EXPLORING THE ROLES OF THE HISTONE DEACETYLASE AND LONGEVITY FACTOR SIRT6 IN CANCER

by

Bernadette Margaretha Maria Zwaans

A dissertation submitted in partial fulfillment
of the requirements for the degree of
Doctor of Philosophy
(Molecular and Cellular Pathology)
in the University of Michigan
2014

Doctoral Committee:

Assistant Professor David B. Lombard, Chair
Professor Kathleen R. Cho
Associate Professor Yali Dou
Professor Eric R. Fearon
Associate Professor Patrick J. Hu

To my parents, I hope I have made you proud.

Acknowledgements

Graduate school has been an immense learning experience for me, both at a professional and personal level. Many friends, family and colleagues, each in their own way, have contributed to my growth and completion of my PhD training at the University of Michigan and I'm grateful for having had such a great support system to fall back on.

First I would like to thank my former mentor Dr. Diane Bielenberg. Prior to joining PIBS at the University of Michigan, I worked in Dr. Bielenberg's laboratory as a research assistant. All the skills and the confidence that I obtained while working with Diane formed the foundation on which I further built my scientific career at the University of Michigan. I'm enormously thankful for having been able to work under her tutelage and hope that in the future our scientific paths will cross again.

Throughout my PhD training I've had the pleasure of working with a number of extraordinary scientists. First and foremost I would like to show my gratitude to my mentor Dr. David Lombard, who has guided me through the daily twist and turns of scientific discovery. I admire his broad knowledge, enthusiasm for science, and positive attitude, and am thankful for his patience and flexibility. Secondly, I would like to thank my thesis committee members Dr. Fearon, Dr. Cho, Dr. Hu and Dr. Dou, for

their support, valuable input, and for sharing reagents and protocols. Additionally, I'm very grateful for the guidance that I have gotten from the PIBS program director Dr. Isom, the pathology program directors Dr. Lukacs and Dr. Nikolovska-Coleska, and the support from our program coordinators Laura Hessler and Laura Labut. Furthermore, I would like to thank the Rackham graduate school for awarding me the Rackham predoctoral fellowship.

I would also like to thank the current and former members of the Lombard lab: Mary Skinner, Billy Giblin, Jeongsoon Park, Surinder Kumar, Kylie Smith, Emily Sluiter, Ray Joe, Daniel Tishkoff, Shawn Loder, Bo Yang, Jiangjun Bao, and Mark Eckersdorf. We have spent countless hours working side-by-side, discussing follow-up experiments, hunting down free food and laughing about silly things. You have all contributed to the person I am today, and I thank you for that.

My thesis work wouldn't have been possible without our numerous collaborators. Thank you to Dr. Elenitoba-Johnson and Dr. Basrur for your help in identifying novel SIRT6 interactors, Dr. Rho and Dr. Giordano for providing human tissue samples for our IHC studies, Dr. Greenson for his pathological expertise, Dr. van Deursen and Janine Van Ree for help with our aneuploidy study, Dr. Cavey for performing the mass spectrometry to identify novel SIRT6 targets. Dr. Cho, Dr. Wu and Dr. Gruber for sharing Affymetrix data, and Dr. Lukacs and Dr. Mukherjee for our collaboration on the T-cell project, which is not discussed in my thesis work. Finally, I would like to thank Dr.

Mostoslavsky and Dr. Sebastian for our productive collaboration on the identification of SIRT6's tumor suppressor function (discussed in Chapter 3).

Last, but definitely not least, I would like to thank my friends and family members for their love and support. In particular my friends Davina, Scott, the Liz's, Molly, Seyth and Dave for being there for me through thick and thin, my husband Jake for putting a smile on my face every day and coping with my daily ups and downs, and my siblings for being the very best friends I could wish for. A special thank you goes out to my parents, without whose love and support my life wouldn't be what it is today. They've worked hard their whole lives to be able to give their children every opportunity they'd like to pursue, even if that meant having them move far away from home. I thank them for their unconditional love, emotional as well as financial support, and the family vacations I was always able to look forward to. But most importantly, I thank them for creating this wonderful family, which, up to this day, I consider my strongest asset.

My thesis work is the result of so many helping hands along the way and I hope I have made everybody proud of this joint accomplishment.

Table of contents

List of Figures

List of Tables

List of Abbreviations

53BP1, tumor suppressor p53 binding protein 1; A-EJ, alternative end-joining; A-FABP, adipocyte fatty acid binding protein; Ac, acetyl group; ADPr, ADP-ribose group; ANGPTL4, angiopoietin-like protein 4; AP-1, activator protein 1; APC, adenomatous polyposis coli; ARP, aldehyde reactive probe; AT, adenine thymine; ATP, adenosine triphosphate; BC, breast cancer; BER, base excision repair; BRCA1, breast cancer 1; BSA, bovine serum albumin; C-NHEJ, classic non-homologous end-joining; CBP, CREB binding protein; CC, colon cancer; cDNA, copy DNA; CHIP, carboxyl terminus of Hsp70-interacting protein; ChIP, chromatin immunoprecipitation; CT, computerized tomography; CtIP, CtBP interacting protein; DAB, 3,3'-diaminobenzidine; DCA, dichloroacetate; DCFDA, dichlorofluorescein diacetate; DGAT1, diglyceride acyltransferase 1; DMEM, Dulbecco's modified eagle medium; DNA, deoxyribonucleic acid; DNA-PKcs, DNA-dependent protein kinase catalytic subunit; DSB, double strand break; DTT, dithiothreitol; EAAs, essental amino acids; EDTA, ethylenediaminetetraacetic acid; EGCG, epigallocatechin gallate; EGTA, ethylene glycol tetraacetic acid; ES cell, embryonic stem cell; FACS, fluorescent activated cell sorter; FACT, facilitates chromatin transcription; FBS, fetal bovine serum; FDG, fluorodeoxyglucose; FITC, fluorescein isothiocyanate; FoxO, forkhead box protein O; G3BP, Ras GTPase-activating protein-binding protein; GLS, glutaminase; GLUT,

Glucose transporter; H&E, heamatoxylin and eosin; H2A, histone H2A; H2B, histone H2B; H_2O_2, hydrogen peroxide; H3, histone H3; H3K56, histone H3 lysine 56; H3K56me3, H3K56 trimethylation; H3K9, histone H3 lysine 9; H3K9me3, H3K9 trimethylation; H4, histone H4; H4K16, histone H4 lysine 16; HAT, histone acetylgransferase; HCC, hepatocellular carcinoma; HDAC, histone deacetylase; HDF, human dermal fibroblasts; HFD, high fat diet; HGBT, high-grade brain tumor; HIF-1, Hypoxia inducible factor 1; HK1/2, hexokinase 1/2; HMGB1, high-mobility group protein B1; Hnf4, hepatocyte nuclear factor 4; HNSCC, head and neck squamous cell carcinoma; HP1, heterochromatin protein 1; HR, homologous recombination; HREs, responsive elements; IEC, intestinal epithelial cell; IGF-1, insulin-like growth factor 1; IGFR, insulin-like growth factor receptor; IHC, immunohistochemistry; IIS, insulin-IGF-1-like signaling; IL-13, interleukin-13; IL-17, interleukin-17; Il-6, Interleukin-6; IL-8, interleukin-8; iMEF, immortalized MEF; IP, immunoprecipitation; KAP1, KRAB-associated protein 1; KD, knockdown; KO, knockout; LDHA, lactate dehydrogenase A; LDL, low density lipoprotein; LIF, leukemia inhibitory factor; LINE-1, long interspersed nuclear element-1; LMNAC, lamin A/C; MCP1, monocyte chemoattractant protein-1; MCT4, monocarboxylate transporter 4; MEFs, mouse embryonic fibroblasts; MeOH, methanol; mMES, mutant NES; mNLS, mutant NLS; mRNA, messenger RNA; MSR, major satellite repeat; mTORC1, mammalian target of rapamycin complex 1; NAC, N-acteyl cysteine; NAD, nicotinamide aldenine dinucleotide; NAM, nicotinamide; NES, nuclear export sequence; NF-κB, nuclear factor-κB; NK cells, natural killer cells; NLS, nuclear localization signal; NRF1, nuclear respiratory factor 1; NSCLC, non-small cell lung cancer; OD, optical density; OE, overexpression; PaC, pancreatic cancer; PARP-

1, poly [ADP-ribose] polymerase 1; PBS, phosphate buffered saline; PCR, polymerase chain reaction; PDC, pyruvate dehydrogenase complex; PDH, phosphate dehydrogenase; PDK1, pyruvate dehydrogenase kinase 1; PDP1, pyruvate dehydrogenase phosphatase catalytic unit 1; PET, positron emission tomography; PFA, paraformaldehyde; PFK1, phosphofructokinase 1; PGC-1α, PPARγ coactivator-1α; PHD, prolyl hydroxylase; PKA, protein kinase A; PMSF, phenylmethylsulfonyl fluoride; PPARγ, peroxisome proliferator-activated receptor γ; PrC, prostate cancer; PTM, post-translation modification; PVDF, polyvinyl difluoride; rDNA, ribosomal DNA; RNA, ribonucleic acid; ROS, reactive oxygen species; rRNA, ribosomal RNA; RT-PCR, real-time polymerase chain reaction; SCID, severe combined immunodeficiency; SD, standard deviation; SDS, sodium dodecyl sulfate; SEM, standard error of the mean; shRNA, short hairpin RNA; SIR2, silent information regulator 2; siRNA, small interfering RNA; SIRT6, sirtuin 6; SREBP1/2, sterol regulatory element binding protein 1/2; SCC, squamous cell carcinoma; SSC, saline-sodium citrate; ssDNA, single strand DNA; SSRP1, structure specific recognition protein 1; SUV, standard uptake value; T2D, type-2 diabetes; TBST, tris-buffered saline and tween; TCA, tricarboxylic acid; TEB, triton extraction buffer; TF, transcription factor; TFAM, mitochondrial transcription factor A; TNFα, tumor necrosis factor α; TPE, telomere position effect; TSA, trichostatin A; USP10, ubiquitin-specific peptidase 10; UTP, uridine 5'-triphosphate; UTR, untranslated region; UV, ultraviolet; V-c, villin-cre-recombinase; VHL, von Hippel-Lindau; WAT, white adipose tissue; WCE, whole cell extract; WRN, Werner protein; WT, wild type

Abstract

Identification of pathways that regulate longevity in an evolutionarily conserved manner is a major focus of modern biogerontology. Interest in the sirtuin family of deacetylases/ADP-ribosyltransferases/deacylases began with the observation that increased expression of SIR2 extends replicative lifespan in budding yeast. The seven mammalian sirtuin homologs have been the focus of intense investigation for their potential impacts on health- and lifespan. My thesis work focuses specifically on the mammalian sirtuin SIRT6. SIRT6 plays multiple roles in metabolic homeostasis and genome integrity through modification of histones and other protein targets; consequently SIRT6 suppresses many age-associated pathologies such as neoplasia, cardiac hypertrophy, and glucose intolerance. SIRT6 overexpression results in extended lifespan in male mice, suggesting that SIRT6 may represent a true functional ortholog of yeast SIR2, and supporting an evolutionarily conserved role for sirtuins in longevity. In this work, we identified a protective role for SIRT6 in suppressing tumorigenesis. First, SIRT6 suppresses aerobic glycolysis, the preferred form of energy metabolism in cancer cells, by inhibiting the expression of various glycolytic proteins. Second, SIRT6 regulates cell growth by reducing ribosomal biogenesis via the proto-oncogene c-MYC. Additionally, we identified H3K56ac, a histone mark involved in DNA repair which is often elevated in cancer, as a novel target for SIRT6

and we identified an increased incidence of aneuploidy in SIRT6-deficient cells. Thus, SIRT6's role in maintaining genomic integrity could possibly provide a third means through which SIRT6 suppresses tumor development. Conversely, examination of established cancer cell lines and tissues, revealed high SIRT6 protein expression and cytoplasmic localization. However, SIRT6 activity appears to be compromised as SIRT6 no longer acts upon its target H3K56. Overall, the identified tumor suppressive properties of SIRT6 are possibly the underlying mechanism through which SIRT6 extends mammalian lifespan, and provides therapeutic potential for the treatment of various malignancies.

Chapter 1

Introduction: The Diverse Roles of SIRT6 in Mammalian Healthspan

Introduction to SIRT6

Aging is a conserved phenomenon, which is associated with loss of function and impaired stress resistance in invertebrate and mammalian model organisms. In humans, most common health conditions – type 2 diabetes (T2D), cardiovascular disease, cancer, and neurodegeneration, among many others – are strongly associated with advancing age. Conversely, genetic and environmental interventions that promote increased longevity typically also delay or even prevent many age-associated pathologies. Therefore, an understanding of molecular mechanisms of aging offers the possibility of improved treatments for many common diseases. This realization has led to a hunt for pathways that regulate health- and lifespan, at least some of which function in a conserved manner across different phyla.

The sirtuins are a conserved NAD^+-dependent enzyme family regulating many cellular functions, in particular stress responses. The *SIR2* (Silent Information Regulator 2) gene in budding yeast was the first sirtuin to be identified and functionally characterized. Increased dosage of *SIR2* or its homologs promotes increased lifespan

in budding yeast, worms and flies (Belenky et al., 2007; Berdichevsky et al., 2006; Hoffmann et al., 2013; Kaeberlein et al., 1999; Rogina and Helfand, 2004; Salvi et al., 2013; Tissenbaum and Guarente, 2001; Viswanathan et al., 2005; Whitaker et al., 2013). As an aside, it should be noted that one prominent study did not reproduce these pro-longevity effects of sirtuins in worms or flies (Burnett et al., 2011), and aspects of the roles of sirtuins in yeast longevity are also still hotly debated (Longo and Kennedy, 2006). The discrepant results obtained by different laboratories likely result from variations in experimental protocols, strain background and/or husbandry conditions. Notwithstanding these controversies, the apparently conserved pro-longevity effect of sirtuins has led to intensive efforts to characterize functions of the seven mammalian sirtuins, termed SIRT1-7 (Figure 1.1). Each of these proteins possesses a fairly conserved catalytic domain; however sirtuins differ at their N- and C-termini, and are a divergent family in terms of sub-cellular localization, targets and functions (Canto et al., 2013). Overexpression of at least two mammalian sirtuins, SIRT1 (in the hypothalamus) or SIRT6 (globally) extends mouse lifespan (Kanfi et al., 2012; Satoh et al., 2013).

In addition to lifespan *per se,* a large body of evidence has revealed major roles for individual sirtuins in suppressing age-associated pathologies (Morris, 2013). Biochemically, mammalian sirtuins function as NAD^+-dependent lysine deacetylases, with varied catalytic efficiencies and substrates. Several mammalian sirtuins have been shown to possess ADP-ribosyltransferase activity (Ahuja et al., 2007; Frye, 1999; Haigis et al., 2006; Liszt et al., 2005), and some sirtuins remove non-canonical lysine

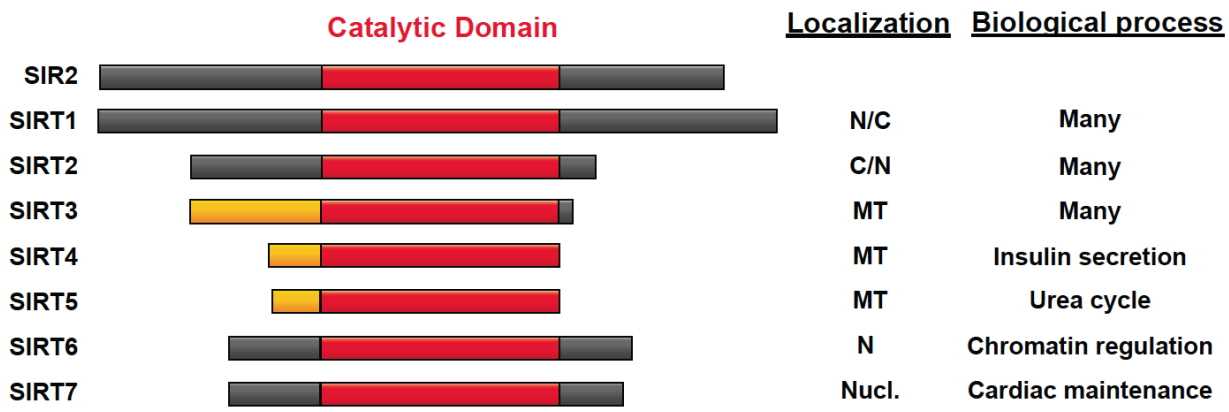

Figure 1.1: Mammalian Sirtuin family

A schematic representation of yeast SIR2 and its mammalian homologs (SIRT1-7). The sirtuins share a conserved catalytic domain but differ in their N and C-termini, resulting in diversity in intracellular localization and function. N, nucleus; C, cytoplasm; MT, mitochondria; Nucl., nucleolus. Yellow depicts mitochondrial localization sequence.

post-translational modifications such as succinyl, malonyl, and acyl groups (Du et al., 2011; Feldman et al., 2013; Jiang et al., 2013; Peng et al., 2011). Through these activities, mammalian sirtuins modulate a diverse array of biological processes such as transcriptional regulation, metabolism, genomic stability, cell cycle control and inflammation (Morris, 2013).

SIRT6, the focus of my dissertation work, has been implicated in suppressing many age-associated pathologies: obesity and metabolic syndrome (Kanfi et al., 2010; Kim et al., 2010; Schwer et al., 2010), inflammation (Lappas, 2012; Lee et al., 2013b; Lee et al., 2013c; Xiao et al., 2012), cardiac hypertrophy (Sundaresan et al., 2012; Yu et al., 2013), neurodegeneration (Jin et al., 2013), cellular senescence (Cardus et al., 2013; Kawahara et al., 2009; Shen et al., 2013; Xie et al., 2012) and cancer (Bauer et al.,

2012; Han et al., 2014; Khongkow et al., 2013b; Lefort et al., 2013; Marquardt et al., 2013b; Min et al., 2012; Sebastian et al., 2012; Thirumurthi et al., 2014; Van Meter et al., 2011).

SIRT6 is a nuclear protein that associates with heterochromatin (Liszt et al., 2005; Michishita et al., 2005; Mostoslavsky et al., 2006; Xiao et al., 2010). Biochemically, SIRT6 functions as a lysine deacetylase, a mono-ADP-ribosyltransferase, and a long-

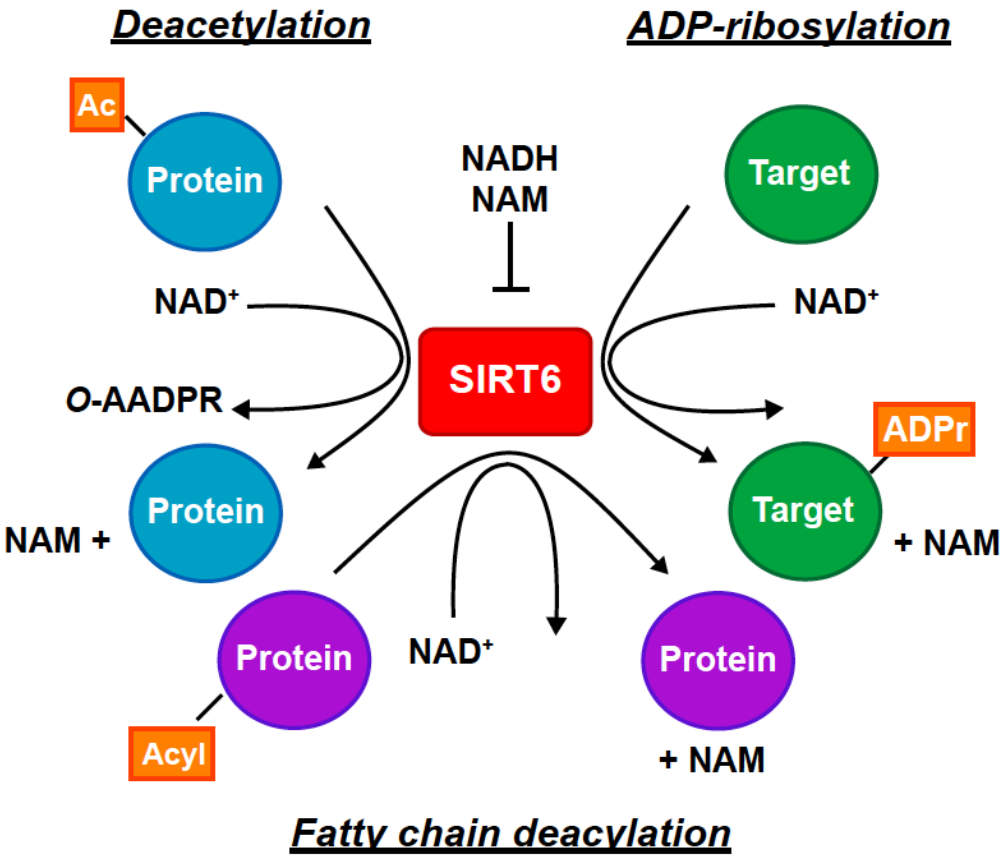

Figure 1.2: SIRT6 biochemical functions

SIRT6 possess three known biochemical functions: deacetylation, ADP-ribosylation and fatty chain deacylation. Each one of these reactions is dependent on the presence of NAD^+. Ac, acetyl group; NAM, nicotinamide; ADPr, ADP-ribose group; NAD, nicotinamide adenine dinucleotide.

chain fatty acid deacylase (Jiang et al., 2013; Liszt et al., 2005; Mao et al., 2011; Michishita et al., 2008) (Figure 1.2). *In vitro* studies suggest that SIRT6 possesses very modest deacetylase activity (Pan et al., 2011). However, a recent study suggested that SIRT6 is more active when interacting with nucleosomes as it is reconfigured there into a more active form (Gil et al., 2013) and that physiological concentrations of various free fatty acids drastically induce SIRT6 catalytic efficiency (Feldman et al., 2013). Nevertheless, as described in depth below, recent work has revealed that SIRT6 functionally deacetylates at least three targets: one histone site (H3K9) (Michishita et al., 2008), and two non-histone proteins (CtIP and GCN5) (Dominy et al., 2012; Kaidi et al., 2010). Initial insights into SIRT6 function came from studies of SIRT6-deficient mice (Mostoslavsky et al., 2006). These animals show severe pleiotropic defects, suggesting that SIRT6 likely impacts multiple processes important for organismal health.

Sirt6-deficient fibroblasts and ES cells grow slowly and show genome instability. *Sirt6* knockout (KO) mice appear normal at birth but soon manifest growth retardation due to very low serum IGF-1 levels. They are frail, with a hunched posture (lordokyphosis) and lose most of their white adipose tissue (WAT), including the subcutaneous fat. At approximately two weeks of age, blood glucose levels begin to decline steeply in *Sirt6* KO animals. These mice also show rapid depletion of lymphocytes via a massive wave of apoptosis. The latter phenotype is most likely a systemic rather than a cell-autonomous defect, as *Sirt6*-deficient bone marrow cells are able to repopulate the

lymphocyte compartment of irradiated recipient mice as efficiently as wild-type bone marrow (Mostoslavsky et al., 2006). Clearly, SIRT6 plays crucial roles in cellular and organismal homeostasis.

As described below, there has been significant recent progress in elucidating molecular functions of SIRT6. A common theme that has emerged is that SIRT6 negatively regulates the transcriptional output of key cellular signaling pathways by deacetylating histones at their target promoters. This is in contrast to SIRT1; though SIRT1 can also deacetylate histones, it exerts many of its functions by directly deacetylating transcription factors and other non-histone targets themselves (Guarente, 2011). Much of the newer functional analysis of SIRT6 has been carried out using tissue-specific *Sirt6* KO animals, avoiding the lethality associated with global Sirt6 deficiency, and permitting a finer dissection of SIRT6's roles.

SIRT6 is a master metabolic regulator

As noted above, SIRT6 is required for glucose homeostasis, a role that is critical for organismal survival. Two different *Sirt6* germline KO mouse strains have been described (Mostoslavsky et al., 2006; Xiao et al., 2010). Both show severe hypoglycemia and greatly reduced serum IGF-1 levels. On a pure 129SvJ strain background, SIRT6 deficiency results in completely penetrant postnatal lethality by one month of age (Mostoslavsky et al., 2006). However, in an outbred background, a minority of *Sirt6*-deficient mice survives this hypoglycemia and lives into adulthood (Xiao et al., 2010).

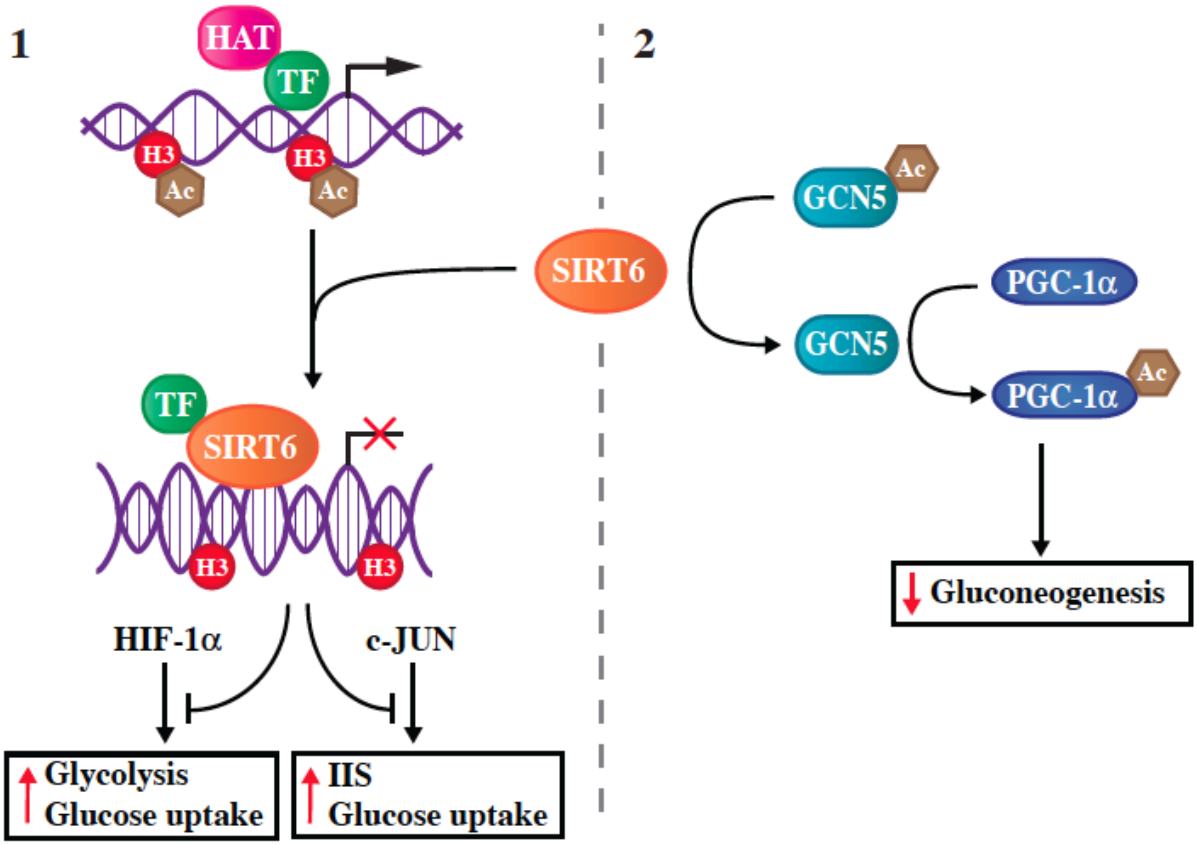

Figure 1.3: SIRT6 as a master regulator of glucose metabolism

SIRT6 regulates glucose metabolism through at least two distinct mechanisms. (1) SIRT6 deacetylates histone H3, thereby attenuating transcriptional output of HIF-1α and c-JUN, which normally enhance glucose uptake and induce glycolysis or activate the insulin-IGF-1-like signaling (IIS) pathway. (2) SIRT6 deacetylates the histone acetyltransferase GCN5 (KAT2A), which in turn acetylates and activates the transcriptional regulator PPARγ coactivator-1α (PGC-1α), reducing de novo production of glucose (gluconeogenesis) in the liver. Ac, acetyl group; HAT, histone acetyltransferase; H3, histone H3; TF, transcription factor.

Glucose supplementation of these *Sirt6*-deficient mice further improves their survival, proving that hypoglycemia is a major cause of death in the absence of SIRT6 during postnatal development (Xiao et al., 2010). Reduced NF-κB signaling can also partially rescue the lethality of SIRT6 deficiency (Kawahara et al., 2009). As described more fully below, NF-κB family transcription factors are implicated in inflammation, apoptosis,

and cellular senescence. SIRT6 attenuates NF-κB mediated gene expression by deacetylating histone H3 lysine K9 (H3K9) at the promoters of NF-κB target genes (Kawahara et al., 2009). Therefore, other factors besides hypoglycemia contribute to the lethality of SIRT6 deficiency.

Recent work has revealed multiple roles for SIRT6 in glucose homeostasis. SIRT6 controls blood glucose levels by regulating at least three distinct pathways: HIF-1α signaling, insulin/IGF-like signaling (IIS), and gluconeogenesis (Dominy et al., 2012; Xiao et al., 2010; Zhong et al., 2010) (Figure 1.3). HIF-1α is a master metabolic regulator; under conditions of low oxygen or glucose, HIF-1α promotes a shift from oxidative metabolism to glycolysis (Koh and Powis, 2012) (Figure 1.4). HIF-1α promotes expression of multiple genes encoding proteins in the glycolytic cascade; conversely, HIF-1α drives increased expression of PDK1, in turn inhibiting carbon flow into mitochondria (see also Figure 3.2). The glucose transporter GLUT1 is another key HIF-1α target. SIRT6 functions as a repressor of HIF-1α transcriptional output by deacetylating H3K9 at the promoters of HIF-1α target genes, and also by reducing overall HIF-1α levels. Hence, in the absence of SIRT6, uncontrolled HIF-1α activity results in increased glycolysis and glucose uptake from the circulation, most evident in skeletal muscle and brown adipose tissue, culminating in hypoglycemia (Zhong et al., 2010). Increased glycolytic gene expression has also been found in the livers of hepatic-specific *Sirt6* KOs (Kim et al., 2010).

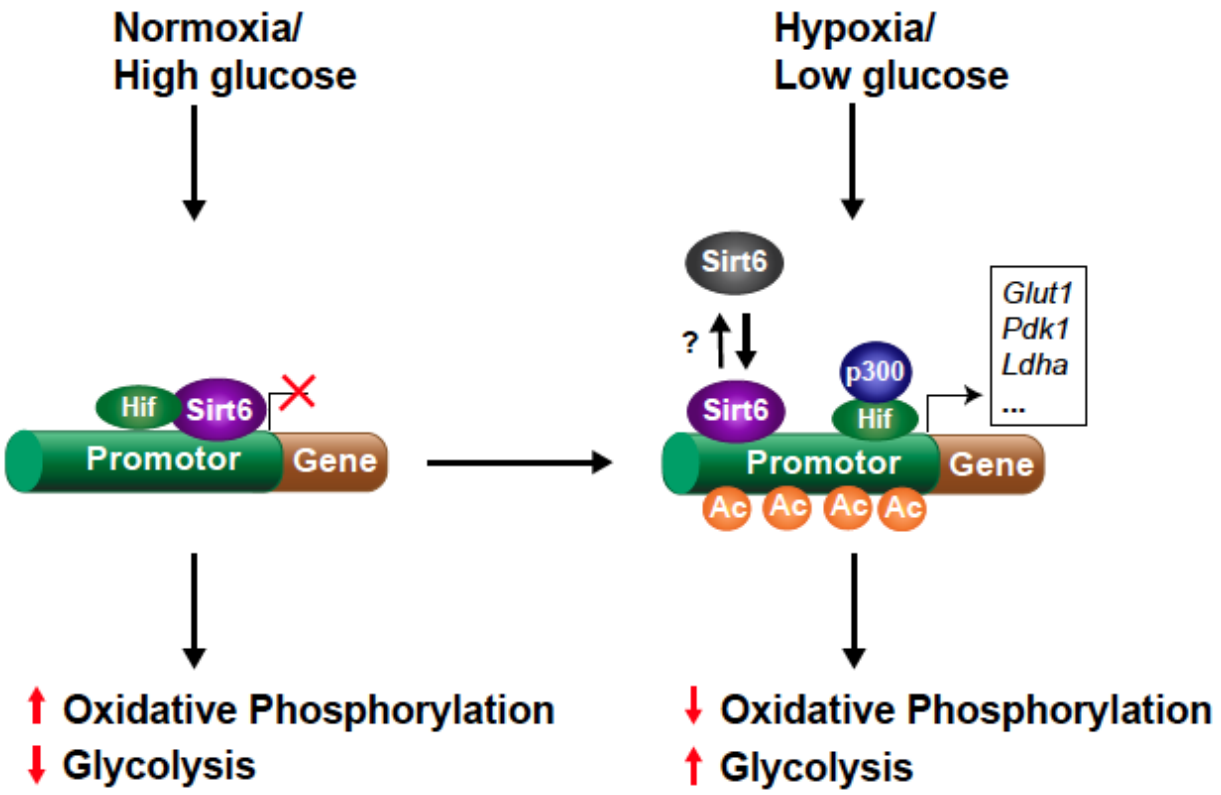

Figure 1.4: SIRT6 regulates glycolysis

Under normal oxygen tension and high glucose conditions, SIRT6 deacetylates histone H3K9ac at the promoter region of HIF-1 target genes and represses HIF-1 activity, thereby suppressing glycolysis and promoting oxidative phosphorylation. When oxygen or glucose levels are low, the removal of SIRT6 allows transcription of glycolytic genes by HIF-1. Figure adapted from (Zhong et al., 2010)

In addition to GLUT1, *Sirt6*-deficient mice show higher levels of the glucose transporter GLUT4 at the cell membrane (Xiao et al., 2010). Unlike GLUT1, GLUT4 translocation is promoted by IIS. Despite lower serum insulin and IGF-1 levels in *Sirt6* mutant mice, IIS is actually much more active in these animals (Sundaresan et al., 2012; Xiao et al., 2010). This may reflect the role for SIRT6 as a co-repressor of c-JUN, as c-JUN promotes expression of many genes involved in IIS (Sundaresan et al., 2012). c-JUN is a component of the activator protein 1 (AP-1) transcription factor, which is involved in

various processes such as apoptosis, cell proliferation and development (Dunn et al., 2002).

SIRT6 also suppresses hepatic gluconeogenesis by deacetylating the acetyltransferase GCN5, activating it to acetylate PGC-1α (Dominy et al., 2012) (Figure 1.3). PGC-1α is a transcriptional co-activator that is a master regulator of mitochondrial biogenesis and other metabolic processes (Puigserver and Spiegelman, 2003). In the liver, PGC-1α promotes gluconeogenesis by coactivation of *FoxO1* and *Hnf4* (Puigserver et al., 2003; Rhee et al., 2003). Acetylation of PGC-1α inhibits PGC-1α transcriptional activity (Rodgers et al., 2005); hence, via activation of GCN5, SIRT6 inhibits hepatic glucose production (Dominy et al., 2012). The twin roles of SIRT6 in suppressing glycolysis while simultaneously inhibiting hepatic glucose output might superficially seem at odds with one another. These functions might be rationalized as a means to avoid futile cycling of glucose production and breakdown (Dominy et al., 2012).

The relationship between SIRT1 and SIRT6 in the context of PGC-1α acetylation is also intriguing. SIRT1 deacetylates PGC-1α to activate its transcriptional function, thus opposing the activity of SIRT6/GCN5 (Rodgers et al., 2005). Consistent with antagonistic functions of these sirtuins, protein kinase A (PKA) suppresses SIRT6 activity while stimulating SIRT1 function (Dominy et al., 2010; Gerhart-Hines et al., 2007; Nin et al., 2012). However, these findings seem inconsistent with the published role of SIRT1 in stimulating SIRT6 expression (Kim et al., 2010). Further studies are

required to elucidate the precise interplay between SIRT1 and SIRT6 in response to varied dietary conditions.

In addition to its role in glucose homeostasis, SIRT6 also controls hepatic fatty acid metabolism by regulating expression of genes involved in this process via promoter H3K9 deacetylation. SIRT6 suppresses accumulation of triglycerides in hepatocytes by inhibiting fatty acid uptake and synthesis, while promoting their breakdown via β-oxidation (Kim et al., 2010). A number of genes involved in these processes are regulated by the nuclear receptor PPARγ. PPARγ induces expression of genes that regulate lipid metabolism and adipocyte differentiation (Zhang et al., 2013a), including angiopoietin-like protein 4 (ANGPTL4) and adipocyte fatty acid binding protein (A-FABP). ANGPTL4 negatively regulates lipoprotein lipase, which hydrolyzes serum triglycerides into free fatty acids, and thus mediates triglyceride clearance from the blood (Kim et al., 2010). A-FABP is a chaperone for cytosolic fatty acids, elevated levels of which are associated with obesity and metabolic syndrome (Xu et al., 2006). Furthermore, SIRT6 binds to the promoter of DGAT1, a key enzyme in triglyceride synthesis, repressing its expression (Kim et al., 2010). Through this mechanism, SIRT6 protects against fatty liver formation in response to a high fat diet (HFD). SIRT6 also inhibits pancreatic inflammation under these dietary conditions (Kanfi et al., 2010). Human fatty livers exhibit lower levels of SIRT6, and liver-specific *Sirt6* knockout mice develop fatty liver and hypercholesterolemia, in particular LDL cholesterol (Tao et al., 2013a, b). Overexpression of SIRT6 protects the liver from excessive lipid accumulation (Kanfi et al., 2010) and lowers LDL cholesterol in response to HFD by

recruiting FOXO3 and repressing transcription of *Pcks9* and *Srebp1/ 2*, major regulators of cholesterol homeostasis (Elhanati et al., 2013; Tao et al., 2013a, b). The SREBPs, or sterol regulatory element binding proteins, are transcription factors that bind the sterol regulatory element DNA sequence and are required for cholesterol and fatty acid biosynthesis (Tao et al., 2013a, b). In addition to suppressing their expression, SIRT6 suppresses SREBP1/2 cleavage into their active forms and SIRT6 inactivates SREBP1 through its phosphorylation (Elhanati et al., 2013).

Given the roles of SIRT6 in glucose and lipid homeostasis, it is perhaps not surprising that it plays protective roles against obesity and T2D, both common age-associated pathologies (Dominy et al., 2012; Schwer et al., 2010). Brain-specific *Sirt6* KO mice become obese in adulthood, which is associated with reduced levels of pituitary growth hormone and the hypothalamic factors proopiomelanocortin (POMC), single-minded homolog 1 (SIM1) and brain-derived neurotrophic factor (BDNF). These factors have all been linked to obesity in humans. SIRT6 deficiency in the brain causes hyperacetylation of H3K9 and H3K56, possibly leading to dysregulation of these and potentially numerous other genes (Schwer et al., 2010). Furthermore, ectopic expression of SIRT6 in a mouse model of diabetes reduces hepatic glucose output and normalizes serum glucose levels (Dominy et al., 2012). Thus, roles of SIRT6 in regulating obesity-associated gene expression and glucose and lipid metabolism might eventually be exploited therapeutically. It will be of great interest to assess roles for SIRT6 in other metabolically critical tissues such as skeletal muscle, adipose tissue, and pancreatic β-cells. Similarly, it remains an outstanding question whether the

depletion of WAT observed in global *Sirt6* KOs indicates a primary role for SIRT6 in maintaining WAT, or a secondary consequence of hypoglycemia and overall disordered metabolism in these animals.

Regulation of SIRT6

Despite its central role in metabolic homeostasis, relatively little is known regarding how SIRT6 levels and activity are regulated. Like other sirtuins, SIRT6 requires the metabolic cofactor NAD^+ for activity. In response to fasting or long term calorie restriction, SIRT6 protein levels are elevated in brain, heart and WAT (Kanfi et al., 2008; Kim et al., 2010), promoting a metabolic switch from glycolysis to oxidative phosphorylation (Dominy et al., 2012; Kim et al., 2010; Xiao et al., 2010; Zhong et al., 2010). However, there is conflicting evidence about the underlying mechanism of altered *Sirt6* expression. SIRT6 levels are decreased in livers of obese and diabetic mice (Dominy et al., 2012). Conversely, *SIRT6* mRNA rises in liver and subcutaneous fat in response to severe weight loss; possibly due to decreased inflammation as TNFα can suppress *SIRT6* expression (Moschen et al., 2013). Likewise, SIRT6 protein levels increase in response to caloric restriction. Kanfi and colleagues showed that SIRT6 protein levels, but not mRNA levels, rise in response to fasting, due to stabilization of the SIRT6 protein (Kanfi et al., 2008). However, Kim and coworkers found that induction of *Sirt6* during fasting occurs transcriptionally and requires SIRT1 (Kim et al., 2010). They found that SIRT1 deacetylates FOXO3a to allow FOXO3a to form a complex with NRF1 and induce *Sirt6* gene expression (Kim et al., 2010). As noted above, PKA also inhibits SIRT6 expression, while simultaneously increasing SIRT1

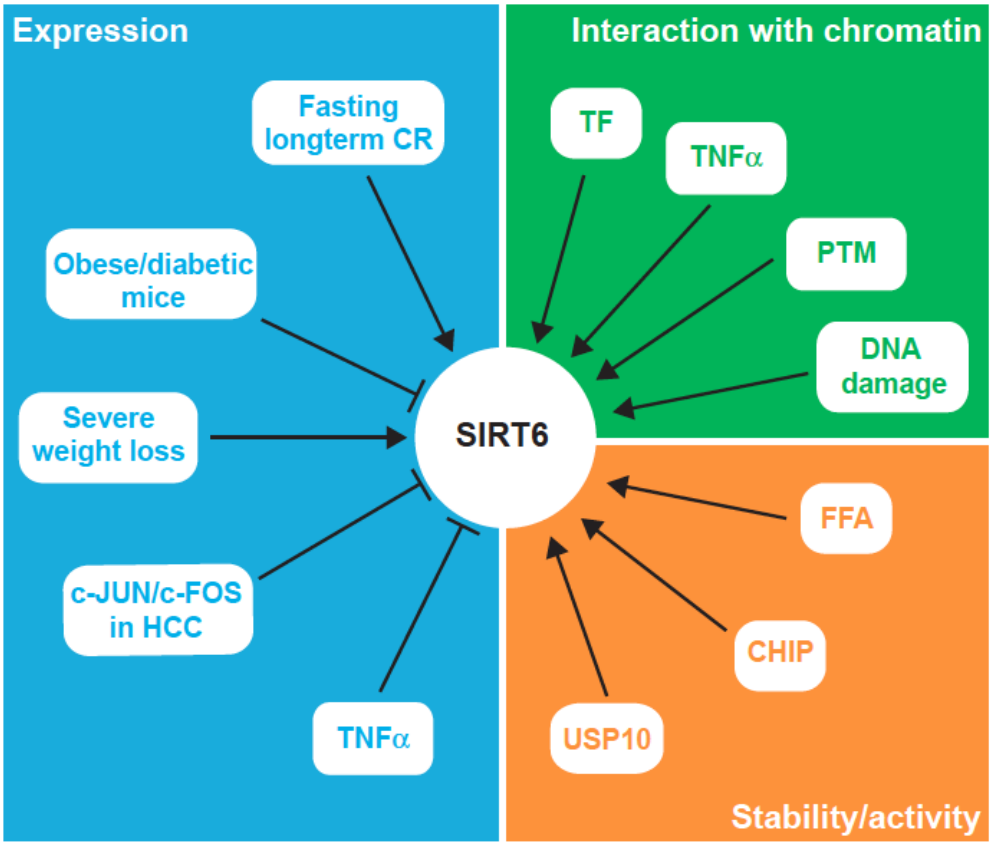

Figure 1.5: Mechanisms of SIRT6 regulation

SIRT6 is regulated through numerous factors that mediate SIRT6 protein expression, SIRT6 binding to the chromatin and SIRT6 stability or activity. CR, calorie restriction; HCC, hepatocellular carcinoma; TNFα, tumor necrosis factor α; USP10, ubiquitin-specific peptidase 10; CHIP, carboxyl terminus of Hsp70-interacting protein; FFA, free fatty acids; PTM, post-translational modification; TF, transcription factor.

levels (Dominy et al., 2010; Gerhart-Hines et al., 2007; Nin et al., 2012). SIRT1 is regulated by a complex network of interactors and post-translational modifications (PTM) (Revollo and Li, 2013); analogously SIRT6 activity is regulated by means other than expression levels. Physiological concentration of free fatty acids induces catalytic efficiency of SIRT6, thereby increasing SIRT6 activity. In addition, the ubiquitin ligase CHIP (carboxyl terminus of Hsp70-interacting protein) ubiquitinates and consequently stabilizes SIRT6 by preventing SIRT6's interaction with other ubiquitin ligases

(Ronnebaum et al., 2013). Likewise, SIRT6 is protected from proteasomal degradation by the ubiquitin-specific peptidase USP10 (Figure 1.5) (Lin et al., 2013).

Other studies, discussed in detail later, report dysregulation of SIRT6 levels under various pathological conditions; however it remains unclear for the most part how this occurs mechanistically. In one case, recent data (discussed below) suggest that altered c-JUN and c-FOS signaling reduce *Sirt6* expression during the initiation of hepatocellular carcinoma (Min et al., 2012). SIRT6 associates with nuclear chromatin and upon stress induction, *e.g.* TNFα treatment, SIRT6 relocalizes dynamically to different promoters (Kawahara et al., 2011). Similarly, SIRT6 relocalizes to sites of DNA damage, perhaps via interaction with DNA repair machinery (McCord et al., 2009). The interaction of SIRT6 with the chromatin appears to be mediated at least in part by transcription factors. Kawahara and coworkers demonstrated that SIRT6 and RELA bind to a large panel of common promoter sites of genes involved in processes such as cell cycle progression, immune system development, anti-apoptosis and glycolysis. For a large fraction of these promoter sites, binding of SIRT6 was dependent on RELA (Kawahara et al., 2011). Other common binding sites in SIRT6 occupied gene promoters are SP1, STAT1/3 and FOXO1/4 (Kawahara et al., 2011) and thus it is reasonable to hypothesize that those transcription factors may also be necessary to recruit SIRT6 to these specific promoters in response to stimuli. Conversely numerous other post-translational modifications present on SIRT6 that have been identified by mass spectrometry (*cf.* www.phosphosite.org), whose functions

have not yet been elucidated, could regulate the interaction of SIRT6 with specific transcriptional activators and/or repressors (Figure 1.5).

SIRT6 regulates inflammation

Increased inflammation is a common feature of aging in many mammalian tissue types (Agrawal et al., 2009; Agrawal et al., 2010). Evidence from global and tissue-specific *Sirt6* KOs suggests that SIRT6 has important roles in limiting the inflammatory response. As part of their overall degenerative syndrome, SIRT6-deficient mice develop severe colitis with erosion of the intestinal mucosa (Mostoslavsky et al., 2006). In outbred SIRT6-deficient mice that survive hypoglycemic crisis, inflammation also develops in the liver, where it eventually leads to fibrosis, and, to lesser extent, in the kidneys, pancreas and lung (Xiao et al., 2012). In the context of hepatic inflammation, using tissue-specific knockouts, it was shown that SIRT6 in lymphocytes and macrophages, and not in hepatocytes, is required to suppress this phenotype. Liver inflammation coincides with increased expression of numerous pro-inflammatory genes, including *Mcp-1* and *Il-6*, in Kuppfer cells and T-cells. Mechanistically, SIRT6 binds the transcription factor c-JUN at the promoters of these pro-inflammatory genes, where it deacetylates H3K9ac and inhibits c-JUN transcriptional output (Figure 1.6) (Xiao et al., 2012).

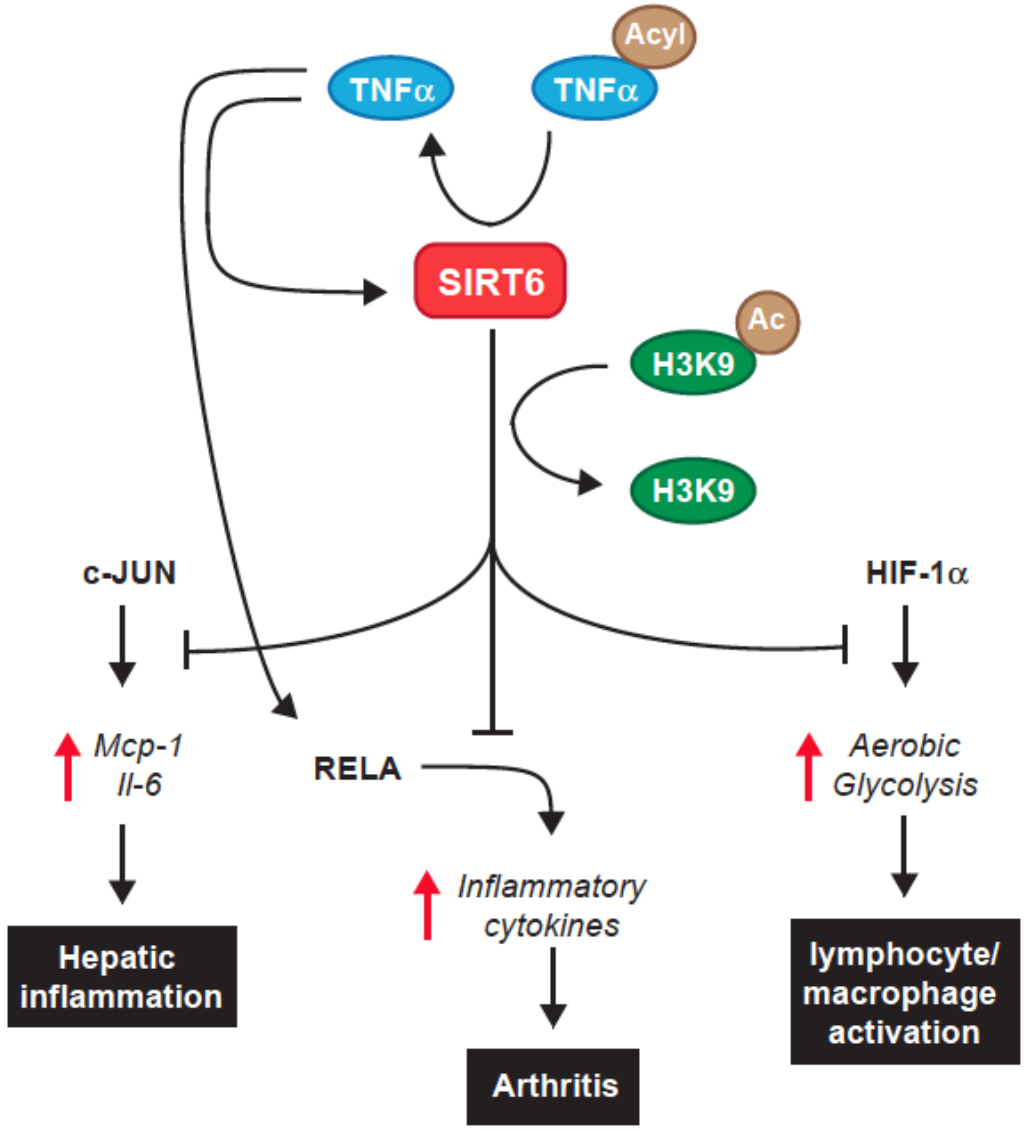

Figure 1.6: SIRT6's regulation of inflammation

Through its deacetylation of H3K9, SIRT6 inhibits at least 3 transcription factors that support an inflammatory response: c-JUN, RELA and HIF-1α. Thereby, SIRT6 aleviates chronic tissue inflammation and arthritis, and prevents the activation of lymphocytes and macrophages. Ac, acetyl group; Acyl, acyl group; TNFα, tumor necrosis factor α; Mcp-1, monocyte chemoattractant protein 1; Il-6, interleukin-6.

In addition to c-JUN, SIRT6 also inhibits the transcriptional output of NF-κB signaling resulting in decreased expression of genes involved in aging (Kawahara et al., 2009). NF-κB is a family of transcription factors implicated in multiple processes such as

inflammation, cell death and proliferation, and development. The NF-κB protein family consists of five members: RELA (p65), RELB, c-REL, p50 and p52, among which RELA interacts with SIRT6. Under basal conditions, they are retained in the cytoplasm by an inhibitor of NF-κB (IκB) family member. In response to diverse stimuli, such as the inflammatory cytokine TNFα, NF-κB is released and consequently moves to the nucleus where it can activate expression of its target genes. The transcriptional output of NF-κB is dependent on various co-regulators and chromatin modulators, including SIRT6 (Kawahara et al., 2009; Wan and Lenardo, 2010). Overexpression of SIRT6 can reduce arthritis in a collagen-induced arthritis mouse model by blocking NF-κB transcriptional output and consequently diminishes secretion of pro-inflammatory cytokines (Figure 1.6) (Lee et al., 2013a). SIRT6 may also mediate the inflammatory response through the pro-inflammatory cytokine TNFα, however their interplay is somewhat complex. Xiao and coworkers showed that TNFα protein levels are elevated in SIRT6-deficient macrophages under both basal and lipopolysaccharide stimulated conditions (Xiao et al., 2012). Conversely, Van Gool and colleagues reported that SIRT6 promotes elevated TNFα protein levels at a post-transcriptional level, indicating that under some conditions, SIRT6 may actually promote secretion of pro-inflammatory cytokines (Van Gool et al., 2009; Xiao et al., 2012). A recent study revealed that SIRT6 stimulates TNFα secretion by removing long-chain fatty acyl groups of lysine 19 and 20 in this protein (Jiang et al., 2013). Conversely, treatment of HeLa cells with TNFα increases SIRT6 translocation to NF-κB/RELA target promoters (Kawahara et al., 2009). Further studies are needed to clarify interactions between TNFα and SIRT6; it is

possible that a negative feedback loop exists in which SIRT6 inhibits TNFα by suppressing NF-κB mediated transcription of pro-inflammatory genes.

In addition to roles for SIRT6 in modulating c-JUN and NF-κB function, the function of SIRT6 in metabolism may be relevant in its suppression of inflammation. Both lymphocytes and macrophages shift their metabolism from respiration to aerobic glycolysis upon activation (Ardawi and Newsholme, 1982; Garedew and Moncada, 2008). Conversely, cells that limit inflammation, such as regulatory T-cells, show relatively low levels of glycolysis (O'Neill and Hardie, 2013). Therefore, it is possible that increased glycolysis occurring in the absence of SIRT6 preferentially drives activation of pro-inflammatory cells.

Overall, most studies have identified roles for SIRT6 in suppressing inflammation. Based on known functions of SIRT6, it is possible that SIRT6 activators might be useful in treating age-associated chronic inflammatory diseases such as diabetes, and cardiovascular and autoimmune diseases characterized by ongoing, chronic inflammation.

SIRT6 promotes genomic stability via diverse mechanisms

Initial studies of SIRT6-deficient cells revealed that SIRT6 plays a major role in genome integrity (Mostoslavsky et al., 2006). *Sirt6* KO cells show reduced proliferation, an elevated incidence of chromosomal abnormalities, and increased sensitivity to DNA damaging agents. Originally it was hypothesized that SIRT6 might play a role in base

excision repair (BER), pathways that repair small DNA lesions, including those induced by oxidative insult (Parsons and Dianov, 2013). This hypothesis was based on the spectrum of sensitivities of SIRT6-deficient cells, as well as the ability of the catalytic domain of Polβ, the major polymerase involved in BER, to rescue cellular phenotypes of SIRT6 deficiency (Mostoslavsky et al., 2006). In support of an involvement of SIRT6 in BER, overexpression of SIRT6 can suppress oxidative DNA damage in porcine fetal fibroblasts, possibly by enhancing BER (Xie et al., 2012). However, there is currently no mechanistic insight into how SIRT6 might facilitate BER. In contrast, there has been significant progress in understanding how SIRT6 promotes DNA double strand break (DSB) repair.

DNA DSBs represent a severe threat to cell viability. They are repaired via three major pathways: classical non-homologous end-joining (C-NHEJ), homologous recombination (HR), and alternative end-joining (A-EJ) (Boboila et al., 2012). Overexpression of SIRT6 increases the clearance of γH2AX foci and accelerates overall DSB repair (Mao et al., 2011). A recent study showed that, in response to DNA insult, SIRT6 is recruited to the breakage site where it interacts with the helicase SNF2H. This complex remodels the nucleosome and consequently attracts various DNA repair factors such as BRCA1 and 53BP1 (Toiber et al., 2013). In support of this idea, SIRT6 stimulates both C-NHEJ and HR by mono-ADP-ribosylating poly (ADP-ribose) polymerase 1, PARP-1 (Mao et al., 2011). PARP-1 binds and stabilizes broken DNA ends and mediates the recruitment of other DNA repair factors. In this context, ectopic SIRT6 expression can rescue the decline of HR capacity associated with

replicative exhaustion (Mao et al., 2012). SIRT6 is required for optimal recruitment of the C-NHEJ factor DNA-PKcs to DNA DSBs, an effect potentially occurring via modulation of local chromatin structure by SIRT6 (McCord et al., 2009). SIRT6 promotes HR by deacetylating and activating CtIP, a factor required for DNA end resection to generate ssDNA for initiation of HR (Kaidi et al., 2010).

In addition to these roles for SIRT6 in promoting global genome stability, SIRT6 in human cells plays a role in stabilizing telomeres specifically. In normal human cells, SIRT6 deacetylates H3K9 at telomeres to promote telomeric heterochromatinization and association of telomeric binding proteins (Michishita et al., 2008; Tennen et al., 2011). Hyperacetylation of telomeric chromatin in the absence of SIRT6 disrupts the interaction of telomeric regions with WRN, a protein involved in telomere maintenance, which is mutated in the premature aging disorder Werner Syndrome. Telomeric attrition is a major cause of replicative senescence in human cells; indeed SIRT6 KD in human fibroblasts causes premature cellular senescence (Michishita et al., 2008; Tennen et al., 2011). Furthermore, SIRT6 is essential for maintaining telomere position effect (TPE), a phenomenon in which telomere-proximal genes are epigenetically silenced (Aparicio et al., 1991; Ng et al., 2002). TPE is lost with replicative aging in yeast (Dang et al., 2009b). This role of SIRT6 is reminiscent of the function of yeast SIR2 in promoting heterochromatinization of the rDNA array to suppress recombination and promote increased replicative lifespan (Ha and Huh, 2011). In contrast, despite the fact that SIRT6 also deacetylates H3K9 at telomeres in mouse cells, telomeres are much longer in mice than humans, and thus do not apparently display dysfunction

upon SIRT6 deletion (Michishita et al., 2008). It would be of interest to determine whether SIRT6 has roles in stabilizing other heterochromatic loci in mammalian cells besides telomeres. Overall, SIRT6 plays many roles through which it can maintain the genomic integrity of the cell.

SIRT6 suppresses cardiac hypertrophy and promotes cardiac stress resistance

Cardiac hypertrophy is a condition characterized by cardiac enlargement, occurring either physiologically in response to normal stimuli such as pregnancy or exercise, or as a consequence of disease states (pathological hypertrophy). Even in the absence of overt stress stimuli, thickening of the ventricular wall occurs with age. In humans, hypertension is a frequent cause of pathological cardiac hypertrophy. Age-associated cardiac hypertrophy is characterized by loss of cardiomyocytes, interstitial fibrosis, and hypertrophy of the remaining cells. Pathological cardiac hypertrophy and consequent ventricular dysfunction is thought to be a mostly irreversible process, which can eventually result in cardiac failure (Dai et al., 2012; Olivetti et al., 2000).

Mice induced to develop cardiac hypertrophy have elevated NF-κB activity in cardiomyocytes, and inhibition of RELA in these mice can revert this phenotype (Gupta et al., 2008). Likewise, overexpression of SIRT6 ameliorates hypertrophy *in vitro* and inhibits the increase in hypertrophic marker genes in cardiomyocytes by repressing NF-κB gene expression (Yu et al., 2013). Sundaresan and colleagues showed a strong reduction in SIRT6 levels in cardiac hypertrophy in both human and mouse hearts (Sundaresan et al., 2012). In contrast, Yu and coworkers reported that SIRT6 levels

are elevated in cardiac hypertrophy in rats, but that this coincides with decreased SIRT6 activity due to decreased NAD^+ levels (Yu et al., 2013). Whole-body *Sirt6* KO and cardiomyocyte-specific *Sirt6* KO mice spontaneously develop cardiac hypertrophy as early as two months after birth, characterized by increased cardiomyocyte size, cellular degenerative changes, and increased expression of aging-associated cytoskeletal proteins, as well as fibrotic and apoptotic markers. Conversely, SIRT6 overexpression protects animals against induction of cardiac hypertrophy (Sundaresan et al., 2012). In the absence of SIRT6, both c-JUN and NF-κB are hyperactive, and silencing either of these transcription factors can prevent hypertrophy *in vitro* (Gupta et al., 2008; Sundaresan et al., 2012; Yu et al., 2013).

The underlying mechanism through which SIRT6 promotes cardiac health is not fully understood. Sundaresan and colleagues reported that SIRT6 protects against cardiac hypertrophy by inhibiting IIS, as *Sirt6* KO hearts showed elevated expression of proteins involved in this pathway. Furthermore, pharmacological inhibition of IGF-1 signaling was able to protect *Sirt6* KO mice from development of cardiac hypertrophy (Sundaresan et al., 2012). Conversely, SIRT6 overexpression was able to decrease the expression of these proteins *in vivo*.

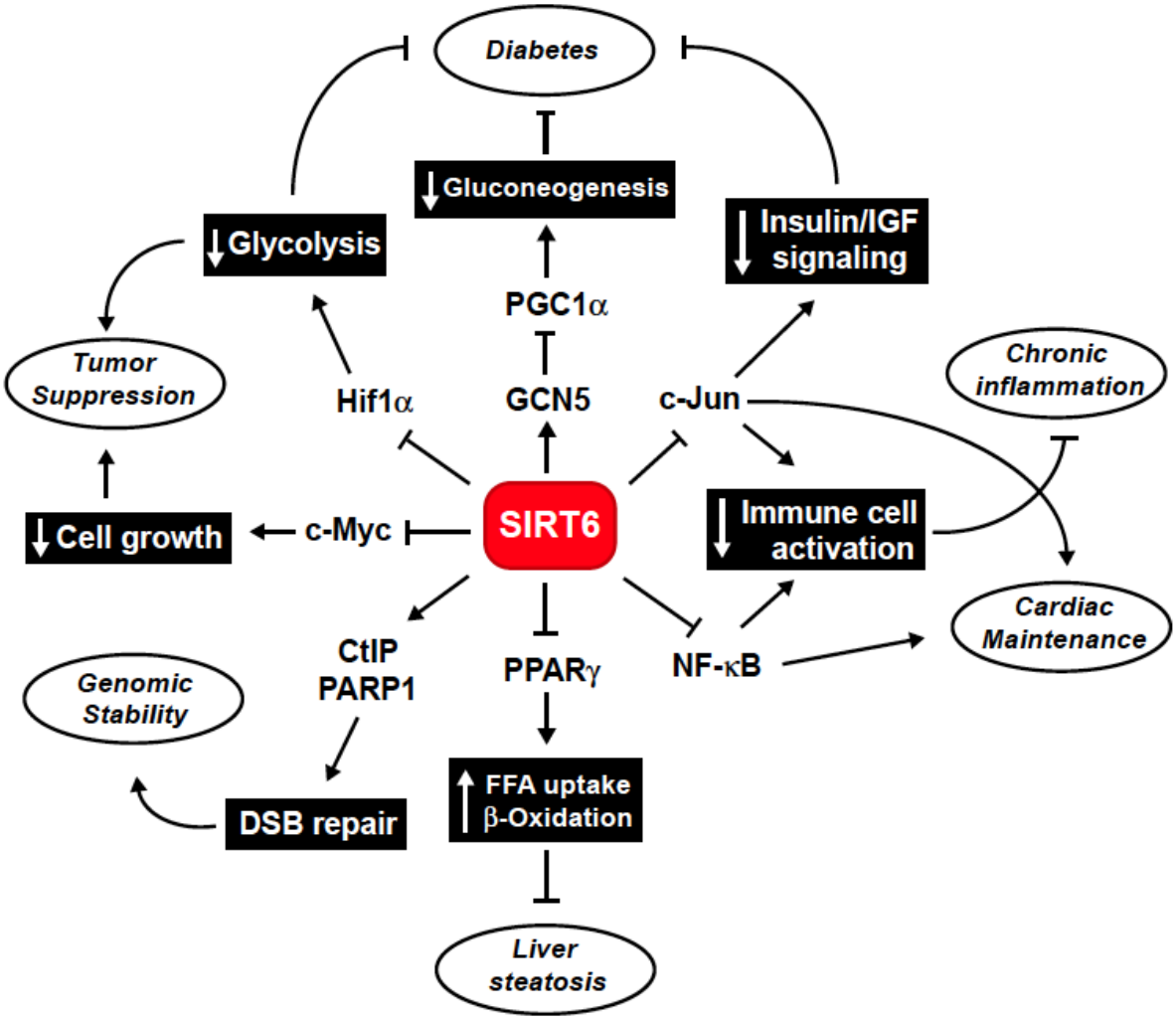

Figure 1.7: Schematic overview of SIRT6 functions

Through its deacetylase and mono-ADP-ribosyltransferase activities, SIRT6 affects activities of transcription factors and other proteins, causing alterations in key cellular processes (black boxes). Through these activities, SIRT6 suppresses multiple metabolic and age-associated pathologies (ovals).

Likewise, both mouse and human hypertrophic hearts showed increased phosphorylated AKT and IGFR expression in comparison to controls, indicative of hyperactivity of the IIS pathway. Indeed, suppression of IIS in *Drosophila* can prevent the age-associated decline in cardiac performance. However, the role of IIS in cardiac health may be at odds with this mechanism, as previous studies have reported that

age-dependent heart failure is associated with low serum IGF-1 levels in elderly with no history of heart disease (Dai et al., 2012), and treatment of cardiomyocytes with a locally-produced IGF-1 isoform can protect these cells from hypertrophy in a SIRT1 dependent manner (Vinciguerra et al., 2010). Therefore, the hypertrophy observed in *Sirt6* KO mice might not mimic age-related cardiac hypertrophy, and possibly other age-associated changes in elderly hearts could contribute to the opposing effects of IIS on cardiac health. Conversely, this discrepancy could be explained by a bimodal effect of IIS on heart health in which both inactive and excessive IIS are harmful and an intermediate level would be desirable for optimal cardiac health.

SIRT6 prolongs mammalian lifespan

Interest in the sirtuin protein family in the context of the biology of aging began with the observation that SIR2 overexpression in budding yeast extends longevity in this organism (Kaeberlein et al., 1999). Therefore, the finding that SIRT6 overexpression increases median and maximal lifespan in male (but not in female mice; C57BL6/J and BALB/cOlaHsd mixed background) represents an extremely significant milestone in sirtuin biology (Kanfi et al., 2012). The mechanisms underlying this effect are not entirely clear. Sahin and colleagues observed an age-dependent increase in methylation of *Sirt6* promoter, meaning that *Sirt6* expression decreases with age (Sahin et al., 2014). Lower IGF-1 levels are observed in male SIRT6 overexpressors; genetic reduction of IIS is associated with increased lifespan in mice as well as invertebrates (Holzenberger et al., 2003; Kenyon, 2010). However, this effect is typically more pronounced in female animals, whereas the impact of SIRT6

overexpression on lifespan is seen in male mice only. While the gender-specific effect on SIRT6-mediated lifespan could be mouse strain specific, it is likely that other functions of SIRT6 may be relevant for its pro-longevity role. A higher incidence of spontaneous tumors is observed in male mice than in females (Kanfi et al., 2012); thus, a tumor suppressor role for SIRT6 might explain why lifespan extension is only observed in male SIRT6-overexpressors (Lombard and Miller, 2012).

Other roles of SIRT6 may also be relevant for its pro-longevity effects. The roles of SIRT6 in DNA repair, maintenance of genomic integrity and epigenetic silencing could contribute to increased longevity of SIRT6-overexpressing male mice. As described above, through its histone deacetylase activity, SIRT6 impacts activities of HIF-1α and NF-κB. Both these factors have been implicated in regulating aging. HIF-1α appears to play a role in longevity; however the data on this topic are somewhat controversial. Deletion of HIF-1α can extend lifespan in *C. elegans* by inhibiting IIS (Zhang et al., 2009). However, others have reported that overexpression of HIF-1α causes lifespan extension, possible by reducing mitochondrial respiration and thus reactive oxygen species (ROS) production, and/or by acting as a stress response factor (Mehta et al., 2009). Hence, both deletion and overexpression of HIF-1α may have beneficial effects depending on context, and it is possible that increased levels of SIRT6 could cause lifespan extension by inhibiting HIF-1α activity. Moreover, pharmacological inhibition of NF-κB can extend lifespan in both male and female *Drosophila* (Moskalev and Shaposhnikov, 2011). NF-κB activity increases with age, promoting increased tissue inflammation (Baker et al., 2011), and blocking the age-associated increase in NF-κB

levels in the skin of aged mice reverts the gene expression profile to that seen in young animals (Adler et al., 2007). In support of this, suppression of NF-κB activity in the hypothalamus extends mouse median and maximal lifespan (Zhang et al., 2013b). Therefore it is possible that SIRT6 overexpression might attenuate age-associated NF-κB mediated inflammation, helping to preserve tissue function.

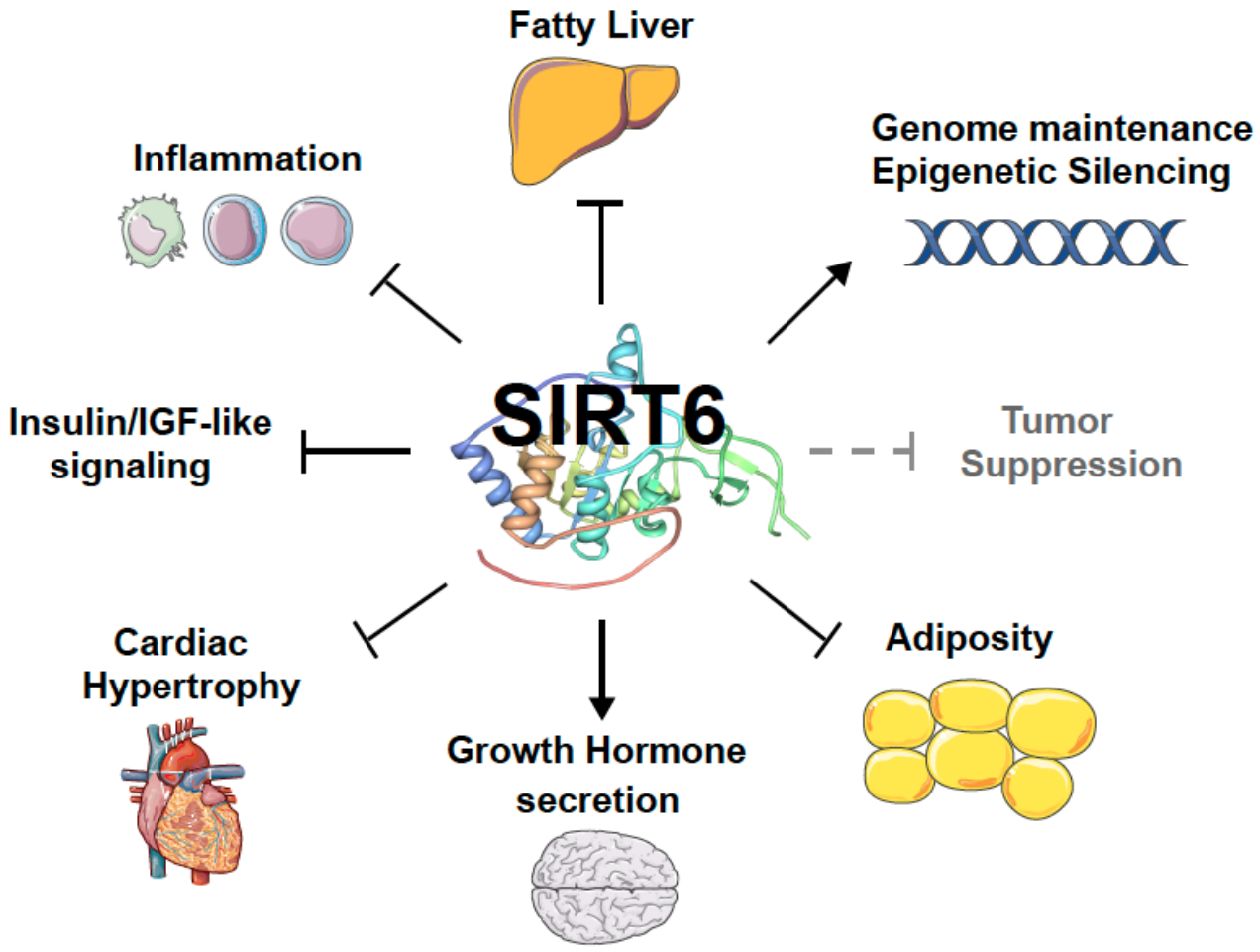

Figure 1.8: Implications of SIRT6 in diseases

SIRT6 improves overall healthspan by impacting diverse physiological processes. The function of SIRT6 as a tumor suppressor protein is the focus of my thesis work (grey). SIRT6 crystal structure was obtained from RCSB Protein Data Bank (Pan et al., 2011). Figure was produced using images from Servier Medical Art (www.servier.com).

Finally, SIRT6 has been implicated in stress responses, which are essential for cellular survival. Mechanistically, SIRT6 translocates to the cytoplasm where it promotes the dephosphorylation of G3BP (Ras GTPase-activating protein-binding protein) and thereby influences stress granule formation and enhances cell viability (Jedrusik-Bode et al., 2013). Overall, SIRT6 is implicated in many processes that could contribute to the longevity phenotype seen in male SIRT6 overexpressing mice.

Rationale

It has been widely accepted that numerous cellular processes need to be disrupted in order for a normal cell to become cancerous. Hanahan and Weinberg originally divided up these processes into the six hallmarks of cancer: continued proliferation, resistance to cell death, avoiding growth suppression, initiating angiogenesis, allowing immortalization, and activating invasion and metastasis (Hanahan and Weinberg, 2000). Based on recent advancements in the field of tumorigenesis, Hanahan and Weinberg revisited their original cancer hallmarks and have added two emerging and two enabling traits: metabolic reprogramming, immune avoidance, tumor-promoting inflammation, and genome instability and mutation (Figure 1.9) (Hanahan and Weinberg, 2011).

Based on these cancer hallmarks and the biological processes regulated by SIRT6, we postulated that SIRT6 has protective properties against tumor formation. The acquisition of the above mentioned hallmarks is in large part dependent on the

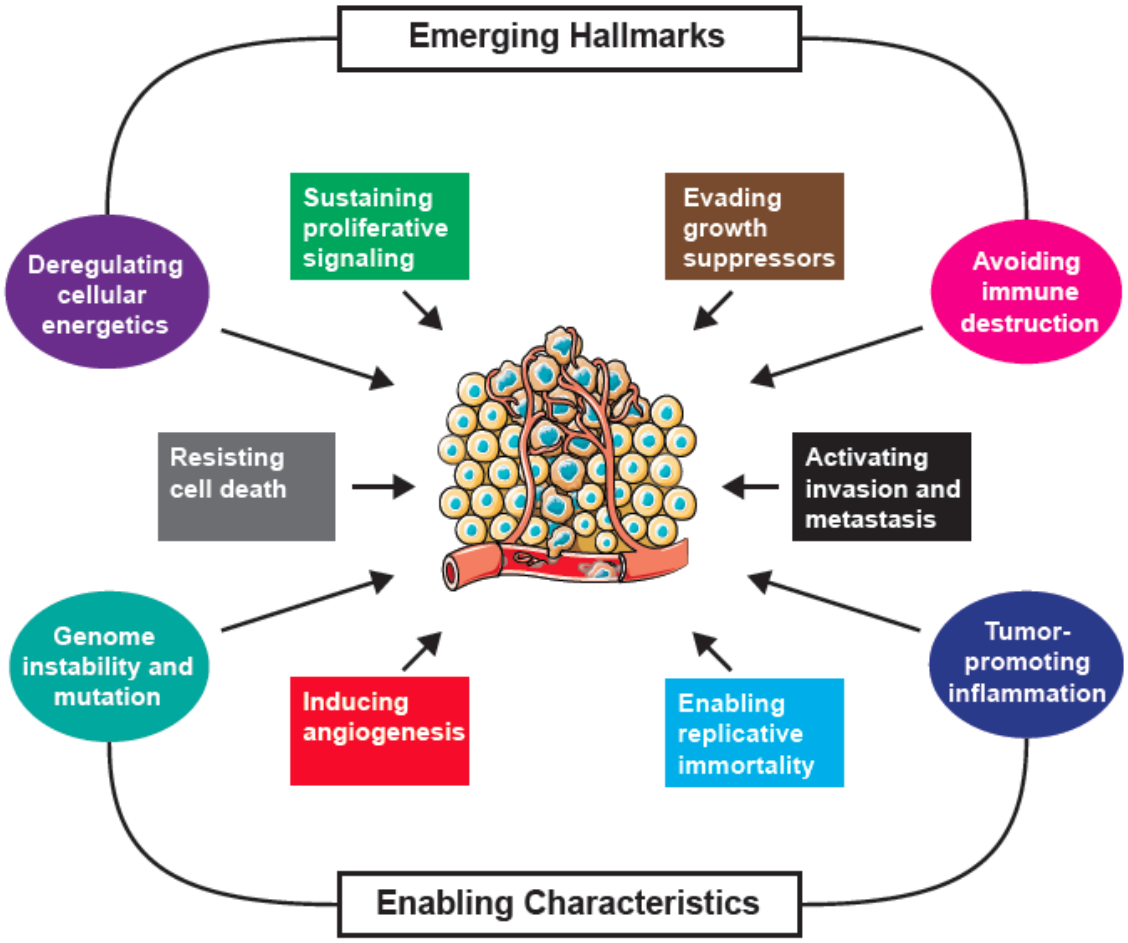

Figure 1.9: The revised hallmarks of cancer

The newly described hallmarks of cancer as described by Hanahan and Weinberg: Resistance to cell death, deregulating cellular energetics, sustaining proliferative signaling, evading growth suppressors, avoiding immune destruction, enabling replicative immortality, tumor promoting inflammation, activating invasion and metastasis, inducing angiogenesis, and genome instability and mutation. Figure was adapted from (Hanahan and Weinberg, 2011)

accumulation of alterations in the genome (= enabling hallmark). As SIRT6 protects against DNA damage by interacting with the double strand DNA repair proteins CtIP and PARP1 (Kaidi et al., 2010; Mao et al., 2012), it is possible that the ablation of SIRT6 can lead to genetic mutations and consequently the acquisition of tumorigenic

properties. Likewise, SIRT6 protects against telomere dysfunction by deacetylating H3K9 and by recruiting WRN to regulate telomere processing during S-phase (Michishita et al., 2008). Patients with a mutation in the *Wrn* gene age prematurely, with cancer and cardiovascular disease being their main causes of death. Furthermore, cancer cells alter their metabolism such that their ATP generation is largely derived from glycolysis. With SIRT6 being an essential regulator of this pathway, SIRT6 deficiency may aid in tumor progression by supporting the preferred form of metabolism in cancer. Therefore, in my thesis work we aimed to elucidate a role for SIRT6 in cancer.

Chapter 2

Identification of novel SIRT6 targets

Abstract

Post-translational modifications of histones drive many important cellular processes such as DNA repair, DNA replication and transcriptional regulation. The latter is generally activated by histone hyperacetylation. Therefore, knowing the acetylation state of histones can provide great insight in the activity of downstream signaling pathways. The histone deacetylase SIRT6 deacetylates H3K9 at various promoter regions, resulting in repression of various transcription factors such as NF-κB, HIF-1 and c-JUN. In doing so, SIRT6 regulates many important cellular processes and is implicated in a wide array of pathologic conditions. In this study we aimed to identify additional histone targets for SIRT6 to further our understanding of SIRT6's molecular functions. Here we report that SIRT6 has three additional histone targets: H3K18ac, H3K23ac and H3K56ac. Misregulation of each of these residues has been shown to impact organismal health.

Introduction

Our genetic information is tightly packaged into chromatin, a complex structure composed of DNA, proteins and RNA. The main functions of chromatin are to regulate gene expression, protect against DNA damage, mediate DNA replication and compact DNA into a smaller volume. The basic unit of chromatin is the nucleosome, which consists of 146bp wrapped around a histone core complex. This complex is an octamer made up of two copies of each of the four core histones: H2A, H2B, H3 and H4. Histones are small proteins that consist of a globular core structure and N- and C-termini called histone tails. Histones are subjected to many different post-translational modifications (PTMs), such as phosphorylation, ubiquitination, methylation and acetylation. Each of these modifications is controlled by enzymes. For example acetylation of lysine residues is carried out by histone acetyltransferases (HATs), which use acetyl-coenzyme A as a cofactor to catalyze the transfer of an acetyl group to a lysine residue resulting in charge reduction. Deacetylation, on the other hand, is mediated by histone deacetylases (HDACs), which cleave off the acetyl groups from lysine residues. Histone acetylation reduces the affinity between histones and DNA, allowing the chromatin to adopt a more relaxed structure, and permits the binding of transcription factors. Because HDACs counteract this action, deacetylation is generally associated with transcriptional repression. Despite their names, HATs and HDACs can also target non-histone proteins (Kouzarides, 2000; Shahbazian and Grunstein, 2007).

The first identified target for SIRT6 was histone H3 acetylated at Lysine 9 (H3K9ac) (Michishita et al., 2008). The interaction of SIRT6 with the chromatin, and its

subsequent deacetylation of H3K9, generates a hypoacetylated region that is associated with compacted chromatin and gene silencing. SIRT6 binds telomeric regions specifically where it deacetylates H3K9. Hypoacetylated telomeres allow for the binding of WRN, the protein that is mutated in the premature aging disease Werner's Syndrome and that is responsible for proper regulation of telomere ends. In SIRT6 deficient cells, hyperacetylation, and subsequently the absence of WRN, results in telomere dysfunction with an increased risk for end-to-end chromosomal fusions, telomere loss and premature cellular senescence (Michishita et al., 2008). In a similar fashion, a number of transcription factors have been described to interact with SIRT6 at the promoter regions of their target genes. By deacetylating H3K9 at these regions, SIRT6 suppresses transcriptional output and thus regulates a wide range of cellular processes. One such transcription factor is NF-κB, which plays an important role in regulating the inflammatory response, immunity, apoptosis and cellular senescence (Kawahara et al., 2009). SIRT6 deficient cells show apoptotic resistance and cellular senescence due to hyperactivity of NF-κB. Strikingly, reduction of NF-κB activity in *Sirt6* germline knockout mice partially rescues their early lethality (Kawahara et al., 2009). Likewise, SIRT6 inhibits HIF-1 and c-JUN transcriptional output, resulting in hypoglycemia (Zhong et al., 2010), cardiac hypertrophy (Sundaresan et al., 2012), and liver inflammation and fibrosis (Xiao et al., 2012).

In addition to the above-mentioned functions, SIRT6 also plays a role in DNA repair as SIRT6 deficiency leads to chromosomal aberrations (Mostoslavsky et al., 2006). Various studies have indicated that SIRT6 enhances base excision repair (BER) and

DNA double strand break repair (Kaidi et al., 2010; Mao et al., 2012; McCord et al., 2009; Mostoslavsky et al., 2006; Toiber et al., 2013). Two modifications that are rapidly and reversible deacetylated in response to DNA damage are H3K9ac and H3K56ac (Tjeertes et al., 2009). H3K56ac is acetylated by the HATs CBP and p300, and deacetylated by the HDACs SIRT1 and SIRT2 (Das et al., 2009; Yuan et al., 2009). Acetylation of H3K56 is critical for chromatin assembly after DNA replication, chromatin disassembly during gene transcription and cell survival (Chen et al., 2008; Li et al., 2008; Williams et al., 2008). Furthermore, proper H3K56ac regulation is crucial for genomic stability and accurate DNA damage response as mutated H3K56 results in spontaneous DNA breaks (Yuan et al., 2009). Due to the importance of H3K56ac in maintaining genomic integrity, a feature shared by SIRT6, we investigated if SIRT6, in addition to H3K9ac, deacetylates H3K56ac or any other histone H3 residues. The subsequent studies were done in collaboration with Dr. B. Yang.

Materials and Methods

Site-directed mutagenesis

The H133Y mutation was introduced into mouse 1xFlag-SIRT6 in pBABE-puro and 3xFlag-SIRT6 in pCMV 7.1 (Sigma) by site-directed mutagenesis using Pfu turbo (Stratagene) per the manufacturer's instructions using the following mutagenesis oligonucleotides: Forward: 5' TGGCAGAGCTGTACGGAAACATGTTTGTAGAGGA 3', Reverse: 5' TCCTCTACAAACATGTTTCCGTACAGCTCTGCCA 3'.

Cells and mice

In our studies we used mouse embryonic fibroblasts (MEFs), isolated from C57/BL6 WT and *Sirt6* KO embryos (E13.5) according to standard conditions (Mostoslavsky et al., 2006). MEFs were grown in DMEM supplemented with 15% fetal bovine serum, 1% L-Glutamine, 1% pen/strep, 1% sodium pyruvate, 1% non-essential amino acids, 2% HEPES and 115 μM beta-mercaptoethanol. MEFs were grown at low oxygen conditions, split 1:3 with each passage and maintained in culture up to passage 8. SIRT6-deficient ES cells and mice were as previously described (Mostoslavsky et al., 2006). For rescue experiments, a SIRT6-deficient MEF line immortalized by serial passage was incubated with retroviral supernatants for 48 hours in the presence of 4 μg/ml polybrene, after which they were selected in media containing 2.5 μg/ml puromycin for 72 hours.

Mass spectrometry analysis

Mass spectrometry was used to identify acetylation sites on histone H3 after incubation with p300 acetyltransferase +/- SIRT6 and was performed in collaboration with Dr. G Cavey. Non-acetylated lysines of histone H3 were propionylated prior to trypsin digestion to restrict enzyme digest to arginine amino acids. Histone H3 has several acetylated and non-acetylated lysine amino acids in close proximity. Without restricting trypsin digestion to arginine amino acids trypsin cleavage at non-acetylated lysines would result in very short peptides or single acetylated lysine that would not bind sufficiently to C18 reverse phase columns during LC-MS analysis and subsequently be missed in the analysis (Garcia et al., 2007). Data was collected with a Waters quadrupole time-of-flight mass spectrometer in data independent MS^E mode that collects accurate mass data for all detectable peptides and also generates fragment ions that are diagnostic of acetylated peptides (Geromanos et al., 2009; Niggeweg et al., 2006).

Immunoblot analysis

For analysis of histone acetylation in cell lines and in mouse tissues, 50 μg of total protein was fractionated on 4-20% gradient gels (Bio-Rad), transferred to PVDF membranes, and probed with the following antibodies in TBST/5% milk at the dilutions indicated: rabbit anti-H3K56ac (Epitomics, catalog number 2134-1), 1:1000; rabbit anti-H3K9ac (Abcam), 1:1000; rabbit anti-H3K18ac (Abcam), 1:2000; rabbit anti-H3K23ac (Millipore), 1:2000; rabbit anti-H3 (Abcam), 1:20,000; rabbit anti-mouse SIRT6 (Novus), 1:1000.

Immunocytochemistry

For H3K56ac analysis, MEFs were grown on multi-chamber slides (Fisher Scientific) and fixed in 100% methanol at -20°C for 10 minutes. All subsequent steps, unless indicated, took place at room temperature. Slides were rehydrated in PBS for 20 minutes and subsequently washed for 20 minutes in PBS/0.1% Tween-20 (PBST). Slides were blocked in PBS/1% BSA/10% goat serum for 1 hour, and then incubated with primary antibody (1:500; Abcam) in blocking buffer for 1 hour, followed by 3 washes (10 minutes each) in PBST. Slides were then incubated with Alexa Fluor-conjugated goat-anti-rabbit (Invitrogen) (1:500) for 1 hour in blocking buffer, washed as above, and mounted in Vectashield with DAPI (Vector Labs). For H3K18ac and H3K23ac staining, MEFs were grown on multi-chamber slides, fixed in 4% PFA for 10 minutes, permeabilized in 100% MeOH for 10 minutes at -20°C and rehydrated in PBS for an additional 10 minutes. Slides were blocked for 30 minutes in 5% goat serum in PBS containing 0.3% triton and subsequently incubated with primary antibody (1:100; H3K18ac, abcam; H3K23ac, Millipore) in blocking buffer 1 hour, followed by 3 washes in PBST. Slides were then incubated with secondary antibody and mounted as described above. Images were captured on an Olympus BX-51 scope with an Olympus DP-70 high-resolution digital camera (University of Michigan Microscopy & Image Analysis lab); images shown were taken at equal exposure times. For quantification, two random fields on each of 3 separate slides were imaged (~100 cells/field) per cell line.

Immunohistochemistry

Immunohistochemistry (IHC) for H3K18ac was performed on brain tissue of WT and *Sirt6* KO mice by the University of Michigan histology core. In brief, slides were deparaffinized and rehydrated through a series of xylene and alcohol washes. Antigen retrieval was performed by heating the slides for 10 minutes in citrate buffer (10mM Citric Acid, 0.05% Tween 20, pH 6.0), followed by a 10 minutes cool down at room temperature. Endogenous peroxide was blocked by incubation in 3% hydrogen peroxide (H_2O_2) for 10 minutes. Additional blocking was performed by incubating the slides in 5% normal goat serum in PBS for one hour. Tissues were incubated with rabbit anti-H3K18ac antibody (Abcam) overnight at 4°C. Signal was visualized using 3,3'-diaminobenzidine (DAB; Vector Laboratories) and slides were mounted using permanent mounting medium (Vector Laboratories). Slides were imaged with an Olympus BX-51 scope with an Olympus DP-70 high-resolution digital camera (University of Michigan Microscopy & Image Analysis lab).

***In vitro* deacetylation**

3xFlag-tagged SIRT6 and 3xFlag-tagged SIRT6-H133Y were generated in 293T cells, and purified in 500mM NaCl using anti-FLAG M2 agarose (Sigma). Histone H3 was acetylated *in vitro* by incubating 10 µg of recombinant histone H3 (New England Biolabs) for 2 hours at 30°C with 150 ng FLAG-tagged p300 acetyltransferase (kindly provided by Yali Dou, University of Michigan) in HAT buffer (50 mM Tris pH 8.0, 0.1 mM EDTA, 1 mM DTT and 10% glycerol). Subsequently, p300 was isolated using 5 ml

of M2-agarose beads (Sigma) for 30 minutes. Histone H3 was deacetylated by incubating acetylated histone H3 with purified SIRT6 or SIRT6-H133Y (1:1 ratio) in HDAC buffer (10 mM Tris pH 8.0, 150 mM NaCl and 0.5 mM NAD^+) for 2 hours at 30^oC. Deacetylation of histone H3K9 (Abcam), H3K18 (Abcam), H3K23 (Millipore) and H3K56 (Millipore) was monitored by immunoblot using site-specific antibodies.

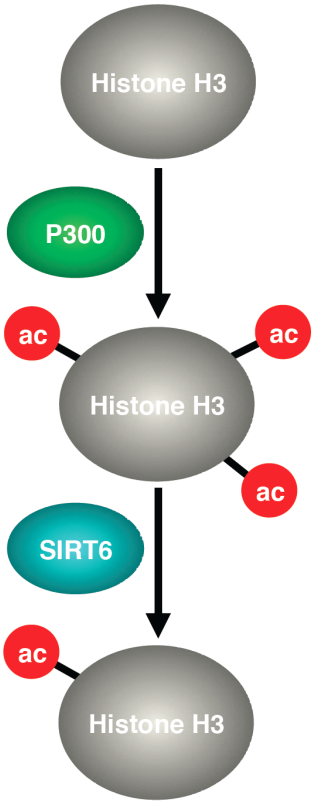

Figure 2.1: Illustration of *in vitro* deacetylation assay

Recombinant histone H3 protein was acetylated by the acetyltransferase p300 and subsequently deacetylated with SIRT6 to identify SIRT6 specific targets on H3.

Results

SIRT6 deacetylates Histone H3 Lysine 56.

To test a potential role for SIRT6 in deacetylating H3K56, levels of this modification were assessed in SIRT6-deficient MEFs and littermate controls. Levels of H3K56ac were dramatically increased in *Sirt6* KO cells (Figure 2.2A, left panel). H3K56ac levels were also elevated in two independent SIRT6-deficient ES cell lines compared with a WT control (Figure 2.2A, middle panel). Reintroduction of wild-type SIRT6, but not a catalytically inactive SIRT6 allele (SIRT6HY), rescued H3K56 hyperacetylation in MEFs (Figure 2.2A, right panel), indicating that H3K56 hyperacetylation in these cells is a direct consequence of loss of SIRT6 function. Interestingly, overall H3K9ac levels were unaltered in SIRT6-deficient MEFs (Figure 2.2A, left panel), although they were modestly elevated in ES cells lacking SIRT6 (Figure 2.2A, middle panel). Thus, SIRT6 plays a critical role in deacetylating H3K56 in MEFs and ES cells; SIRT6 regulates global H3K9 acetylation levels in ES cells but is dispensable for this function in MEFs. To assess H3K56ac levels on a single cell level, immunofluorescence analysis was performed on SIRT6-deficient MEFs and littermate controls. H3K56ac staining was markedly brighter in SIRT6-deficient MEFs, and also present in a much greater fraction of cells (Figure 2.2B, left panel). H3K56ac was detectable in 96.6% of SIRT6-deficient cells, whereas H3K56ac was only detectable in 21.5% of control MEFs. Thus SIRT6 deficiency leads to both higher levels of H3K56ac on a per-cell basis, as well as an increased fraction of cells with detectable acetylated H3K56.

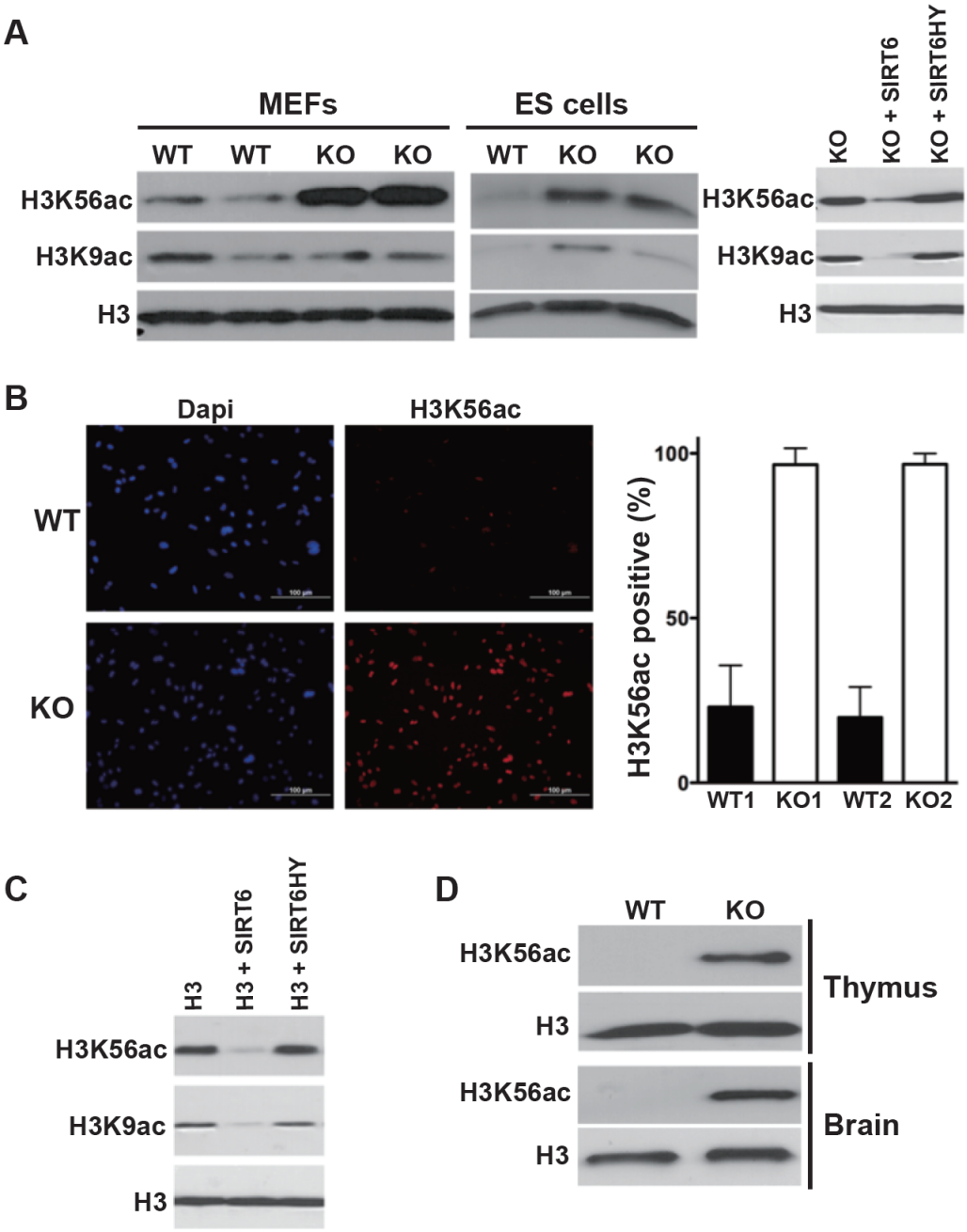

Figure 2.2: SIRT6 deacetylates Histone H3 Lysine 56

(A) H3K56 is hyperacetylated in the absence of SIRT6 in both MEFs (left) and ES cells (middle). Reconstitution of a SIRT6 deficient immortalized MEF cell line with SIRT6, but not the catalytic inactive mutant, reduces H3K56ac levels (right). (B) Immunofluorescence analysis for H3K56Ac in SIRT6-deficient MEFs and littermate controls. (C) Recombinant SIRT6, but not catalytic null SIRT6, deacetylates H3K56 *in vitro*. (D) H3K56 is hyperacetylated in thymus and brain tissue from SIRT6-null mice compared to littermate controls. Figures A, C and D were generated by Dr. B. Yang (Yang et al., 2009).

To rule out the possibility that hyperacetylation of H3K56 in SIRT6-deficient cells might be an indirect result of genomic instability associated with SIRT6 deficiency, the ability of SIRT6 to deacetylate this site was assessed. Acetylated H3 was incubated with catalytically active SIRT6 or the SIRT6 catalytic mutant SIRT6-H133Y. WT SIRT6 robustly deacetylated both H3K56ac and H3K9ac, whereas this activity was completely abrogated in the mutant (Figure 2.2C). We conclude that SIRT6 directly deacetylates H3K56 to regulate global H3K56Ac levels.

To test the role of SIRT6 in deacetylating H3K56ac *in vivo*, H3K56 acetylation was assessed in tissues from SIRT6-deficient mice and littermate controls. We focused on thymus and brain, tissues where SIRT6 is highly expressed (Mostoslavsky et al., 2006). SIRT6 deficiency was associated with dramatically higher levels of H3K56ac in both tissues (Figure 2.2D). Thus SIRT6 is a critical H3K56ac deacetylase *in vivo*.

SIRT6 targets Histone H3 Lysine 18 and 23.

The identification of SIRT6 as a potent deacetylase of H3K56, prompted us to test if SIRT6 had additional histone H3 targets. Therefore, we performed an *in vitro* deacetylation assay in which we incubated recombinant histone H3, acetylated by the acetyltransferase p300, with SIRT6. Following this deacetylation reaction we looked for lysine residues that were no longer acetylated after SIRT6 treatment using mass spectrometry analysis (in collaboration with Dr. Cavey, van Andel Institute). When comparing histone H3, H3ac, and H3ac treated with SIRT6, we found a peak that appeared after acetylation of H3 but disappeared after SIRT6 treatment (Figure 2.3A, purple star).

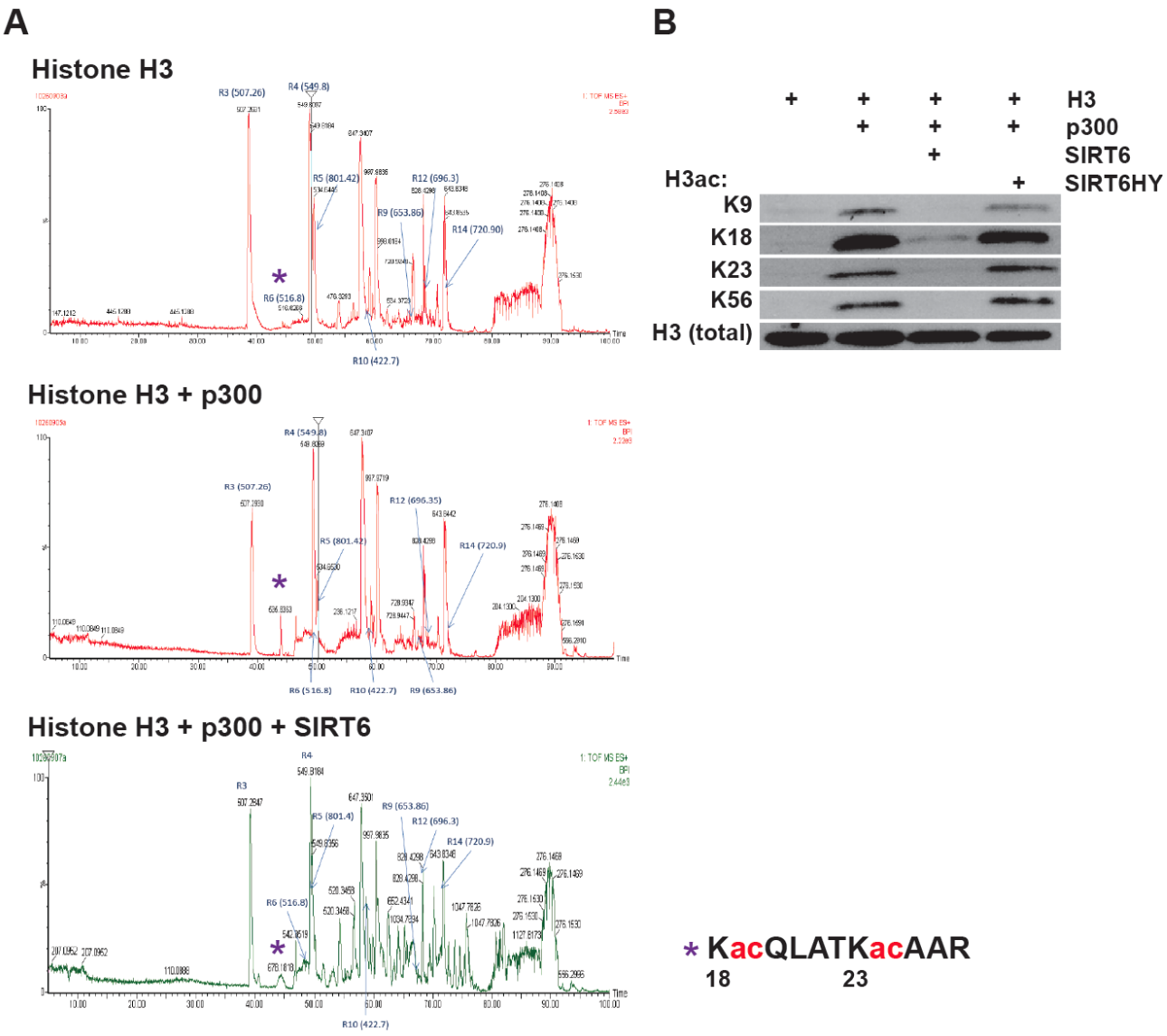

Figure 2.3: *In vitro* deacetylation of Histone H3 residues by SIRT6

(A) MS/MS spectrum of H3 peptide KQLATKAAR acetylated at K18 and K23. The 1070.62 M+H mass is consistent with two acetylated lysine amino acids (purple star). (B) After acetylation of H3 with the acetyltransferase p300, H3 is deacetylated by SIRT6, but not the catalytic mutant SIRT6HY, at the indicated lysine residues. Figure A was generated by Dr. G. Cavey, Figure B was generated by Dr. B. Yang.

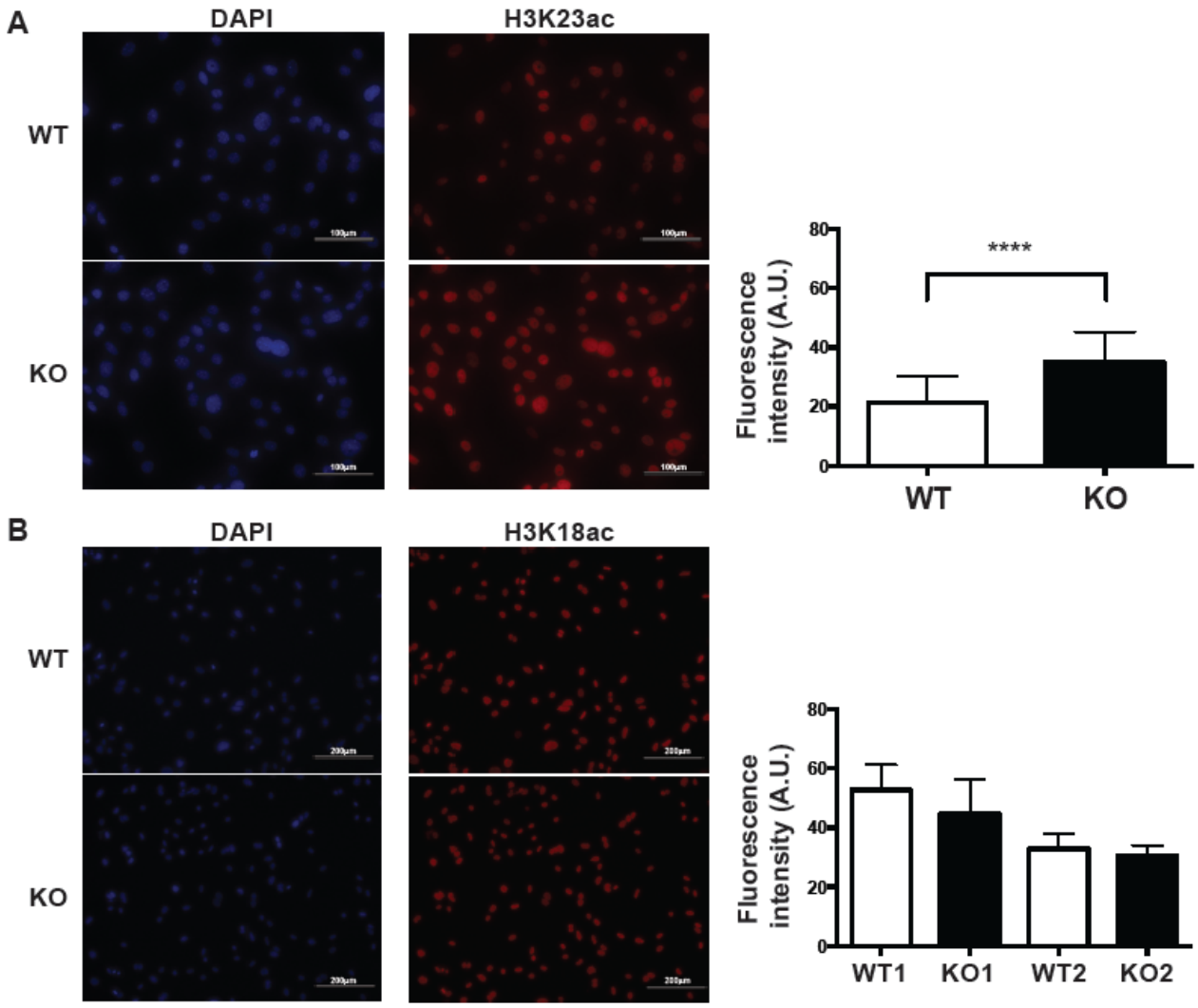

Figure 2.4: Immunocytochemistry of histone marks in Sirt6 MEFs

Immunofluorescence staining of *Sirt6* WT and *Sirt6* KO MEFs for (A) H3K23ac and (B) H3K18ac. Fluorescence intensity was measured with ImageJ and represented in bar graph.

This peak corresponds with a protein sequence containing the lysine residues K18 and K23. To test if either histone H3 residues were targets for SIRT6, we repeated the *in vitro* deacetylation and ran the reactions on a western blot. When probing with antibodies specific for either modification, we confirmed that, under *in vitro* conditions,

SIRT6, but not the catalytic inactive mutant SIRT6HY, was able to deacetylate H3K18ac and H3K23ac (Figure 2.3B). As positive controls for the deacetylation reaction we confirmed the deacetylation of the previously described targets H3K9ac and H3K56ac.

Next, we investigated if SIRT6 was able to deacetylate H3K18 and H3K23 in living cells. Thus we isolated MEFs from 13.5 days old embryos from our *Sirt6* germline knockout strain and performed immunocytochemistry for both histone modifications. As predicted, we observed an increase in fluorescence intensity for H3K23ac in the absence of SIRT6 (Figure 2.4A). However, H3K18ac does not appear to be different between WT and Sirt6KO MEFs (Figure 2.4B). Even more so, it appears SIRT6 deficient cells show a slight decline in H3K18ac levels compared to control cells. Since histone modifications can be cell type specific, we performed IHC on *Sirt6* WT and KO brain sections for H3K18ac, and detected a marked increase in this modification with SIRT6 ablation (Figure 2.5). To strengthen this finding, we tested the levels of H3K18/23ac in various tissues derived from germline Sirt6 KO and littermate control mice by western blot analysis, in conjunction with the previously described histone H3 targets of SIRT6, H3K9 and H3K56. In both brain and thymus, two high Sirt6 expressing organs, H3K18 and H3K23 acetylation levels appear to be elevated in the absence of SIRT6 (Figure 2.6). Although less apparent, this finding holds up for H3K23ac in heart, kidney and spleen. H3K18ac, on the other hand, is mildly elevated in Sirt6 KO hearts, but does not appear to be different in kidney or spleen tissues (Figure 2.6). As for the previously described SIRT6 histone targets, global H3K56ac are elevated in each tissue analyzed, while H3K9ac is only different in thymus and

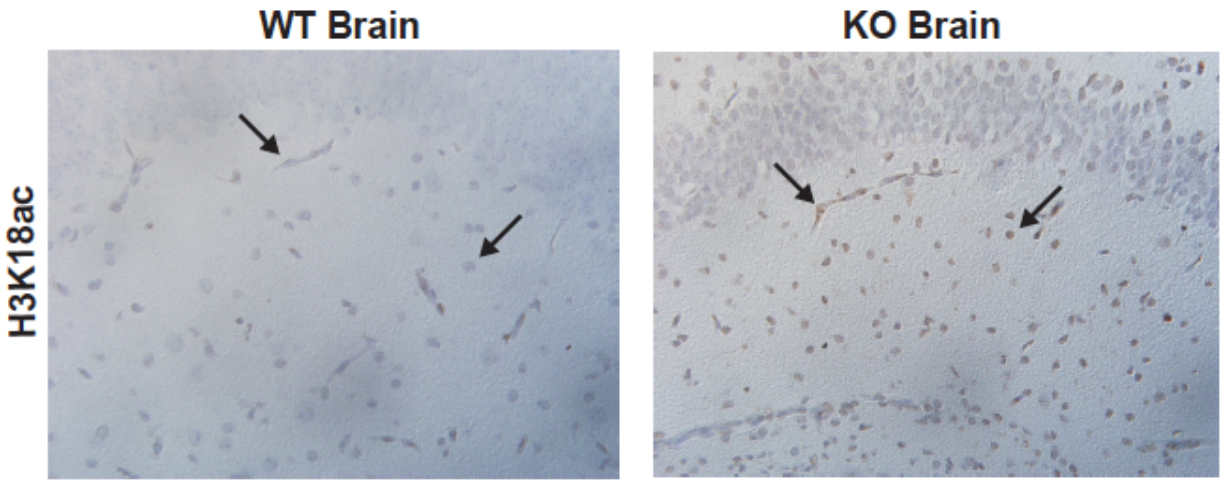

Figure 2.5: SIRT6 deacetylates H3K18ac in the brain

Brain sections of germline *Sirt6* KO and control mice were stained for H3K18ac. Arrows point at representative neuronal nuclei in WT and KO tissue indicating higher H3K18ac staining in *Sirt6* KO brains.

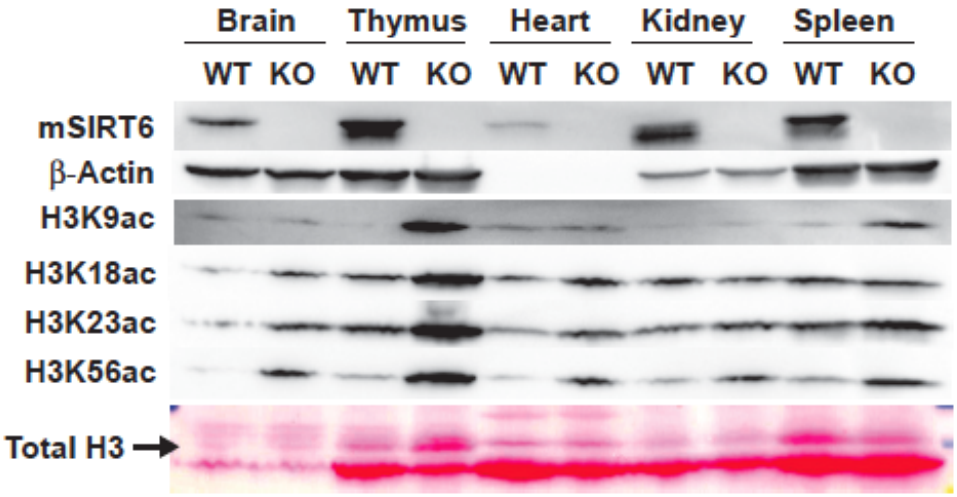

Figure 2.6: SIRT6 deacetylates histone H3 *in vivo*

50 µg of tissue extract was loaded per lane and probed for the indicated proteins and histone marks. Total H3 is visible (arrow) on ponceau staining of immunoblot. Figure was generated in collaboration with Mary Skinner.

spleen. Overall, these findings suggest that SIRT6 globally deacetylates H3K23, similar to H3K56, while overall H3K18 deacetylation by SIRT6 appears to be more tissue specific as seen for H3K9ac.

Discussion

In our study we identified three novel targets for SIRT6 *in vivo*: H3K18ac, H3K23ac and H3K56ac. H3K56 acetylation levels are normally very low in mammalian cells, but rise dramatically in the context of SIRT6 deficiency (Yang et al., 2009). Improper regulation of H3K56 acetylation in mammalian cells leads to impaired cell cycle progression, sensitivity to genotoxins and spontaneous DNA damage (Michishita et al., 2009; Yang et al., 2009; Yuan et al., 2009), phenotypes reminiscent of SIRT6 deficiency. The exact mechanism through which deacetylation of H3K56ac by SIRT6 might repress DNA damage accumulation is not fully understood. A recent study has demonstrated that, in the event of a double strand break, SIRT6 is one of the first factors recruited to the damaged locus where it deacetylates H3K56 and consequently recruits the chromatin remodeler SNF2H and other DNA repair factors (Toiber et al., 2013). It has been hypothesized that H3K56 acetylation is asymmetric around the replication fork during S-phase: acetylated behind the fork on newly synthesized DNA, and non-acetylated ahead of the replication fork. Thus, H3K56 acetylation may allow newly-replicated DNA to be distinguished from unreplicated DNA for proper targeting of HR during S-phase (Munoz-Galvan et al., 2013). H3K56 acetylation is also required for chromatin reassembly following DSB repair (Chen et al., 2008) and for recovery from post-repair

checkpoint arrest following UV irradiation (Battu et al., 2011). In SIRT6-deficient cells, which show dramatically elevated levels of H3K56ac, it is possible that any or all of these processes may be perturbed. It should be noted however that SIRT6-deficient cells are not hypersensitive to UV, despite their dramatic H3K56 hyperacetylation (Mostoslavsky et al., 2006).

The global deacetylation of H3K18 and H3K23, like H3K9, appears to show more tissue specificity, which would imply that these modifications are involved in transcriptional regulation of genes whose expression is dependent on cell type. Conversely, SIRT6 mediated regulation of these histone residues could be restricted to specific genomic regions, and thus we would not observe any global changes in acetylation in the absence of SIRT6. Both modifications are markers of active gene expression. Understanding the regulation of these histone modifications is clinically of great relevance as both H3K18ac and H3K23ac have been implicated in various disease states. High levels of H3K23ac have been reported in advanced diabetic kidney disease (Sayyed et al., 2010). Low levels of H3K18ac are associated with poor survival in pancreatic adenocarcinoma (Manuyakorn et al., 2010), and a higher risk of prostate, lung and kidney cancer recurrence (Seligson et al., 2009). However, thyroid tumors appeared to have higher levels of H3K18ac in comparison to normal tissue (Puppin et al., 2011). A previous study has identified H3K18ac as a target of SIRT7. SIRT7 does not alter global acetylation levels of H3K18, instead it is recruited by the cancer-associated transcription factor ELK4 to specific promoter sites where it represses downstream transcription. Through H3K18 deacetylation, high levels of

SIRT7 in prostate cancer cells stimulate anchorage-independent growth and cellular proliferation, and reduce contact inhibition and cell death (Barber et al., 2012). However, SIRT7 mediated H3K18 deacetylation is most likely highly region specific since SIRT7 promotes rRNA expression, which is under the influence of the MYC transcription factor, while on the other hand MYC, like the oncogenes Ras and Braf, binding to its target genes has been described to enhance H3K18ac levels (Martinato et al., 2008; Puppin et al., 2011). In addition to SIRT6 and SIRT7, H3K18 is also deacetylated by SIRT2. In the event of an infection with bacterium Listeria monocytogenes, SIRT2 facilitates the infection by translocating to the nucleus where it deacetylates H3K18. This deacetylation results in gene repression, of which a subset are involved in the immune response. Through this mechanism, SIRT2 supports the bacterium in taking over cellular control of the host cell (Eskandarian et al., 2013). Our finding that SIRT6 deacetylates histone H3 K18, K23 and K56 is of great importance in understanding the cellular functions of SIRT6. SIRT6 suppresses the activity of multiple transcription factors by deacetylating H3K9ac (Kawahara et al., 2009; Sundaresan et al., 2012; Xiao et al., 2012; Zhong et al., 2010). With the identification of three additional histone targets for SIRT6, further studies will clarify whether SIRT6 deacetylates these novel targets at the same genomic regions as H3K9 or if this indicates that more chromatin binding sites for SIRT6 are yet to be identified. As previously described, SIRT6 plays a role in overall healthspan, thus understanding the molecular functions of SIRT6 is essential when considering its therapeutic potential.

Future directions

In addition to the known SIRT6 target H3K9ac, we have identified three histone H3 residues that are targeted by SIRT6: H3K18ac, H3K23ac and H3K56ac. By deacetyling H3K9ac, SIRT6 silences HIF-1 mediated transcription of glycolytic genes (Zhong et al., 2010). Furthermore, our recent work (see chapter 3) has identified SIRT6 as a transcriptional inhibitor of ribosomal gene expression by targeting H3K56ac at their promoter regions (Sebastian et al., 2012). Thus it would be of interest to test H3K18 and H3K23 acetylation status at these promoter sites. In a pilot experiment we performed ChIP for these four acetylated histone H3 lysine residues followed by qPCR for glycolytic and ribosomal genes (Figure 2.7). Overall, H3K23 and H3K56 acetylation levels were elevated at all four analyzed promoter regions, while surprisingly we did not observe a change in H3K9ac. Furthermore, H3K18ac levels appeared to be lower for each of the sites tested (Figure 2.7). These results suggest that SIRT6 mainly targets K23 and K56 on histone H3 at the tested promoter regions. Our previous results indicated an apparent global change of these residues in the absence of SIRT6 across all tissues analyzed, while both H3K9ac and H3K18ac appeared to be more tissue specific (Figure 2.6). The lack of SIRT6-dependent change in acetylation of K9 and K18 might thus reflect tissue specificity. Alternatively, SIRT6 could target H3K9 and H3K18 at still unknown regions, which should be clarified through further studies.

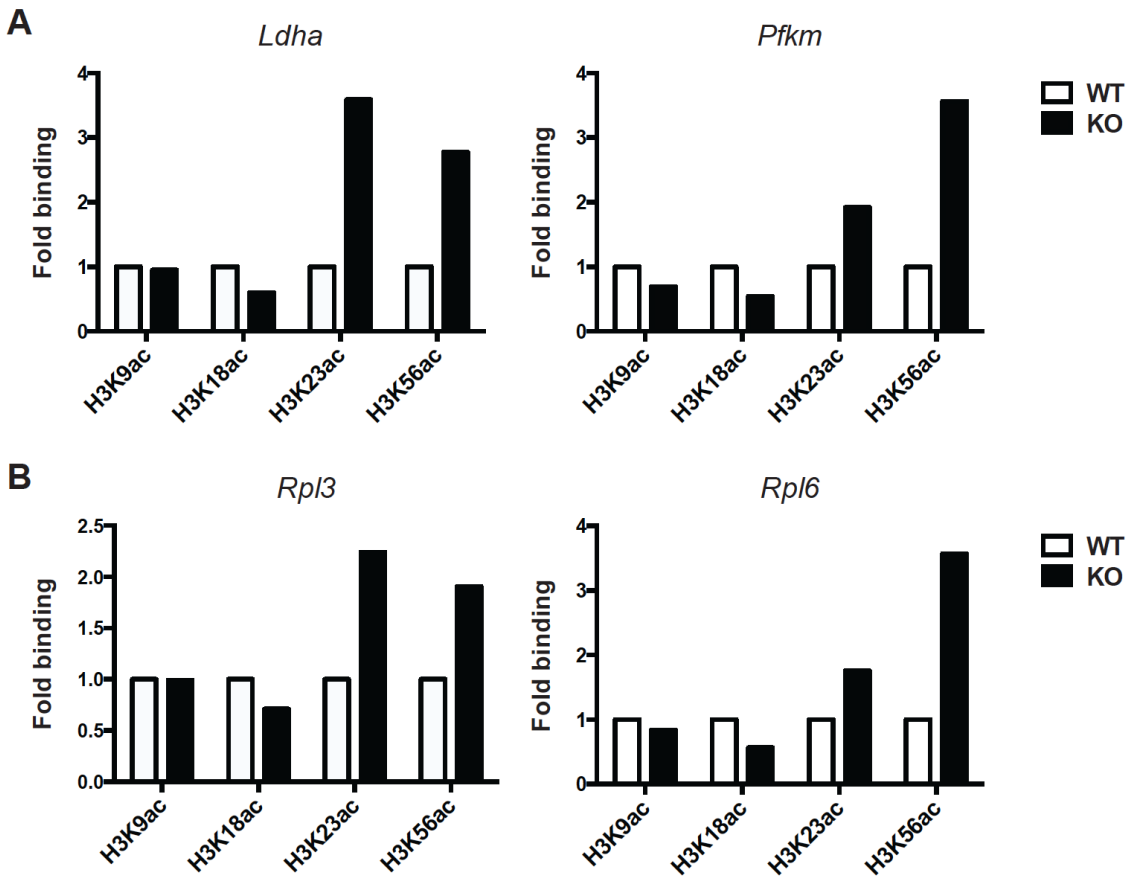

Figure 2.7: Histone H3 acetylation changes at SIRT6 target promoter regions

ChIP for indicated acetylated histone H3 residues at promoters of (A) glycolytic and (B) ribosomal genes WT and *Sirt6* KO MEFs (n=3 technical replicates). Primer sequences (Table 3.1) and methods (chapter 3) are described at indicated locations.

The three newly identified SIRT6 targets have been shown to be implicated in cancer (Barber et al., 2012; Das et al., 2009; Manuyakorn et al., 2010; Puppin et al., 2011; Seligson et al., 2009), diabetic kidney disease (Sayyed et al., 2010) and bacterial infection (Eskandarian et al., 2013). From a therapeutic perspective, it would be of interest to know if SIRT6 plays a role in mediating their acetylation state in these pathological conditions and whether SIRT6 modulation could prevent disease onset or progression.

Chapter 3

SIRT6 acts as a tumor suppressor through inhibition of glycolysis

Abstract

Cancer cells derive much of their energy from aerobic glycolysis, a phenomenon called the Warburg Effect. Despite being known for decades, the underlying mechanism driving the metabolic switch in cancer cells is largely unknown. Here we demonstrate that the histone deacetylase SIRT6 acts as a tumor suppressor protein in part by inhibiting aerobic glycolysis. Loss of SIRT6 drives tumorigenesis in immortalized cells and supports tumor growth and glycolysis in already transformed cells. Furthermore, deletion of *Sirt6* in the intestinal epithelial cells of mice predisposed to developing intestinal adenomas results in an increase in the number, size and aggressiveness of these tumors. In addition, SIRT6 also inhibits cell growth by repressing c-MYC driven transcription of ribosomal genes. And lastly, SIRT6 protein levels are decreased in human colorectal adenomas. Thus our studies strongly support a role for SIRT6 as a potent tumor suppressor protein.

Introduction

Warburg effect

Cells regulate glucose metabolism based on their differentiation and growth state, and the availability of oxygen. Differentiated tissues preferentially metabolize glucose to pyruvate through glycolysis; pyruvate subsequently enters the mitochondrial tricarboxylic acid (TCA) cycle to be fully oxidized to CO_2 (oxidative phosphorylation). However, oxidative phosphorylation is dependent on the availability of O_2. Under hypoxic conditions, pyruvate is converted instead into lactate in anaerobic glycolysis (Vander Heiden et al., 2009). In 1924, Otto Warburg observed that cancer cells preferentially convert glucose into lactate, irrespective of the presence of oxygen (aerobic glycolysis) (Warburg, 1956). This phenomenon, termed the Warburg effect, is also observed in non-neoplastic proliferating cells, such as lymphocytes (Wu and Zhao, 2013) and LPS-stimulated macrophages (Tannahill et al., 2013) (Figure 3.1).

It might at first seem surprising that cancer cells carry out a form of metabolism that is relatively inefficient at generating ATP. For each molecule of glucose that enters the cell, oxidative phosphorylation generates up to 36 molecules of ATP, whereas aerobic glycolysis provides only 2 net ATP molecules (Vander Heiden et al., 2009). Thus, glycolysis must provide rapidly proliferating cells with benefits that outweigh a lower efficiency of ATP production. A large body of recent work indicates that glycolysis and lactate production provide cancer cells with a number of advantages that drive tumorigenesis. First, in the presence of ample glucose, glycolysis generates ATP more rapidly than oxidative phosphorylation (Wu and Zhao, 2013). Second, aerobic

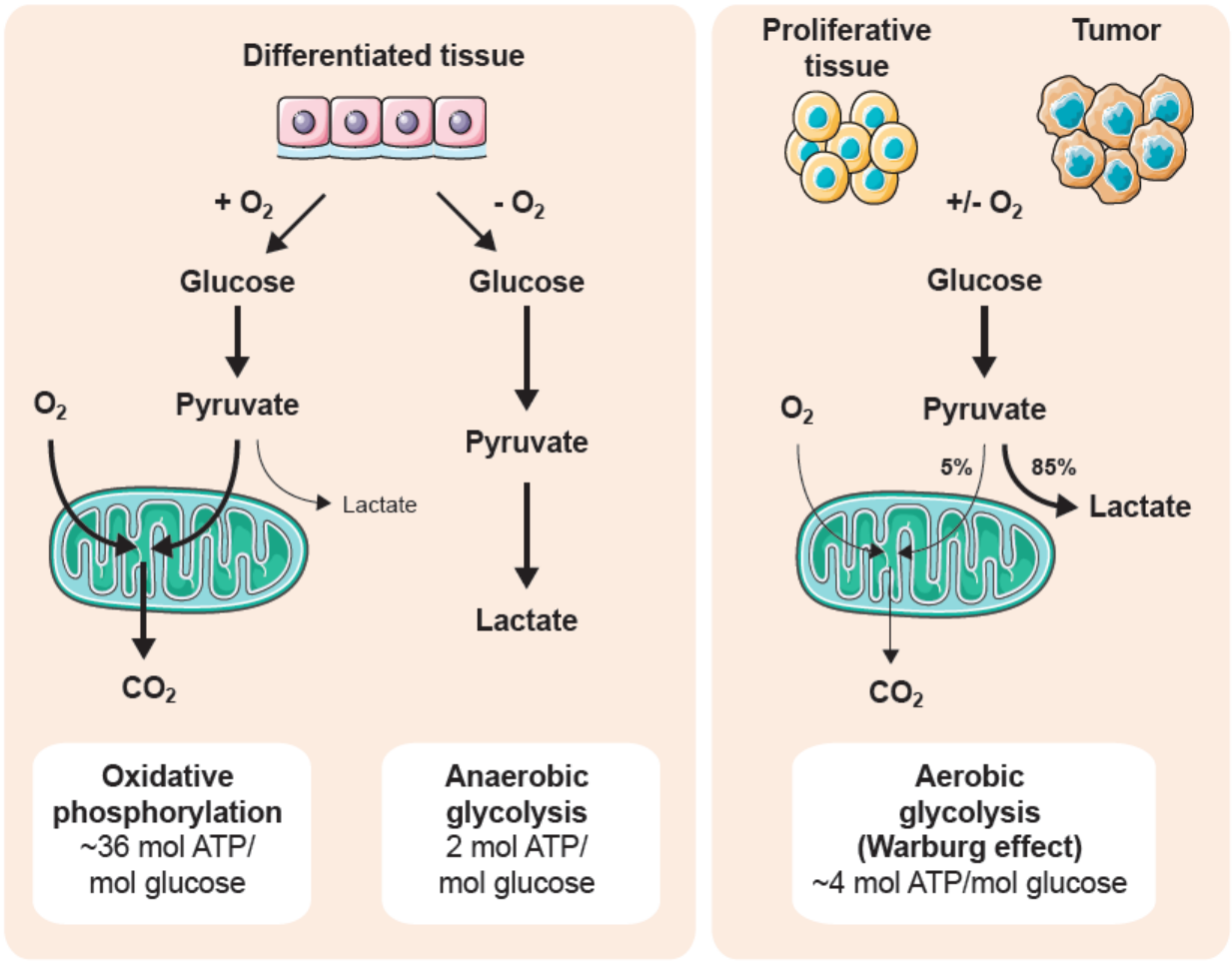

Figure 3.1: Illustration of the Warburg Effect

In the presence of ample oxygen, differentiated tissue preferentially generates energy through oxidative phosphorylation, hereby producing 36mol ATP/mol glucose. However, under low oxygen condition pyruvate is converted into lactate instead (anaerobic glycolysis), hereby providing the cell with a mere 2mol ATP/mol glucose. Proliferative or cancerous tissue, independent of oxygen levels, preferentially generates ATP through conversion of glucose to pyruvate and lactate, a phenomenon referred to as the Warburg Effect. Figure is adapted from (Vander Heiden et al., 2009)

glycolysis provides the cell with increased capacity to generate precursors for synthesis of macromolecules (lipids, nucleic acids, and proteins) essential for rapid cell division (Soga, 2013; Vander Heiden et al., 2009; Wu and Zhao, 2013). Finally, lactate secretion by tumors creates a toxic environment for immune cells, thereby inhibiting

immune surveillance, and stimulates endothelial cells to form new blood vessels, facilitating tumor metastasis (Hirschhaeuser et al., 2011). Lactate levels are negatively correlated with survival in patients with diverse tumor types, including cervical cancer, head and neck squamous cell carcinoma, and glioblastoma multiforme (Hirschhaeuser et al., 2011). In addition, high blood lactate levels are associated with radioresistance (Hirschhaeuser et al., 2011). It is now known that aerobic glycolysis is a part of the broader metabolic reprogramming that occurs in cancer cells (Ward and Thompson, 2012).

SIRT6 plays a particularly crucial physiologic role in maintaining glucose homeostasis. The first observation linking SIRT6 and glucose metabolism was made in SIRT6-deficient mice. Loss of SIRT6 in a 129Sv strain background caused severe hypoglycemia that resulted in death by one month post-partum (Mostoslavsky et al., 2006). Subsequent studies have shown that this hypoglycemia results from elevated tissue uptake of blood glucose in SIRT6-deficient mice, despite their lower circulating insulin levels. Collectively, these studies have revealed that SIRT6 is a master regulator of glucose homeostasis (Dominy et al., 2012; Kim et al., 2010; Xiao et al., 2010; Zhong et al., 2010). SIRT6 exerts this function through three distinct pathways: (1) inhibiting activity of HIF-1α, a transcription factor that drives glycolysis and simultaneously inhibits oxidative phosphorylation (Zhong et al., 2010), (2) attenuating IIS and glucose uptake by reducing c-JUN transcriptional activity (Sundaresan et al., 2012; Xiao et al., 2012), and (3) inhibiting hepatic gluconeogenesis by promoting acetylation of the transcription factor PGC-1α (Dominy et al., 2012) (Figure 1.3).

Highlighting the central role of metabolic reprogramming in neoplasia, mutations in genes that encode proteins involved in mitochondrial metabolism can promote tumorigenesis (Wu and Zhao, 2013). A number of transcription factors have been identified as the drivers of cancer metabolism (Soga, 2013; Ward and Thompson, 2012). Two such transcription factors are HIF-1α and c-MYC.

HIF-1 is a driver of metabolic reprogramming in cancer

Hypoxia-inducible factors (HIFs), HIF-1, HIF-2 and HIF-3, are transcription factors that drive glycolysis and lactate production when the oxygen supply is limited. HIFs consist of an α-subunit whose levels are sensitive to oxygen concentration, and a stable β-subunit. Under physiological oxygen tension, the α-subunit undergoes hydroxylation by prolyl hydroxylase (PHD) and subsequent proteasomal degradation mediated by von Hippel-Lindau (VHL) protein and E3 ligase (Keith et al., 2012; Semenza, 2010). However, under hypoxic conditions, oxygen shortage and/or the generation of reactive oxygen species (ROS) by the mitochondria inhibits the activity of PHD resulting in stabilization of the α-subunit, resulting in the HIF complex binding to hypoxia-responsive elements (HREs) in the promoters of HIF target genes. The ubiquitously expressed HIF-1α was first identified in 1995, followed shortly after by the discovery of HIF-2α (Ema et al., 1997; Flamme et al., 1997; Hogenesch et al., 1997; Tian et al., 1997; Wang et al., 1995). HIF-2α was initially thought to be mainly expressed in endothelial cells; however, expression of HIF-1α and HIF-2α overlaps in many cell types, and they regulate common as well as unique target genes (Hu et al., 2003; Keith et al., 2012; Raval et al., 2005; Wiesener et al., 2003).

HIF-1 induces expression of a number of glycolytic genes, such as *SLC2A1* and *SLC2A3*, hexokinases 1 and 2 (HK1/2), *PFK1*, *LDHA*, *MCT4,* and *PDK1* (Figure 3.2). *SLC2A1* and *SLC2A3* encode the glucose transporters GLUT1 and GLUT3 respectively, which are responsible for basal, non-insulin-responsive glucose uptake.

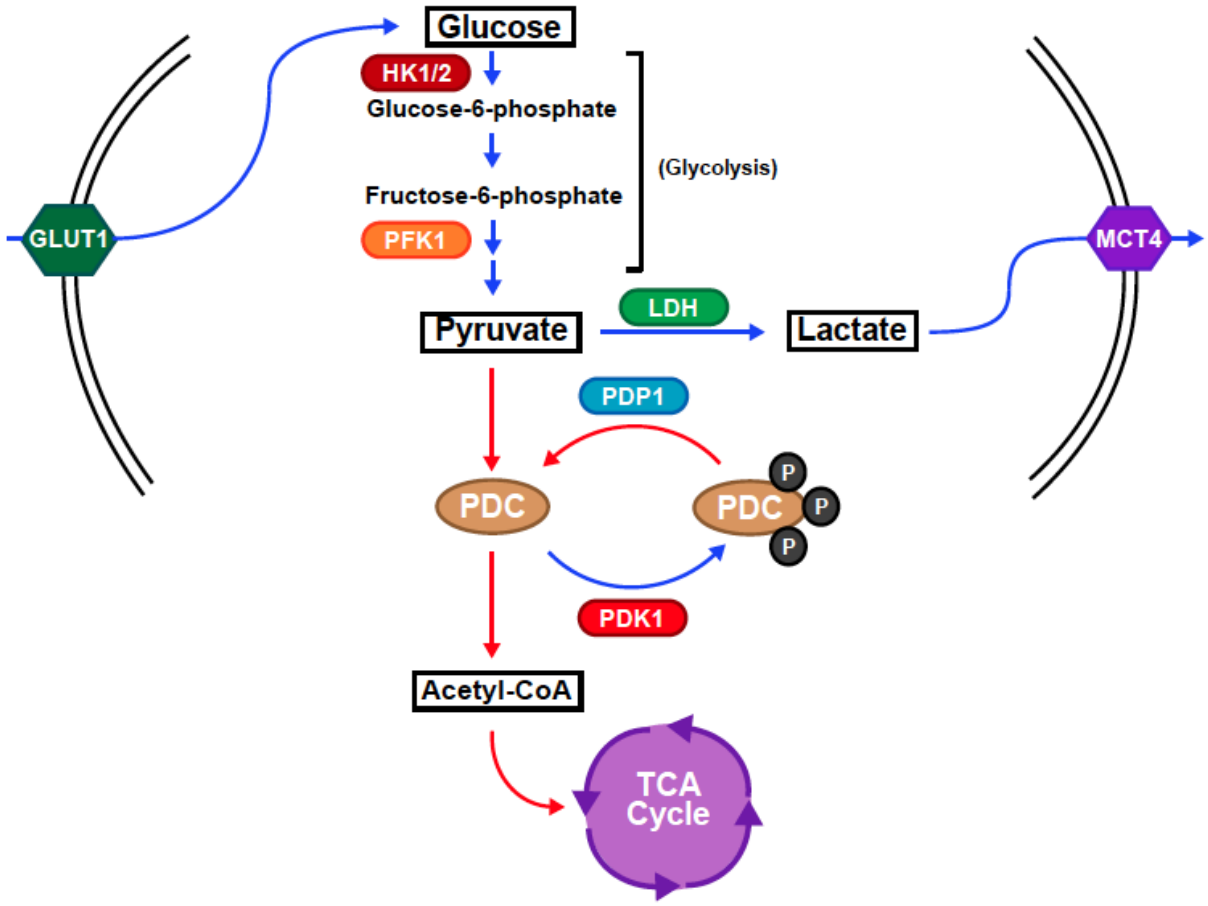

Figure 3.2: HIF-1 transcriptional activity positively regulates glycolysis and lactate production

HIF-1 regulates transcription of a number of glycolytic genes that drive aerobic glycolysis (blue arrows) and inhibit oxidative phosphorylation (red arrows). GLUT, glucose transporter; HK1/2, hexokinase 1/2, PFK1, phosphofructokinase 1; LDH, lactate dehydrogenase; PDC, pyruvate dehydrogenase complex; PDK1, pyruvate dehydrogenase kinase 1; PDP1, pyruvate dehydrogenase phospatase 1; MCT4, monocarboxylate transporter 4.

Once imported into the cell, glucose is converted to glucose-6-phosphate in the initial step of glycolysis by hexokinases. Another important enzyme in glycolysis is phosphofructokinase 1 (PFK1) which converts fructose-6-phosphate into fructose-1,6-biphosphate. Pyruvate generated in the final step of glycolysis can either be converted into acetyl-CoA by pyruvate dehydrogenase complex (PDC) for further metabolism in the TCA cycle, or be converted to lactate. Under hypoxic conditions, HIF-1 upregulates expression of glycolytic enzymes and favors lactate production, while inhibiting pyruvate entry into the TCA cycle. Two of HIF-1's major transcriptional targets are pyruvate dehydrogenase kinase 1 (*PDK1*) and lactate dehydrogenase (*LDH*). PDK1 phosphorylates the E1α subunit of PDC, thereby inhibiting holoenzyme activity. LDH catalyzes conversion of pyruvate into lactate. Once formed, lactate is transported out of the cell by the monocarboxylate transporter MCT4 (Keith et al., 2012; Semenza, 2010). Increased expression of HIF-1α and HIF-2α has been detected in many different cancer types as well as tumor-associated stromal cells, and in both cases high HIF levels are associated with a poor clinical outcome (Bonuccelli et al., 2010; Keith et al., 2012; Pavlides et al., 2010; Semenza, 2010).

Oncogenic c-Myc regulates biomass production in cancer

c-MYC, l-MYC and n-MYC are the three members of the oncogenic MYC transcription factor family. n-MYC and c-MYC possess overlapping functions, though expression of n-MYC is more tissue-restricted, being more prevelant in postmitotic cells undergoing differentiation (Dang, 2012; Malynn et al., 2000). c-MYC heterodimerizes with its partner protein MAX (MYC-associated factor X) to bind specific DNA sequences,

termed E-boxes, on promoter regions of 30% of all genes (Dang et al., 2009a). In this regard, recent data indicate that MYC functions as an amplifier of the expression of essentially all expressed genes, in a cell-type specific manner (Lin et al., 2012; Nie et al., 2012). To regulate gene expression, the c-MYC/MAX complex requires interaction with other transcription factors such as E2F1 and HIF-1. c-MYC positively regulates ribosomal biogenesis, glucose metabolism, and mitochondrial respiration in most cell types (Dang et al., 2009a). Ribosomal genes are particularly important c-MYC targets in the context of cellular transformation; heterozygosity for a ribosomal gene (*L24*) is sufficient to attenuate MYC-driven oncogenesis in B-lymphocytes (Barna et al., 2008).

With respect to glucose metabolism and mitochondrial function, a complex interplay exists between MYC and HIF proteins. Under hypoxic conditions, HIF-1 inhibits MYC activity, either through interruption of MYC/MAX binding, or through stimulation of proteasomal degradation of MYC (Corn et al., 2005; Gordan et al., 2007b). However, oxygen levels tend to fluctuate in cancer cells (Dewhirst, 2007). Therefore, in tumor cells, where c-MYC levels are generally elevated, HIF-1α will only inhibit MYC activity during short periods of severe hypoxia, while at other times the high c-MYC levels can drive cellular proliferation (Gordan et al., 2007b). In contrast to HIF-1, HIF-2 was reported to promote MYC/MAX heterodimerization under hypoxic conditions and enhance MYC activity (Gordan et al., 2007a). Because HIF-2 is expressed in endothelial cells, it has been postulated that, via this mechanism, HIF-2 stimulates endothelial proliferation and angiogenesis. However, endothelial-specific deletion of

HIF-2α does not affect endothelial proliferation per se; instead it results in defective tumor vessel formation and increased tumor hypoxia and apoptosis (Skuli et al., 2009).

Increased c-MYC activity is a feature of many diverse human tumors (Dang et al., 2008; Dang et al., 2009a). A key function of c-MYC in cancers is regulating the absorption and metabolism of the non-essential amino acid glutamine. In 1955, Dr. H. Eagle observed that cellular proliferation of normal and malignant cells in culture requires exogenous glutamine (Eagle, 1955). Glutamine uptake by cancer cells exceeds that of any other amino acid by 10-fold, and glutamine deprivation of transformed cells induces apoptosis (Wise et al., 2008; Yuneva et al., 2007). The importance of glutamine in cancer cell survival and growth is due largely to its involvement in macromolecular synthesis (Dang, 2010; Wise and Thompson, 2010). Glutamine is essential for protein translation in cancer cells as it drives the uptake of extracellular essential amino acids (EAAs), which in turn activate mTORC1, a master regulator of protein translation (Wise and Thompson, 2010). In addition, glutamine and glucose are important carbon and nitrogen sources for synthesis of all non-essential amino acids except tyrosine (Wise and Thompson, 2010). In addition, through various processes, glutamine metabolism generates important substrates for energy production (DeBerardinis et al., 2007), carbon and nitrogen to support protein, nucleotide, and lipid synthesis (Jones and Thompson, 2009) (Wise and Thompson, 2010), and high levels of NADPH (Wise and Thompson, 2010).

C-MYC can regulate glutamine uptake and metabolism in cancer cells in at least three distinct ways. First, c-MYC directly increases the expression of the amino acid transporters SLC5A1 and SLC7A1 (Gao et al., 2009). Second, c-MYC stimulates glutamine metabolism by indirectly regulating the expression of the enzyme glutaminase (GLS) (Gao et al., 2009). Finally, c-MYC promotes the expression of several enzymes involved in nucleotide biosynthesis using glutamine (Dang, 2010; Wise and Thompson, 2010).

In addition to c-MYC's regulation of glutamine uptake and metabolism, c-MYC also plays an important role in promoting cellular growth, a feature that depends on c-MYCs ability to stimulate ribosomal gene expression and ribosomal biogenesis (Arabi et al., 2005; Grandori et al., 2005; Grewal et al., 2005). Ribosomal biogenesis encompasses the synthesis and processing of ribosomal RNA (rRNA), the synthesis and import of ribosomal proteins, and the assembly and export of pre-ribosomal subunits. The human ribosomal genes are clustered together on various chromosomes. Each one of these clusters co-localizes with a nucleolus where rRNA transcription and processing takes place and ribosomal proteins are integrated to form the immature ribosome (Gonzalez and Sylvester, 1995). The rate at which rRNA is synthesized is essential in ribosomal biogenesis and protein synthesis, which in turn are rate-limiting steps for cellular proliferation (Dai and Lu, 2008). In mammals, c-MYC regulates the transcription of ribosomal genes by recruiting RNA polymerase I to the nucleolus (Grandori et al., 2005). As a result, the expression of the majority of genes dedicated to ribosomal biogenesis are regulated by c-MYC (Grewal et al., 2005). Cells expressing

high levels of c-MYC have an abundance of rRNA, large numbers of ribosomes and have dense endoplasmatic reticulum network (Grewal et al., 2005). These features coincide with the increased nucleolar size and enhanced rRNA synthesis that is commonly seen in transformed cells (Derenzini et al., 1998).

Based on the role of SIRT6 in maintaining genomic stability and glucose homeostasis (Cardus et al., 2013; Kaidi et al., 2010; Mao et al., 2012; McCord et al., 2009; Mostoslavsky et al., 2006; Toiber et al., 2013; Zhong et al., 2010), we hypothesized that SIRT6 could function as a tumor suppressor protein. In this study we confirm that the absence of SIRT6 drives tumorigenesis in immortalized cells through at least two pathways. First, SIRT6 controls HIF-1 activity, hereby preventing the switch to aerobic glycolysis, the main mode of energy production in cancer cells (Warburg Effect). Second, SIRT6 regulates cell growth by co-repressing c-MYC transcriptional activity, and thereby inhibits ribosomal gene expression. Manipulation of either pathway rescues the tumorigenic potential of SIRT6 deficient cells *in vitro* and *in vivo*. Furthermore, we find that SIRT6 protein levels are decreased in human adenomas in comparison to normal colon tissues, consistent with the notion that SIRT6 is a potent tumor suppressor. These studies were performed in collaboration with Dr. R. Mostoslavsky and Dr. C. Sebastiàn at Massachusetts General Hospital and Harvard Medical School.

Materials and Methods

Immortalized and transformed MEFs

Primary MEFs were isolated from 13.5 day-old embryos as previously described (Mostoslavsky et al., 2006). These cells were further immortalized through 3T3 serial passaging or transformed by KD of p53 expression.

Cell culture

MEFs were grown in DMEM supplemented with 15% fetal bovine serum, 1% L-Glutamine, 1% pen/strep, 1% sodium pyruvate, 1% non-essential amino acids, 2% HEPES and 115 μM β-mercaptoethanol. ES cells were grown on gelatinized tissue culture dishes in MEF growth media supplemented with 1 ng/ml recombinant mouse leukemia inhibitory factor (LIF; Life Technologies). U2OS and 293T cells were grown in DMEM with 10% FBS, 2 mM Glutamine and 1% pen/strep.

Xenograft studies

5 x 10^6 cells in 100 ul matrigel were injected subcutaneously into the flanks of SCID mice (Taconic Farms, Inc., Hudson, NY) or athymic nude (*Foxn1*^{nu}/*Foxn1*^{nu}) mice (Jackson Laboratories). Mice were checked for the appearance of tumors twice a week, and the tumors were harvested and measured after 4 weeks.

Immuno Blot analysis and Immunoprecipitation

Western analysis was carried out as previously described (Zhong et al., 2010). The following primary antibodies were used in 5% milk in TBST: anti-SIRT6 (Abcam,

ab62739), anti-FLAG (Sigma, F1804), anti-PDK1 (Cell Signaling), anti-LDHa (Santa Cruz), anti-p53, anti-phospho-AKT (Ser473), anti-total-AKT (Cell Signaling), anti-phospho-ERK (Sigma), anti-ERK (Santa Cruz), anti-phospho-PDH-E1a-Ser293 (Abcam), anti-MYC (Epitomics), anti-actin (Sigma). To determine the interaction between SIRT6 and MYC, Flag-SIRT6, FLAG-SIRT2 or FLAG-SIRT5 were co-transfected with MYC into U2OS cells and after anti-Flag immunoprecipitation the presence of MYC was evaluated by western blot (according to manufacturers instructions). Endogenous immunoprecipitation was performed in mouse ES cells. Cells were grown to approximately 70% confluency, then washed twice with 1xPBS and collected in CHAPS buffer (25 mM HEPES, 2 mM EGTA, 2.5 mM $MgCl_2$ and 0.3% CHAPS). After a 20 min incubation on ice and a 20 min centrifugation at 4°C, the supernatants were transferred to fresh tubes. Lysates (1 mg) were pre-cleared with 50 µl Protein A Agarose beads (Roche) for two hours and supernatants were collected after short centrifugation (1 min, 1000 rpm and 4°C). IPs were performed by adding 5 µg of SIRT6 antibody or IgG control (Abcam) together with 50 µl of protein A Agarose beads overnight at 4°C. After three washes in CHAPS buffer containing 150 mM NaCl, the immuno-complexes were eluted by boiling the samples for 10 min in 4x SDS loading buffer.

Lactate, Glutamine, and Glucose Uptake Assays

Lactate and glutamine concentration were measured in the media using the Lactate Assay Kit and the EnzyChrom Glutamine Assay Kit (BioVision), respectively. *In vitro* glucose uptake was performed as previously described (Zhong et al., 2010).

Luciferase Reporter Assays

MYC transcriptional activity was determined by luciferase experiments as previously described (Zhong et al., 2010). In short, 293T cells were co-transfected with 1 μg of pCMV-3xFlag-SIRT6 or empty vector, 950 ng of pMYC-luc (Signosis, Inc., Sunnyvale, CA) and 50 ng of pGL3-Renilla. Twenty-four hours after transfection, cells were harvested and luciferase activity was deteremined using the Dual-Luciferase Reporter Assay system (Promega). An aliquot of the same lysates was used to confirm protein expression of Flag-SIRT6.

RNA Extraction and Real-Time PCR

Total RNA was extracted with the TriPure Isolation Reagent (Roche) per manufacturers instructions. For cDNA synthesis, 1 μg total RNA was reverse-transcribed using the QuantiTect Reverse Transcription Kit (Qiagen). Real-time PCR was carried out using the SYBR green master mix (Roche) as described by the manufacturer, with the exception that SYBR green reaction mix was adjusted to a total volume of 12.5 μl. The real-time PCR reaction was run on a LightCycler 480 detection system (Roche). Data are represented as relative mRNA levels normalized to β-actin levels in each sample. The primer sequences are shown in Table 3.1.

Table 3.1: Primer sequences for Real-Time PCR

	Forward sequence	Reverse sequence
Rpl3	cgtttcgctaagcttgaacc	aggagccagtgcaggctat
Rpl6	gagtcgcaaggctcaaagtc	ataagcaatgacgggaggtg
Rpl23	catcttaagcgcagctttcc	gggacactgggatatgaacg
Rps15a	cctcgcattggttgtcctat	gatggcacagataccacacg
LDHA	agggggtgtgtgaaaacaag	atggcttgccagcttacatc
LDHB	agagagagcgcttcgcatag	ggctggatgagacaaagagc
ALDOC	aagtggggcactgttaggtg	gttggggattaagcctggtt
PFKM	ttaagacaaagcctggcaca	caaccacagcaattgaccac
Pkd4	ctgtagtccccccttccctgt	gagcttttggagcagactgg
β-actin	gaggtatcctgaccctgaagta	cacacgcagctcattgtaga

FDG-PET Assays

Glucose uptake in tumors was measured as previously described (Zhong et al., 2010). Briefly, H-RasV12/shp53 cells were injected into the flanks of SCID mice 15 days prior to glucose measurement. Prior to imaging with an Inveon (Siemens) small animal scanner, animals were fasted for 12 hours and intravenously injected with approximately 700 μCi ^{18}FDG 45 minutes prior to PET acquisition (Boiselle et al., 1998). CT preceded PET, acquiring 360 cone beam projections, and PET data sets acquired 600 million counts. During CT acquisition, iodine contrast was infused intravenously at a rate of 20 μl/min to enhance intravascular contrast. Data analysis consisted of region of interest analysis on standard uptake value (SUV) PET images superimposed on anatomic contrast enhanced CT images. Images were analyzed using OsiriX software and FDG-PET data were calculated as SUV_{max} for selected regions of interest. 120-days old $Apc^{min/+}$ mice were imaged similarly to analyze *in vivo* adenoma glucose uptake. FDG-PET was performed in collaboration with Dr. R. Weissleder's group.

Proliferation Assay

Cells were plated in triplicate in 12-well plates and cultured in complete media. At the indicated time points, cells were harvested with trypsin and counted. For colony formation assays, 250 cells were plated in 6-well plates and kept in culture for 10-15 days.

Apoptosis Assay

Cells were plated in triplicate in 12-well plates and grown in complete media overnight. The next day, medium was replaced by DMEM with 10% FBS and 0.3 mM Glutamine with or without glucose. After 6 days, cells were collected and stained with Annexin-V (BD Bioscience) to analyze cell death.

Anchorage-independent Cell Growth Assay

7.5×10^3 cells were resuspended in 0.4% agar and plated in triplicate in 6 cm dishes containing a 0.8% base agar layer. Colonies were stained with 0.005% Crystal Violet in 2% methanol and counted.

Viral Infection

The following plasmids were used to generate viral particles: pBabe-H-RasV12, pLMS-shp53.1224, pLKO.1-shPDK1 (The MGH RNAi Consortium Library), pLKO.1-shMYC (Open biosciences), pMSCV-3xFlag-SIRT6 (generated by subcloning Flag-SIRT6 from pCMV-3xFlag-SIRT6 to pMSCV-puro). Viral infection was carried out as previously

described (Zhong et al., 2010). These plasmids and viral infections were generated by Dr. R. Mostoslavsky's group.

Chromatin Immunoprecipitation Assay

Chromatin immunoprecipitation (ChIP) was performed as previously described (Sebastian et al., 2008) with minor modifications. Cells were cross-linked with 1% paraformaldehyde for 20 minutes at room temperature. The reaction was quenched for 10 minutes by adding 0.125 M glycine. After three washes with 1x PBS, cells were lysed with lysis buffer (1% SDS, 10 mM EDTA pH 8, 50 mM Tris-HCl pH 8) supplemented with protease and deacetylase (TSA) inhibitors. Lysates were sonicated on ice using a Bioruptor sonicator (2 pulses of 10 minutes, 0.5 minute soication) to obtain 200-1200bp fragments. Soluble chromatin was collected after centrifugation at 14,000 rpm at 4°C for 10 minutes and 1 mg (for MYC IP) or 0.2 mg (for H3K9ac and H3K56ac IP) of protein was diluted to 1:10 in dilution buffer (1% Triton X-100, 2 mM EDTA, 150 mM NaCl, 20 mM Tris-HCl pH 8.1) supplemented with protease and deacetylase inhibitors. 1-5% of the soluble chromatin was kept as input control. The soluble chromatin was pre-cleared with 100 µg/ml of salmon sperm DNA (Amersham Biosciences), 2.5 µg/ml of control IgG, and protein-A-Sepharose at 50% overnight at 4°C while rotating. After centrifugation at 1000 rpm for 1 minute, supernatants were collected and specific antibodies were added: 7.5 µl MYC (Epitomics), 3 µl H3K9ac (Millipore), 3 µl H3K56ac (Epitomics) or control IgG (Abcam). Mixtures were incubated at 4°C for 6 hours while rotating and subsequently incubated overnight at 4°C with 50% protein-A-Sepharose (Roche). Beads were collected and

washed sequentially at 4°C for 10 minutes with buffer I (150 mM NaCl, 0.1% SDS, 1% Triton X-100, 2 mM EDTA, and 20 mM Tris-HCl (pH 8.1)), buffer II (500 mM NaCl, 0.1% SDS, 1% Triton X-100, 2 mM EDTA and 20 mM Tris-HCl (pH8.1)), and buffer III (0.25 mM LiCl, 1% Nonidet P-40, 1% deoxycholate, 1 mM EDTA and 10 mM Tris-HCl (pH 8.1)). After one wash with 1x PBS, the immunoprecipitates were eluted from the beads twice for 20 minutes with elution buffer (0.1 M $NaHCO_3$ and 1% SDS). The eluates and the input controls were incubated overnight at 65°C to reverse the cross-linking, and DNA was subsequently purified using the QIAquick spin kit (Qiagen). Real time PCR was performed as described above.

Generation of *Sirt6* Conditional KO Mice

To generate mice lacking SIRT6 specifically in the intestinal epithelial cells, we crossed previously described homozygous *Sirt6*$^{f/f}$ mice (Kim et al., 2010) with C57BL6/J mice expressing Cre-recombinase under the *Villin-1* promoter. Cre-recombinase exposure leads to deletion of exon 2 and 3. These crossed mice were consequently interbred with C57BL/6J-*Apc*$^{min/+}$ mice (Jackson Laboratories) to generate mice heterozygous for *Apc* in which *Sirt6* is specifically deleted in the intestinal epithelial cells (Figure 3.3). Mice were euthanized at 120 days, the intestines harvested and analyzed for the presence of polyps. Subsequently, the intestines were fixed in 10% formaldehyde and processed for H&E staining according to standard procedures by the University of Michigan histology core.

A subset of *Sirt6*$^{f/f}$;*V-c*;*Apc*$^{min/+}$ and control;*Apc*$^{min/+}$ mice were treated just after weaning with dichloroacetic acid (DCA; 5 g/l of drinking water) or regular water and euthanized

at 108 days of age. Intestines were harvested and processed as described above. Of each mouse one polyp was collected for protein extraction to analyze PDH-E1α phosphorylation.

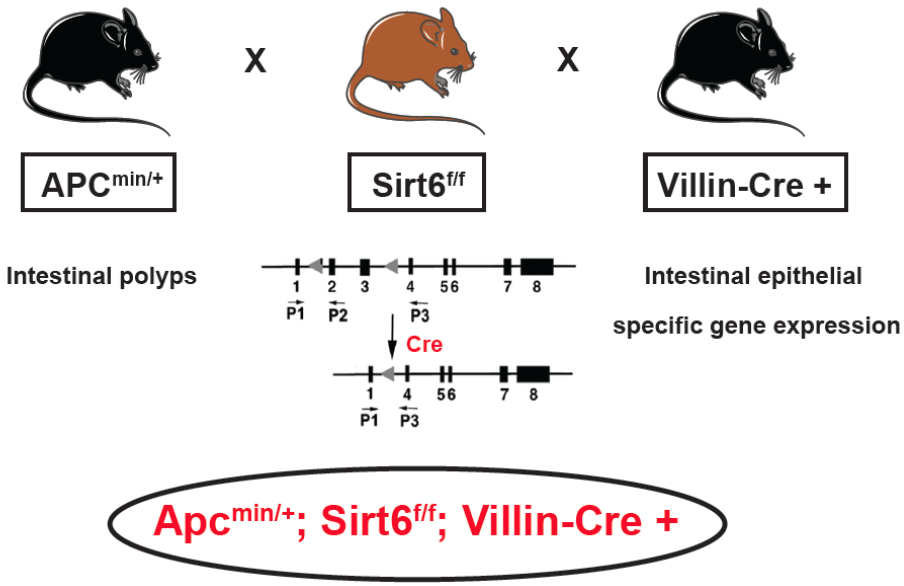

Figure 3.3: Adenoma-prone mouse model breeding scheme

Mice containing the *Sirt6* allele with loxP sites flanking exons 2 and 3 were crossed with mice carrying the *cre-recombinase* gene driven by the *Villin-1* promoter to generate intestinal epithelial specific knockouts for Sirt6. These mice were further crossed with *Apc*$^{min/+}$ mice that are predisposed to developing intestinal adenomas.

Immunohistochemistry

IHC for SIRT6 was performed on human normal colon and adenomas by the University of Michigan histology core. In brief, slides were deparaffinized and rehydrated through a series of xylene and alcohol washes. Antigen retrieval was performed by first heating the slides for 10 minutes in citrate buffer (10 mM Citric Acid, 0.05% Tween 20, pH 6.0) and then slides were allowed to cool down for 10 minutes at room temperature.

Endogenous peroxide was blocked by incubation in 3% hydrogen peroxide (H_2O_2) for 10 minutes. Additional blocking was performed by incubating the slides in 5% normal goat serum in PBS for one hour. Tissues were incubated with anti-SIRT6 antibody (Cell Signaling Technology) overnight at 4°C. Signal was visualized using 3,3'-diaminobenzidine (DAB; Vector Laboratories) and slides were mounted using permanent mounting medium (Vector Laboratories). Slides were imaged with an Olympus BX-51 scope with an Olympus DP-70 high-resolution digital camera (University of Michigan Microscopy & Image Analysis lab).

Results

SIRT6-deficient cells are tumorigenic

It was previously shown that SIRT6 plays a role in maintaining genomic integrity (Mostoslavsky et al., 2006) and in controlling glucose homeostasis in part by regulating aerobic glycolysis (Zhong et al., 2010). Both these processes are key features in cancer cells, and thus we hypothesized that the absence of SIRT6 might result in tumorigenesis. To investigate this hypothesis, we obtained mouse embryonic fibroblasts (MEFs) from *Sirt6* WT and KO embryos and immortalized them through serial passaging according to a standard 3T3 protocol. *Sirt6* KO MEFs had a higher proliferative rate (Figure 3.4A) and formed larger colonies when plated at very low density (Figure 3.4B) than *Sirt6* WT MEFs. Subsequently, we injected *Sirt6* WT and KO cells into the flanks of nude mice to assess tumor growth *in vivo*. Immortalized MEFs normally do not grow in this setting except when transformed with an activated

oncogene. However, the SIRT6-deficient MEFs easily formed tumors indicating that the absence of SIRT6 is sufficient to drive tumorigenesis in immortalized MEFs (Figure 3.4C).

Genomic instability can cause cellular transformation by activating oncogenes or inactivating tumor suppressor genes. Since SIRT6 is known to maintain genomic integrity through its stimulatory function in various DNA repair pathways (Kaidi et al., 2010; Mao et al., 2012; McCord et al., 2009; Mostoslavsky et al., 2006), we first wanted to verify if the tumorigenesis observed in *Sirt6* KO MEFs was due to genomic instability. To test this, we reintroduced SIRT6 in KO MEFs and injected these cells into nude mice. If cellular transformation were caused by genomic instability due to the absence of SIRT6, we would expect tumor growth even when reintroducing SIRT6. We observed that these rescued cells were no longer capable to form tumors *in vivo* (Figure 3.4C), indicating that an alternative pathway is responsible for mediating SIRT6's tumor suppressor function. In support of this, KO MEFs reconstituted with the catalytic inactive mutant SIRT6-H133Y still formed tumors *in vivo* (Figure 3.4C), suggesting that SIRT6 catalytic activity is required for tumor suppression.

Finally, we examined whether SIRT6 deficiency influenced tumor growth in the presence of activated oncogenes. Therefore, we expressed an activated form of H-Ras (H-RasV12) and knocked down *p53* expression (shp53) in both WT and *Sirt6* KO MEFs and found that even in this setting SIRT6 deficiency provided transformed MEFs with a growth advantage when subjected to an anchorage-independent soft agar assay (Figure 3.4E). Indicating that SIRT6 protects against both tumor initiation and tumor progression.

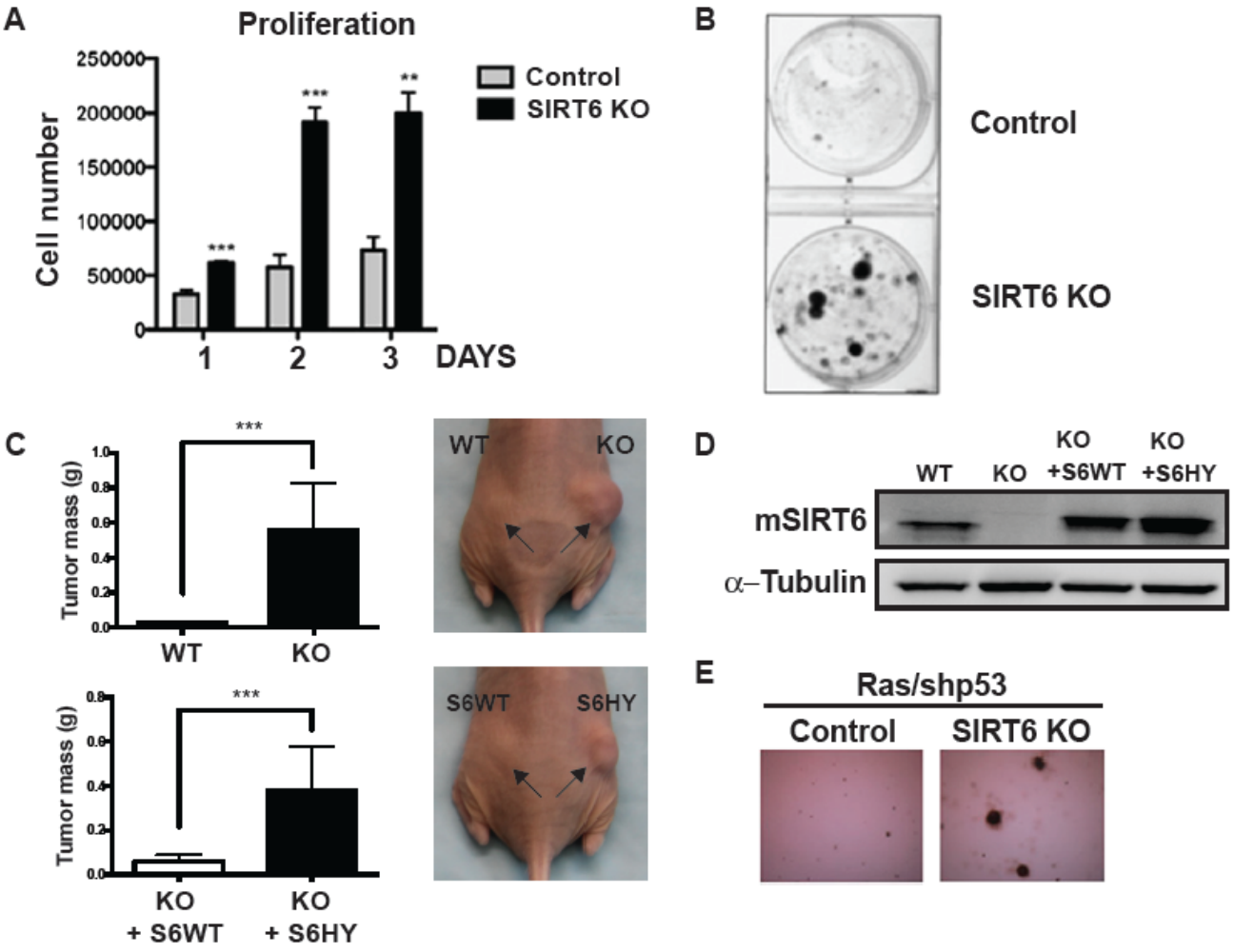

Figure 3.4: SIRT6-deficient cells are tumorigenic

(A) *Sirt6* WT and KO immortalized MEFs (two independent cell lines for each) were plated, and cells were counted on indicated days. Error bars indicate SEM. (B) *Sirt6* WT and KO immortalized MEFs were plated at a low density and cultured to assess colony formation. (C) Immortalized MEFs were injected into the flanks of nude mice to assess their tumorigenic potential. Likewise, *Sirt6* KO MEFs were infected with lentiviruses encoding Flag-SIRT6 or Flag-SIRT6HY (catalytic inactive mutant) and grown in nude mice. (D) SIRT6 protein levels were assessed in the indicated immortalized MEFs. (E) Anchorage-independent cell growth assay of *Sirt6* WT and KO H-RasV12/shp53 transformed cells. (Sebastian et al., 2012) Experiments in figures A, B and E were performed by Dr. C. Sebastian.

SIRT6 deficient cells and tumors exhibit enhanced aerobic glycolysis

To identify the underlying mechanism associated with the tumorigenic phenotype of SIRT6 deficient cells, we concentrated on SIRT6's role in regulating glucose metabolism. Immortalized MEFs showed increased glucose uptake and lactate production in the absence of SIRT6 (Figure 3.5A). Additionally, reintroduction of SIRT6 in KO MEFs, in addition to decreasing tumor growth *in vivo* (Figure 3.4C), reduced cellular glucose absorption (Figure 3.5B), suggesting that compromising the inhibitory role of SIRT6 on aerobic glycolysis could mediate tumorigenesis. To analyze the glycolytic phenotype of these cells, we measured the expression levels of various glycolytic genes that have previously been shown to be regulated by SIRT6 (Zhong et al., 2010). In comparison to WT MEFs, SIRT6-deficient MEFs show higher expression of *Glut1*, *Pfk1*, *Pdk1* and *Ldha* (Figure 3.5C). Further enhanced expression of these genes was observed in *Sirt6* KO tumors derived from *Sirt6* KO MEFs (Figure 3.5C), suggesting a selective advantage within *Sirt6* KO tumors for cells with elevated glycolytic activity. Enhanced glycolytic activity is indicative of glucose addiction. To test this, we measured cellular apoptosis of *Sirt6* WT and KO MEFs under high and low glucose conditions. Strikingly, almost 50% of SIRT6-deficient cells died after glucose withdrawal, while most SIRT6-proficient cells survived (Figure 3.5D). These results strongly suggest that SIRT6 acts as a tumor suppressor protein by inhibiting aerobic glycolysis and thereby glucose addiction, a hallmark of cancer cells.

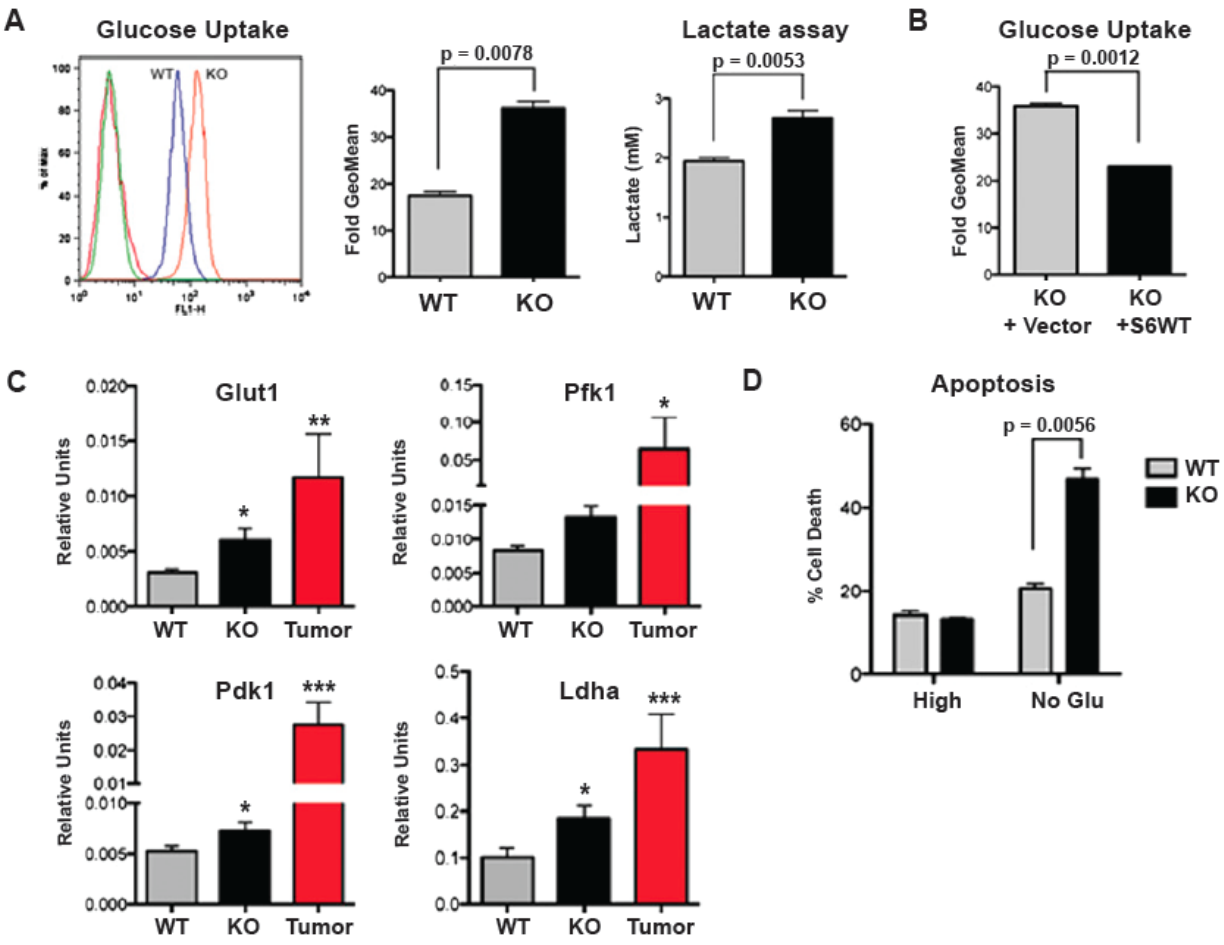

Figure 3.5: SIRT6 deficient cells and tumors show elevated aerobic glycolysis

(A) Glucose uptake (left and middle) and lactate production in *Sirt6* WT and KO immortalized MEFs (two independent cell lines; error bars indicate SEM). (B) Glucose uptake in *Sirt6* KO immortalized MEFs virally infected with empty vector or WT *Sirt6* (error bars indicate SD). (C) Real-time PCR showing the expression of the indicated genes in *Sirt6* WT and KO immortalized MEFs (n=20 experiments from two independent lines) and for cells derived from *Sirt6* KO tumors (n=8 experiments from three independent lines) (error bars indicate SEM). (D) *Sirt6* WT and KO MEFs were cultured with or without glucose. After 6 days cell death was measured using Annexin V staining (error bars indicate SEM). Experiments were performed by Dr. C. Sebastián (Sebastian et al., 2012)

Inhibition of glycolysis suppresses tumorigenesis in Sirt6 KO cells

The above results suggest that SIRT6 acts as a tumor suppressor protein by mediating aerobic glycolysis. In addition to changes at a transcriptional level, both LDHA and PDK1 protein levels are elevated in immortalized and transformed *Sirt6* KO MEFs, in comparison to control cells (Figure 3.6A). To further assess the importance of aerobic glycolysis in driving tumorigenesis in the absence of SIRT6, we hypothesized that reversing this metabolic switch by stimulating the conversion of pyruvate to Acetyl-CoA instead of to lactate, would rescue the tumorigenesity phenotype in SIRT6 deficient cells. Therefore, we virally infected immortalized *Sirt6* KO MEFs with *shPdk1* or vector control. This resulted in efficient knockdown of PDK1 and, as a consequence, reduced PDH phosphorylation (Figure 3.6B). Furthermore, PDK1 downregulation reversed both the proliferative potential and the glucose addiction of *Sirt6* KO MEFs (Figure 3.6C). In addition, inhibition of PDK1 activity diminished anchorage-independent cell growth in soft agar that was previously observed in SIRT6-deficient cells (Figure 3.6D). Overall, these results indicate that SIRT6 acts as a tumor suppressor protein by preventing the switch from oxidative phosphorylation to aerobic glycolysis and that reactivation of oxidative phosphorylation is sufficient to revert this phenotype.

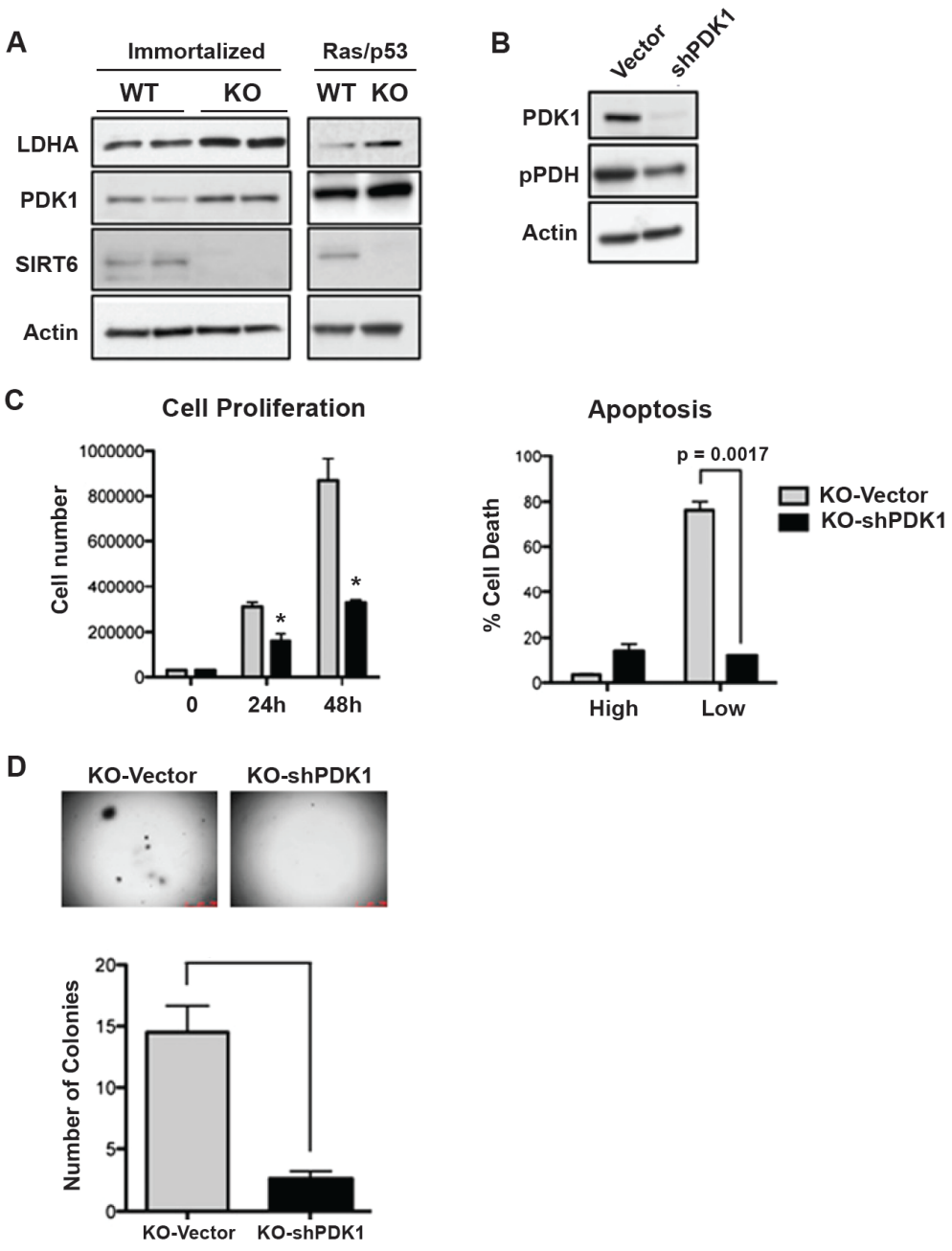

Figure 3.6: Inhibition of glycolysis suppresses tumorigenesis in *Sirt6* KO cells

(A) Western blot showing the expression of PDK1 and LDHA in *Sirt6* WT and KO immortalized and transformed MEFs. (B) Western blot showing PDK1 and phospho-PDH-E1α (Ser293) protein levels in *Sirt6* KO cells infected with *shPdk1* and vector control. (C) Cell proliferation assay (left) and glucose-starvation-induced cell death assay (right) in *Sirt6* KO-vector and *Sirt6* KO-*shPdk1* MEFs (error bars indicate SD). (D) Anchorage-independent cell growth of the same cells as in (C) (error bars indicate SD). Experiments were performed by Dr. C. Sebastián and members of Mostoslavsky laboratory (Sebastian et al., 2012).

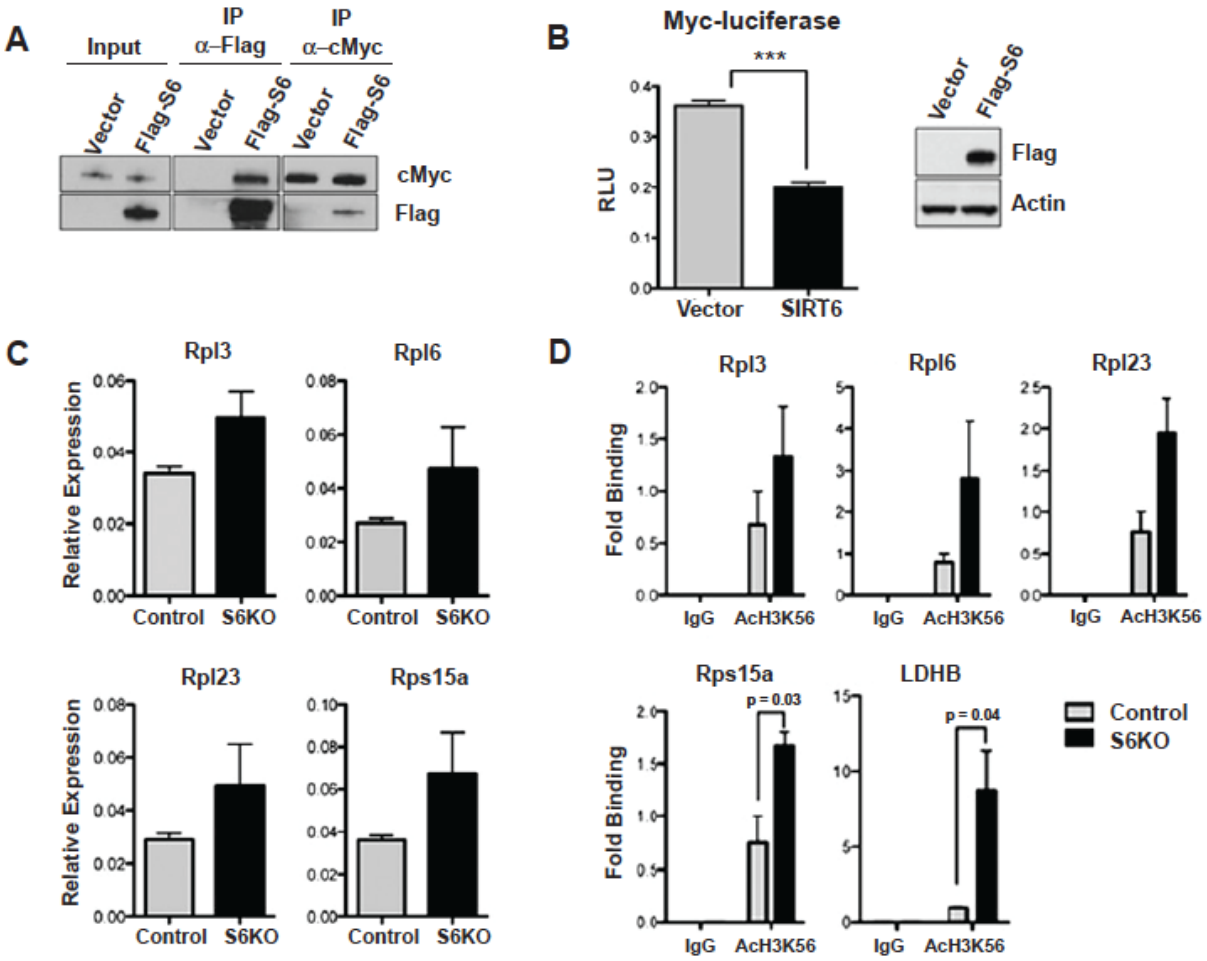

Table 3.7: SIRT6 inhibits ribosomal gene expression by co-repressing MYC transcriptional activity

(A) IPs of Flag-SIRT6 and cMYC indicating their physical interaction. (B) Luciferase activity measured in 293T cells which were co-transfected with a luciferase reporter gene under the regulation of a MYC-responsive element and with Flag-SIRT6 or empty vector (error bars indicate SEM). (C) Relative expression of the indicated genes in *Sirt6* WT and KO H-RasV12/shp53 tumors (n=4; error bars indicate SEM). (D) ChIP analysis of H3K56ac levels at indicated loci for *Sirt6* WT and KO H-RasV12/*shp53* MEFs (n=4; error bars indicate SEM). IP was performed by Dr. E. Guccione and remaining experiments were performed by Dr. C. Sebastián (Sebastian et al., 2012).

SIRT6 inhibits ribosomal gene expression by co-repressing MYC

In general, a metabolic switch to glycolysis alone is not sufficient to provide cells with a growth advantage. Therefore we hypothesized that SIRT6 might regulate cellular

proliferation in addition to glycolysis. Based on data sets from SIRT6 chromatin immunoprecipitation followed by DNA sequencing (ChIP-seq) performed in collaboration with Dr. Bernstein and Dr. Regev's research groups using their newly developed method to study chromatin regulator binding (Ram et al., 2011), we found that SIRT6 binds ribosomal and ribonucleoprotein genes. Interestingly, these genes are under the transcriptional regulation of MYC (Arabi et al., 2005; Grandori et al., 2005; Grewal et al., 2005), and therefore we hypothesized that SIRT6 might suppress MYC transcriptional activity. We first confirmed that SIRT6 and MYC physically interact by co-transfecting 293T cells with Flag-SIRT6 and c-MYC followed by immunoprecipitation (Figure 3.7A). Since SIRT6 has been previously identified as a transcriptional repressor, we verified if SIRT6 could also inhibit MYC activity. Thus, we measured the expression of a MYC-dependent luciferase reporter in 293T cells in the presence or absence of SIRT6. We found that SIRT6 suppressed the luciferase expression significantly (Figure 3.7B), demonstrating that SIRT6 represses MYC activity in this setting. To confirm this *in vivo*, we measured the expression of various ribosomal genes in SIRT6-deficient tumors, which were all upregulated in the absence of SIRT6 (Figure 3.7C). As it was previously shown that SIRT6 deacetylates multiple residues on histone H3 (Michishita et al., 2008; Michishita et al., 2009; Yang et al., 2009), and that this deacetylation can repress activity of multiple transcription factors (Kawahara et al., 2009; Zhong et al., 2010), we performed ChIP to assess if SIRT6 represses MYC in a similar fashion. We found that SIRT6 specifically deacetylates H3K56ac, and not H3K9ac (data not shown), on the promoter regions of ribosomal protein genes (Figure 3.7D). In summary, we have shown that SIRT6 physically

interacts with MYC on the promoter regions of ribosomal genes and that SIRT6 functions as a transcriptional repressor of MYC to inhibit ribosomal gene expression. Thus we provide another mechanism through which SIRT6 can suppress tumorigenesis.

To assess the importance of SIRT6 suppression of MYC activity in preventing tumorigenesis, we knocked down MYC in SIRT6-deficient MEFs using a viral short hairpin vector (Figure 3.8A). Upon knockdown of Myc, cellular proliferation in culture (Figure 3.8B) and *in vivo* (Figure 3.8C) was reduced in the absence of SIRT6. Additionally, MYC knockdown inhibited ribosomal gene expression as well as *glutaminase* (*Gls*) expression in *Sirt6* KO MEFs (Figure 3.8D). However, glucose uptake and glycolytic gene expression was unaffected by *Myc* knockdown (Figure 3.8E-F), indicating that MYC regulates tumor growth in SIRT6-deficient cells specifically by enhancing expression of glutamine and ribosomal genes and that the metabolic switch observed in the absence of SIRT6 is likely through hyperactivation of HIF-1α.

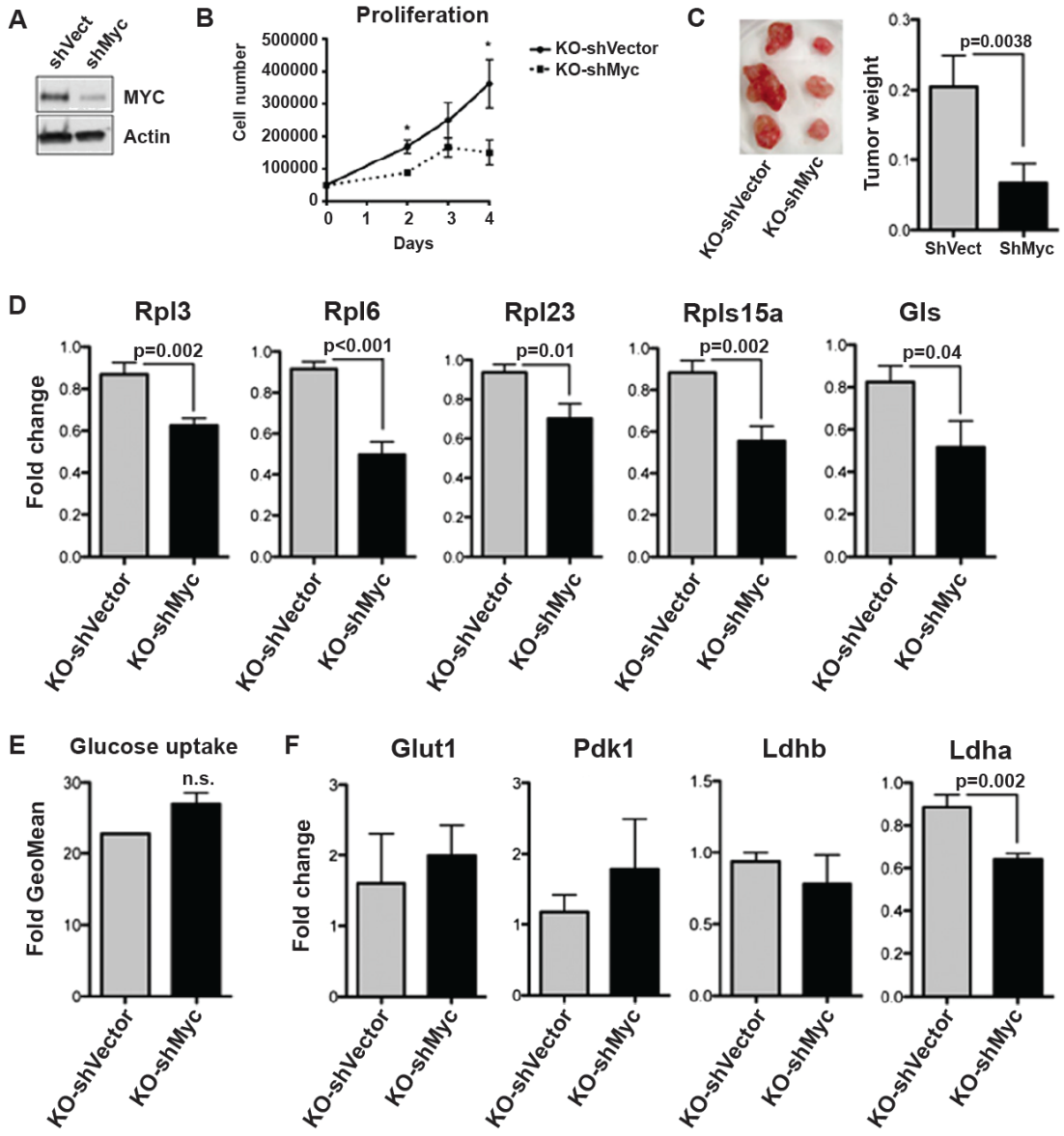

Figure 3.8: MYC regulates growth of SIRT6-deficient cells

(A) Western blot showing MYC protein levels in Sirt6 KO-shMYC and vector control MEFs. (B) Proliferation assay in which 5 x 10^5 MEFs were plated in triplicate and counted at the indicated time points (error bars indicate SD). (C) 5 x 10^5 MEFs were injected into either side of the flanks of SCID mice. The weights of the harvested tumors are depicted in the bar graph (error bars indicate SD). (D) Relative expression of ribosomal genes and glutaminase (Gls) in Sirt6 KO-shVector and Sirt6 KO-shMYC cells (n=9; error bars indicate SEM). (E) Glucose uptake in Sirt6 KO-shVector and Sirt6 KO-shMYC cells (error bars indicate SD). (F) As in (D) relative expression of glycolytic genes (error bars indicate SEM). Experiments were performed by Dr. C. Sebastián (Sebastian et al., 2012).

SIRT6 functions as a tumor suppressor in vivo

Our studies so far strongly suggest a tumor suppressor role for SIRT6. To test whether our findings would hold *in vivo*, we took advantage of a well-described mouse model of colorectal adenomatosis in which mice lack a mutation in the Apc gene ($Apc^{min/+}$) (Moser et al., 1990; Su et al., 1992). To overcome the early lethality of Sirt6 germline KO mice, we deleted Sirt6 specifically in the mouse epithelial cells by crossing a previously described mouse strain with a floxed *Sirt6* allele (Kim et al., 2010) with a mouse strain expressing cre-recombinase under the *Villin-1* promoter (*V-c*+) (Madison et al., 2002). Mice with intestinal epithelial specific deletion of Sirt6 were further bred with $Apc^{min/+}$ mice to obtain $Apc^{min/+}$; $Sirt6^{f/f}$; *V-c*+ (Figure 3.3). Littermate controls were $Apc^{min/+}$; *V-c*+ mice either null ($Sirt6^{+/+}$) or heterozygous ($Sirt6^{f/+}$) for the floxed *Sirt6* allele. Remarkably, a three-fold increase in polyp number was observed upon deletion of *Sirt6* (Figure 3.9B-C). Furthermore, the average polyp size was greater than in the littermate controls (Figure 3.9D). Finally, as graded by Dr. J. Greenson, a pathologist in our department, the SIRT6 deficient adenomas had a higher grade and, in some instances, showed invasive properties, a phenotype rarely seen in $Apc^{min/+}$ animals (Figure 3.9E). In these polyps, glycolytic (Figure 3.10A) and ribosomal (Figure 3.10B) gene expression were both elevated in $Sirt6^{f/f}$; *V-c*; $Apc^{min/+}$ mice in comparison to their littermates. Strikingly, treatment of $Sirt6^{f/f}$; *V-c*; $Apc^{min/+}$ mice and controls with the PDK1 inhibitor DCA specifically inhibited tumor formation in the absence of SIRT6 as we observed smaller, fewer and lower-grade tumors upon treatment with DCA (Figure 3.9). Finally, to assess whether SIRT6 levels are altered in human adenomas, we

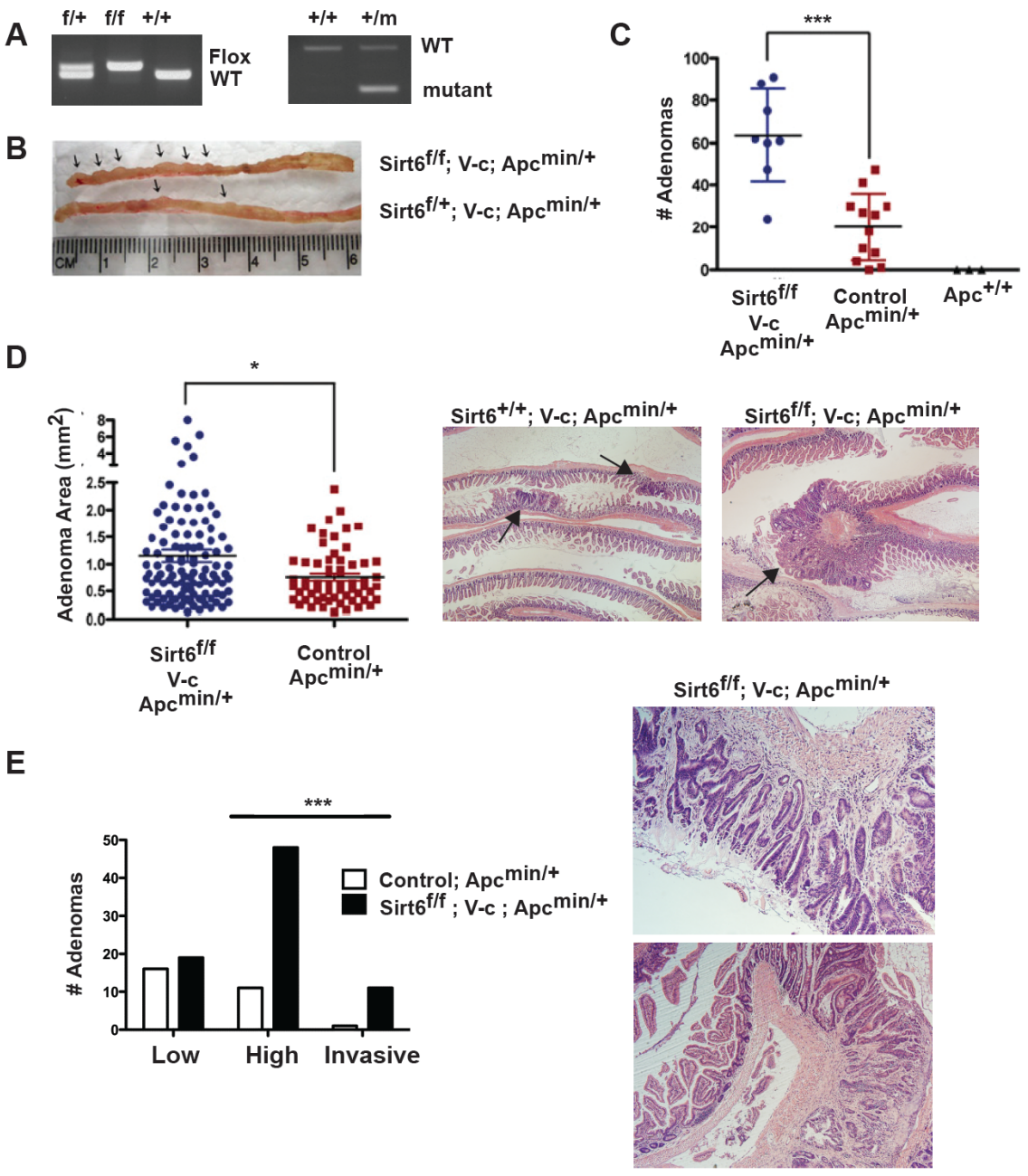

Figure 3.9: Increased tumorigenesis in SIRT6-deficient intestinal mouse model

(A) PCR showing the floxed *Sirt6* allele (left) and the Apc mutant allele (right). (B) Representative image of intestines from *Sirt6*$^{f/f}$; *V-c*; *Apc*$^{min/+}$ and littermate controls. (C) Adenoma count in intestines of SIRT6-deficient *Apc*$^{min/+}$ mice and littermate controls. (D) Adenoma area from indicated mice (left) with representative images from hematoxylin and eosin (H&E) stained intestines (right). (E) Quantification of the tumor grade in indicated mice (left) with representative images of invasive phenotype in *Sirt6*$^{f/f}$; *V-c*; *Apc*$^{min/+}$ mice. Tumor grading in figure E was carried out by Dr. J. Greenson (Sebastian et al., 2012).

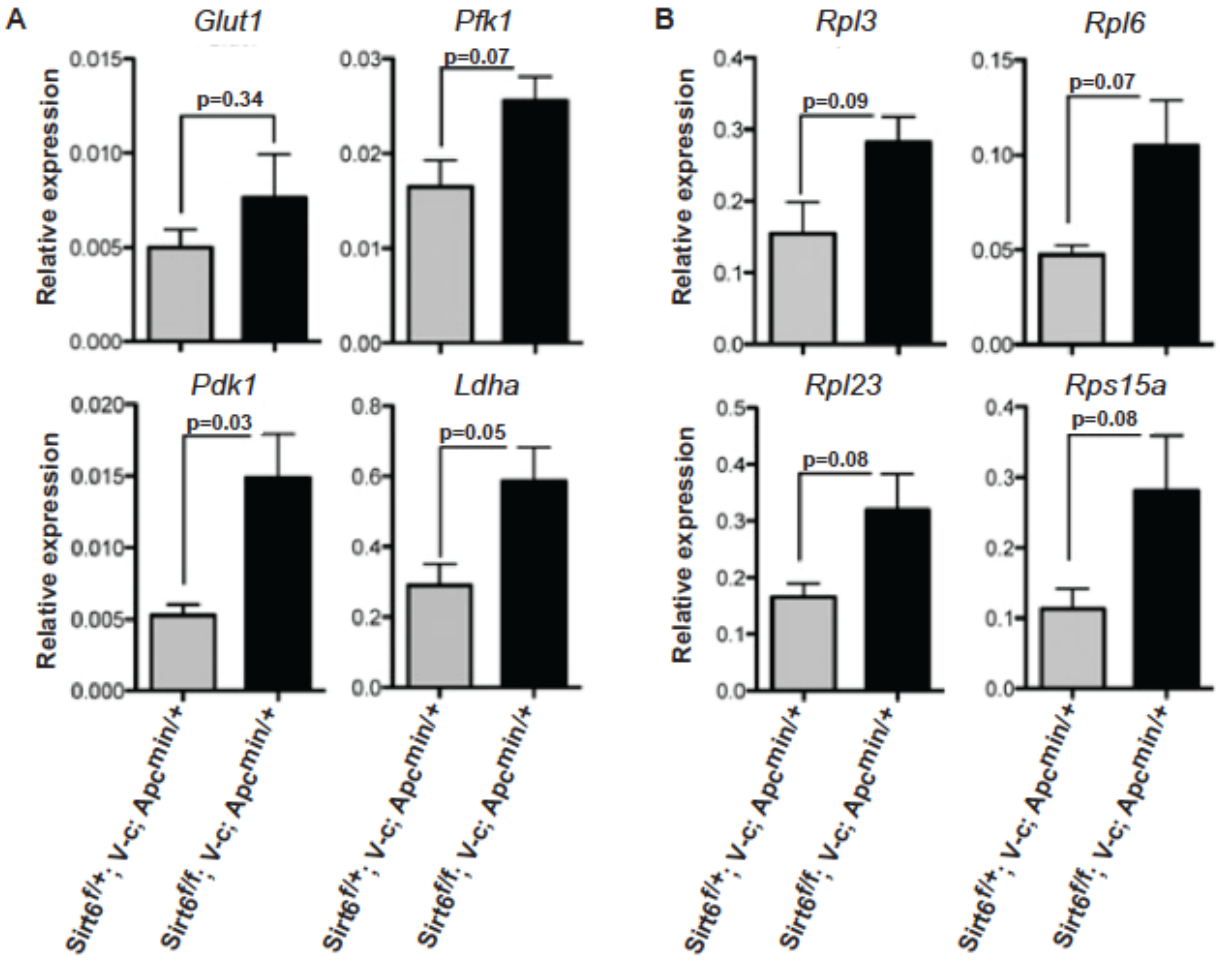

Figure 3.10: Enhanced glycolytic and ribosomal gene expression in mouse adenomas

Expression of various glycolytic (A) and ribosomal (B) genes in Sirt6 proficient and deficient adenomas derived from *Apc*$^{min/+}$ mice (n=3) (error bars indicate SEM). Experiments were performed by Dr. C. Sebastián (Sebastian et al., 2012).

stained normal human colons and human adenomas for SIRT6 and observed a decrease in SIRT6 levels in adenomas in comparison to normal tissue (Figure 3.12). Overall our study shows that SIRT6 inhibits the initiation of colorectal cancer *in vivo* by repressing aerobic glycolysis and ribosomal gene expression (Figure 3.13).

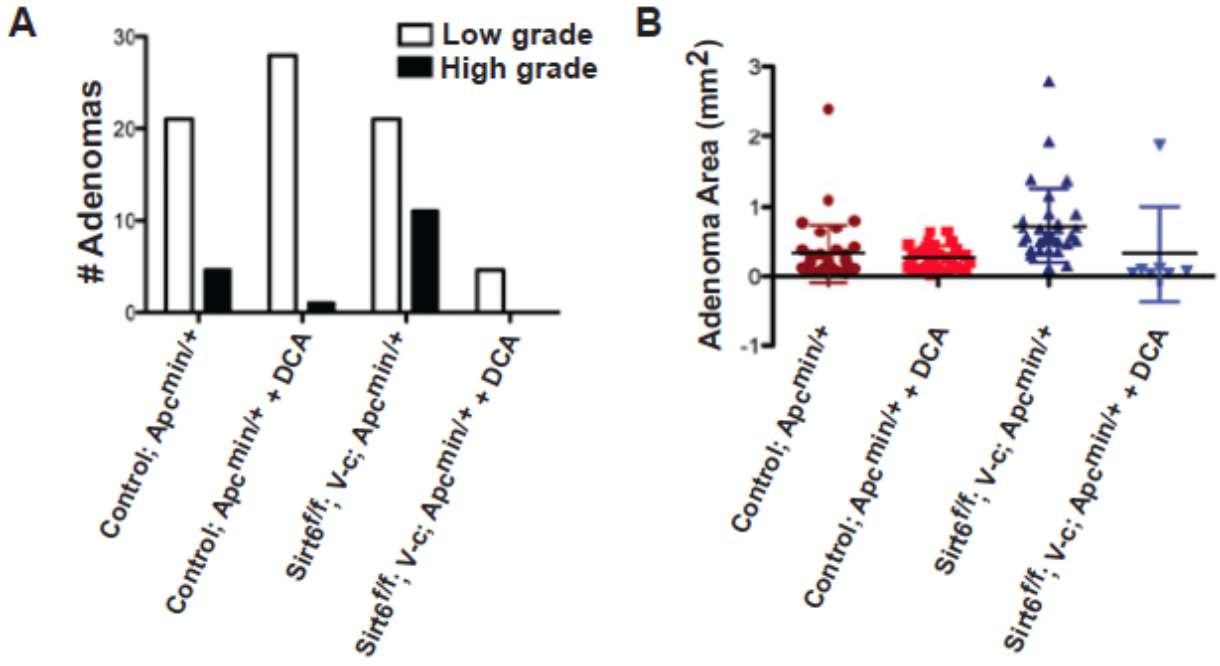

Figure 3.11: Inhibition of glycolysis decreases tumorigenesis of SIRT6-deficient adenomas

Tumor grade (A) and area (B) of *Sirt6*$^{f/f}$; *V-c*; *Apc*$^{min/+}$ and Control; *Apc*$^{min/+}$ mice untreated or treated with DCA (5g/L). Experiments were performed by Dr. C. Sebastián, tumor grading was carried out by Dr. J. Greenson (Sebastian et al., 2012).

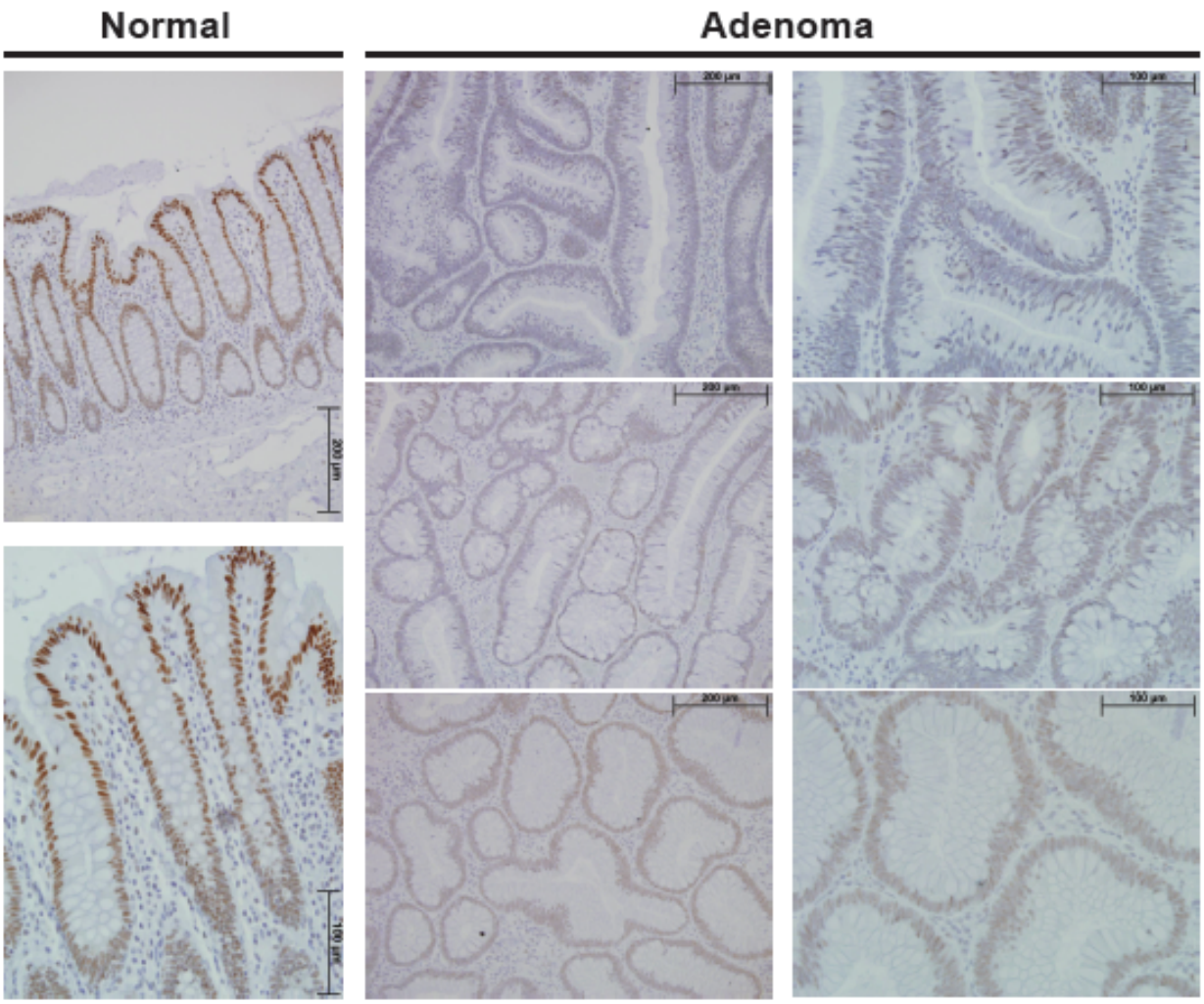

Figure 3.12: SIRT6 expression is decreased in human adenomas

Immunohistochemistry for human SIRT6 in human normal colon and colorectal adenomas. Right column is higher magnification of middle column.

Discussion

An increased incidence of neoplasia is a major feature of aging in mammals. SIRT6's functions in regulating glucose homeostasis, genomic stability and cellular senescence have prompted multiple groups to assess roles for SIRT6 in cancer. Our work has revealed that SIRT6 functions as a tumor suppressor, at least in part by modulating cellular metabolism and c-Myc induced cellular proliferation. SIRT6-deficient mouse embryonic fibroblast cell lines, immortalized by a 3T3 serial passage protocol or p53 knockdown, show increased proliferation relative to controls. In contrast to controls, these cells are able to form colonies *in vitro* and tumors *in vivo*. These results are consistent with a cell-autonomous tumor suppressor role for SIRT6. Furthermore, conditional deletion of *Sirt6* in intestinal epithelial cells in the $Apc^{min/+}$ adenomatosis model results in a three-fold increase in the number of tumors, which are larger and of higher grade than lesions in littermate controls. Furthermore, SIRT6 protein levels are reduced in human adenomas relative to normal tissue. These data support a tumor suppressor role for SIRT6 in mice and potentially in humans as well.

Molecularly, SIRT6 deficiency leads to increased levels of glycolytic gene expression. Ribosomal biogenesis and glutaminase expression are also elevated in the absence of SIRT6; these are regulated by the proto-oncogene c-MYC. Mechanistically, SIRT6 interacts with c-MYC and deacetylates H3K56 at the promoters of c-MYC target genes, attenuating their expression. Inhibition of c-MYC in the absence of SIRT6 reduces cellular proliferation and inhibits tumor growth, indicating that SIRT6 acts as a tumor suppressor at least in part by inhibiting c-MYC activity.

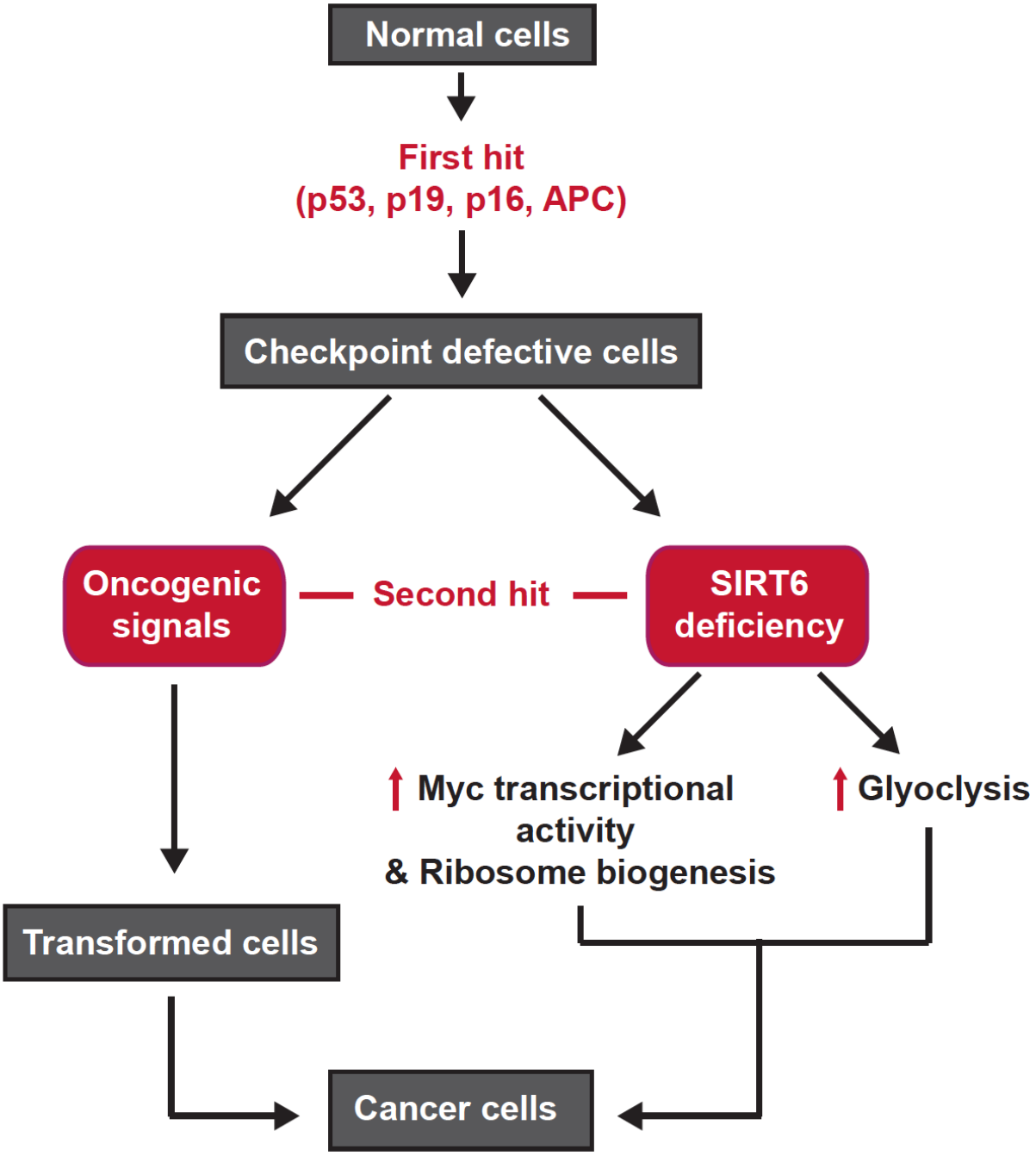

Figure 3.13: Schematic overview of the role of SIRT6 as a tumor suppressor

A first mutation in cell cycle or growth regulatory genes renders normal cells checkpoint defective. Inactivation of SIRT6 in these cells drives tumorigenesis through two distinct pathways: (1) enhancing glycolysis and (2) increasing Myc transcriptional activity and ribosome biogenesis. Figure adapted from (Sebastian et al., 2012)

In addition to targeting c-MYC, SIRT6 inhibits HIF-1α transcriptional activity resulting in decreased glycolysis. Cancer cells shift their energy production from mitochondrial respiration to glycolysis and lactate production (Warburg effect) (Warburg, 1956). Upon SIRT6 ablation, increased HIF-1α activity causes reprogramming of cellular metabolism by enhancing glucose uptake and glycolysis, providing SIRT6 deficient cells with tumorigenic potential. Conversion of pyruvate to lactate is the rate-limiting step in glycolysis, and blocking this step is able to enhance mitochondrial respiration, reducing proliferation and inhibiting colony formation of SIRT6-deficient cells. Similarly, treating adenoma-prone SIRT6 deficient mice with dichloroacetate (DCA), a small molecule that promotes mitochondrial respiration, reverts increased tumorigenesis of these mice *in vivo*. Finally, lower SIRT6 protein levels were observed in human adenomas. Consistent with this finding, decreased SIRT6 expression has been reported in hepatocellular carcinomas (HCC), and low levels of SIRT6 are associated with shortened time to recurrence in patients with this disease. Furthermore, liver-specific SIRT6 KO mice have elevated levels of HCC biomarkers (e.g. AFP, IGF2 and H19) and re-expression of SIRT6 in HCC cell lines sensitizes these cells to chemotherapeutic drugs resulting in increased apoptosis (Marquardt et al., 2013a). This indicates that decreased SIRT6 expression in some tumors is correlated with more aggressive clinical behavior.

SIRT6 plays tumor suppressor functions in other contexts as well. Overexpression of SIRT6 can induce apoptosis specifically in cancer cells through p53 or p73 (Van Meter et al., 2011). P53 is a tumor suppressor that is mutated or inactivated in most human cancers. Both p53 and its homolog p73 are involved in cell cycle regulation and induction of apoptosis (Murray-Zmijewski et al., 2006). Additionally, SIRT6 can prevent tumor formation in liver cells by blocking RELA-mediated expression of survivin to promote cell survival (Min et al., 2012). Survivin is a member of the inhibitor of apoptosis (IAP) family and inhibits cell death. It is mainly expressed during embryogenesis and, with the exception of a few cell types, is not normally expressed in adult tissue (Church and Talbot, 2012). In human dysplastic liver nodules, c-JUN interferes with c-FOS transcriptional output. As *Sirt6* is a target of c-FOS, c-JUN thereby inhibits *Sirt6* expression. Decreased SIRT6 levels coincide with increased acH3K9 levels at the survivin promoter, allowing for increased NF-κB-driven expression of this gene (Min et al., 2012). Survivin is only upregulated during the initiation phase of liver cancer, as survivin levels were not altered in normal livers or in advanced hepatic carcinomas (Min et al., 2012). Furthermore, a recent study showed that Sirt6 mRNA levels are decreased in human non-small cell lung cancer (NSCLC) and that overexpression of SIRT6 in lung cancer cell lines decreased cellular proliferation by inhibiting the expression of *Twist1* (Han et al., 2014). Finally, in breast cancer cell lines, SIRT6 is phosphorylated by AKT and consequently degraded by MDM2. Inhibition of MDM2 mediated degradation of SIRT6 suppresses cellular proliferation, and low levels of phosphorylated SIRT6 (Ser 338) is positively correlated

with breast cancer patient survival (Thirumurthi et al., 2014). These findings indicate that SIRT6 functions as a tumor suppressor in multiple tissues, and suggest that SIRT6 activators could be useful therapeutic tools for cancer treatment, potentially in both early-stage and advanced lesions.

Future directions

Our striking results demonstrating SIRT6 as a potent tumor suppressor, raises the question whether SIRT6 activators would provide protection against tumor formation. Kanfi and colleagues demonstrated that whole body SIRT6 overexpressing mice have an extended lifespan (Kanfi et al., 2012) and it was postulated by others that this could be explained by a decrease in cancer incidence (Lombard and Miller, 2012). In a small pilot study we crossed *Apc*$^{min/+}$ mice with an inducible SIRT6 overexpressor, in which an extra copy of the *Sirt6* gene, at the Rosa26 locus driven by a tet inducible promoter, was inserted in the genome. At five weeks of age, doxycycline was added to the drinking water resulting in whole body SIRT6 overexpression. After 150 days, mice were sacrificed and polyps were counted (Figure 3.14). We observed no difference between *Sirt6* WT and *Sirt6* OE *Apc*$^{min/+}$ mice, which could indicate that overexpression of SIRT6 does not provide additional protection against tumor development. It is also possible that SIRT6's tumor suppressor function is dependent on co-factors, which could be the rate-limiting factor in increasing SIRT6 activity. Furthermore, we observed that the number of polyps in the *Sirt6* OE mice varied strongly between each mouse, possibly due to the variability in doxycycline water consumption by each mouse. To overcome this issue, a constitutive SIRT6 overexpressor might be a more suitable

model (Kanfi et al., 2012). Finally, it is plausible that long-term treatment with doxycycline could have adverse effects, which could affect adenoma formation *in vivo*. Thus, due to many confounding factors, we cannot conclude at this point that high levels of SIRT6 provide additional protection against tumor formation. Further studies with either a constitutive Sirt6 overexpressor or with Sirt6 activators would be a superior approach. Aditionally, we could reexpress SIRT6 using adenoviral infection in our *Apc*$^{min/+}$ mouse model shortly after adenoma formation. Based on the role of SIRT6 in suppressing aerobic glycolysis and c-MYC mediated cellular growth, we would assume that *Sirt6* reexpression could prevent tumor growth and would support the therapeutic potential of SIRT6 activators, especially in tumors with the actived oncogene c-MYC. However, if Sirt6 reexpression is unable to rescue the enhanced tumorigenesis phenotype in *Sirt6* mutant mice, SIRT6 likely exerts its tumor suppressor function through additional mechanisms.

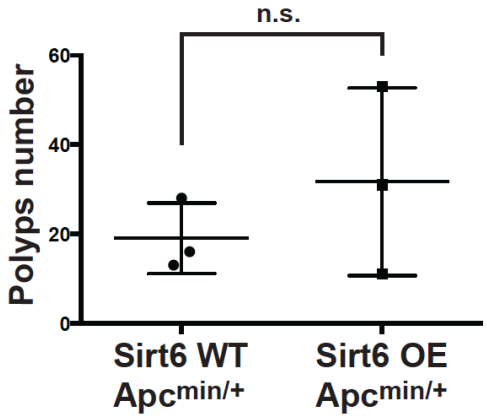

Figure 3.14: Polyp number in SIRT6 overexpressing mice

Mice carrying an inducible SIRT6 OE system (Rosa 26) were crossed with *Apc*$^{min/+}$ mice. The number of adenomas were counted macroscopically at day 150 (n=3; Man Whitney t-test).

Despite our identification of a tumor suppressor function for SIRT6, multiple other groups demonstrated that SIRT6 possess tumor-promoting properties (Bauer et al., 2012; Khongkow et al., 2013b; Liu et al., 2013). It is feasible that SIRT6 has different properties based on tumor stage, with protective properties in the initial stages of tumorigenesis and tumor enhancing traits in established cancer. Furthermore, it is likely that SIRT6's role in cancer is tissue dependent. Thusfar, no other research group has assessed a role for SIRT6 in tumor development as all other studies were done using already established cancer cells. The pathways affected in the absence of SIRT6, as described in this chapter, are derailed in many cancer types. Thus it is likely that deletion of SIRT6 in other tumor models would provide a similar outcome. It would be of interest to develop additional mouse tumor models to assess the tumor suppressor role for SIRT6 in different tissues and to rule out a tissue specific effect of SIRT6.

Chapter 4

SIRT6 protects against aneuploidy

Abstract

Identification of novel genes and pathways with functional roles in cancer holds out the eventual prospect of improved treatments. We recently identified a major function for SIRT6 as a tumor suppressor through the regulation of cellular metabolism. In addition to mediating glucose metabolism, SIRT6 plays a crucial role in maintaining genomic integrity by enhancing various DNA repair pathways. In this study we aspired to identify a second mechanism through which SIRT6 protects against tumorigenesis. We found that SIRT6 maintains normal chromosome number in mouse embryonic fibroblasts and intestinal epithelial cells. Aberrant chromosomal number is a major feature of human cancers. In this study we explore two potential pathways that can lead to aneuploidy in cells: major satellite repeat instability and elevated reactive oxygen species.

Introduction

The acquisition of cancer hallmarks is in large part dependent on genomic instability and the accumulation of mutations (Hanahan and Weinberg, 2011). One form of chromosomal abnormality, as a result of genomic instability, is the gain or loss of whole chromosomes resulting in cells containing an odd chromosome number (= aneuploidy). At least one quarter of the genome of cancer cells is affected by chromosome copy number alterations (Beroukhim et al., 2010) and gain or loss of specific chromosomes is associated with particular cancer types. For example, loss of chromosome 3 is observed in 50% of melanomas tested, while an additional copy of this chromosome is detected in approximately 22% of multiple myeloma cases (Gordon et al., 2012). It is debated whether aneuploidy in cancer cells is a consequence of genome instability or a driver of tumorigenesis (Gordon et al., 2012). The consequences of aneuploidy can be two-sided. Individuals with trisomy 21 have a significantly increased incidence for hematological cancers, but a notable decrease in the occurence of solid tumors (Malinge et al., 2009). The maintenance of euploidy requires proper chromosome segregation. While a basal rate of spontaneous chromosome missegregation is common under tissue culture conditions, disruption of pathways or genes involved in this process can result in increased aneuploidy (Gordon et al., 2012). For example, centrosome amplification, which often occurs in tumors *in vivo*, has a strong correlation with chromosome instability (Pihan et al., 2003). Additionally, loss of major satellite repeats silencing has also been associated with increased aneuploidy. Major satellite repeats (MSR), a pericentromeric region comprised of an AT rich sequence of approximately 234bp, repeated about 10,000 times in every chromosome and making

up 10% of the mouse genome, play an important role in regulating chromosome separation during cell division (Guenatri et al., 2004). Furthermore, chromosome missegregation due to impaired MSR silencing has been associated with neoplasia (Bernard et al., 2001; David et al., 2006; Peters et al., 2001). The expression of MSRs is elevated in mouse tumors (Eymery et al., 2009; Ting et al., 2011), and enforced expression of this region is sufficient to induce genomic instability (Zhu et al., 2011). Alternatively, elevated reactive oxygen species (ROS), which are chemically reactive molecules that contain oxygen with one or more unpaired electrons, can induce aneuploidy. ROS cause the most frequent DNA damage in living cells and can trigger aneuploidy by interfering with some of the pathways involved in mitosis (Wang et al., 2013). Numerous cellular defense mechanisms are in place to protect against ROS-induced DNA damage, such as antioxidants and DNA repair systems. Malfunctioning ROS defense systems can therefore also drive aneuploidy.

As discussed previously, SIRT6 deficiency results in genomic instability and increased sensitivity to DNA damaging agents due to SIRT6's role in regulating several DNA repair pathways (Cardus et al., 2013; Kaidi et al., 2010; Mao et al., 2012; McCord et al., 2009; Mostoslavsky et al., 2006; Toiber et al., 2013). SIRT6 was initially postulated to play a role in BER (Mostoslavsky et al., 2006). While this finding has not been further explored, multiple studies have identified a role for SIRT6 in regulating DNA double strand break repair by recruiting a number of DNA repair factors to the breakage site (Kaidi et al., 2010; Mao et al., 2012; McCord et al., 2009; Toiber et al., 2013). We previously reported that SIRT6 acts as a tumor suppressor protein by

regulating glucose metabolism; however the genomic instability observed in *Sirt6*-null cells suggests that SIRT6, at least in part, can protect against tumor initiation by inhibiting the accumulation of chromosomal aberrations. In this study we aimed to identify a second mechanism through which SIRT6 protects against tumorigenesis.

Materials and Methods

Cell culture

In our studies we used mouse embryonic fibroblasts (MEFs), which were isolated from C57Bl/6 wild type and *Sirt6* knockout embryos (E13.5) according to standard conditions. MEFs were grown in DMEM supplemented with 15% fetal bovine serum, 1% L-Glutamine, 1% pen/strep, 1% sodium pyruvate, 1% non-essential amino acids, 2% HEPES and 115 µl beta-mercaptoethanol. MEFs were grown at low oxygen conditions, split 1:3 with each passage and maintained in culture up to passage 8. For the aneuploidy study, MEFs were cultured for 4 passages in normoxia prior to inducing cell cycle arrest in metaphase with colcemid (Life Technologies). Wild-type and *Suv39h1/2* KO immortalized MEFs (iMEFs) were grown in the same media as the primary MEFs.

Wild type and *Sirt6* KO embryonic stem (ES) cells were used for endogenous co-immunoprecipitation of SIRT6. ES cells were grown on 0.2% gelatin coated plates in MEF media supplemented with LIF (Invitrogen).

Intestinal epithelial cells (IEC-6) were grown in DMEM supplemented with 10% FBS, 4 mM L-glutamine, 1.5 g/L sodium bicarbonate, 4.5 g/L glucose and 0.1 Unit/ml bovine insulin.

Metaphase spreads

Mouse embryonic fibroblasts were treated with colcemid (10 µg/ml) for 4 hours to arrest cells in metaphase. MEFs were harvested, washed twice with PBS and resuspended in 0.4% KCl. After 15 minutes of incubation at 37°C, 2 ml of freshly prepared fixative (methanol:glacial acedic acid – 3:1) was added. The cells were pelleted at 1200 rpm for 8 minutes and subsequently subjected to 4 rounds of fixation – 10 ml of fixative was slowly added to the cell pellet while gently vortexing the tube and spun down. Finally the fixed cells were resuspended in a small amount of fixative, dropped on slides and mounted with prolong gold containing dapi stain (Invitrogen).

Immunoprecipitation

HCT116 cells knocked down for *Sirt6* (shRNA TripZ vector) (see chapter 5) were transfected with the pCDNA3.1 vector containing human FLAG-SIRT6 using Lipofectamine LTX reagent (Life Technologies). After 48 hours, cells were gently scraped of the dish and washed twice in PBS. The cell pellet was resuspended in cell lysis buffer (1% triton x-100, 0.5% NP-40, 150 mM NaCl, 50 mM Tris pH 7.4, 10% glycerol, protease inhibitor cocktail (Roche)) and allowed to lyse for 30 minutes on ice. Cells were sonicated for 2 x 20 seconds using a Branson Sonifier 450 sonicator at 2.5% output control and 50% duty cycle. After centrifugation, the supernatant was collected and protein concentration was measured using DC assay (Bio-Rad).
For the immunoprecipitation, 50 µl of protein G agarose beads (Roche) were added to 2 mg protein lysate diluted in a total volume of 1ml lysis buffer and rotated for 1 hour at 4°C to preclear. The samples were spun down for 5 minutes at 1000 rpm and the

pelleted beads were discarded. The supernatant was subsequently incubated overnight in 50 ul of FLAG-M2 agarose beads (Sigma). The samples were spun down 5 minutes at 1000 rpm in a refrigerated tabletop centrifuge at 4°C. The supernatant was discarded and the beads were washed 3 times in 1 ml lysis buffer. FLAG-SIRT6 was eluted 2 times using 250 ng/ml of FLAG peptide in PBS + proteinase inhibitors by rotating 15 minutes at RT and both elutions were combined. IP reactions were fractionated on a 4-20% gradient gel (Bio-Rad) and proteins were subsequently visualized with Coomassie stain (BioRad). Mass spectrometry was performed to identify proteins co-immunoprecipitated with FLAG-SIRT6.

For endogenous IPs, mouse embryonic stem cells were grown in a 15 cm dish and harvested at 90% confluency. Nuclei were isolated by resuspending the cell pellet in hypotonic buffer (10 mM HEPES pH 7.5, 10 mM KCl, 1.5 mM $MgCl_2$, 0.5 mM DTT) supplemented with 0.5% NP-40 and proteinase inhibitor cocktail (Roche), incubated on ice for 10 minutes and spun down for 5 minutes at 500 x g. The pellet was washed once in hypotonic buffer and then resuspended in lysis buffer (450 mM NaCl, 20 mM HEPES and 0.5% NP-40. After rotation at 4°C for 20 minutes, the samples were sonicated using a Branson Sonifier 450. Subsequently, the samples were treated with DNase for 25 minutes in a 37°C water bath and spun down at maximal speed at 4°C to discard of any cellular debris. At this point, protein concentration was measured (DC assay, BioRad) and 1 mg of protein was diluted with 20 mM HEPES + proteinase inhibitor cocktail to a final concentration of 115 mM NaCl, 20 mM HEPES and 0.125% NP-40. Samples were pre-cleared with protein A agarose beads (Invitrogen) for 1 hour on a rotator at 4°C. After removal of the beads with a brief centrifugation, the protein

samples were incubated with mouse SIRT6 antibody (Cell Signaling) overnight at 4°C on a rotator. Mouse SIRT6 was precipitated with protein A agarose beads, washed three times in 115 mM NaCl, 20 mM HEPES, 0.125% NP-40 and proteinase inhibitor cocktail. Beads were boiled in 2x Laemmli buffer (100mM Trish-HCl pH 6.8, 2% SDS, 20% glycerol, 4% beta-mercaptoethanol and a dash of bromophenol blue).

Chromatin immunoprecipitation (ChIP)

ChIP was performed using standard conditions (see chapter 3). MEFs were cross-linked using formaldehyde, lysed and sonicated to obtain 200-1000bp DNA fragments. For each immunoprecipitation reaction, 10 µg protein was used. The following antibodies were utilized for ChIP to MSR: rabbit anti-mSIRT6 (Cell Signaling Technologies), rabbit anti-H3K9ac (Abcam), rabbit anti-H3K56ac (Abcam), rabbit anti-H3K9me3 (Abcam), rabbit anti-H3K56me3 (kind gift of Dr. S Hake), and rabbit anti-KAP1 (Abcam).

Real-time PCR

Wild type and *Sirt6* KO MEFs were grown to 80% confluency, harvested and lysed in TRIzol reagent (Life Technologies). According to manufacturer's instructions, RNA was further isolated by performing phenol:chloroform (pH 4.3) extraction and subsequently precipitated with 100% ethanol. The RNA pellet was washed once in 75% ethanol and resuspend in RNAse/DNAse free water. 50 µg RNA was treated with 5 µl DNAseI (Roche) according to the manufacturer's instructions, subjected to phenol/chloroform extraction and resuspended at a final concentration of 500 ng/µl in DNAse/RNAse free

water. Reverse transcription was performed using the high capacity cDNA reverse transcription kit (Life Technologies) and quantitave PCR was performed using SYBR green select PCR master mix (Life Technologies). Primers for the detection of major satellite repeat transcripts: MSR 5' GACGACTTGAAAAATGACGAAATC, MSR 3' CATATTCCAGGTCCTTCAGTGTGC.

Northern Blot

Total RNA was extracted from WT and *Sirt6* KO MEFs using TRIzol reagent (Invitrogen), according to the manufacturer's instructions. Precipitated RNA was resuspended in 500 ml of RNAse-free H_2O and incubated at 56ºC for 10 minutes and returned to room temperature. To remove contaminating genomic DNA, RNA was incubated with 100 units of RNAse-free DNAse I (Roche) at 37ºC for 30 minutes in the presence of 40 units of RNAse inhibitor (Roche). RNA was precipitated with two rounds of phenol (pH 5.2):chloroform extraction was preformed, followed by a final extraction using only chloroform. RNA was then ethanol precipitated in the presence of 0.3 M sodium acetate pH 5.2 overnight at -20ºC, spun down and washed twice with 500ml of 70% ethanol. RNA was resuspended in RNAse-free H_2O. RNA integrity was confirmed by gel electrophoresis.

An equal volume of NorthernMax-Gly Sample Loading Dye (Ambion) was added to 5 mg of total RNA and incubated for 30 minutes at 56ºC. Samples were resolved on a 1% Bis-Tris-PIPES-EDTA agarose gel at 5 V/cm (as measured between electrodes). Resolved RNA was transferred overnight onto a pre-wet Zeta Probe membrane (Bio Rad) by upward capillary action using 10X SSC as the solvent. Once transferred, the

membrane was briefly rinsed in 2X SSC and UV crosslinked in a Stratalinker (Stratagene). The membrane was prehybridized for 1 hour at 68ºC in ULTRAhyb Hybridization Buffer (Ambion). During prehybridization, 1 mg of the MSR dsDNA template containing the T7 promoter was used to generate a radiolabelled riboprobe using the T7 MAXIscript Kit (Ambion) and isotopically labeled UTP, [a-32P] (Perkin Elmer), according to manufacturer's instructions. The labeled probe was purified in a MicroSpin G-25 column (GE Healthcare). The prehybridized membrane was incubated with the probe overnight at 68ºC and washed for 30 minutes at 68ºC twice in 2X SSC, twice in 2X SSC, 0.1% SDS and twice in 0.1X SSC, 0.1%SDS. The membrane was imaged by autoradiography.

Immunocytochemistry

MEFs were grown on chamberslides (BD biosciences) for 24 hours prior to staining. Each well was briefly washed with 1x PBS, CSK buffer (100 mM NaCl, 300 mM sucrose, 3 mM $MgCl_2$, 10 mM PIPES, at final pH 6.8) and subsequently incubated in CSK/0.5% Triton x100 for 5 minutes. After a wash in CSK, cells were fixed in 3% PFA in PBS for 10 minutes. Following 30 minutes of incubation in blocking buffer (1% BSA, 0.1% Tween-20 in PBS), cells were treated for 1 hour with primary antibody in blocking buffer: rabbit anti-KAP1 (Abcam), 1:100; rabbit anti-HP1α (Abcam), 1:50; rabbit anti-H3K9me3 (Abcam), 1:100; rabbit anti-H3K56me3 (kind gift of Dr. S Hake), 1:200. Slides were washed three times in PBST (PBS with 0.2% Tween-20), incubated in blocking buffer containing FITC conjugated goat anti-rabbit (Invitrogen, 1:200) for 30 minutes, and washed again in PBST. Slides were mounted with ProLong Gold antifade

mounting media with DAPI (Life Technologies) and imaged with an Olympus BX-51 scope with an Olympus DP-70 high-resolution digital camera (University of Michigan Microscopy & Image Analysis lab).

Immunoblot analysis

For analysis of immunoprecipitated samples, 25% of the immunoprecipitate was fractionated on 4-20% gradient gels (Bio-Rad), transferred to PVDF membranes, and probed with the following antibodies in TBST/5% milk at the dilutions indicated: rabbit anti-HP1α (Abcam), 1:1000; rabbit anti-HP1β (Abcam), 1:1000; rabbit anti-HP1γ (Abcam) 1:1000; mouse anti-SPT16 (Santa Cruz Biotechnology), 1:500; mouse anti-SSRP1 (Santa Cruz Biotechnology), 1:500; rabbit anti-mouse SIRT6 (Cell Signaling), 1:1000; rabbit anti-H3 (Abcam), 1:10.000; rabbit anti-HMGB1 (Proteintech), 1:1000.

NAC treatment mice

Apc$^{min/+}$ with specific deletion of Sirt6 in the mouse epithelial cells (*Sirt6*$^{f/f}$; *V-c*) were bred and instestines were harvested and processed as previously described (Chapter 3). Mice treated with the antioxidant N-acetyl cysteine (NAC) were given drinking water containing 40 mM NAC (Sigma) starting at two months of age. Water bottles were exchanged every 5 days.

ROS levels

In each well of a 6-well dish 2 x 10^5 WT or *Sirt6* KO MEFs were plated for 3 different treatment conditions: untreated, H_2O_2 or NAC (Sigma). The NAC treated cells were

grown in culture media supplemented with 1 mM NAC for 24 hours prior to harvesting. Four hours prior to harvesting fresh media was added to the cells. Cells were treated with 5 μM DCFDA (dichlorofluorescin diacetate; Invitrogen) for 30 minutes and harvested with trypsin. After two washes with PBS, the cells were resuspended in PBS. For the treatment groups, the PBS was supplemented with 0.03% H_2O_2, or 1 mM NAC. After an incubation of 15 minutes at room temperature in the dark, the cells were analyzed using a FACSCanto II and a 488 nm laser provided by the University of Michigan flow cytometry core facility.

Oxidative damage detection

Oxidative DNA damage was detected using an antibody-based immunoassay (DNA damage – AP site-assay kit; Abcam). The assay was performed according to manufacturers instructions. Briefly, *Sirt6* WT and KO MEFs were plated in 6-well dishes in the presence or absence of NAC. After 48 hours, cells were harvested through trypsinzation, fixed and incubated over night in ARP-binding solution. After a DNA denaturing step, the cells were incubated in a blocking solution and consequently stained with avidin-FITC. The samples were analyzed using a FACSCanto II and a 488nm laser provided by the University of Michigan flow cytometry core facility.

Results

Increased aneuploidy in the absence of SIRT6

Numerous studies have indicated that SIRT6-deficient cells are more sensitive to DNA damaging agents and have an increased number of chromosomal aberrations (Cardus et al., 2013; Kaidi et al., 2010; Mao et al., 2012; McCord et al., 2009; Mostoslavsky et al., 2006; Toiber et al., 2013). Mostoslavsky et al. identified elevated anomalies such as chromosome breaks and detached centromeres. In order to determine if these chromosomal abnormalities could explain the increased tumor incidence in SIRT6 deficiency, we made metaphase spreads from WT and *Sirt6* KO MEFs. In contrast to previous report, we did not observe chromosomal aberrations such as chromosomal breaks and detached centromeres (Figure 4.1A) however we did find increased aneuploidy in *Sirt6* KO MEFs in comparison to littermate controls. While a certain degree of aneuploidy is expected in primary cells due to increased oxidative damage as a result of *ex vivo* tissue culture (Foudah et al., 2009; Liu et al., 2012; Miyai et al., 2008), the absence of SIRT6 resulted in up to two-fold increase of anueploid cells in comparison to littermate controls (Figure 4.1B-C). Furthermore, when *Sirt6* was knocked down in immortalized rat intestinal epithelial cells (IEC-6) using a constitutive knockdown vector (GipZ), we again observed an increase in aneuploidy (Figure 4.1D). This data suggests that SIRT6 can protect against chromosome gain or loss in both primary and immortalized cells.

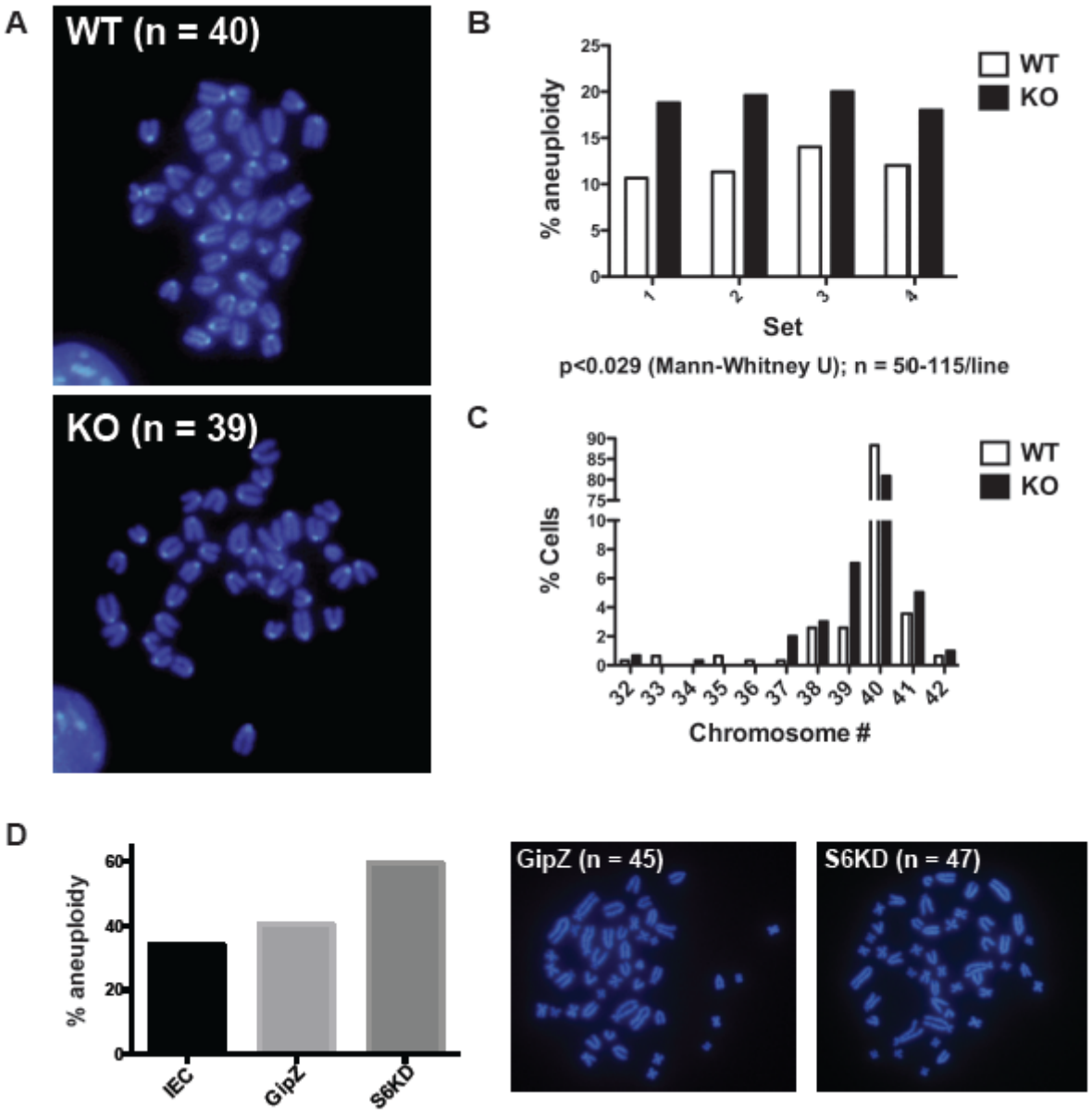

Figure 4.1: SIRT6-deficient cells show increased aneuploidy

(A) Metaphase spread of WT and *Sirt6* KO MEFs stained with Dapi. (B) percentage of aneuploid metaphase spreads in four sets of WT and *Sirt6* KO MEFs (n=50-115 spreads/cell line). Two sets were tested for aneuploidy by Dr. J. van Deursen and Janine Van Ree. (C) Percentage of cells containing the indicated number of chromosomes from the MEFs mentioned in (B). (D) Percentage of aneuploid IEC-6 cells, IEC-6 infected with control GipZ vector and IEC-6 infected with *Sirt6* KD GipZ vector. Experiments were done in collaboration with M. Skinner.

SIRT6 interacts with chromatin silencing factors

In conjunction with our aneuploidy study, we performed mass spectrometry in collaboration with Dr. Elenitoba-Johnson and Dr. Basrur to identify novel SIRT6 interactors. In this study, we transfected HCT116 cells with pCDNA3.1 FLAG-SIRT6 or empty vector and isolated SIRT6 with its interactors via FLAG IP. On a Coomassie stain we saw enrichment for SIRT6 and could identify histones, which SIRT6 is known to interact with (Figure 4.2A). Furthermore, mass spectrometry revealed a number of other known interactors of SIRT6, such as PARP1, which we confirmed by immunoblot (Figure 4.2A). In addition to these known SIRT6 binding partners, we identified a series of novel SIRT6 interactors that play a role in silencing and/or chromatin remodeling. Two such factors are KAP1 (KRAB-associated protein 1) and HP1β/γ (heterochromatin protein 1) (Figure 4.2B). KAP1 binding to the chromatin mediates gene silencing by suppressing H3K9 acetylation, promoting H3K9 methylation and recruiting HP1 to inhibit gene expression (Iyengar and Farnham, 2011; White et al., 2012). Thus KAP1 is a scaffold protein that assembles epigenetic factors and interacts with histone methyl transfereases and HDACs to remodel chromatin. To verify the mass spectrometry data, we performed endogenous SIRT6 IP in mouse WT and Sirt6KO ES cells. We confirmed that SIRT6 interacts with KAP1 and the three members of the HP1 protein family (HP1α, β and γ) (Figure 4.2C). In addition, SIRT6 binds both members of the FACT (facilitates chromatin transcription) complex, SPT16 and SSRP1, which are involved in multiple processes such as mRNA elongation, DNA replication and DNA repair (Figure 4.2C). Furthermore, we were not able to IP HMGB1,

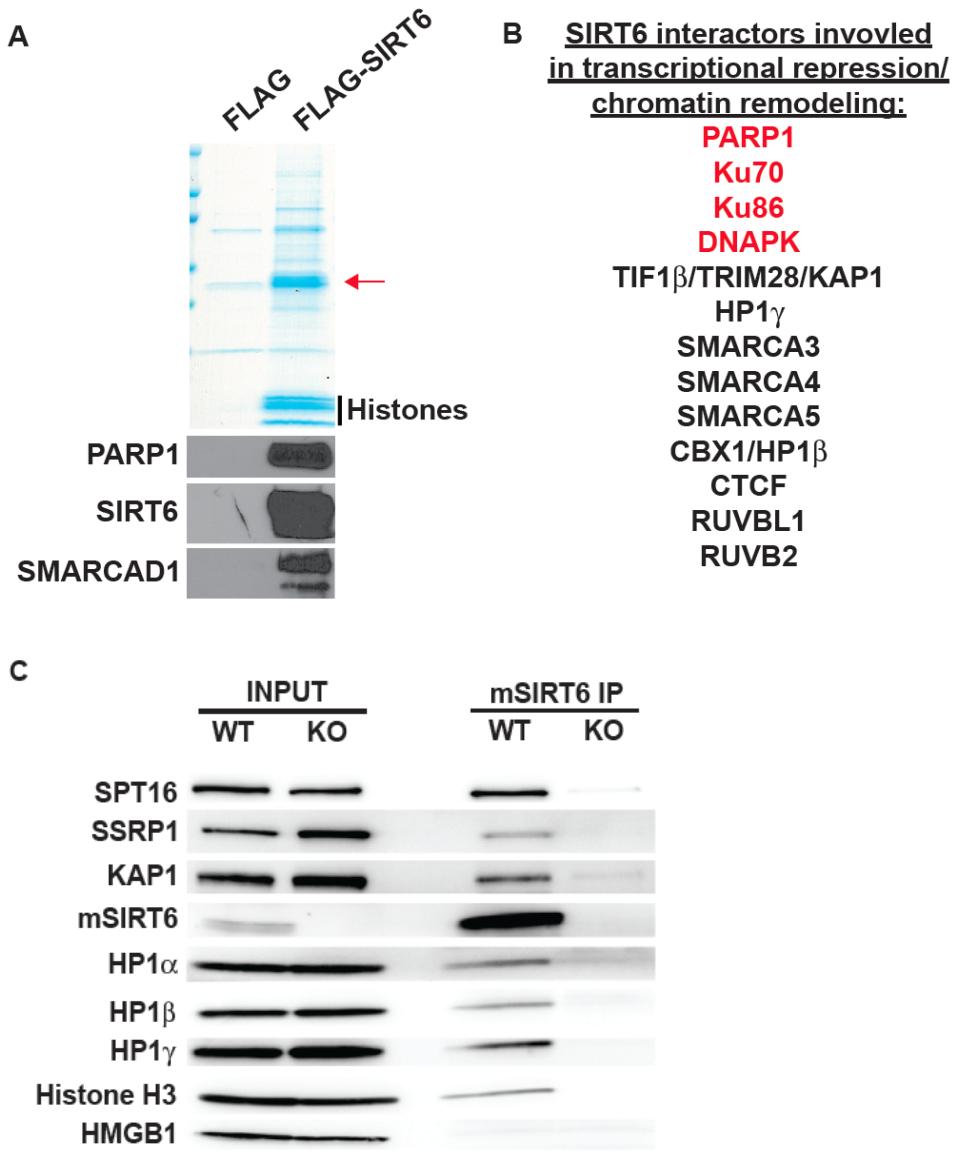

Figure 4.2: SIRT6 interacts with silencing factors

HCT116 cells containing *shSirt6* TripZ vector were transfected with pCDNA3.1 FLAG-SIRT6 or control vector and subjected to FLAG IP. (A) Coomassie stain of FLAG IP, red arrow indicates FLAG-SIRT6 band (top). The presence of SIRT6 and known interactor PARP1 were confirmed by immunoblot (below). (B) List of chromatin factors that were identified using mass spectrometry. Red factors indicate previously described interactors. (C) Endogenous IP of mSIRT6 in mouse ES cells shows interaction of SIRT6 with the chromatin factors SPT16, SSRP1, KAP1, HP1α/β/γ and histone H3. No iteraction of SIRT6 with HMGB1 was found. Mass spectrometry was performed in collaboration with Dr. K. Elenitoba-Johnson and Dr. V. Basrur.

which, according to our mass spectrometry data, is a chromatin factor that does not interact with SIRT6 (Figure 4.2C).

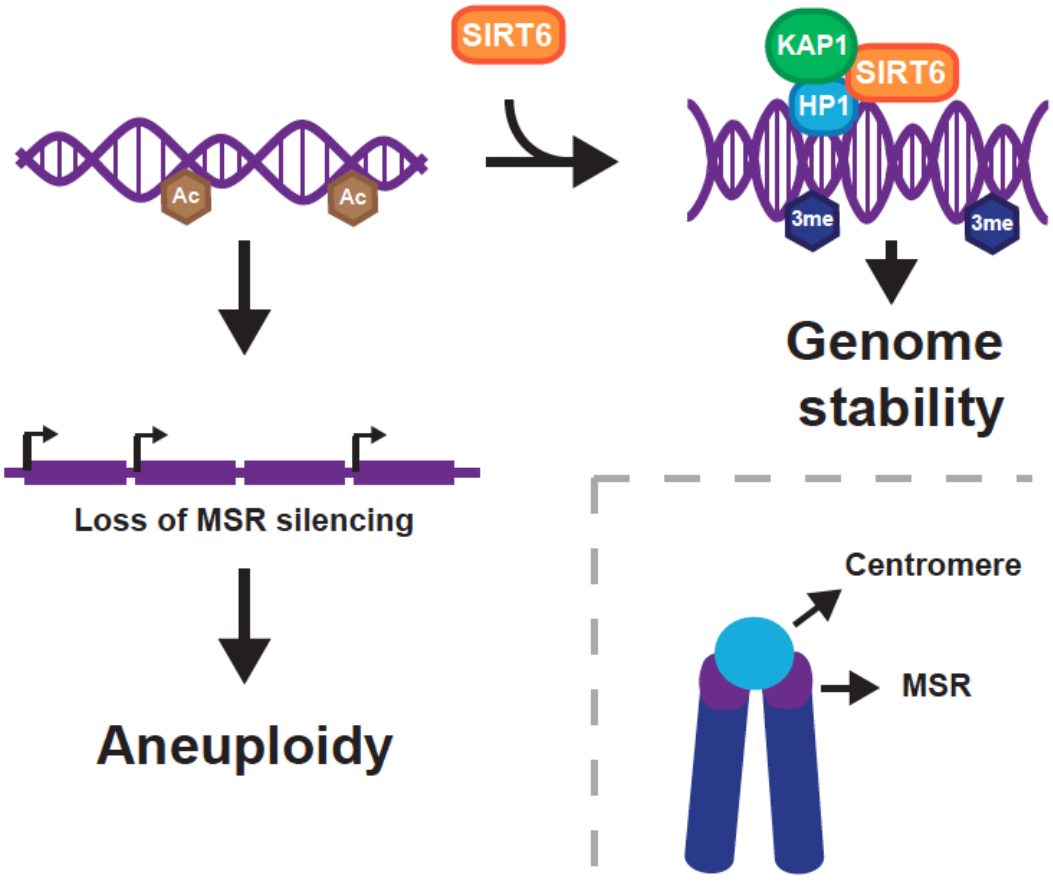

Figure 4.3: Hypothesis for SIRT6 mediated aneuploidy

SIRT6 binds and deacetylates Histone H3 residues at MSR, resulting in their methylation. In doing so, SIRT6 recruits the silencing factors KAP1 and HP1 to aid in compacting the DNA structure and prevent MSR expression. In the absence of SIRT6, histone acetylation at MSR results in high MSR expression and causes aneuploidy.

SIRT6 does not regulate histone modifications at MSR

The majority of aneuploidy occurs due to improper chromosome segregation (Gordon et al., 2012). Considering the importance of MSR stability in maintaining euploidy, that SIRT6 interacts with numerous silencing factors and the fact that yeast SIR2 has been shown to silence heterochromatin (Kaeberlein et al., 1999), we hypothesized that SIRT6 maintains proper chromosome number by deacetylating histone H3 at the MSR region, enhancing H3 methylation and recruiting the silencing factors KAP1 and HP1 (Figure 4.3).

To test whether SIRT6 plays a role in regulating pericentromeric heterochromatin, we performed a series of ChIP experiments in which we assessed SIRT6 binding to the MSR, the level of acetylation and methylation at MSR, and KAP1 interaction with MSR in response to *Sirt6* deletion. Due to the high abundance of MSR in the mouse genome and, consequently, the high risk of sample contamination, we first tested if we could observe a change in histone modification in immortalized *Suv39h1/2* WT and KO MEFs. SUV39H1/2 is a methyltransferase that methylates H3K9 at pericentric heterochromatin (Peters et al., 2001). Loss of SUV39H1/2 results in hypomethylation, increased MSR expression and increased chromosomal instabilities associated with an elevated tumor incidence (Peters et al., 2001). As predicted, loss of SUV39H1/2 resulted in a decrease in H3K9me3 levels, which coincided with an increase in H3K9ac (Figure 4.4A). However, we were unable to observe an interaction of SIRT6 with the MSR (Figure 4.4B), nor did we see a change in histone modifications

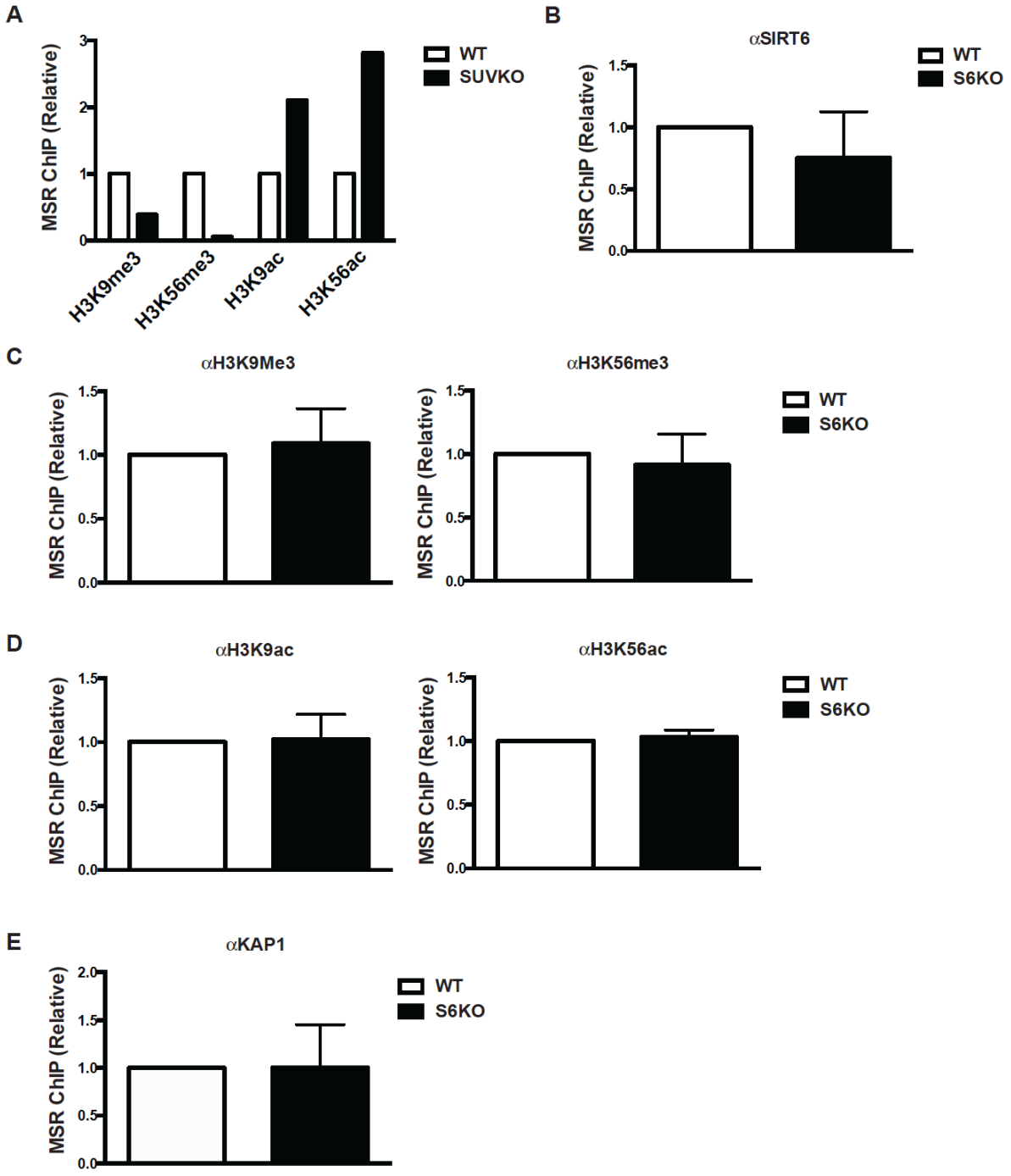

Figure 4.4: SIRT6 does not bind or regulate MSR

(A) ChIP of indicated histone marks at MSR in WT and *Suv39h1/2* KO iMEFs. (B) ChIP for SIRT6 to MSR (n=5). (C) ChIP for histone trimethylation to MSR in WT and *Sirt6* KO MEFs (n=6). (D) ChIP for H3K9ac (n=2) and H3K56ac (n=4) to MSR in same MEFs as (C). (E) ChIP for KAP1 to MSR same MEFs as (C) (n=6). N-value represents biological replciates

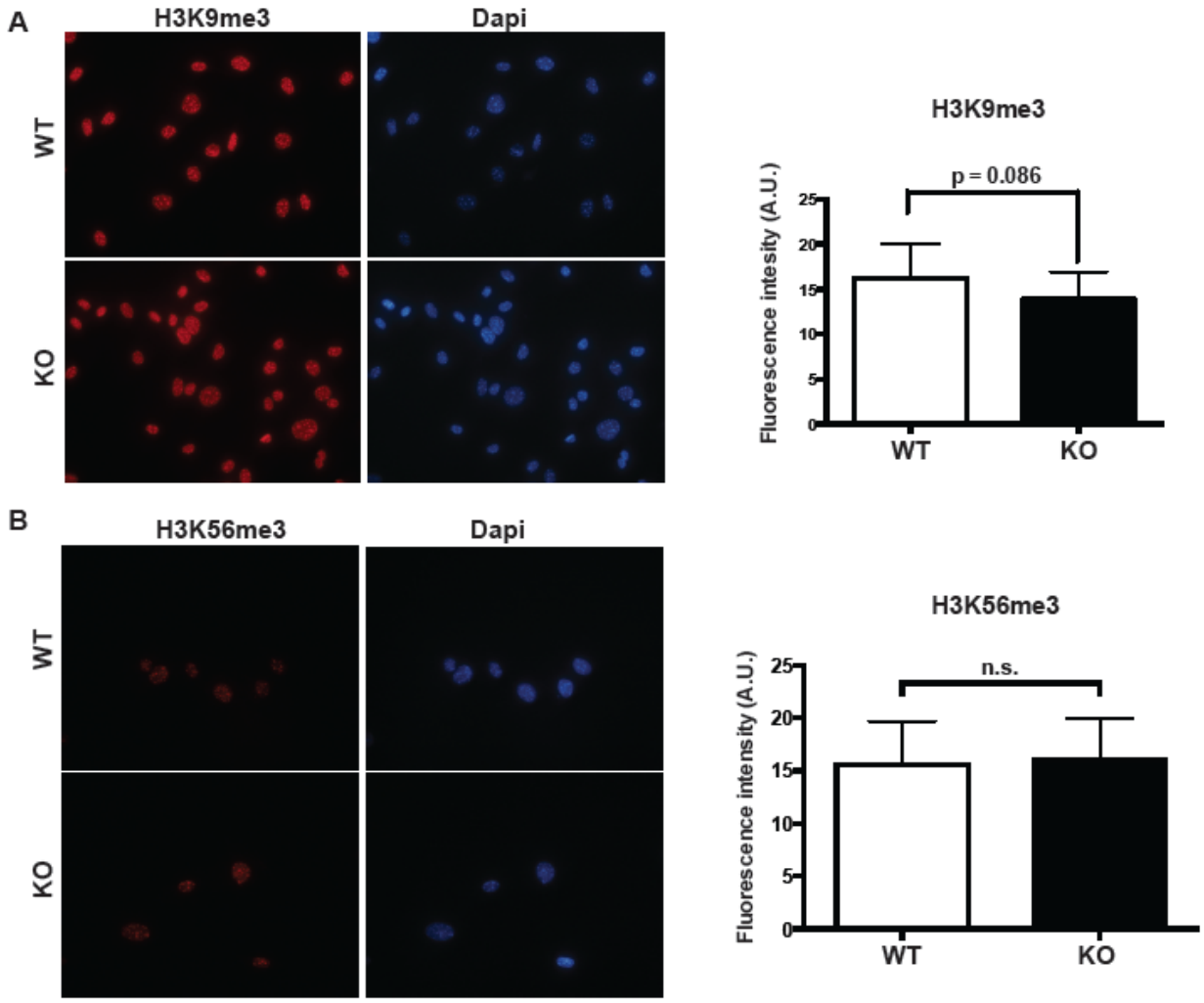

Figure 4.5: SIRT6 does not alter histone trimethylation in MEFs

Immunocytochemistry of WT and *Sirt6* KO MEFs for H3K9me3 (A) and H3K56me3 (B). The fluorescence intensity was measured using ImageJ (n= ~30 cells) and represented in bar graphs (right).

in response to Sirt6 deletion (Figure 4.4C-D). Finally, the interaction of KAP1 at the MSR was not disrupted in SIRT6-deficient MEFs. These results indicate that SIRT6 does not bind and deacetylate its known histone H3 targets at the MSR and it does not impact KAP1 recruitment to the MSR.

Histone H3 Lysine 9 and 56 methylation are not altered in SIRT6-deficient cells

To verify these findings, we performed immunocytochemistry for H3K9 and H3K56 trimethylation, marks for silenced chromatin (Jack et al., 2013; Peters et al., 2002; Peters et al., 2001), on WT and *Sirt6* KO MEFs. Heterochromatic regions can be visualized by Dapi staini as they appear as small bright foci in the nucleus. H3K9me3 and H3K56me3 levels were similar in WT and KO MEFs (Figure 4.5A-B). Even more so, in both cell lines the histone marks overlapped perfectly with the heterchromatic foci suggesting that SIRT6 might not regulate these histone modifications at these regions.

MSR expression is not regulated by SIRT6

Increased expression of MSR is a measure of altered MSR regulation which can impact MSR stability. Therefore, we isolated RNA from WT and *Sirt6* KO MEFs, and from WT and *Sirt6* KO ES cells and performed RT- PCR and northern blot for the MSR. As a positive control we included WT and *Suv39h1/2* KO iMEFs, which, as predicted, showed a dramatic increase in MSR expression in the absence of SUV39H1 (Figure 4.6A-B). Unlike SUV39H1, SIRT6 does not impact MSR expression levels ES cells or MEFs. A slight increase was observed in one of the *Sirt6* KO ES cell lines, but not in the second KO cell line (Figure 4.6B). The ES cells used for these experiments are not littermate controls, and thus slight biological variation between these cell lines can be expected.

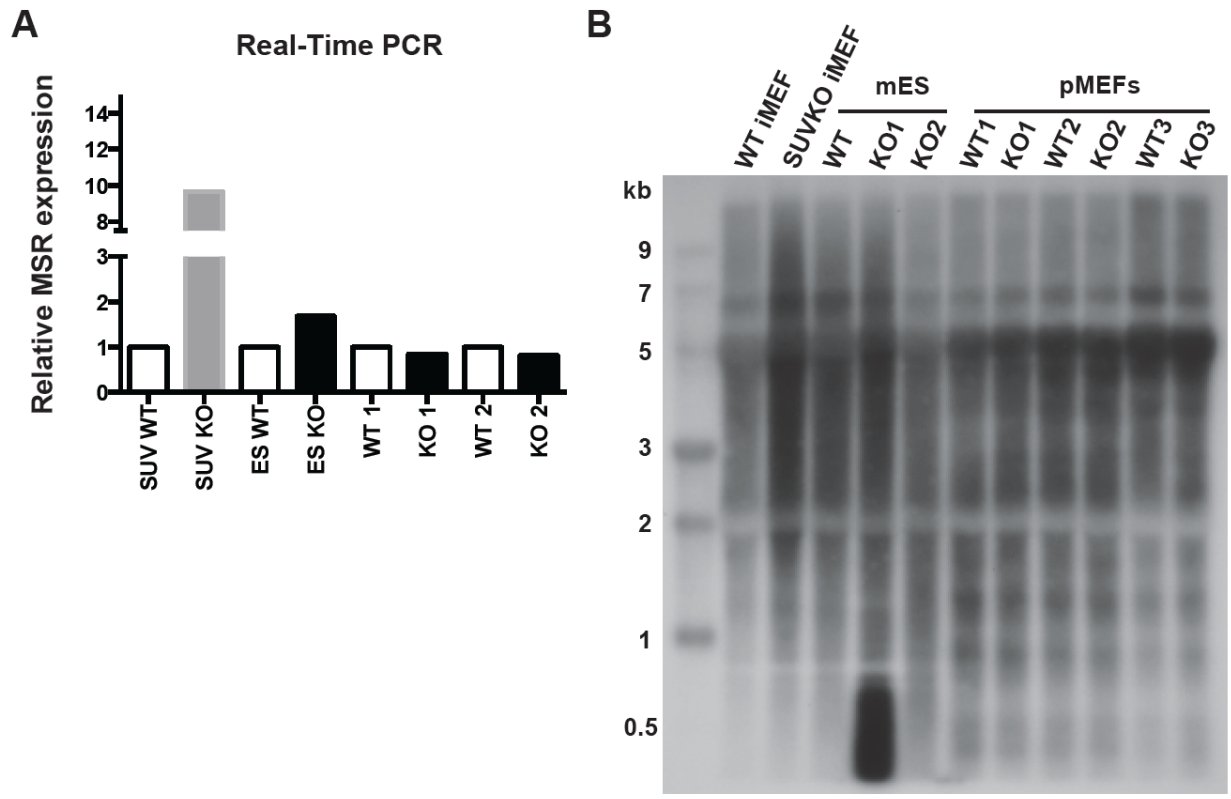

Figure 4.6: MSR expression is not regulated by SIRT6

(A) Real-time PCR for MSR expression in indicated cell lines. (B) northern blot analysis for MSR RNA transcripts using same cell lines as in (A). Experiment in figure B was performed by W. Giblin.

SIRT6 does not impact KAP/HP1 localization and protein levels

Finally, we tested by immunocytochemistry whether protein levels or localization of the silencing factors HP1 and KAP1 was affected with respect to SIRT6 status. In both WT and *Sirt6* KO MEFs, HP1α and KAP1 appeared to be associated with the heterochromatic foci in these cells (Figure 4.7). Furthermore, we did not observe a change in protein levels, as measured by fluorescence intensity, between genotypes

(Figure 4.7). We can conclude that, despite SIRT6's interaction with these factors, SIRT6 is not responsible for their protein stability or their interaction with pericentromeric MSR.

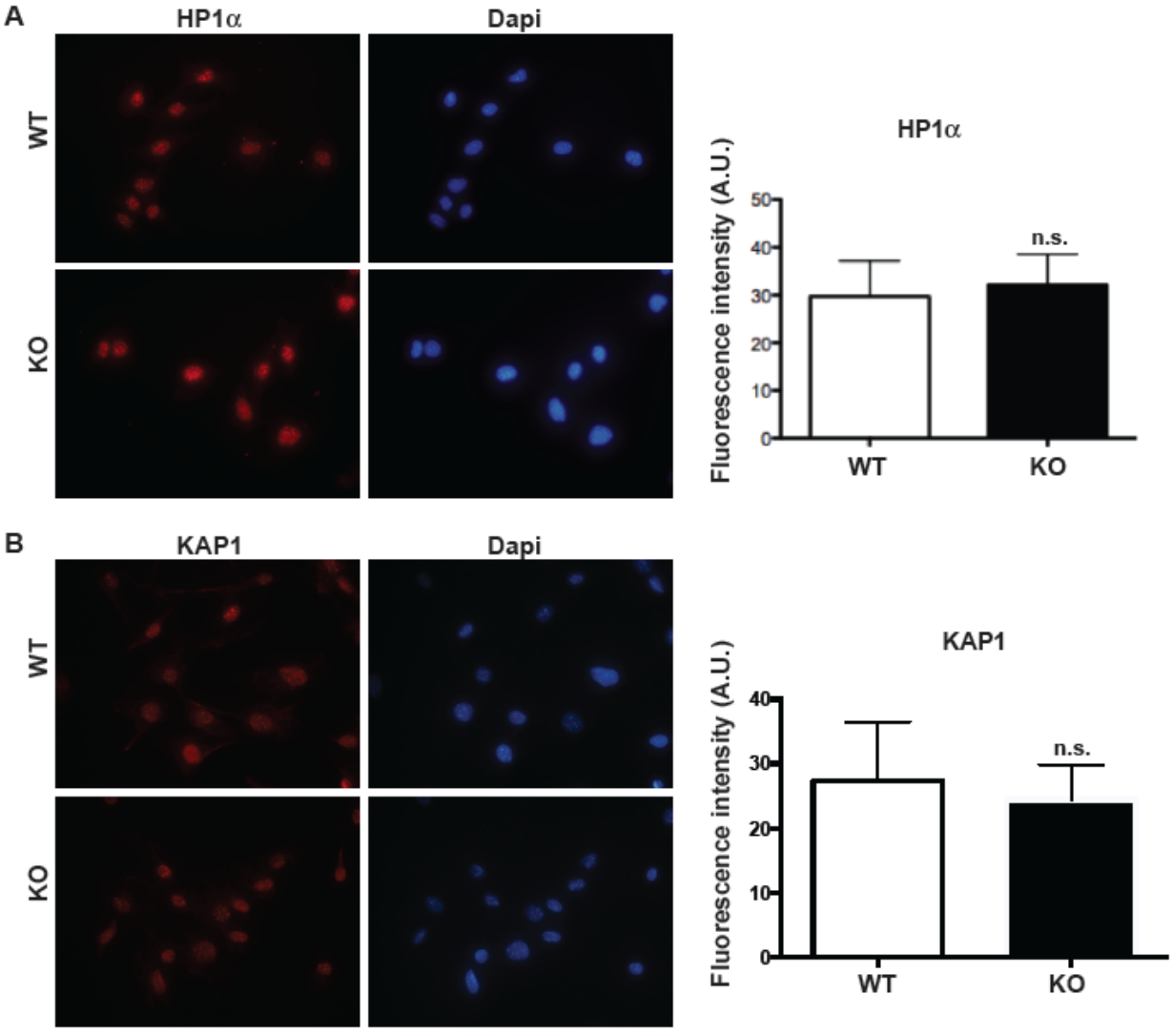

Figure 4.7: SIRT6 does not regulate protein level or localization of silencing factors

Immunocytochemistry of HP1α (A) and KAP1 (B) in WT and Sirt6KO MEFs. Fluorescence intensity was measured using ImageJ (n=~30 cells) and represented in bar graphs (right). Experiments were done in collaboration with K. Smith.

The antioxidant NAC rescues tumorigenesis in absence of SIRT6

Based on the above data the SIRT6 dependent aneuploidy cannot be explained by impaired regulation of MSR. Another possible culprit of aneuploidy is abnormal levels of reactive oxygen species (ROS) (Wang et al., 2013). Thus we hypothesized that high levels of ROS in SIRT6 could lead to aneuploidy and subsequently an increase in tumorigenesis in the absence of SIRT6. To test this hypothesis we treated $Apc^{min/+}$ mice lacking SIRT6 in the intestinal epithelial cells (chapter 3) with the antioxidant N-acetyl cysteine (NAC) for two months. At four months, the mice were sacrificed and polyp numbers were counted. While we saw an increase in polyp number in the absence of SIRT6, treatment with NAC completely rescued this phenotype in SIRT6 conditional mutant mice (Figure 4.8A-B). Furthermore, the polyps of SIRT6 deficient NAC treated mice were of equal grade as their littermate controls (Figure 4.8C). These results indicate that treatment with the antioxidant NAC can rescue the increased tumorigenesity seen in $Apc^{min/+}$; V-c; $Sirt6^{f/f}$ mice.

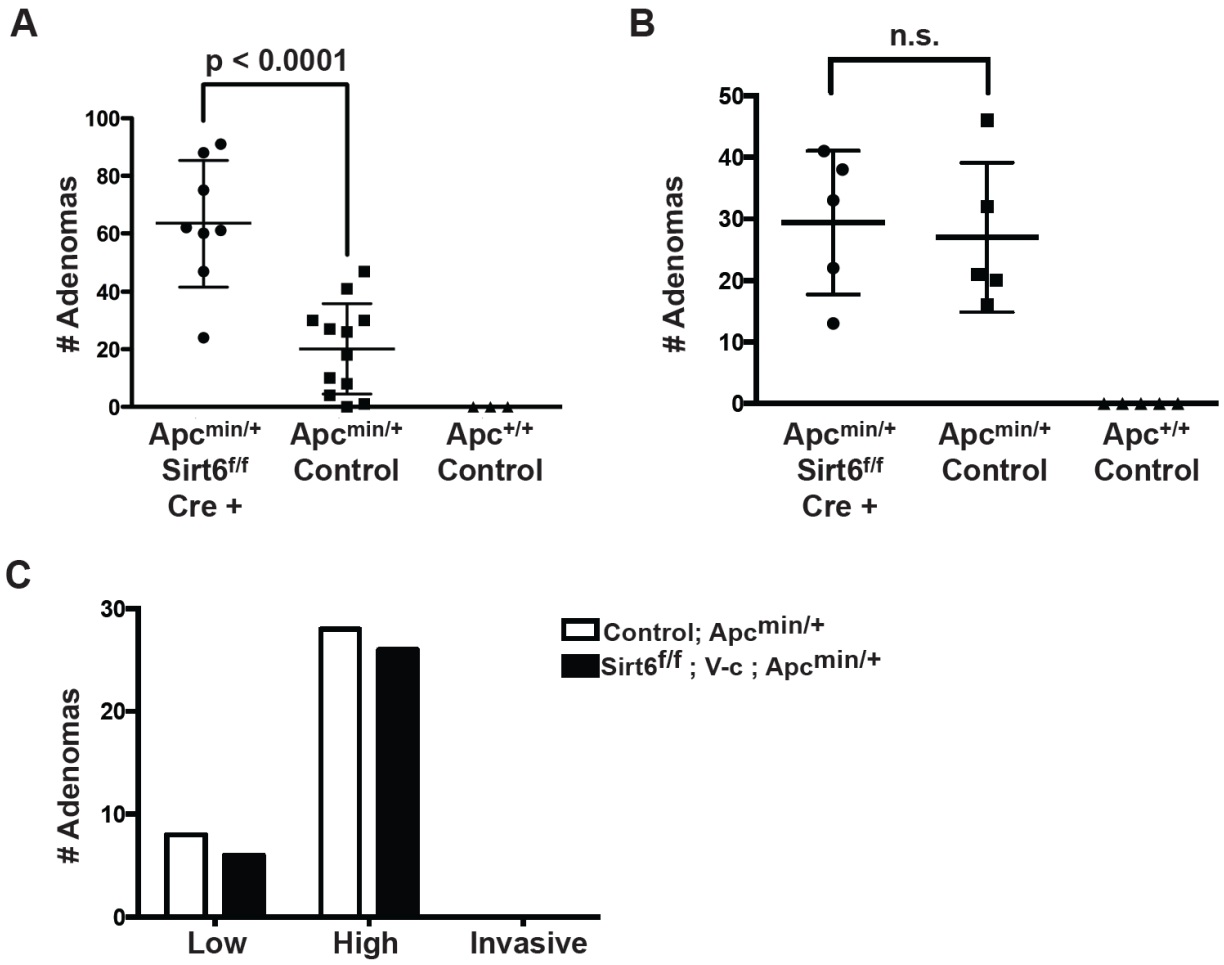

Figure 4.8: NAC treatment rescues increased tumorigenesis in absence of SIRT6

(A) increased polyp number observed in Sirt6$^{f/f}$; V-c; Apc$^{min/+}$ mice in comparison to their littermate controls (Sebastian et al., 2012). (B) Similar mice as in (A) but subjected to NAC treatment. (C) tumor grading of Sirt6$^{f/f}$; V-c; Apc$^{min/+}$ mice and littermate controls treated with NAC. Tumor grade was analyzed by Dr. J. Greenson.

SIRT6 does not regulate ROS levels or ROS induced DNA damage

Next we tested if SIRT6 deficient cells showed altered ROS levels. Therefore we took WT and Sirt6KO MEFs and measured ROS using the compound DCFDA, a fluorescent dye that measures various ROS such as peroxyl, alkoxyl, carbonate and hydroxyl radicals (Eruslanov and Kusmartsev, 2010). As a positive control, we treated MEFs with hydrogen peroxide to increase ROS levels and pre-treated MEFs with NAC to decrease ROS. When analysed by FACS (fluorescent activated cell sorter), we indeed observed an increase and decrease in ROS upon H_2O_2 and NAC treatment respectively. However, we did not observe altered ROS levels in the absence of SIRT6 (Figure 4.9).

Next we determined oxidative DNA damage in the absence of SIRT6 by using a probe that binds specifically to aldehyde groups, which are a result from DNA modifications. While treatment with the compound EGCG (epigallocatechin gallate) increased oxidative damage when used at high concentrations, and NAC was able to reduce oxidative DNA adducts, we again were unable to detect a difference between WT and *Sirt6* KO MEFs (Figure 4.10). Based on the lack of changes in ROS or oxidative DNA damage upon *Sirt6* deletion, we can conclude that SIRT6 does not seem to regulate intracellular ROS levels and thus changes in ROS is likely not the underlying cause of the previously observed aneuploidy.

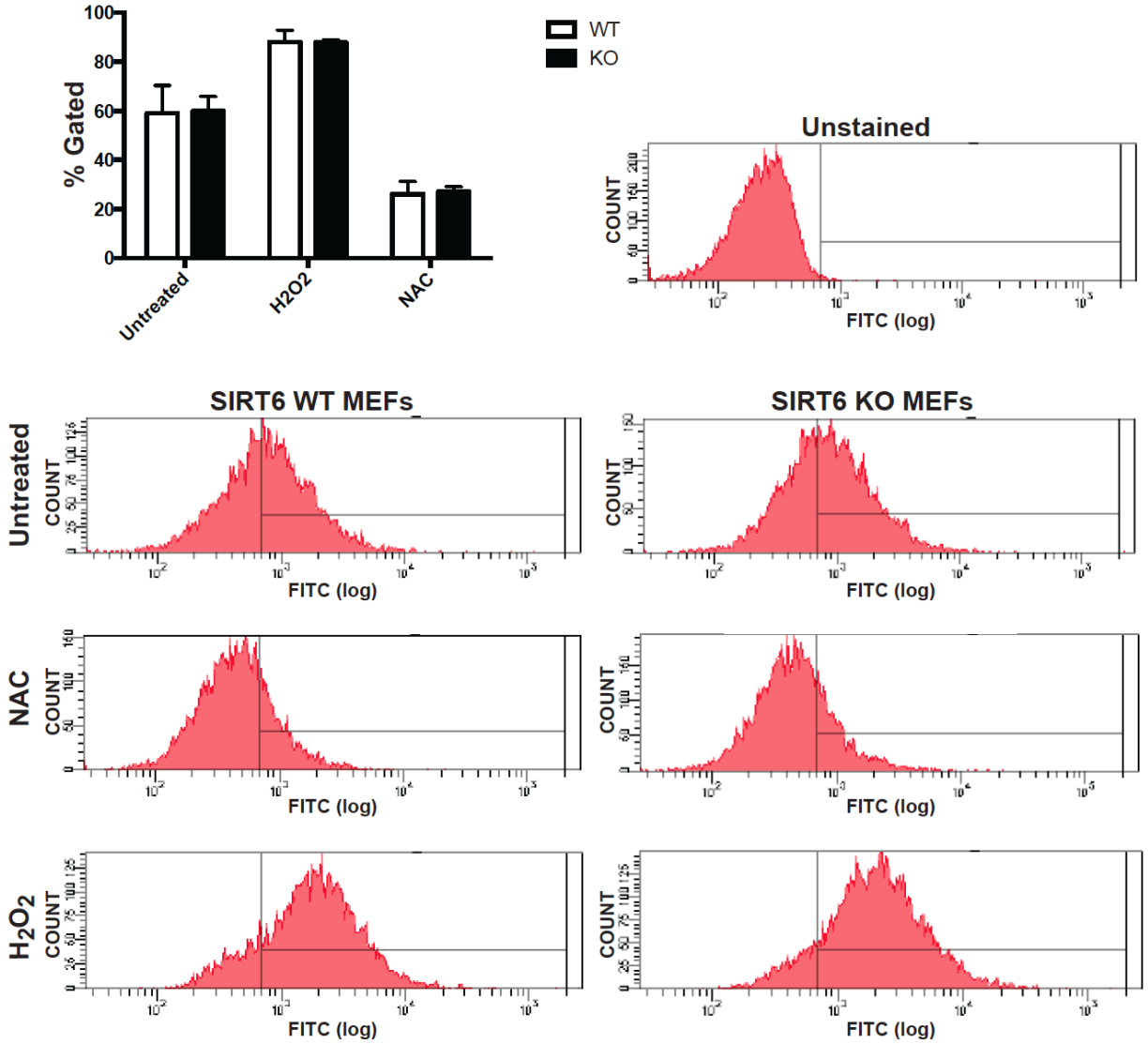

Figure 4.9: ROS levels are unaltered in SIRT6 null cells

ROS levels were measured with DCFDA compound in MEFs untreated, or treated with NAC or H_2O_2 (n=3). Data is represented in a bar graph as percentage of cells gated in the histogram graphs below.

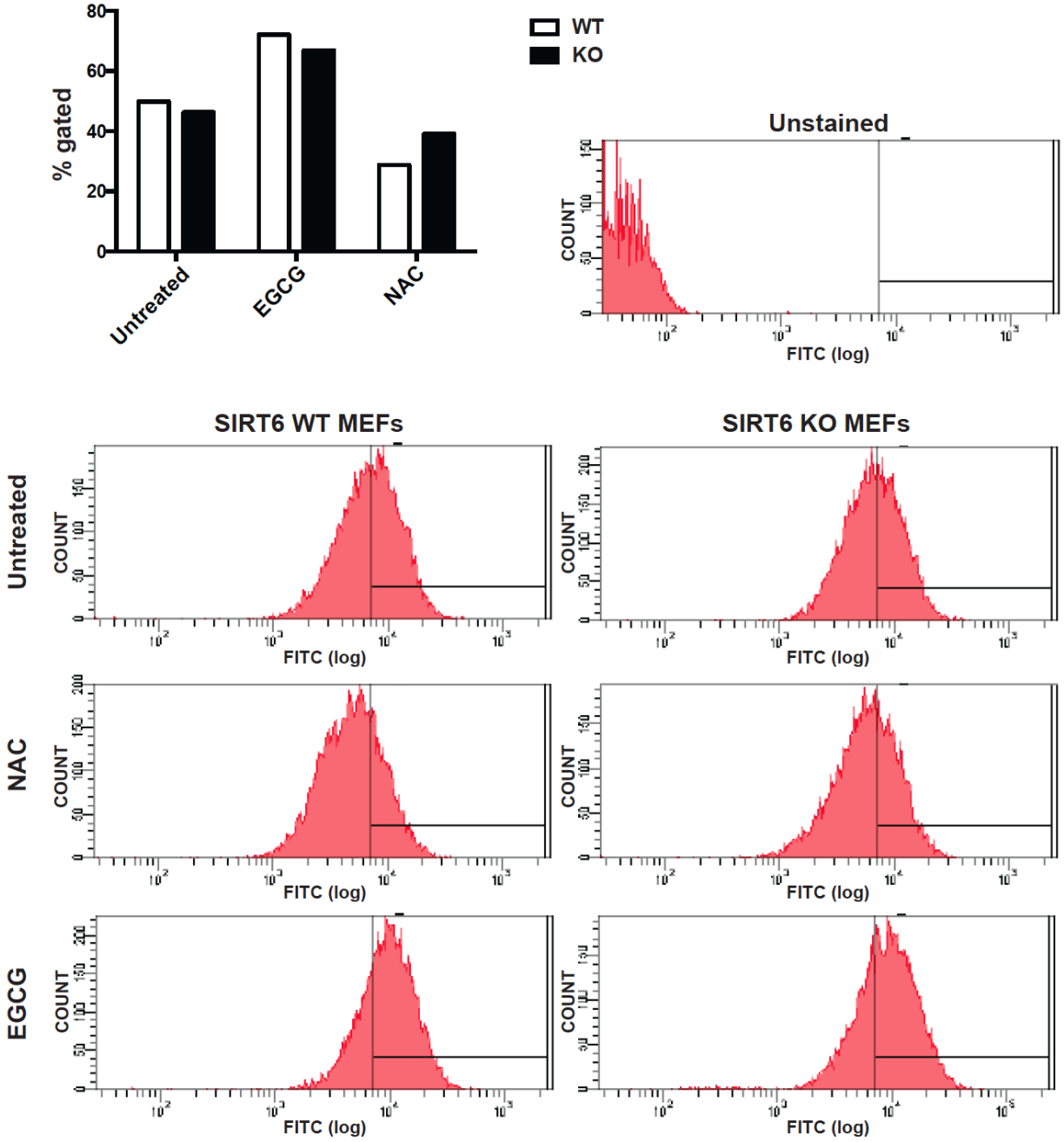

Figure 4.10: SIRT6 does not affect oxidative DNA damage

Oxidative DNA damage in WT and *Sirt6* KO MEFs untreated, or treated with NAC or EGCG (n=1). Data is represented in a bar graph as percentage of cells gated in the histogram graphs below.

Discussion

The six hallmarks of cancer encompass those traits that cells acquire to become carcinogenic. Hannahan and Weinberg, in their most recent review, described the concept of enabeling characteristics, mechanisms through which the cancer hallmarks can be obtained (Hanahan and Weinberg, 2011). The mutational rate in primary cells is generally very low due to the abundant genome maintenance mechanisms that are in place. However, the acquisition of a mutation in one of the genome surveillance and repair pathways can accelerate the mutational rate, leading to the acquisition of additional genomic alterations that provide the cells survival and growth advantage (Hanahan and Weinberg, 2011). Considering the role of SIRT6 in guarding genomic integrity and the aneuploidy defect that we observe in SIRT6 deficient cells, loss of SIRT6 could well be an enabler of tumorigenesis. Therefore we sought to investigate the underlying mechanism responsible for SIRT6's role in mediating euploidy.

The pericentromeric heterochromatic major satellite repeat region is essential in proper chromatid segregation during mitosis. Disruption of MSRs due to improper silencing and higher MSR expression can result in aneuploidy and increased cancer incidence (Bernard et al., 2001; David et al., 2006; Ekwall et al., 1997; Peters et al., 2001). SIRT1 was previously shown to interact with the pericentromeric MSRs where it deacetylates H1K26. While treatment with the sirtuin inhibitor NAM could enhance MSR expression, SIRT1 stable knockout cells did not alter MSR transcript levels, suggesting the involvement of other sirtuin proteins (Oberdoerffer et al., 2008). Our results indicate that SIRT6, in addition to SIRT1, does not silence MSR. Despite the previous report that SIRT6 co-localizes with heterochromatin (Michishita et al., 2005), we were unable

to detect an association of SIRT6 with MSR or identify SIRT6 mediated epigenetic alterations at these repeats. However, a recent study did identify SIRT6 as a potent silencer of LINE-1 (long interspersed nuclear element-1) retrotransposons. Mechanistically, SIRT6 binds the 5' UTR of LINE-1 elements where it raises H3K9me3 levels and recruits the chromating silencing factors KAP1 and HP1α (Van Meter et al., 2014). LINE-1 elements are long DNA repeats that actively translocate to different regions within the genome with each cell cycle. While no relationship exists between LINE-1 elements and aneuploidy, derepressed LINEs are associated with genomic alterations such as DNA double strand breaks (Gasior et al., 2006; Gilbert et al., 2002; Iskow et al., 2010), and can be found in human lung carcinomas (Iskow et al., 2010). Therefore, it is likely that the protection against DNA damage by silencing LINE-1 elements provides an additional mechanism through which SIRT6 protects against tumor formation.

The aneuploidy phenotype in SIRT6-null cells could not be explained by changes in ROS levels either. While it has previously been shown that SIRT6 responds to oxidative stress by relocating to DNA damage sites (Mao et al., 2012), SIRT6 does not appear to impact ROS levels itself *in vitro*, nor do SIRT6 deficient cells show more oxidative DNA damage. In some respect this seems surprising as SIRT6 deficient cells are more glycolytic, and thus should generate less ROS. However, treatment of *Sirt6*$^{f/f}$; *V-c*; *Apc*$^{min/+}$ mice with the antioxidant NAC resulted in a rescue of the increased tumorigenesis phenotype in the absence of SIRT6, insinuating that NAC protects against tumorigenesis in these mice through an alternate mechanism. As aneuploidy is predominantly a result of chromosome missegregation, an in depth study of mitosis in

SIRT6 deficient cells might reveal the underlying mechanism of SIRT6-mediated ploidy changes.

Future directions

Even though changes in ROS are not the underlying mechanism for the increased aneuploidy in the absence of SIRT6, we were able to rescue the increased tumorigenesis in our *Apc*$^{min/+}$; *V-c*; *Sirt6*$^{f/f}$ mice by treating them with the antioxidant NAC. In our study we identified elevated aneuploidy in MEFs and we were able to rescue the tumorigenesis *in vivo* with NAC treatment, though at this point we don't know if treatment of MEFs with NAC can protect against ploidy changes or if the adenomas in our *Apc*$^{min/+}$ model show a higher degree of aneuploidy. Nevertheless, the tumor suppression of NAC in SIRT6 deficient intestines would be worthwhile exploring further. As previously mentioned, Hanahan and Weinberg discussed the existence of two emerging hallmarks: genome instability and tumor-promoting inflammation (Hanahan and Weinberg, 2011). Virtually every tumor contains some level of immune-infiltrate, which was historically viewed as an anti-tumor strategy. While this might still be the case in some instances, immune cells can also help tumor cells acquire additional cancer hallmarks, e.g. by supplying growth or angiogenic factors. Immune cells secrete ROS that can result in an increased mutational rate in cancer cells. Thus the decrease in tumorigenesis through NAC treatment could be a result of inhibition of ROS secreted by the immune cells. In a small pilot experiment, we analyzed intestines from our *Apc*$^{min/+}$; *V-c*; *Sirt6*$^{f/f}$ and control mice for cytokine levels (Figure 4.11). Cytokines are small proteins that are secreted by various cells to regulate the behavior

of others. In this experiment we identified a striking increase in interleukin-17 (IL-17) levels in SIRT6-deficient tissues. IL-17 can be produced by various immune cells such as T-helper cells, natural killer cells (NK cells) and neutrophils, and elicits a pro-inflammatory response (Lonnberg et al., 2014). Furthermore, high IL-17 levels are associated with increased tumor growth (Chang et al., 2014; Cochaud et al., 2013; He et al., 2012; Wu et al., 2013; Xiang et al., 2013). While we are not aware how and in what cell type IL-17 is produced and what the subsequent role of IL-17 is in this setting, it is plausible that SIRT6 deficiency indirectly causes an immune response, resulting in increased proliferative potential of the surrounding epithelial cells.

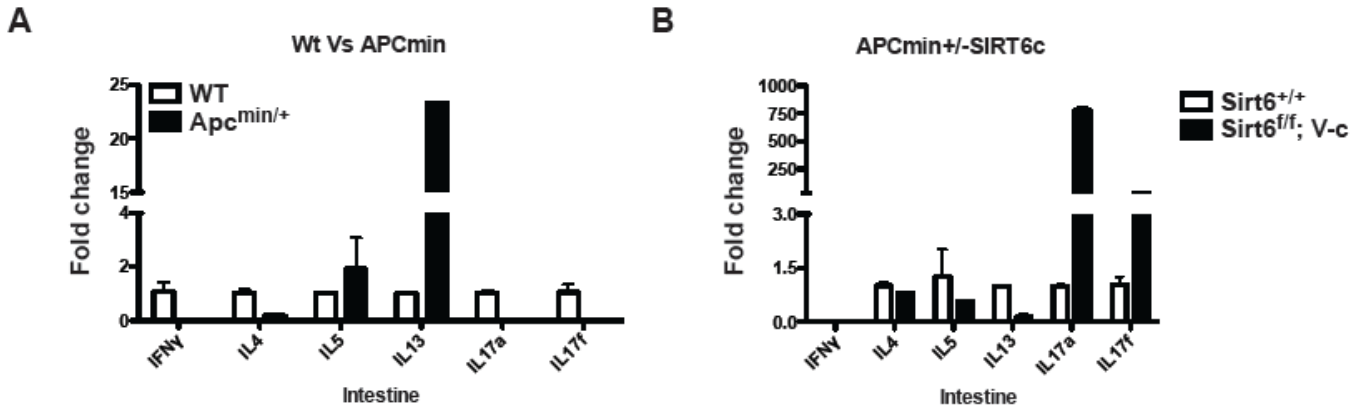

Figure 4.11: IL-17 is elevated in SIRT6-deficient colorectal adenomas

Frozen intestine sections of *Apc*$^{min/+}$; *V-c*; *Sirt6*$^{f/f}$ and *Apc*$^{min/+}$ control mice were processed and tested for indicated cytokines using the Bio-Plex Multiplex system (BioRad). (A) IL-13 levels were elevated in WT versus *Apc*$^{min/+}$ mice (n=3). (B) In the absence of SIRT6 in the intestinal epithelial cells, IL-17a and IL-17F cytokine levels were significantly higher than in control tissue (n=3). (Dr. S. Mukherjee; n-values represents technical replicates)

Chapter 5

A study of SIRT6 localization in cancer

Abstract

SIRT6 is a member of the sirtuin family of NAD^+-dependent protein deacetylases that promote longevity in *C. elegans, Drosophilla* and yeast. We, and others, have shown that SIRT6 deacetylates histone 3 acetylated at lysine 56 (H3K56ac), a histone mark that is elevated in many tumor types. Additionally, SIRT6 deficiency increases susceptibility to tumor development. We assessed the expression and localization pattern of SIRT6 in cancer and identified high SIRT6 protein levels in both nuclear and cytoplasmic fractions of the cell. Our data is suggestive of loss of SIRT6-mediated H3K56 deacetylation in cancer cells and of a role for SIRT6 in transcriptional regulation of mitochondrial genes. Furthermore, examination of the SIRT6 protein sequence revealed a conserved nuclear export sequence, implying a tight regulation of SIRT6 localization in the cell. Finally we propose SIRT6 immunohistochemistry as a useful marker for identifying cancer cells in peritoneal and pleural fluids derived from ovarian cancer patients.

Introduction

In chapters 3 and 4 we have provided evidence for SIRT6's role as a tumor suppressor protein. Loss of SIRT6 can drive tumorigenesis by enhancing c-MYC mediated ribosomal biogenesis, by supporting a metabolic switch to aerobic glycolysis and possibly by increasing chromosomal instability. As an epigenetic regulator, SIRT6 impacts many transcription factors and their downstream signaling pathways, and thus SIRT6 can likely suppress tumorigenesis through other pathways as well. As loss of SIRT6 enhances tumor susceptibility, SIRT6 activators or SIRT6 molecules are potential therapeutic tools for treatment of malignancies. With this in mind, we analyzed SIRT6 expression in various human cancer samples and made an initial assessment of SIRT6 function in established cancers.

Materials and Methods

Cell culture

Colon cancer cell lines (HCT116, DLD1 and LOVO) were kindly provided by Dr. E. Fearon and were grown in high glucose DMEM supplemented with 10% FBS, 1% L-Glutamine and 1% pen/strep. Ovarian cancer cell lines (OVCA 433, OVCAR5, OVCAR8 and HeyA8) were grown in RPMI 1640 containing 10% FBS, 1% L-Glutamine and 1% pen/strep. MEFs were isolated as previously described from germline Sirt6KO mice and were grown in a low oxygen incubator (3% O_2, 5% CO_2) in 15% FBS, 1% L-Glutamine, 1% pen/strep, 1% sodium pyruvate, 1% non-essential amino acids, 2% HEPES and 115 µl beta-mercaptoethanol. IEC-6 cells were grown in DMEM supplemented with 10% FBS, 4 mM L-glutamine, 1.5 g/L sodium bicarbonate, 4.5 g/L

glucose and 0.1 Unit/ml bovin insulin. Mouse myofibroblast C2C12 cells were grown in DMEM containing 10% FBS. All cells were grown at 37°C and 5% CO_2.

Immunohistochemistry

Tissue microarrays of various human carcinomas (colorectal, ovarian, breast, lung and pancreatic), melanoma and glioblastoma were obtained from Dr. T. Giordano. Cytoblocks of pleural or peritoneal fluids from ovarian cancer patients were provided by Dr. M. Roh. Intestines from SIRT6 inducible overexpressing mice on an *Apc*$^{min/+}$ background were fixed in 4% formaldehyde over night, processed by the University of Michigan histology core.

IHC was performed by the University of Michigan histology core. Briefly, slides were deparaffinized and rehydrated through a series of xylene and alcohol washes. Antigen retrieval was performed by first heating the slides for 10 minutes in citrate buffer (10 mM Citric Acid, 0.05% Tween 20, pH 6.0) and then allowing them to cool down for 10 minutes at room temperature. Endogenous peroxide was blocked by incubation in 3% hydrogen peroxide (H_2O_2) for 10 minutes. Additional blocking was performed by incubating the slides in 5% normal goat serum in PBS for one hour. Tissues were incubated with human SIRT6 antibody (Abcam, ab88494 or CST, 2590), mouse SIRT6 (Novus) or H3K56ac (Epitomics) overnight at 4°C. Signal was visualized using 3,3'-diaminobenzidine (DAB; Vector Laboratories) and slides were mounted using permanent mounting medium (Vector Laboratories). Slides were imaged with an Olympus BX-51 scope with an Olympus DP-70 high-resolution digital camera (University of Michigan Microscopy & Image Analysis lab).

Fractionation

Nuclear/cytoplasmic fractionation was performed based on the Abcam Histone Extraction Protocol with modest alterations. Freshly isolated cells (15 cm dish) were incubated for 10 minutes on ice in 500 µl triton extraction buffer (TEB: 0.5% Triton x100, 2 mM phenylmethylsulfonyl fluoride (PMSF), 0.02% NaN_3 in PBS). A small fraction of samples was saved for whole cell extract (WCE) and the remaining lysed cells were spun down at 2000 rpm and 4°C for 10 minutes. The supernatant was saved (= cytoplasmic fraction) and the pellet was washed once in 1 ml TEB. The supernatant was discarded and the nuclear pellet was resuspended in lysis buffer (1% Triton X-100, 0.5% NP-40, 150 mM NaCl, 50 mM Tris pH 7.4 and 10% Glycerol). WCE and nuclear fractions were sonicated using a Branson Sonifier 450 sonicator at 2.5% output control and 50% duty cycle and all samples were spun down at maximum speed in a refrigerated table top centrifuge. The supernatants were collected and protein concentration was measured using DC protein assay (Bio-Rad).

For histone extraction, nuclei were isolated as described above and were rotated over night in 0.2N HCl at 4°C. After the acid extraction, samples were centrifuged at 2000 rpm for 10 minutes. Protein concentration of the supernatants containing histones was measured using DC protein assay (Bio-Rad).

For the isolation of mitochondria, cells were resuspended in 4 ml cell homogenization medium (CHM: 25 mM KCl, 5 mM $MgCl_2$, 10 mM Tris-HCl pH 7.4 supplemented with NAM, TSA and proteinase inhibitors) and allowed to swell for 2 minutes. For each sample, cells were homogenized with 20 strokes in a 7ml dounce with b-pestle. 1 M

sucrose was added to each cell homogenate to a final concentration of 0.25 M sucrose. Homogenate was inverted for 5 minutes at 4°C and centrifuged for an additional 5 minutes at 900xg. Supernantant was further centrifuged at 6200xg in a piramoon rotor for 10 minutes to collect mitochondria. Mitochondrial pellets were resuspended in lysis buffer and allowed to lyse for 30 minutes on ice. Protein concentration was measured as described earlier.

Migration assay

Cell migration was measured using the CytoSelect 24-well Cell Migration Assay (Cell Biolabs) according to the manufacturer's instructions. In short, 500 µl of growth media was added to 12 wells of a 24-well plate. Subsequently, small inserts (8 µm pore size) were placed in each well and these insert were filled with 0.5 x 10^6 cells (in triplicate) in serum free media. After 24 hours the cells that migrated through the inserts were stained following which the stain was extracted. The extracted stain density was measured at OD 560 nm in a plate reader.

Proliferation assay

Proliferation assay was performed using cell-counting kit-8 (Dojindo Molecular Technologies). In quadruplicate, 2.5 x 10^3 cells were plated per well of a 96-wells plate. After 48 hours, 10 µl of CCK-8 solution was added to each well and incubated at 37°C for 2 hours. The absorbance was measured at 450nm using a microplate reader.

Immunoblot

For analysis of fractionated cells, histone extracts or SIRT6 knockdown protein samples were seperated on 4-20% gradient gels (Bio-Rad), transferred to PVDF membranes, and probed with the following antibodies in TBST/5% milk at the dilutions indicated: rabbit anti-SIRT6 (Abcam), 1:1000; rabbit anti-SIRT6 (CST), 1:1000; rabbit anti-H3 (Abcam), 1:10.000; rabbit anti-LDHA (Santa Cruz biotechnology), 1:2000; rabbit anti-H3K56ac (Epitomics), 1:1000; rabbit anti-H4K16ac (Cell Signaling Technology), 1:1000; rabbit anti-H3K9ac (Abcam), 1:1000; rabbit anti-Lamin A/C (Cell Signaling Technology), 1:2000.

Sirt6 knockdown

For viral infection of constitutive or inducible knockdown of *SIRT6*, indicated cancer cell lines were infected with lentivirus *shSIRT6*-GipZ or *shSIRT6*-TripZ respectively or with their respective shControl vectors. shRNA vectors were obtained from Open Biosystems and viral particals were made by the University of Michigan vector core facility at 100x concentration. Cells were plated in a 6-well dish and after 12 hours 50 µl of concentrated virus was added to one well of a 6-well dish containing 1ml of media and 4 µg/ml polybrene (Sigma). After 24 hours, media was replaced and cells were treated for 48 hours with puromycin (2.5 µg/ml) to select for virally infected cells. Following selection, cells were maintained in normal growth media.

For transient Sirt6 knockdown, cells were transfected with siRNA for *SIRT6* or control siRNA (Dharmacon) using Lipofectamine LTX transfection reagent (Life Technologies).

Transfection was performed according to the manufacturer's instructions. For proliferation assay, cells were plated in quadruplicate and each well, containing 100 µl pen/strep free media, was transfected with 0.25 µl siRNA and 0.25 µl Lipofectamine LTX in 50 µl Opti-MEM (Life Technologies). After 24 hours media was refreshed and 48 hours post transfection cellular proliferation was measured. To assess efficient *SIRT6* knockdown, cells were plated in 6-well dish and to each well 500 µl Opti-MEM containing 5 µl siRNA and 5 µl Lipofectamine LTX was added. After 48 hours knockdown was verified through western blot analysis.

Transfection

For transient transfection of SIRT6 mutants, WT *hSIRT6*, mNES *SIRT6* and mNLS *SIRT6* were transfected into HCT116 *SIRT6* KD-GipZ using the transfection reagent Lipofectamine LTX. HCT116 cells were plated into 15 cm dishes and after 24 hours (~60% confluency), media was replaced and Opti-MEM containing plasmid and transfection reagent were gently added. Cells were harvested after 48 hours and fractionated as described above.

Mutagenesis

The identified consensus sequences in the SIRT6 protein sequence (Figure 5.A) were each mutated in two steps: NES Leucine 209 (1) and Leucine 213 (2) were replaced by two alanine residues, NLS lysine/arginine 230/231 (1) and 346/347 (2) were mutated to two alanine residues (see Table 5.1). As a template Flag-tagged human *SIRT6* in pCDNA3.1, obtained from Addgene (plasmid 13817), was used. The DNA polymerase

PFU Ultra II fusion HS (Agilent) was used for the mutagenesis as recommended by the manufacturer. PCR products were verified by gelelctrophoresis for correct size, then treated with DPN-1 for 1 hour at 37°C to digest original DNA template, and DH5α competent cells were transformed with the generated PCR products by mixing 50 µl DH5α with 1 µl PCR product, incubating on ice for 30 minutes, heat shock 45 seconds at 42°C, recovering DH5α 45 minutes at 37°C in LB media (Miller's LB broth, Sigma) and plating the transformed bacteria onto LB agar plates containing carbenicillin (500 µg/ml). After 18 hours, colonies were picked, expanded into a large culture and plasmids were isolated with Qiagen maxiprep kit. Mutations were confirmed by the University of Michigan sequencing core using pCDNA3.1 specific sequencing primers (Table 5.1). The generated plasmids were used as a template to generate the second mutation and the above-described procedure was repeated.

Table 5.1: Primer sequences *Sirt6* mutagenesis

	Forward (5')	**Reverse (3')**
mNES step 1 (L209A)	GCCAGCAGGAACGCCGACGCGTCCATCACG CTGGGTACA	TGTACCCAGCGTGATGGACGCGTCGGCGTT CCTGCTGGC
mNES step 2 (L213A)	GCCGACGCGTCCATCACGGCGGGTACATCG CTGCAGATC	GATCTGCAGCGATGTACCCGCCGTGATGGA CGCGTCGGC
mNLS step 1 (KR230/1AA)	CTGCCGCTGGCTACCGCGGCCCGGGGAGGC CGCCTG	CAGGCGGCCTCCCCGGGCCGCGGTAGCCA GCGGCAG
mNLS step 2 (KR246/7AA)	CCCCACAGACCCCCCGCAGCGGTGAAGGCC AAGGCG	CGCCTTGGCCTTCACCGCTGCGGGGGGTC TGTGGGG
pCDNA3.1 seq	TAATACGACTCACTATAGGG	TAGAAGGCACAGTCGAGG

Results

SIRT6 protein levels are elevated in human carcinomas in vivo

We recently identified a role for SIRT6 as a potent tumor suppressor in part by suppressing aerobic glycolysis and c-myc mediated cell growth (Sebastian et al., 2012). In addition, our studies suggest that SIRT6 could protect against tumorigenesis by promoting euploidy, though the underlying mechanism remains to be elucidated (chapter 4). Based on SIRT6's protective role in tumor formation, we wanted to assess SIRT6 expression levels in human cancer tissues, hypothesizing that SIRT6 levels would be strongly reduced in established malignancies. Dr. T. Giordano (University of Michigan) kindly provided us with tissue microarrays containing tissue samples from various normal and malignant tumors. First we assessed SIRT6 staining intensity in normal colon tissue, adenomas and carcinoma (Figure 5.1). In normal tissue, SIRT6 is localized to the nucleus and has a higher staining intensity at the top of the vilii versus the base of the crypts. In adenomas, SIRT6 remains nuclear but is less abundant than in normal tissue, which is consistent with our hypothesis. However, SIRT6 protein levels in colorectal carcinomas are strongly elevated and SIRT6 appears to be localized in both the nuclear and cytoplasmic region of the cell (Figure 5.1A). We quantified these results by comparing SIRT6 staining intensity in carcinoma samples with normal tissue and found that approximately 38% of colon cancers showed similar SIRT6 expression to normal colon tissue, while in the remaining samples SIRT6 levels were elevated (Figure 5.1B). In addition to the high SIRT6 levels observed in colon cancer, SIRT6 appears to be highly abundant in the cytoplasm. To determine if this finding was consistent in other

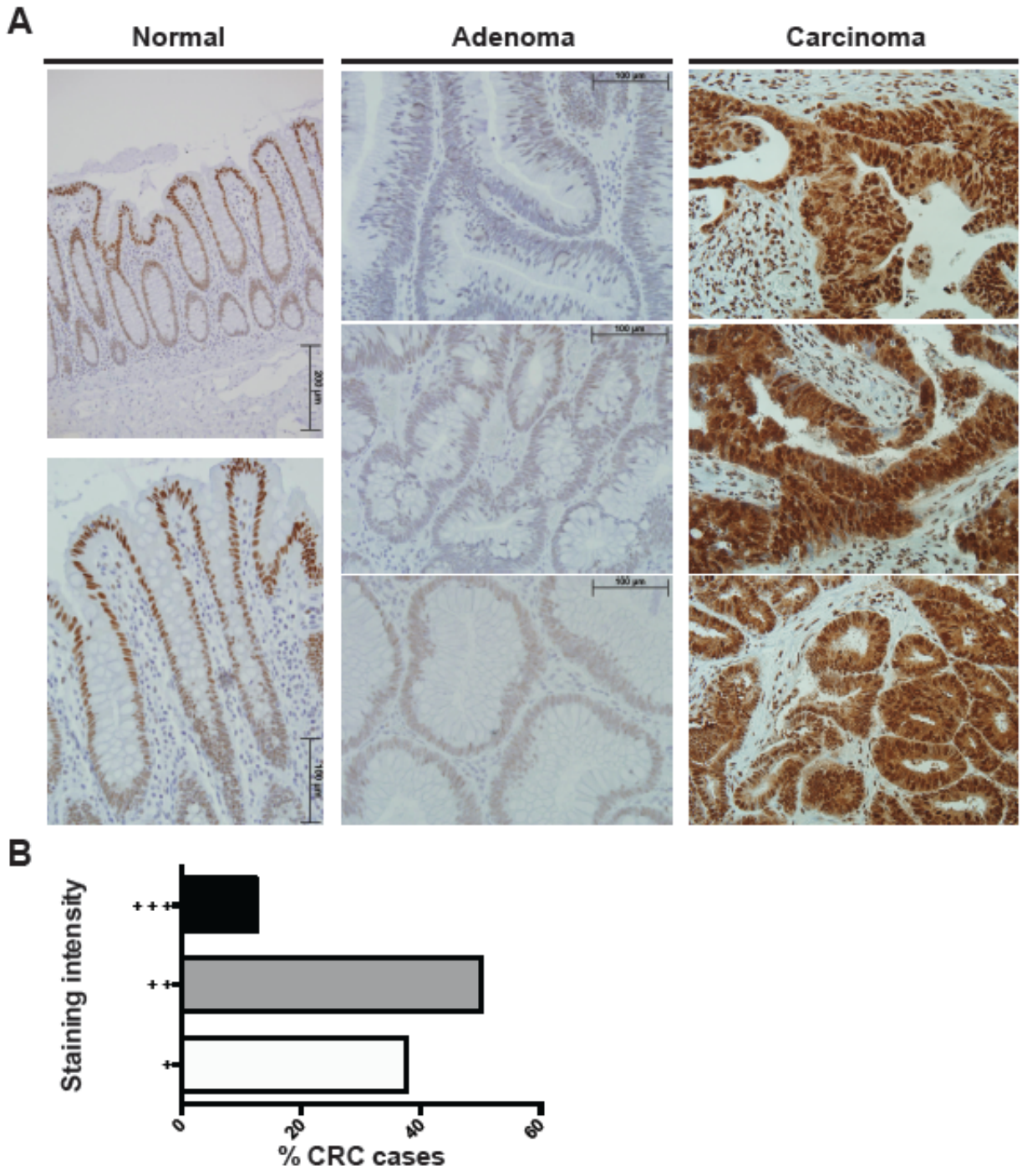

Figure 5.1: SIRT6 protein levels in colon tissue

(A) Human normal colon, adenomas and colorectal carcinomas stained for human SIRT6. (B) Staining intensity for SIRT6 with one plus sign equals SIRT6 levels in normal colon tissue.

tumor types, we assessed SIRT6 protein levels and localization in other carcinomas, melanoma and glioblastoma (Figure 5.2). Strikingly, although SIRT6 levels did not appear to change in cancerous tissue compared to normal brain tissue or melanocytes, our previous finding did hold up for other carcinomas such as breast and ovarian cancer (Figure 5.2A). Furthermore, while almost every tissues sample analyzed was positive for SIRT6 (Figure 5.2B – brackets), SIRT6 cytoplasmic localization was generally associated with carcinomas and is rarely visible in melanomas and glioblastomas (Figure 5.2B).

SIRT6 is elevated and relocalized in human carcinoma cell lines

To verify the above findings, we assessed SIRT6 levels and localization in human ovarian (HeyA8, OVCA 433, OVCAR5 and OVCAR8) and colon cancer cell lines (HCT116, DLD1 and LOVO) by immunoblot. Nuclear/cytoplasmic fractionation of these cells revealed a high abuncance of SIRT6 in both compartments of the cell. We used an inducible Sirt6 knockdown vector (TripZ) to confirm the specificity of our antibody, and lactate dehydrogenase A and lamin A/C were used as cytoplasmic and nuclear loading controls respectively. To test if SIRT6 cytoplasmic localization is tumor specific, we fractionated various non-cancerous cell lines: myoblasts (C2C12), primary MEFs, human dermal fibroblasts, 3T3 immortalized MEFs (Figure 5.3B-E), and intestinal epithelial cells (IEC-6; Figure 5.5B). While SIRT6 levels were dramatically lower in these cell lines in comparison to the carcinoma cell lines (Figure 5.3A vs D), we did observe cytoplasmic localized SIRT6, suggesting that SIRT6 has functional importance in the cytoplasm.

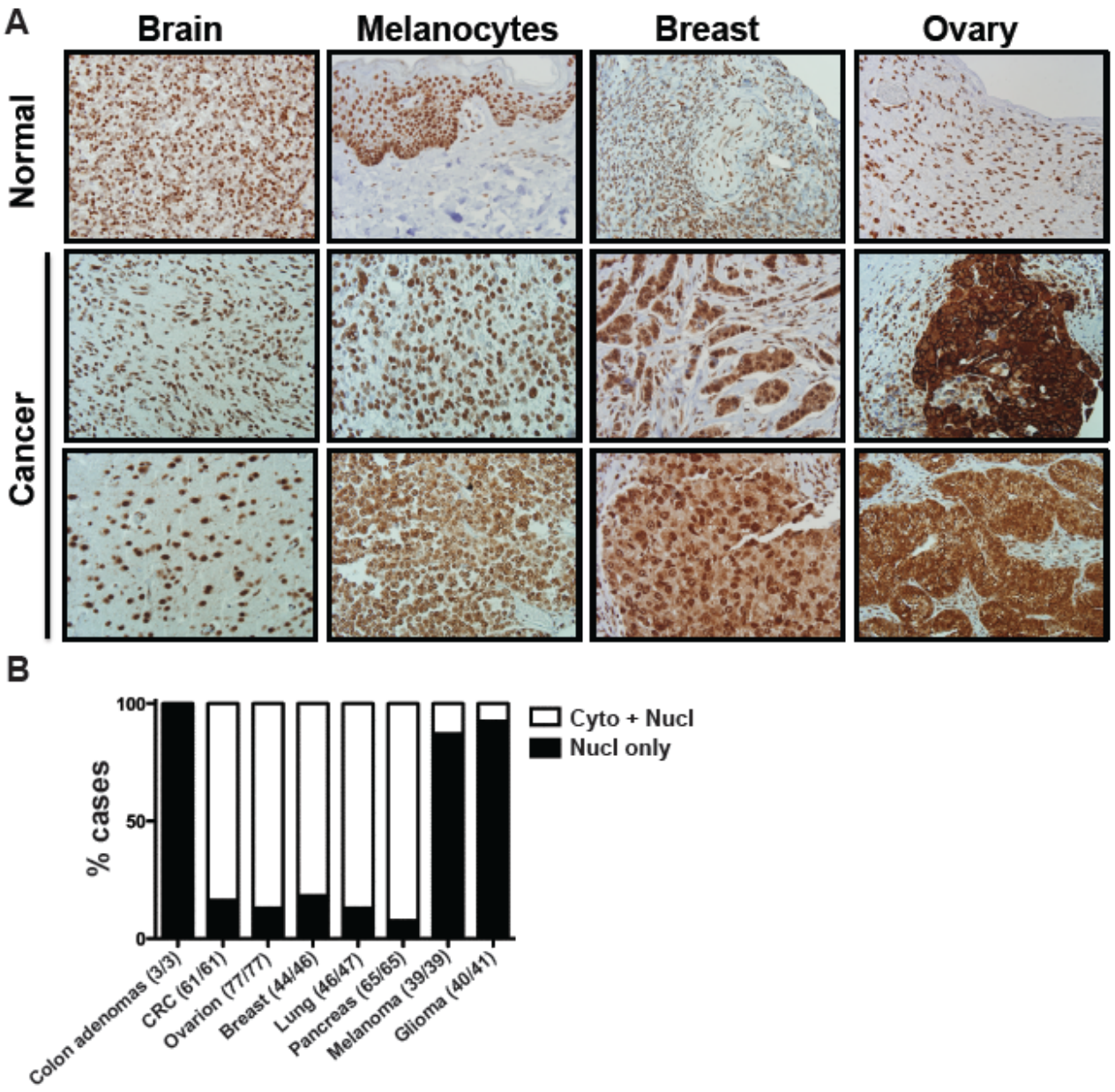

Figure 5.2: SIRT6 localization in human malignancies

(A) Expression and localization of human SIRT6 was assessed in the tumor types indicated using immunohistochemistry. (B) The majority of ovarian, colon and breast carcinomas contain a significant fraction of cytoplasmic SIRT6, in contrast to melanomas and high-grade brain tumors (HGBT). The numbers between brackets indicate the number of samples positive for SIRT6 staining out of the number of tissues analyzed.

SIRT6 mRNA expression not altered in carcinomas

To determine if *SIRT6* expression was altered in carcinomas, we analyzed *SIRT6* mRNA levels using Affymetrix-based data previously generated in the laboratories of Dr. S. Gruber (colon cancer) and Dr. K. Cho (ovarian cancer). *SIRT6* expression in 4 normal colon samples was compared to its expression in 227 colorectal cancers, and only a modest (not significant) increase in *SIRT6* RNA levels was observed in the colon tumors (Figure 5.4A). Likewise, *SIRT6* expression was assessed in ovarian adenoma, ovarian cancer and normal ovarian surface epithelial cells (Figure 5.4B). Overall, no change in *SIRT6* mRNA levels was observed when comparing normal ovarian cells to benign or malignant tumor cells. Thus the elevated SIRT6 protein levels are likely due to increased SIRT6 protein stability or a decrease in proteasomal degradation. Recent work has identified the ubiquitin-specific peptidase USP10 as a novel SIRT6 interactor in colon cancer cells (HCT116). Through its interaction with USP10, SIRT6 is protected against ubiquitination and subsequent degradation (Lin et al., 2013). Future studies should verify the correlation between SIRT6 and USP10 protein levels in various carcinoma cell lines and tissues.

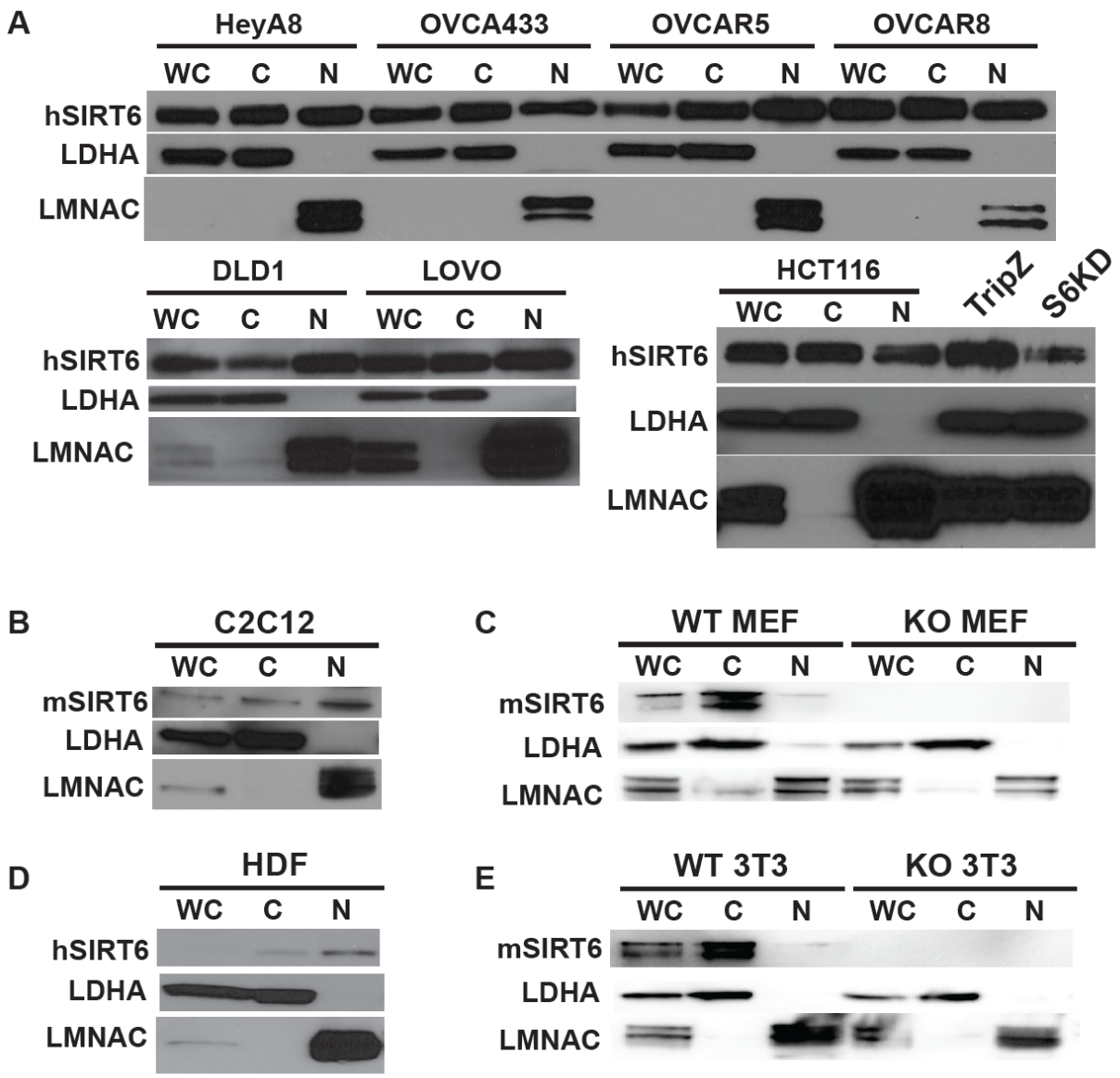

Figure 5.3: SIRT6 localization in cell lines

SIRT6 levels were assessed in subcellular fractions from (A-top) four ovarian and (A-bottom) three colon carcinoma cell lines, (B) mouse myoblast cells (C2C12), (C) WT and *SIRT6* KO MEFs, (D) human dermal fibroblasts (HDF), and (E) 3T3 immortalized WT and *SIRT6* KO MEFs. Equal amounts of protein were loaded in each lane (50 µg). Fractions were probed for SIRT6 or LDHA and LMNA as controls for cytoplasmic and nuclear fractionation, respectively. Both normal and malignant cell lines have detectable levels of SIRT6 in the cytoplasm.

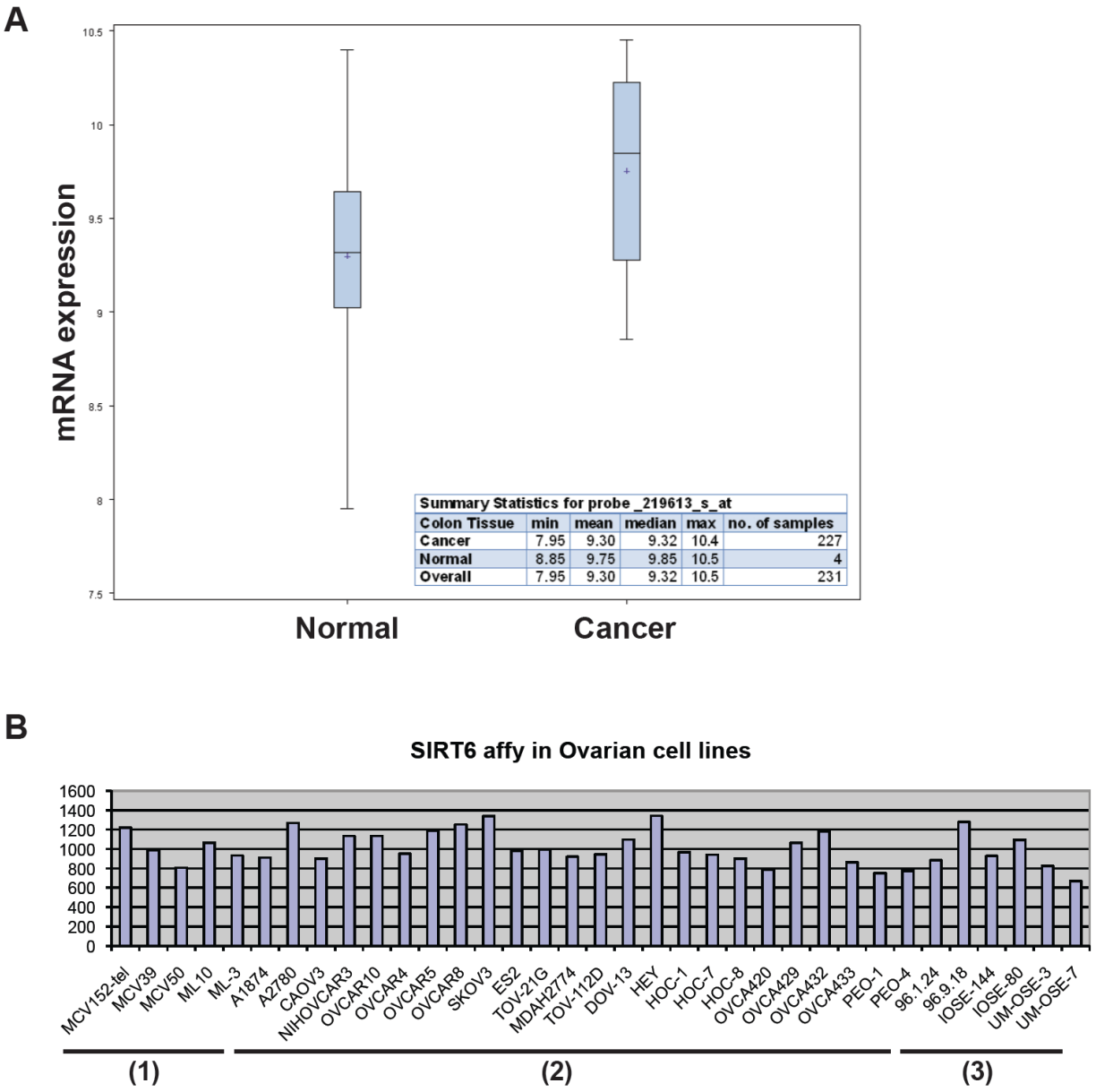

Figure 5.4: *SIRT6* mRNA expression in carcinomas

SIRT6 mRNA expression levels were assessed in (A) colon cancer tissue and (B) ovarian cell lines based on affimetrix data generated by Dr. S. Gruber and Dr. K. Cho respectively. (1) Spontaneously immortalized cystadenomas, (2) Ovarian carcinomas, (3) ovarian surface epithelial cells.

Loss of SIRT6 deacetylase activity in adenoma lesion

We, and others, have identified SIRT6 as a H3K56 deacetylase (Michishita et al., 2009; Yang et al., 2009). Because elevated H3K56ac is found in various tumor types (Das et al., 2009), we predicted that SIRT6 levels would either be decreased or that SIRT6 deacetylase activity would be inactivated in cancer. To assess H3K56ac levels in cancer cells with respect to SIRT6 status, we isolated histones from HCT116 cells infected with an inducible shSirt6 TripZ vector (or scrambled shRNA). As a negative control we included H4K16ac, which is not targeted by SIRT6. We did not observe an increase in H3K56ac or H3K9ac levels with *SIRT6* KD (Figure 5.5A). In fact, it appeared that global histone acetylation was slightly decreased in the SIRT6 depleted cells. Likewise, *Sirt6* knockdown in IEC-6 did not result in augmented H3K56ac (Figure 5.5B). These results indicate that SIRT6 either loses its ability to deacetylate some or all histone targets, or that the remaining amount of SIRT6 after *SIRT6* KD is sufficient to maintain histone acetylation status. To answer this question, we assessed H3K56ac and SIRT6 levels in normal intestines and adenomas of an inducible Sirt6 overexpressing mouse with an $Apc^{min/+}$ background. By using an inducible SIRT6 overexpressor, we would circumvent the decrease in SIRT6 protein levels, which we previously observed in adenomas. In normal tissue, SIRT6 was strictly nuclear and coincided with the absence of H3K56ac (Figure 5.5C). However, in pre-cancerous epithelial cells, SIRT6 levels were elevated and relocalized to the cytoplasm. Furthermore, cytoplasmic localization of SIRT6 corresponded with higher levels of H3K56ac. These results suggest that in normal tissue SIRT6 is a potent H3K56 deacetylase, a function that may be lost in pre-malignant lesions.

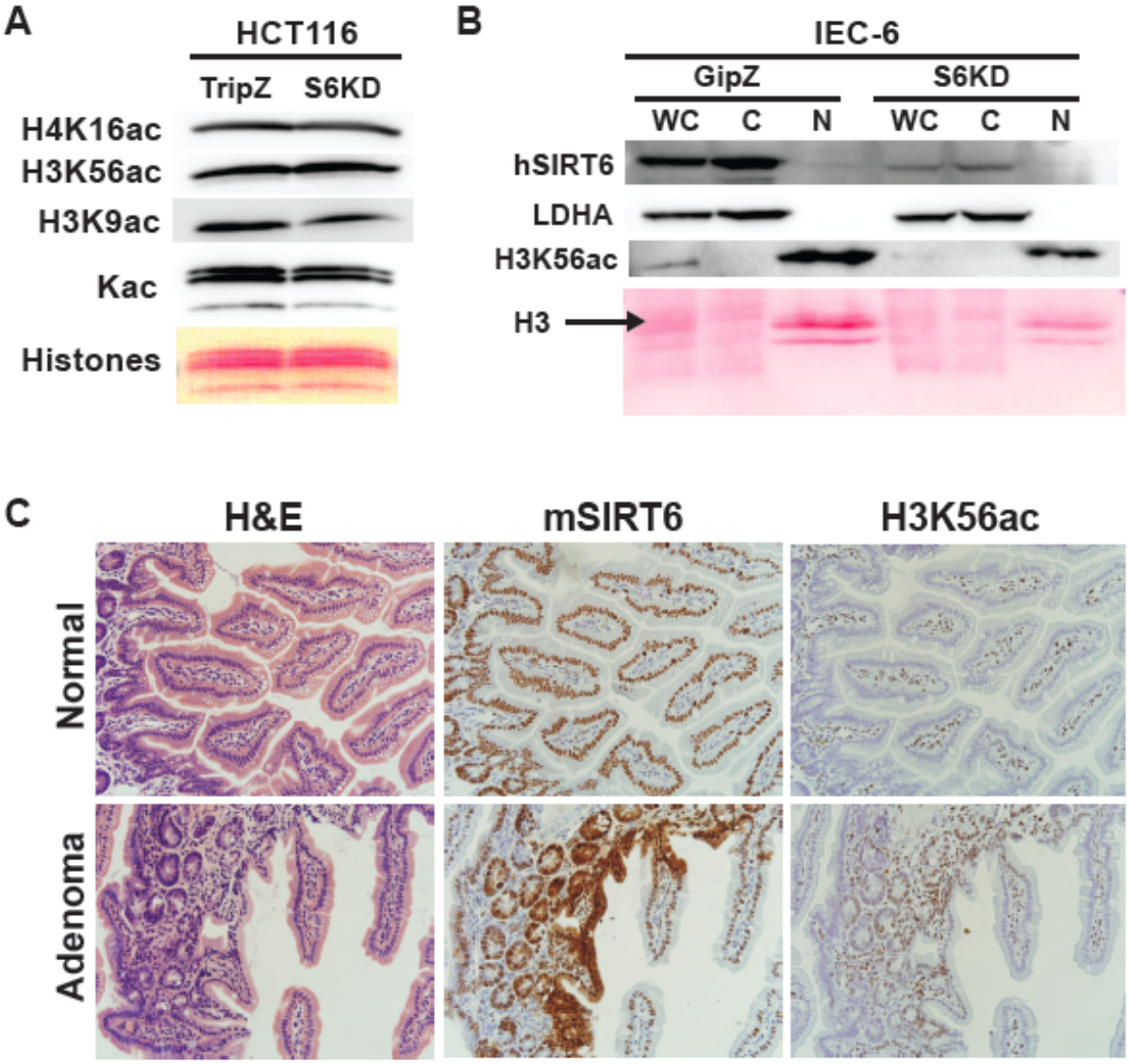

Figure 5.5: SIRT6 loses global deacetylation function upon cellular transformation

(A) Western blot analysis of isolated histones from HCT116 TripZ or *Sirt6* KD for histone acetylation. (B) Nuclear/cytoplasmic fractionation of IEC-6 cells infected with *Sirt6* shRNA vector or control. Ponceau staining serves as loading control (A-B). (C) IHC of normal intestine and adenoma in *Sirt6* OE *Apc*$^{min/+}$ for mSIRT6 and H3K56ac. Sections were imaged with Olympus BX-51 scope at 40X magnification.

SIRT6 actively shuttles to the cytoplasm

The cytoplasmic localization of SIRT6 suggests that SIRT6 is actively transported in and out of the nucleus. Transport across the nuclear envelope requires interaction with karyopherins (importins and exportins) that bind their target protein at specific amino acid sequences. These specific sequences are called nuclear localization signal (NLS) and nuclear export sequence (NES). A close look at the SIRT6 protein sequence revealed one NES and two NLS conserved between mouse and human (Figure 5.6A). We mutated both leucine residues in the NES and the first lysine and arginine residues of both NLSs of SIRT6. We performed transient transfection of HCT116 with WT, mutant NES (mNES) or mutant NLS (mNLS) followed by nuclear/cytoplasmic fractionation (Figure 5.6B). Strikingly, mutation of NES resulted in strictly nuclear SIRT6. Furthermore, mNES is present at a much lower concentration in the nucleus than WT SIRT6. While this may be attributed to lower transfection efficiency, it is also possible that strictly nuclear localized SIRT6 is less stable than WT. mNLS did not alter SIRT6 cellular distribution. In the human SIRT6 protein sequence a third NLS can be found that is absent in mouse SIRT6. It is also possible that all three NLSs need to be mutated to restrict SIRT6 to the cytoplasm.

In an attempt to identify a potential role for SIRT6 in the cytoplasm, we assessed whether SIRT6, like some other sirtuin proteins, is localized to the mitochondria. We isolated mitochondria from two colon cancer cell lines (HCT116 and DLD1) and found SIRT6 to be present in the mitochondria (Figure 5.6C). This was further confirmed in our previously performed interaction screen (Chapter 4) in which we identified

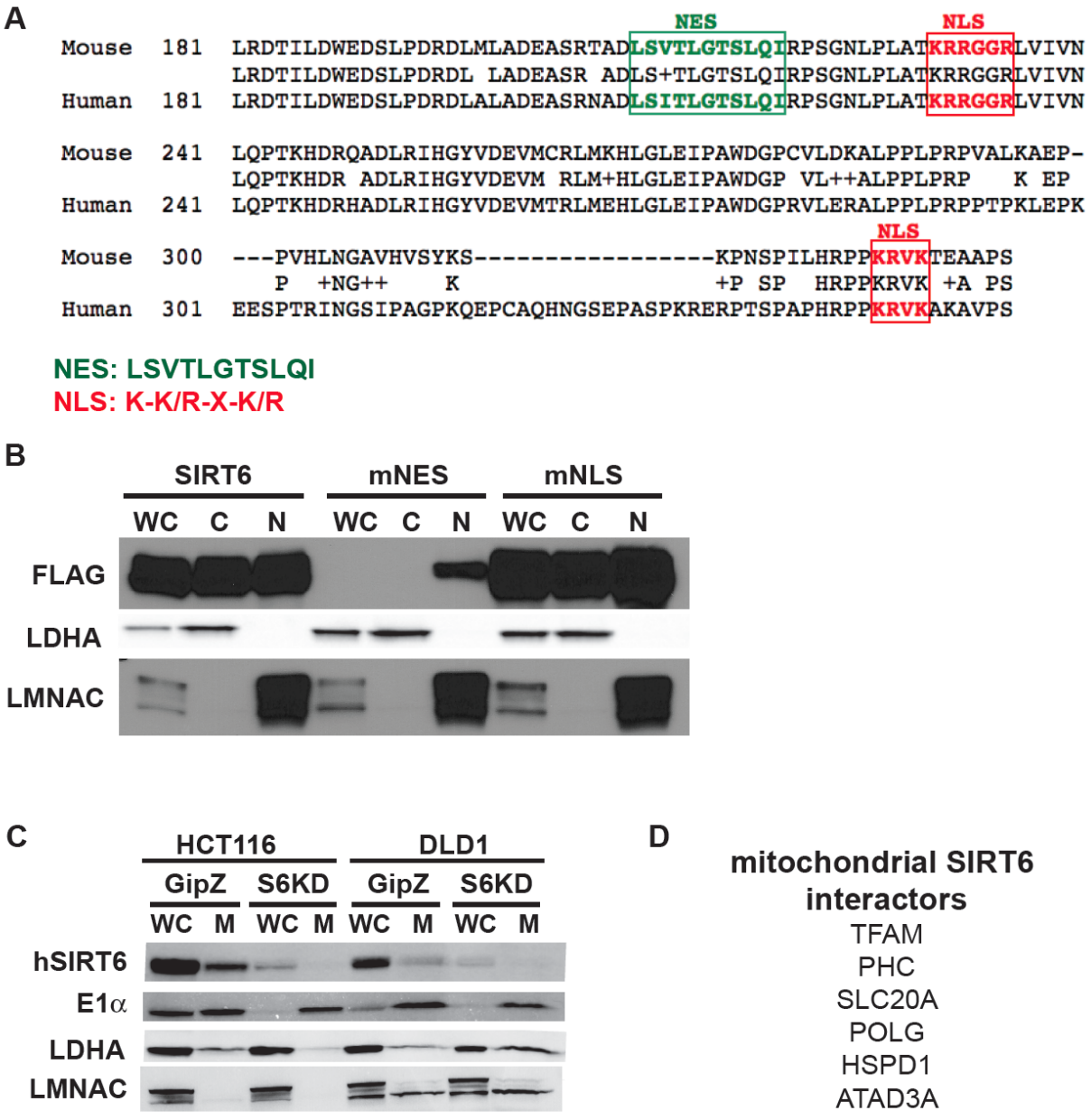

Figure 5.6: Conserved nuclear export sequence and nuclear localization signals in SIRT6

(A) Two nuclear localization signals (NLS) and one nuclear export sequence (NES) are conserved in the C-termini of the mouse and human SIRT6 sequences. (B) Mutagenesis of NES, but not NLS, results in strictly nuclear SIRT6 when transfected into HCT116. (C) SIRT6 may be localized to the mitochondria (50 µg protein/lane) and (D) interacts with a number of mitochondrial factors. E1α, mitochondrial marker; LDHA, cytoplasmic marker; LMNAC, nuclear marker.

numerous mitochondrial factors as SIRT6 interactors (Figure 5.6D). Overall, these results indicate that SIRT6 might have functions outside the nucleus.

SIRT6 does not regulate cancer cell growth or migration

The high levels of SIRT6 in various carcinoma tissues and cell lines raise the question whether SIRT6 provides the tumor cells with a growth advantage. Therefore, we generated two constitutive Sirt6 knockdown ovarian cancer cell lines (Figure 5.7B) and found that the absence of SIRT6 resulted in increased proliferation (Figure 5.7A). To verify our findings, we repeated this experiment using an inducible Sirt6KD vector (TripZ). Unlike the constitutive Sirt6 knockdown, doxycycline induced knockdown resulted in decreased proliferation. As *Sirt6*-null MEFs are sensitive to DNA damaging agents and are genomically unstable, the proliferation results might be due to side effects of doxycycline treatment rather than a direct cause of SIRT6 ablation. Thus we reassessed proliferative potential of three carcinoma cell lines by using transient SIRT6 knockdown (Figure 5.7F). HCT116 and OVCAR8 showed a mild decrease in proliferation in the absence of SIRT6, while no change in cell growth was observed in HeyA8 cells (Figure 5.7E). Due to the variaton of this data, we cannot conclude at this point whether SIRT6 impacts growth of carcinoma cells.

In addition to proliferation, invasive potential is also an important trait of cancer cells. Thus we analyzed the migration ability of two ovarian cancer cell lines using both the constitutive and the inducible knockdown systems. While a mild increase in migration was observed in the constitutive knockdown cell lines (Figure 5.8A), these results were not reproducible in doxycycline inducible knockdowns (Figure 5.8B).

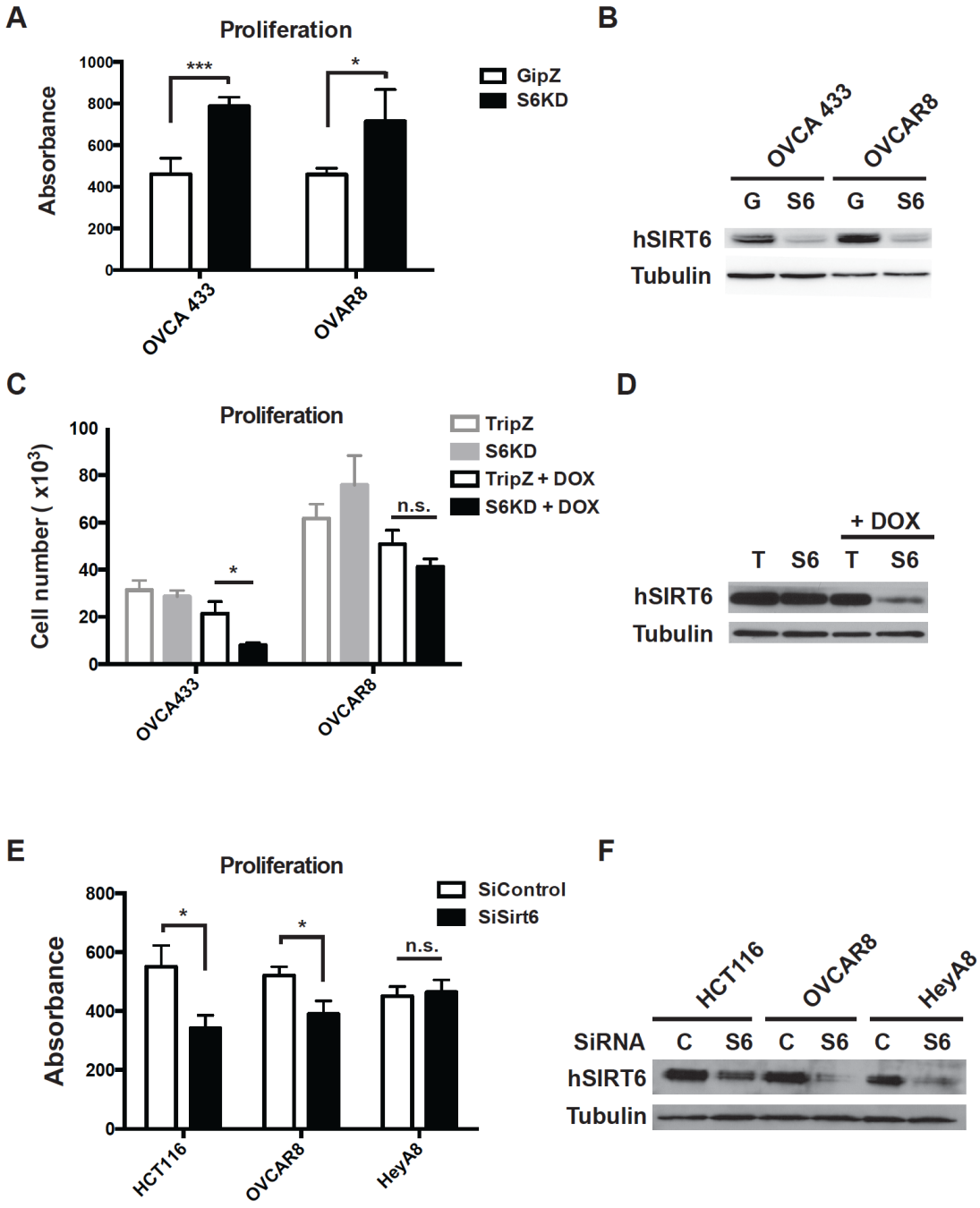

Figure 5.7: Assessment of SIRT6-dependent cellular proliferation

(A) Cellular proliferation in OVCA 433 and OVCAR8 cell lines infected with *shSIRT6* and shControl in GipZ vector. (B) *shSIRT6*-GipZ efficiently knockdowns SIRT6 in indicated cell lines. (C) Cellular proliferation of same cells as in (A) using the inducible TripZ *SIRT6* KD vector. (D) *shSIRT6*-TripZ efficiently knocked down SIRT6 in OVCA 433 cells. (E) Proliferation assay of indicated cell lines using transient siRNA knockdown. (F) SIRT6 proteins levels upon *siSIRT6* treatment. * $p < 0.05$, *** $p < 0.001$

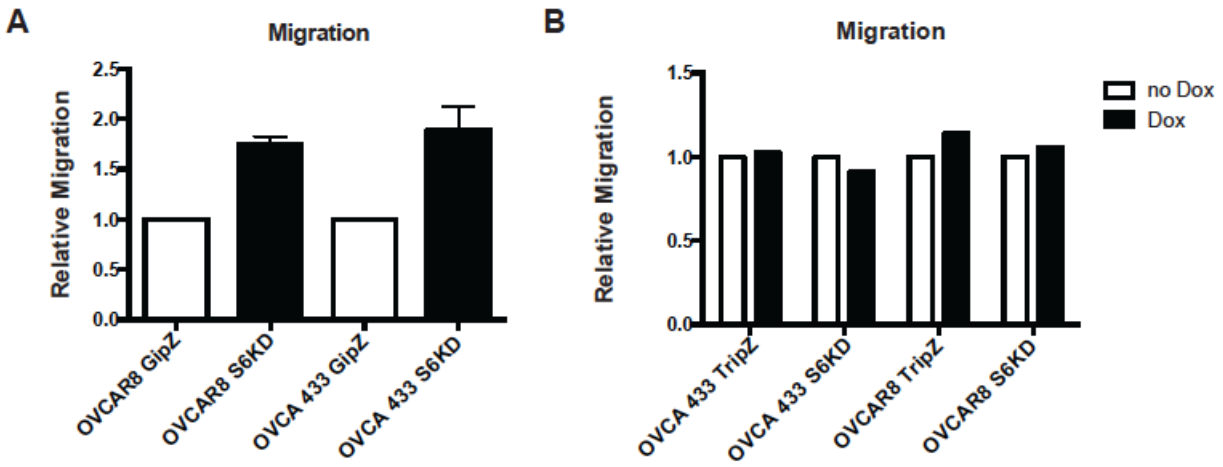

Figure 5.8: SIRT6-mediated tumor cell migration

Migration of OVCAR8 and OVCA433 cell lines with respect to SIRT6 status using (A) constitutive (n = 2) or (B) doxycycline (Dox) inducible knockdown system. Values were normalized to control vector (A) or untreated sample (B).

SIRT6 as a diagnostic tool

While we were unable to identify a role for SIRT6 in carcinoma cells or assess how SIRT6 cellular localization is regulated, the high SIRT6 protein levels and localization might be useful from a diagnostic perspective. In collaboration with Dr. M. Roh, we stained cytoblocks made of pleural or peritoneal fluids, obtained from ovarian cancer patients, for SIRT6 using two independent SIRT6 antibodies (Figure 5.9). Overall, both antibodies clearly visualized the tumor cells with elevated and cytoplasmic staining. When comparing both antibodies, the Abcam antibody showed a higher staining intensity in all cell types and identified cytoplasmic SIRT6 in macrophages. SIRT6-CST (SIRT6 antibody from Cell Signaling Technology) staining, on the other hand, only showed postive cytoplasmic staining in tumor cells and was largely negative in normal cells. No distinction could be made in SIRT6 staining pattern between low versus high-grade adenocarcinomas.

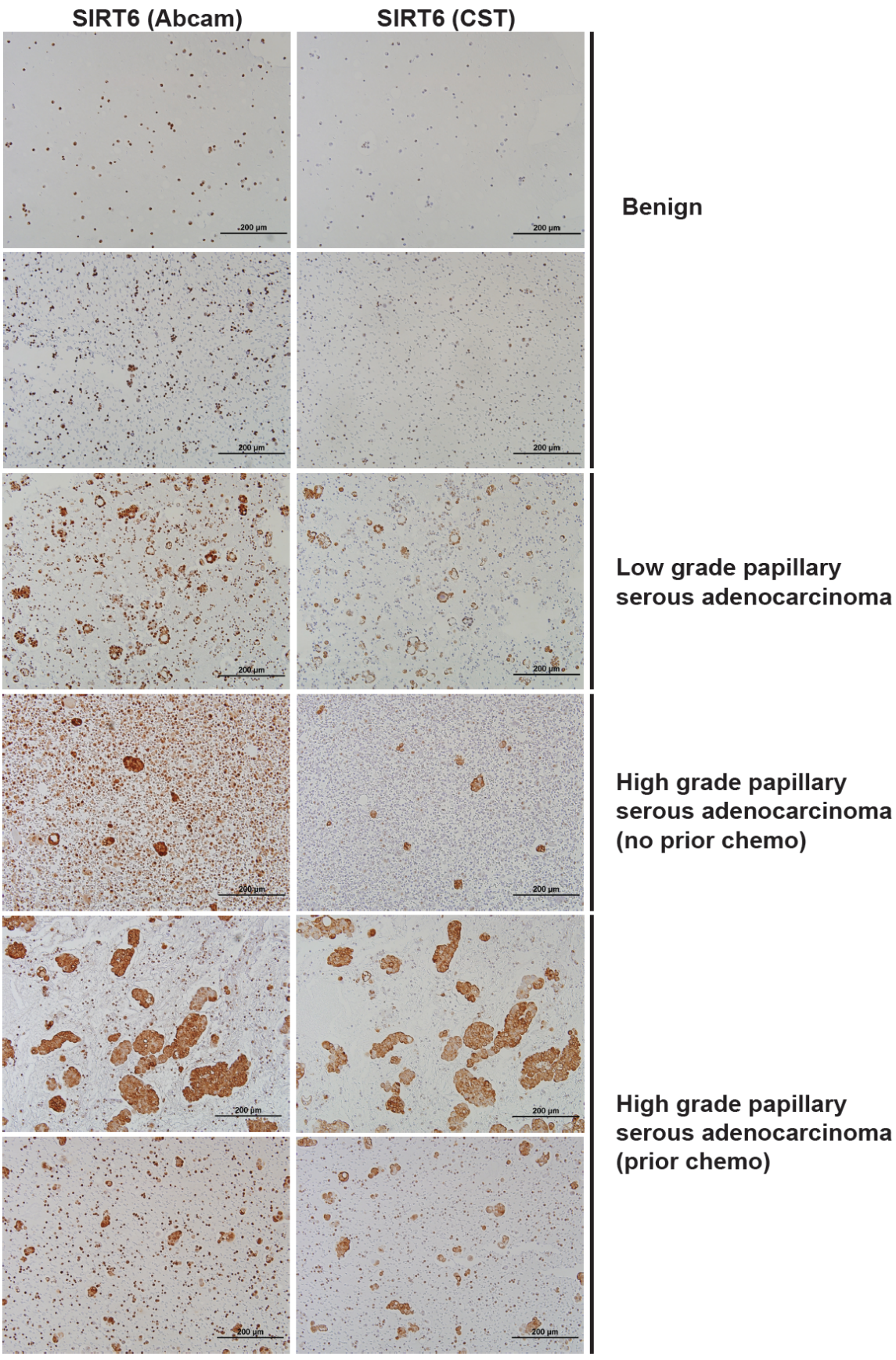
SIRT6 (Abcam)
SIRT6 (CST)
Benign
Low grade papillary serous adenocarcinoma
High grade papillary serous adenocarcinoma (no prior chemo)
High grade papillary serous adenocarcinoma (prior chemo)

Figure 5.9: Detection of ovarian cancer in pleural fluids/ascites

Cytoblocks from pleural or peritoneal fluids were analyzed for the presence of ovarian cancer cells using SIRT6 staining. Two commercial SIRT6 antibodies were compared for specificity. CST, Cell Signaling Technologies.

Discussion

A number of recent studies have provided compelling evidence for a role of SIRT6 as a tumor suppressor protein by regulating numerous pathways such as apoptosis, cell growth and metabolism (discussed in detail in chapter 3) (Han et al., 2014; Min et al., 2012; Sebastian et al., 2012; Van Meter et al., 2011). Others have reported tumor-promoting properties for SIRT6 (Figure 5.10). Elevated SIRT6 levels are associated with chemotherapeutic drug resistance in MCF-7 breast cancer cells (Khongkow et al., 2013a). Deacetylation of the tumor suppressor proteins FOXO3A and p53 by SIRT6, resulting in reduced cell cycle arrest and apoptosis in response to chemotherapeutic treatment, has been proposed to explain this effect. However, importantly there currently is no direct evidence *in vitro* that SIRT6 can deacetylate these proteins. In addition, Khongkow and colleagues reported that high nuclear levels of SIRT6 correlated with a poor prognosis in breast cancer patients (Khongkow et al., 2013a). Furthermore, high SIRT6 levels are associated with undifferentiated squamous cell carcinoma (SCC) (Lefort et al., 2013). The tumor suppressor and tumor promoting functions of SIRT6 are likely to result from different underlying functions of this protein.

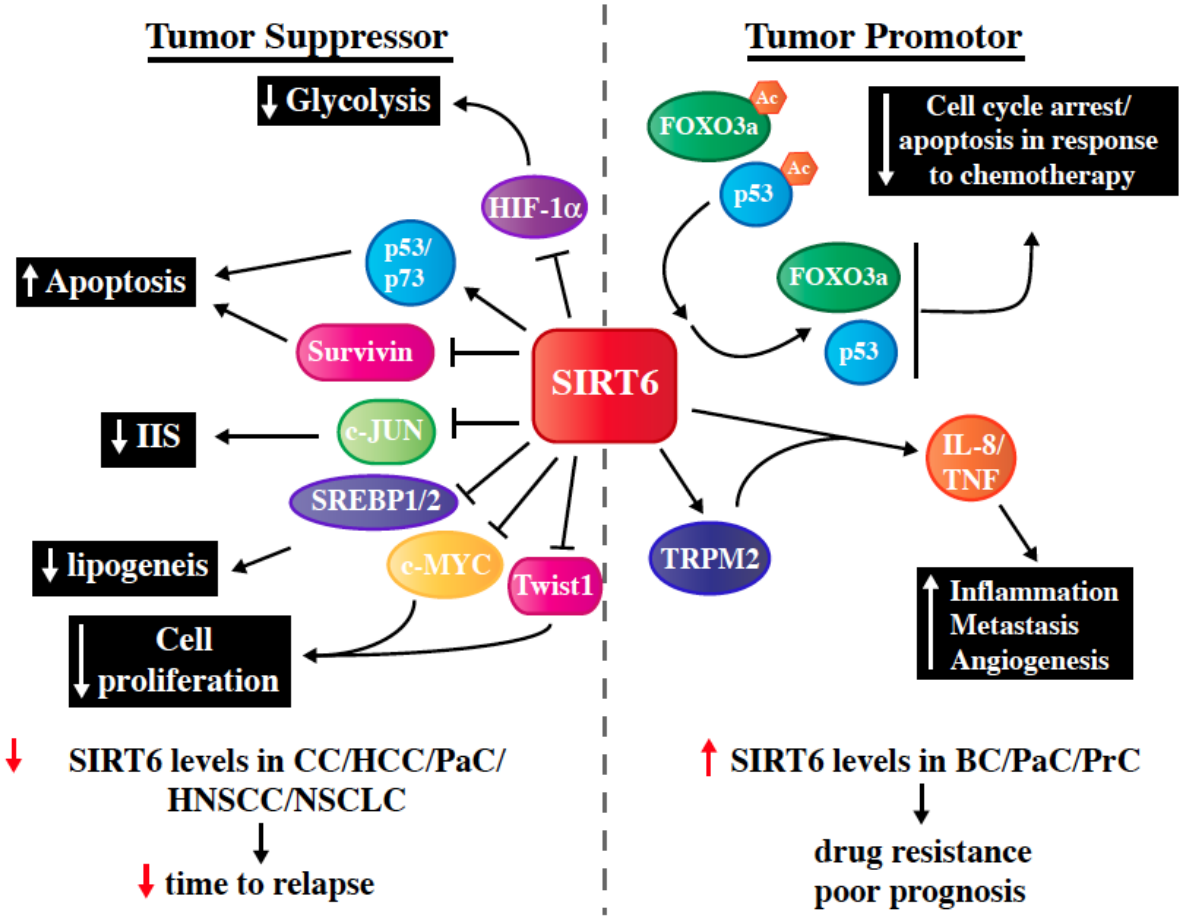

Figure 5.10: Dual roles for SIRT6 in cancer
SIRT6 has been reported to have both tumor suppressor and oncogenic properties. Low levels of SIRT6 have been described in colon cancer (CC), hepatocellular carcinoma (HCC), pancreatic cancer (PaC), head and neck squamous cell carcinoma (HNSCC) and non-small cell lung cancer (NSCLC), and correlates with a shortened time to relapse. By contrast, high SIRT6 levels have been reported in breast cancer (BC), PaC and prostate cancer (PrC), and is associated with drug resistance and poor prognosis. Ac, acetyl group; TNF, tumor necrosis factor; IL-8, interleukin-8.

In conjunction with these studies, we found SIRT6 protein, but not mRNA, levels in human carcinoma tissues and cell lines to be significantly elevated. Furthermore, SIRT6, a previously described nuclear protein (Liszt et al., 2005; Michishita et al., 2005; Mostoslavsky et al., 2006; Xiao et al., 2010), is highly abundant in the cytoplasmic fraction of the normal and cancer cells analyzed. Khongkow et al. also

identified cytoplasmic localization of SIRT6 in breast cancer cells and reported that the cytoplasmic fraction of SIRT6, in contrast to nuclear SIRT6, correlated with a better clinical outcome in breast cancer (Khongkow et al., 2013b). The presence of SIRT6 outside the nucleus in both normal and cancerous cells implies that SIRT6 targets non-nuclear proteins as well. However, we were not able to detect cytoplasmic localized SIRT6 in normal cells by immunohistochemistry. While this could be explained by technical variability, it is also likely that cells grown in culture are subjected to a mild form of stress. Jedrusik-Bode and colleagues reported that cellular stress causes SIRT6 to relocalize to the cytoplasm where it is essential for rapid stress granule formation and disassembly (Jedrusik-Bode et al., 2013). Currently other cytoplasmic functions for SIRT6 are unknown.

Further cellular subfractionation revealed the presence of SIRT6 in the mitochondria (Figure 5.6C). In support of this, we identified a number of mitochondrial factors in a SIRT6 interaction screen (Figure 5.6D). Among these the mitochondrial transcription factor TFAM, the mitochondrial transporters PHC and SLC20A, the catalytic subunit of mitochondrial DNA polymerase POLG, HSPD1, which is essential for folding and assembly of newly imported proteins in the mitochondria, and ATAD3A, a mitochondrial protein that stabilizes nucleoids (mitochondrial DNA protein complexes). While SIRT6's interaction with these mitochondrial proteins needs to be confirmed, SIRT6's interaction with the transporters PHC and SLC20A suggests that SIRT6 may be actively transported into the mitochondria, while SIRT6's binding to TFAM implies

that SIRT6 could act as a transcriptional regulator, similar to its function in the nucleus. Future studies are needed to test this hypothesis.

Examination of the SIRT6 protein sequence revealed the presence of three conserved localization sequences: one NES and two NLSs. These sequences indicate that SIRT6 cellular localization is tightly regulated. Indeed, mutating the NES allowed us to confine SIRT6 to the nucleus (Figure 5.6B). Mutagenesis of the two NLSs did not result in SIRT6 relocalization. However, deletion of the N- and C-termini of SIRT6 does drive SIRT6 out of the nucleus (Tennen et al., 2010) and thus other or additional sequences are likely responsible for nuclear localization of SIRT6.

The high protein levels of SIRT6 in carcinoma cells, possibly due to enhanced protein stability or decreased protein degradation, would seem to oppose the previously described tumor suppressor function of SIRT6. H3K56ac, a target of SIRT6, is associated with DNA instability and cancer (Das et al., 2009). Knockdown of SIRT6 in HCT116 cells did not result in increased H3K9 or H3K56 acetylation (Figure 5.5A). Strikingly, SIRT6 knockdown did not alter H3K56ac levels in IEC-6 cells either (Figure 5.5B). We, and others, have previously shown that SIRT6 deacetylates H3K56 using germline Sirt6KO MEFs (Michishita et al., 2009; Yang et al., 2009). Knockdown of Sirt6 with shRNA is about 90% effective and thus it is possible that the small fraction of remaining SIRT6 is sufficient to regulate H3K56ac. However, *in vivo* overexpression of SIRT6 resulted in complete loss of H3K56 acetylation in normal intestinal epithelial cells. Notably, in polyps, H3K56ac reappeared, which coincided with SIRT6

relocalization to the cytoplasm (Figure 5.5C). These results suggest that SIRT6 relocalization to the cytoplasm is a means to attenuate nuclear SIRT6 function.

Finally, in an effort to identify functional properties of SIRT6 in cancer, we measured the proliferative and migratory capacity of cancer cells with respect to SIRT6 status using various Sirt6 knockdown systems. When knocking down Sirt6 constitutively, cancer cells grew and migrated faster, while inducible Sirt6 knockdown with doxycycline had the opposite effect on cellular growth and did not impact cell migration (Figures 5.7-5.8). Furthermore, the change in cellular growth was variable between cancer cell lines when using transient siRNA transfection. We previously identified increased aneuploidy upon constitutive knockdown of Sirt6 in IEC-6. Thus long-term SIRT6 ablation could result in genomic instability and possible accumulation of mutations that provide cancer cells with additional cancer traits. Likewise, SIRT6 deficient cells are sensitive to genotoxins and thus SIRT6 depleted cancer cells might be vulnerable to doxycycline treatment resulting in decreased growth.

While we cannot provide mechanistic insight in SIRT6 function in cancer cells, our results suggest that SIRT6 relocalization results in loss of SIRT6's H3K56 deacetylation function. In this regard, treatment with SIRT6 activators might be a usefull therapeutic tool. The distinct staining pattern of SIRT6 does provide a valuable diagnostic tool as we can clearly identify ovarian carcinoma cells in ascites and pleural lavages from ovarian cancer patients by performing IHC for SIRT6.

Future directions

In this study we identified SIRT6 relocalization to the cytoplasmic fraction of carcinoma cells. SIRT6 cellular localization is likely tightly regulated as we were able to confine SIRT6 to the nuclear fraction by mutating the NES. A more indepth study of SIRT6 shuttling across the nuclear membrane will provide the means to identify the importance of nuclear versus cytoplasmic SIRT6 in normal and cancerous cells. Except for SIRT6's role in mediating stress granule formation (Jedrusik-Bode et al., 2013), no cytoplasmic functions for SIRT6 have been described. The initial observation that SIRT6 interacts with a number of mitochondrial proteins could imply that SIRT6 plays a role in regulating mitochondrial gene expression and possibly maintaining the integrity of mitochondrial DNA (mtDNA). Mice heterozygous for TFAM have a 30-50% reduction of mtDNA (Larsson et al., 1998) and changes in mtDNA content are associated with tumorigenesis (Lan et al., 2008; Lee et al., 2005). Therefore, it is feasible that SIRT6 could maintain mitochondrial integrity and suppress tumor formation by regulating TFAM. However, further studies are necessary to test this a possible role for SIRT6 in the mitochondria.

In addition to exploring a role for SIRT6 in various cellular compartments, a better understanding of how SIRT6 protein levels are regulated in cancer cells is essential when considering SIRT6 as a potential therapeutic target. We did not observe a change in SIRT6 transcripts, suggesting increased SIRT6 stability or a decrease in SIRT6 proteasomal degradation. Ubiquitination of SIRT6 by CHIP enhances SIRT6 stability (Ronnebaum et al., 2013). Changes in PTMs on SIRT6 might be a means through which SIRT6 is stabilized in cancer cells.

Chapter 6

Concluding remarks

A cancer cell is generated through the accumulation of multiple mutations that provide the initial cell the ability to surpass the many defense mechanisms in place to protect the organism from malignancies, such as DNA repair systems, antioxidants, cell cycle checkpoints and immune response. Hanahan and Weinberg described the 6 halmarks, and the four enabling and emerging characteristics of cancer (Hanahan and Weinberg, 2011). In my thesis work we have identified the histone deacetylase SIRT6 as a potent tumor suppressor protein, possibly by inhibiting several of these cancer traits. First SIRT6 suppresses aerobic glycolysis, the preferred method of energy generation in cancer cells (Hallmark: deregulating cellular energetics). Secondly, SIRT6 inhibits ribosomal biogenesis and subsequent cell growth through c-MYC (Hallmark: sustaining proliferative signaling). In addition to these two traits, we have suggestive data that SIRT6 can protect against tumor formation through two additional mechanisms. SIRT6 deficient cells have a higher percentage of aneuploidy, possibly through SIRT6's role in DNA repair (Hallmark: genome instability and mutation). Furthermore, enterocyte specific SIRT6-deficient mice in an *Apc*$^{min/+}$ background have elevated levels of the cytokine Il-17, a cytokine that can promote tumor growth by inducing an inflammatory response (Hallmark: tumor-promoting inflammation).

In addition, we have identified various novel cellular activities of SIRT6 that contribute to the current understanding of SIRT6 biology. In addition to H3K9ac, we found that SIRT6 deacetylates histone H3 acetylated at K18, 23 and 56. The latter is specifically target by SIRT6 at the promoter sites of ribosomal genes normally transcribed by c-MYC. Additionally, we identified an interaction of SIRT6 with the silencing factors KAP1 and HP1, and the members of the FACT complex, possibly to regulate gene transcription. Furthermore, *in vivo* treatment with the antioxidant NAC rescues the increased tumor incidence seen in the absence of SIRT6. In cancer, we observed that SIRT6 protein levels, but not mRNA, are elevated in numerous carcinoma cell lines and tissues. Here SIRT6 is localized in both the nuclear and cytoplasmic fraction of the cell, and it appears to be actively transported out of the nucleus through a conserved nuclear export sequence. Finally, we have generated suggestive evidence that SIRT6 is present in the mitochondrial compartment of the cell where it interacts with several mitochondrial proteins.

The work in this dissertation has given further insight in the diverse roles of SIRT6. Although many questions about SIRT6 function under physiological and pathological conditions remain to be answered, we believe that SIRT6 has strong therapeutic potential for the treatment of cancer or other age-related conditions.

References

Adler, A.S., Sinha, S., Kawahara, T.L., Zhang, J.Y., Segal, E., and Chang, H.Y. (2007). Motif module map reveals enforcement of aging by continual NF-kappaB activity. Genes Dev *21*, 3244-3257.

Agrawal, A., Tay, J., Ton, S., Agrawal, S., and Gupta, S. (2009). Increased reactivity of dendritic cells from aged subjects to self-antigen, the human DNA. J Immunol *182*, 1138-1145.

Agrawal, A., Tay, J., Yang, G.E., Agrawal, S., and Gupta, S. (2010). Age-associated epigenetic modifications in human DNA increase its immunogenicity. Aging (Albany NY) *2*, 93-100.

Ahuja, N., Schwer, B., Carobbio, S., Waltregny, D., North, B.J., Castronovo, V., Maechler, P., and Verdin, E. (2007). Regulation of insulin secretion by SIRT4, a mitochondrial ADP-ribosyltransferase. J Biol Chem *282*, 33583-33592.

Aparicio, O.M., Billington, B.L., and Gottschling, D.E. (1991). Modifiers of position effect are shared between telomeric and silent mating-type loci in S. cerevisiae. Cell *66*, 1279-1287.

Arabi, A., Wu, S., Ridderstrale, K., Bierhoff, H., Shiue, C., Fatyol, K., Fahlen, S., Hydbring, P., Soderberg, O., Grummt, I.*, et al.* (2005). c-Myc associates with ribosomal DNA and activates RNA polymerase I transcription. Nat Cell Biol *7*, 303-310.

Ardawi, M.S., and Newsholme, E.A. (1982). Maximum activities of some enzymes of glycolysis, the tricarboxylic acid cycle and ketone-body and glutamine utilization pathways in lymphocytes of the rat. Biochem J *208*, 743-748.

Baker, R.G., Hayden, M.S., and Ghosh, S. (2011). NF-kappaB, inflammation, and metabolic disease. Cell Metab *13*, 11-22.

Barber, M.F., Michishita-Kioi, E., Xi, Y., Tasselli, L., Kioi, M., Moqtaderi, Z., Tennen, R.I., Paredes, S., Young, N.L., Chen, K.*, et al.* (2012). SIRT7 links H3K18 deacetylation to maintenance of oncogenic transformation. Nature *487*, 114-118.

Barna, M., Pusic, A., Zollo, O., Costa, M., Kondrashov, N., Rego, E., Rao, P.H., and Ruggero, D. (2008). Suppression of Myc oncogenic activity by ribosomal protein haploinsufficiency. Nature *456*, 971-975.
Battu, A., Ray, A., and Wani, A.A. (2011). ASF1A and ATM regulate H3K56-mediated cell-cycle checkpoint recovery in response to UV irradiation. Nucleic Acids Res *39*, 7931-7945.
Bauer, I., Grozio, A., Lasiglie, D., Basile, G., Sturla, L., Magnone, M., Sociali, G., Soncini, D., Caffa, I., Poggi, A.*, et al.* (2012). The NAD+-dependent histone deacetylase SIRT6 promotes cytokine production and migration in pancreatic cancer cells by regulating Ca2+ responses. J Biol Chem *287*, 40924-40937.
Belenky, P., Racette, F.G., Bogan, K.L., McClure, J.M., Smith, J.S., and Brenner, C. (2007). Nicotinamide riboside promotes Sir2 silencing and extends lifespan via Nrk and Urh1/Pnp1/Meu1 pathways to NAD+. Cell *129*, 473-484.
Berdichevsky, A., Viswanathan, M., Horvitz, H.R., and Guarente, L. (2006). C. elegans SIR-2.1 interacts with 14-3-3 proteins to activate DAF-16 and extend life span. Cell *125*, 1165-1177.
Bernard, P., Maure, J.F., Partridge, J.F., Genier, S., Javerzat, J.P., and Allshire, R.C. (2001). Requirement of heterochromatin for cohesion at centromeres. Science *294*, 2539-2542.
Beroukhim, R., Mermel, C.H., Porter, D., Wei, G., Raychaudhuri, S., Donovan, J., Barretina, J., Boehm, J.S., Dobson, J., Urashima, M.*, et al.* (2010). The landscape of somatic copy-number alteration across human cancers. Nature *463*, 899-905.
Boboila, C., Alt, F.W., and Schwer, B. (2012). Classical and alternative end-joining pathways for repair of lymphocyte-specific and general DNA double-strand breaks. Adv Immunol *116*, 1-49.
Boiselle, P.M., Patz, E.F., Jr., Vining, D.J., Weissleder, R., Shepard, J.A., and McLoud, T.C. (1998). Imaging of mediastinal lymph nodes: CT, MR, and FDG PET. Radiographics *18*, 1061-1069.
Bonuccelli, G., Whitaker-Menezes, D., Castello-Cros, R., Pavlides, S., Pestell, R.G., Fatatis, A., Witkiewicz, A.K., Vander Heiden, M.G., Migneco, G., Chiavarina, B.*, et al.*

(2010). The reverse Warburg effect: glycolysis inhibitors prevent the tumor promoting effects of caveolin-1 deficient cancer associated fibroblasts. Cell Cycle *9*, 1960-1971.
Burnett, C., Valentini, S., Cabreiro, F., Goss, M., Somogyvari, M., Piper, M.D., Hoddinott, M., Sutphin, G.L., Leko, V., McElwee, J.J.*, et al.* (2011). Absence of effects of Sir2 overexpression on lifespan in C. elegans and Drosophila. Nature *477*, 482-485.
Canto, C., Sauve, A.A., and Bai, P. (2013). Crosstalk between poly(ADP-ribose) polymerase and sirtuin enzymes. Mol Aspects Med *34*, 1168-1201.
Cardus, A., Uryga, A.K., Walters, G., and Erusalimsky, J.D. (2013). SIRT6 protects human endothelial cells from DNA damage, telomere dysfunction, and senescence. Cardiovasc Res *97*, 571-579.
Chang, S.H., Mirabolfathinejad, S.G., Katta, H., Cumpian, A.M., Gong, L., Caetano, M.S., Moghaddam, S.J., and Dong, C. (2014). T helper 17 cells play a critical pathogenic role in lung cancer. Proc Natl Acad Sci U S A *111*, 5664-5669.
Chen, C.C., Carson, J.J., Feser, J., Tamburini, B., Zabaronick, S., Linger, J., and Tyler, J.K. (2008). Acetylated lysine 56 on histone H3 drives chromatin assembly after repair and signals for the completion of repair. Cell *134*, 231-243.
Church, D.N., and Talbot, D.C. (2012). Survivin in solid tumors: rationale for development of inhibitors. Curr Oncol Rep *14*, 120-128.
Cochaud, S., Giustiniani, J., Thomas, C., Laprevotte, E., Garbar, C., Savoye, A.M., Cure, H., Mascaux, C., Alberici, G., Bonnefoy, N.*, et al.* (2013). IL-17A is produced by breast cancer TILs and promotes chemoresistance and proliferation through ERK1/2. Sci Rep *3*, 3456.
Corn, P.G., Ricci, M.S., Scata, K.A., Arsham, A.M., Simon, M.C., Dicker, D.T., and El-Deiry, W.S. (2005). Mxi1 is induced by hypoxia in a HIF-1-dependent manner and protects cells from c-Myc-induced apoptosis. Cancer Biol Ther *4*, 1285-1294.
Dai, D.F., Chen, T., Johnson, S.C., Szeto, H., and Rabinovitch, P.S. (2012). Cardiac aging: from molecular mechanisms to significance in human health and disease. Antioxid Redox Signal *16*, 1492-1526.
Dai, M.S., and Lu, H. (2008). Crosstalk between c-Myc and ribosome in ribosomal biogenesis and cancer. J Cell Biochem *105*, 670-677.

Dang, C.V. (2010). Rethinking the Warburg effect with Myc micromanaging glutamine metabolism. Cancer Res *70*, 859-862.
Dang, C.V. (2012). MYC on the path to cancer. Cell *149*, 22-35.
Dang, C.V., Kim, J.W., Gao, P., and Yustein, J. (2008). The interplay between MYC and HIF in cancer. Nat Rev Cancer *8*, 51-56.
Dang, C.V., Le, A., and Gao, P. (2009a). MYC-induced cancer cell energy metabolism and therapeutic opportunities. Clin Cancer Res *15*, 6479-6483.
Dang, W., Steffen, K.K., Perry, R., Dorsey, J.A., Johnson, F.B., Shilatifard, A., Kaeberlein, M., Kennedy, B.K., and Berger, S.L. (2009b). Histone H4 lysine 16 acetylation regulates cellular lifespan. Nature *459*, 802-807.
Das, C., Lucia, M.S., Hansen, K.C., and Tyler, J.K. (2009). CBP/p300-mediated acetylation of histone H3 on lysine 56. Nature *459*, 113-117.
David, G., Dannenberg, J.H., Simpson, N., Finnerty, P.M., Miao, L., Turner, G.M., Ding, Z., Carrasco, R., and Depinho, R.A. (2006). Haploinsufficiency of the mSds3 chromatin regulator promotes chromosomal instability and cancer only upon complete neutralization of p53. Oncogene *25*, 7354-7360.
DeBerardinis, R.J., Mancuso, A., Daikhin, E., Nissim, I., Yudkoff, M., Wehrli, S., and Thompson, C.B. (2007). Beyond aerobic glycolysis: transformed cells can engage in glutamine metabolism that exceeds the requirement for protein and nucleotide synthesis. Proc Natl Acad Sci U S A *104*, 19345-19350.
Derenzini, M., Trere, D., Pession, A., Montanaro, L., Sirri, V., and Ochs, R.L. (1998). Nucleolar function and size in cancer cells. Am J Pathol *152*, 1291-1297.
Dewhirst, M.W. (2007). Intermittent hypoxia furthers the rationale for hypoxia-inducible factor-1 targeting. Cancer Res *67*, 854-855.
Dominy, J.E., Jr., Lee, Y., Gerhart-Hines, Z., and Puigserver, P. (2010). Nutrient-dependent regulation of PGC-1alpha's acetylation state and metabolic function through the enzymatic activities of Sirt1/GCN5. Biochim Biophys Acta *1804*, 1676-1683.
Dominy, J.E., Jr., Lee, Y., Jedrychowski, M.P., Chim, H., Jurczak, M.J., Camporez, J.P., Ruan, H.B., Feldman, J., Pierce, K., Mostoslavsky, R.*, et al.* (2012). The deacetylase Sirt6 activates the acetyltransferase GCN5 and suppresses hepatic gluconeogenesis. Mol Cell *48*, 900-913.

Du, J., Zhou, Y., Su, X., Yu, J.J., Khan, S., Jiang, H., Kim, J., Woo, J., Kim, J.H., Choi, B.H.*, et al.* (2011). Sirt5 is a NAD-dependent protein lysine demalonylase and desuccinylase. Science *334*, 806-809.

Dunn, C., Wiltshire, C., MacLaren, A., and Gillespie, D.A. (2002). Molecular mechanism and biological functions of c-Jun N-terminal kinase signalling via the c-Jun transcription factor. Cell Signal *14*, 585-593.

Eagle, H. (1955). Nutrition needs of mammalian cells in tissue culture. Science *122*, 501-514.

Ekwall, K., Olsson, T., Turner, B.M., Cranston, G., and Allshire, R.C. (1997). Transient inhibition of histone deacetylation alters the structural and functional imprint at fission yeast centromeres. Cell *91*, 1021-1032.

Elhanati, S., Kanfi, Y., Varvak, A., Roichman, A., Carmel-Gross, I., Barth, S., Gibor, G., and Cohen, H.Y. (2013). Multiple regulatory layers of SREBP1/2 by SIRT6. Cell Rep *4*, 905-912.

Ema, M., Taya, S., Yokotani, N., Sogawa, K., Matsuda, Y., and Fujii-Kuriyama, Y. (1997). A novel bHLH-PAS factor with close sequence similarity to hypoxia-inducible factor 1alpha regulates the VEGF expression and is potentially involved in lung and vascular development. Proc Natl Acad Sci U S A *94*, 4273-4278.

Eruslanov, E., and Kusmartsev, S. (2010). Identification of ROS using oxidized DCFDA and flow-cytometry. Methods Mol Biol *594*, 57-72.

Eskandarian, H.A., Impens, F., Nahori, M.A., Soubigou, G., Coppee, J.Y., Cossart, P., and Hamon, M.A. (2013). A role for SIRT2-dependent histone H3K18 deacetylation in bacterial infection. Science *341*, 1238858.

Eymery, A., Horard, B., El Atifi-Borel, M., Fourel, G., Berger, F., Vitte, A.L., Van den Broeck, A., Brambilla, E., Fournier, A., Callanan, M.*, et al.* (2009). A transcriptomic analysis of human centromeric and pericentric sequences in normal and tumor cells. Nucleic Acids Res *37*, 6340-6354.

Feldman, J.L., Baeza, J., and Denu, J.M. (2013). Activation of the Protein Deacetylase SIRT6 by Long-chain Fatty Acids and Widespread Deacylation by Mammalian Sirtuins. J Biol Chem *288*, 31350-31356.

Flamme, I., Frohlich, T., von Reutern, M., Kappel, A., Damert, A., and Risau, W. (1997). HRF, a putative basic helix-loop-helix-PAS-domain transcription factor is closely related to hypoxia-inducible factor-1 alpha and developmentally expressed in blood vessels. Mech Dev *63*, 51-60.

Foudah, D., Redaelli, S., Donzelli, E., Bentivegna, A., Miloso, M., Dalpra, L., and Tredici, G. (2009). Monitoring the genomic stability of in vitro cultured rat bone-marrow-derived mesenchymal stem cells. Chromosome Res *17*, 1025-1039.

Frye, R.A. (1999). Characterization of five human cDNAs with homology to the yeast SIR2 gene: Sir2-like proteins (sirtuins) metabolize NAD and may have protein ADP-ribosyltransferase activity. Biochem Biophys Res Commun *260*, 273-279.

Gao, P., Tchernyshyov, I., Chang, T.C., Lee, Y.S., Kita, K., Ochi, T., Zeller, K.I., De Marzo, A.M., Van Eyk, J.E., Mendell, J.T.*, et al.* (2009). c-Myc suppression of miR-23a/b enhances mitochondrial glutaminase expression and glutamine metabolism. Nature *458*, 762-765.

Garcia, B.A., Mollah, S., Ueberheide, B.M., Busby, S.A., Muratore, T.L., Shabanowitz, J., and Hunt, D.F. (2007). Chemical derivatization of histones for facilitated analysis by mass spectrometry. Nat Protoc *2*, 933-938.

Garedew, A., and Moncada, S. (2008). Mitochondrial dysfunction and HIF1alpha stabilization in inflammation. J Cell Sci *121*, 3468-3475.

Gasior, S.L., Wakeman, T.P., Xu, B., and Deininger, P.L. (2006). The human LINE-1 retrotransposon creates DNA double-strand breaks. J Mol Biol *357*, 1383-1393.

Gerhart-Hines, Z., Rodgers, J.T., Bare, O., Lerin, C., Kim, S.H., Mostoslavsky, R., Alt, F.W., Wu, Z., and Puigserver, P. (2007). Metabolic control of muscle mitochondrial function and fatty acid oxidation through SIRT1/PGC-1alpha. EMBO J *26*, 1913-1923.

Geromanos, S.J., Vissers, J.P., Silva, J.C., Dorschel, C.A., Li, G.Z., Gorenstein, M.V., Bateman, R.H., and Langridge, J.I. (2009). The detection, correlation, and comparison of peptide precursor and product ions from data independent LC-MS with data dependant LC-MS/MS. Proteomics *9*, 1683-1695.

Gil, R., Barth, S., Kanfi, Y., and Cohen, H.Y. (2013). SIRT6 exhibits nucleosome-dependent deacetylase activity. Nucleic Acids Res *41*, 8537-8545.

Gilbert, N., Lutz-Prigge, S., and Moran, J.V. (2002). Genomic deletions created upon LINE-1 retrotransposition. Cell *110*, 315-325.
Gonzalez, I.L., and Sylvester, J.E. (1995). Complete sequence of the 43-kb human ribosomal DNA repeat: analysis of the intergenic spacer. Genomics *27*, 320-328.
Gordan, J.D., Bertout, J.A., Hu, C.J., Diehl, J.A., and Simon, M.C. (2007a). HIF-2alpha promotes hypoxic cell proliferation by enhancing c-myc transcriptional activity. Cancer Cell *11*, 335-347.
Gordan, J.D., Thompson, C.B., and Simon, M.C. (2007b). HIF and c-Myc: sibling rivals for control of cancer cell metabolism and proliferation. Cancer Cell *12*, 108-113.
Gordon, D.J., Resio, B., and Pellman, D. (2012). Causes and consequences of aneuploidy in cancer. Nat Rev Genet *13*, 189-203.
Grandori, C., Gomez-Roman, N., Felton-Edkins, Z.A., Ngouenet, C., Galloway, D.A., Eisenman, R.N., and White, R.J. (2005). c-Myc binds to human ribosomal DNA and stimulates transcription of rRNA genes by RNA polymerase I. Nat Cell Biol *7*, 311-318.
Grewal, S.S., Li, L., Orian, A., Eisenman, R.N., and Edgar, B.A. (2005). Myc-dependent regulation of ribosomal RNA synthesis during Drosophila development. Nat Cell Biol *7*, 295-302.
Guarente, L. (2011). Franklin H. Epstein Lecture: Sirtuins, aging, and medicine. N Engl J Med *364*, 2235-2244.
Guenatri, M., Bailly, D., Maison, C., and Almouzni, G. (2004). Mouse centric and pericentric satellite repeats form distinct functional heterochromatin. J Cell Biol *166*, 493-505.
Gupta, S., Young, D., Maitra, R.K., Gupta, A., Popovic, Z.B., Yong, S.L., Mahajan, A., Wang, Q., and Sen, S. (2008). Prevention of cardiac hypertrophy and heart failure by silencing of NF-kappaB. J Mol Biol *375*, 637-649.
Ha, C.W., and Huh, W.K. (2011). The implication of Sir2 in replicative aging and senescence in Saccharomyces cerevisiae. Aging (Albany NY) *3*, 319-324.
Haigis, M.C., Mostoslavsky, R., Haigis, K.M., Fahie, K., Christodoulou, D.C., Murphy, A.J., Valenzuela, D.M., Yancopoulos, G.D., Karow, M., Blander, G.*, et al.* (2006). SIRT4 inhibits glutamate dehydrogenase and opposes the effects of calorie restriction in pancreatic beta cells. Cell *126*, 941-954.

Han, Z., Liu, L., Liu, Y., and Li, S. (2014). Sirtuin SIRT6 suppresses cell proliferation through inhibition of Twist1 expression in non-small cell lung cancer. Int J Clin Exp Pathol *7*, 4774-4781.
Hanahan, D., and Weinberg, R.A. (2000). The hallmarks of cancer. Cell *100*, 57-70.
Hanahan, D., and Weinberg, R.A. (2011). Hallmarks of cancer: the next generation. Cell *144*, 646-674.
He, D., Li, H., Yusuf, N., Elmets, C.A., Athar, M., Katiyar, S.K., and Xu, H. (2012). IL-17 mediated inflammation promotes tumor growth and progression in the skin. PLoS One *7*, e32126.
Hirschhaeuser, F., Sattler, U.G., and Mueller-Klieser, W. (2011). Lactate: a metabolic key player in cancer. Cancer Res *71*, 6921-6925.
Hoffmann, J., Romey, R., Fink, C., Yong, L., and Roeder, T. (2013). Overexpression of Sir2 in the adult fat body is sufficient to extend lifespan of male and female Drosophila. Aging (Albany NY) *5*, 315-327.
Hogenesch, J.B., Chan, W.K., Jackiw, V.H., Brown, R.C., Gu, Y.Z., Pray-Grant, M., Perdew, G.H., and Bradfield, C.A. (1997). Characterization of a subset of the basic-helix-loop-helix-PAS superfamily that interacts with components of the dioxin signaling pathway. J Biol Chem *272*, 8581-8593.
Holzenberger, M., Dupont, J., Ducos, B., Leneuve, P., Geloen, A., Even, P.C., Cervera, P., and Le Bouc, Y. (2003). IGF-1 receptor regulates lifespan and resistance to oxidative stress in mice. Nature *421*, 182-187.
Hu, C.J., Wang, L.Y., Chodosh, L.A., Keith, B., and Simon, M.C. (2003). Differential roles of hypoxia-inducible factor 1alpha (HIF-1alpha) and HIF-2alpha in hypoxic gene regulation. Mol Cell Biol *23*, 9361-9374.
Iskow, R.C., McCabe, M.T., Mills, R.E., Torene, S., Pittard, W.S., Neuwald, A.F., Van Meir, E.G., Vertino, P.M., and Devine, S.E. (2010). Natural mutagenesis of human genomes by endogenous retrotransposons. Cell *141*, 1253-1261.
Iyengar, S., and Farnham, P.J. (2011). KAP1 protein: an enigmatic master regulator of the genome. J Biol Chem *286*, 26267-26276.
Jack, A.P., Bussemer, S., Hahn, M., Punzeler, S., Snyder, M., Wells, M., Csankovszki, G., Solovei, I., Schotta, G., and Hake, S.B. (2013). H3K56me3 is a novel, conserved

heterochromatic mark that largely but not completely overlaps with H3K9me3 in both regulation and localization. PLoS One *8*, e51765.
Jedrusik-Bode, M., Studencka, M., Smolka, C., Baumann, T., Schmidt, H., Kampf, J., Paap, F., Martin, S., Tazi, J., Muller, K.M.*, et al.* (2013). The sirtuin SIRT6 regulates stress granule formation in C. elegans and mammals. J Cell Sci *126*, 5166-5177.
Jiang, H., Khan, S., Wang, Y., Charron, G., He, B., Sebastian, C., Du, J., Kim, R., Ge, E., Mostoslavsky, R.*, et al.* (2013). SIRT6 regulates TNF-alpha secretion through hydrolysis of long-chain fatty acyl lysine. Nature *496*, 110-113.
Jin, J., Albertz, J., Guo, Z., Peng, Q., Rudow, G., Troncoso, J.C., Ross, C.A., and Duan, W. (2013). Neuroprotective effects of PPAR-gamma agonist rosiglitazone in N171-82Q mouse model of Huntington's disease. J Neurochem *125*, 410-419.
Jones, R.G., and Thompson, C.B. (2009). Tumor suppressors and cell metabolism: a recipe for cancer growth. Genes Dev *23*, 537-548.
Kaeberlein, M., McVey, M., and Guarente, L. (1999). The SIR2/3/4 complex and SIR2 alone promote longevity in Saccharomyces cerevisiae by two different mechanisms. Genes Dev *13*, 2570-2580.
Kaidi, A., Weinert, B.T., Choudhary, C., and Jackson, S.P. (2010). Human SIRT6 promotes DNA end resection through CtIP deacetylation. Science *329*, 1348-1353.
Kanfi, Y., Naiman, S., Amir, G., Peshti, V., Zinman, G., Nahum, L., Bar-Joseph, Z., and Cohen, H.Y. (2012). The sirtuin SIRT6 regulates lifespan in male mice. Nature *483*, 218-221.
Kanfi, Y., Peshti, V., Gil, R., Naiman, S., Nahum, L., Levin, E., Kronfeld-Schor, N., and Cohen, H.Y. (2010). SIRT6 protects against pathological damage caused by diet-induced obesity. Aging Cell *9*, 162-173.
Kanfi, Y., Shalman, R., Peshti, V., Pilosof, S.N., Gozlan, Y.M., Pearson, K.J., Lerrer, B., Moazed, D., Marine, J.C., de Cabo, R.*, et al.* (2008). Regulation of SIRT6 protein levels by nutrient availability. FEBS Lett *582*, 543-548.
Kawahara, T.L., Michishita, E., Adler, A.S., Damian, M., Berber, E., Lin, M., McCord, R.A., Ongaigui, K.C., Boxer, L.D., Chang, H.Y.*, et al.* (2009). SIRT6 links histone H3 lysine 9 deacetylation to NF-kappaB-dependent gene expression and organismal life span. Cell *136*, 62-74.

Kawahara, T.L., Rapicavoli, N.A., Wu, A.R., Qu, K., Quake, S.R., and Chang, H.Y. (2011). Dynamic chromatin localization of Sirt6 shapes stress- and aging-related transcriptional networks. PLoS Genet *7*, e1002153.
Keith, B., Johnson, R.S., and Simon, M.C. (2012). HIF1alpha and HIF2alpha: sibling rivalry in hypoxic tumour growth and progression. Nat Rev Cancer *12*, 9-22.
Kenyon, C.J. (2010). The genetics of ageing. Nature *464*, 504-512.
Khongkow, M., Olmos, Y., Gong, C., Gomes, A.R., Monteiro, L.J., Yague, E., Cavaco, T.B., Khongkow, P., Man, E.P., Laohasinnarong, S*., et al.* (2013a). SIRT6 modulates paclitaxel and epirubicin resistance and survival in breast cancer. Carcinogenesis.
Khongkow, M., Olmos, Y., Gong, C., Gomes, A.R., Monteiro, L.J., Yague, E., Cavaco, T.B., Khongkow, P., Man, E.P., Laohasinnarong, S*., et al.* (2013b). SIRT6 modulates paclitaxel and epirubicin resistance and survival in breast cancer. Carcinogenesis *34*, 1476-1486.
Kim, H.S., Xiao, C., Wang, R.H., Lahusen, T., Xu, X., Vassilopoulos, A., Vazquez-Ortiz, G., Jeong, W.I., Park, O., Ki, S.H*., et al.* (2010). Hepatic-specific disruption of SIRT6 in mice results in fatty liver formation due to enhanced glycolysis and triglyceride synthesis. Cell Metab *12*, 224-236.
Koh, M.Y., and Powis, G. (2012). Passing the baton: the HIF switch. Trends Biochem Sci *37*, 364-372.
Kouzarides, T. (2000). Acetylation: a regulatory modification to rival phosphorylation? EMBO J *19*, 1176-1179.
Lan, Q., Lim, U., Liu, C.S., Weinstein, S.J., Chanock, S., Bonner, M.R., Virtamo, J., Albanes, D., and Rothman, N. (2008). A prospective study of mitochondrial DNA copy number and risk of non-Hodgkin lymphoma. Blood *112*, 4247-4249.
Lappas, M. (2012). Anti-inflammatory properties of sirtuin 6 in human umbilical vein endothelial cells. Mediators Inflamm *2012*, 597514.
Larsson, N.G., Wang, J., Wilhelmsson, H., Oldfors, A., Rustin, P., Lewandoski, M., Barsh, G.S., and Clayton, D.A. (1998). Mitochondrial transcription factor A is necessary for mtDNA maintenance and embryogenesis in mice. Nat Genet *18*, 231-236.

Lee, H.C., Yin, P.H., Lin, J.C., Wu, C.C., Chen, C.Y., Wu, C.W., Chi, C.W., Tam, T.N., and Wei, Y.H. (2005). Mitochondrial genome instability and mtDNA depletion in human cancers. Ann N Y Acad Sci *1042*, 109-122.

Lee, H.S., Ka, S.O., Lee, S.M., Lee, S.I., Park, J.W., and Park, B.H. (2013a). Overexpression of SIRT6 suppresses inflammatory responses and bone destruction in collagen-induced arthritic mice. Arthritis Rheum.

Lee, H.S., Ka, S.O., Lee, S.M., Lee, S.I., Park, J.W., and Park, B.H. (2013b). Overexpression of sirtuin 6 suppresses inflammatory responses and bone destruction in mice with collagen-induced arthritis. Arthritis Rheum *65*, 1776-1785.

Lee, O.H., Kim, J., Kim, J.M., Lee, H., Kim, E.H., Bae, S.K., Choi, Y., Nam, H.S., and Heo, J.H. (2013c). Decreased expression of sirtuin 6 is associated with release of high mobility group box-1 after cerebral ischemia. Biochem Biophys Res Commun *438*, 388-394.

Lefort, K., Brooks, Y., Ostano, P., Cario-Andre, M., Calpini, V., Guinea-Viniegra, J., Albinger-Hegyi, A., Hoetzenecker, W., Kolfschoten, I., Wagner, E.F.*, et al.* (2013). A miR-34a-SIRT6 axis in the squamous cell differentiation network. EMBO J *32*, 2248-2263.

Li, Q., Zhou, H., Wurtele, H., Davies, B., Horazdovsky, B., Verreault, A., and Zhang, Z. (2008). Acetylation of histone H3 lysine 56 regulates replication-coupled nucleosome assembly. Cell *134*, 244-255.

Lin, C.Y., Loven, J., Rahl, P.B., Paranal, R.M., Burge, C.B., Bradner, J.E., Lee, T.I., and Young, R.A. (2012). Transcriptional amplification in tumor cells with elevated c-Myc. Cell *151*, 56-67.

Lin, Z., Yang, H., Tan, C., Li, J., Liu, Z., Quan, Q., Kong, S., Ye, J., Gao, B., and Fang, D. (2013). USP10 Antagonizes c-Myc Transcriptional Activation through SIRT6 Stabilization to Suppress Tumor Formation. Cell Rep *5*, 1639-1649.

Liszt, G., Ford, E., Kurtev, M., and Guarente, L. (2005). Mouse Sir2 homolog SIRT6 is a nuclear ADP-ribosyltransferase. J Biol Chem *280*, 21313-21320.

Liu, A.M., Qu, W.W., Liu, X., and Qu, C.K. (2012). Chromosomal instability in in vitro cultured mouse hematopoietic cells associated with oxidative stress. Am J Blood Res *2*, 71-76.

Liu, Y., Xie, Q.R., Wang, B., Shao, J., Zhang, T., Liu, T., Huang, G., and Xia, W. (2013). Inhibition of SIRT6 in prostate cancer reduces cell viability and increases sensitivity to chemotherapeutics. Protein Cell.
Lombard, D.B., and Miller, R.A. (2012). Ageing: Sorting out the sirtuins. Nature *483*, 166-167.
Longo, V.D., and Kennedy, B.K. (2006). Sirtuins in aging and age-related disease. Cell *126*, 257-268.
Lonnberg, A.S., Zachariae, C., and Skov, L. (2014). Targeting of interleukin-17 in the treatment of psoriasis. Clin Cosmet Investig Dermatol *7*, 251-259.
Madison, B.B., Dunbar, L., Qiao, X.T., Braunstein, K., Braunstein, E., and Gumucio, D.L. (2002). Cis elements of the villin gene control expression in restricted domains of the vertical (crypt) and horizontal (duodenum, cecum) axes of the intestine. J Biol Chem *277*, 33275-33283.
Malinge, S., Izraeli, S., and Crispino, J.D. (2009). Insights into the manifestations, outcomes, and mechanisms of leukemogenesis in Down syndrome. Blood *113*, 2619-2628.
Malynn, B.A., de Alboran, I.M., O'Hagan, R.C., Bronson, R., Davidson, L., DePinho, R.A., and Alt, F.W. (2000). N-myc can functionally replace c-myc in murine development, cellular growth, and differentiation. Genes Dev *14*, 1390-1399.
Manuyakorn, A., Paulus, R., Farrell, J., Dawson, N.A., Tze, S., Cheung-Lau, G., Hines, O.J., Reber, H., Seligson, D.B., Horvath, S.*, et al.* (2010). Cellular histone modification patterns predict prognosis and treatment response in resectable pancreatic adenocarcinoma: results from RTOG 9704. J Clin Oncol *28*, 1358-1365.
Mao, Z., Hine, C., Tian, X., Van Meter, M., Au, M., Vaidya, A., Seluanov, A., and Gorbunova, V. (2011). SIRT6 promotes DNA repair under stress by activating PARP1. Science *332*, 1443-1446.
Mao, Z., Tian, X., Van Meter, M., Ke, Z., Gorbunova, V., and Seluanov, A. (2012). Sirtuin 6 (SIRT6) rescues the decline of homologous recombination repair during replicative senescence. Proc Natl Acad Sci U S A *109*, 11800-11805.
Marquardt, J.U., Fischer, K., Baus, K., Kashyap, A., Ma, S., Krupp, M., Linke, M., Teufel, A., Zechner, U., Strand, D.*, et al.* (2013a). SIRT6 dependent genetic and

epigenetic alterations are associated with poor clinical outcome in HCC patients. Hepatology.
Marquardt, J.U., Fischer, K., Baus, K., Kashyap, A., Ma, S., Krupp, M., Linke, M., Teufel, A., Zechner, U., Strand, D.*, et al.* (2013b). Sirtuin-6-dependent genetic and epigenetic alterations are associated with poor clinical outcome in hepatocellular carcinoma patients. Hepatology *58*, 1054-1064.
Martinato, F., Cesaroni, M., Amati, B., and Guccione, E. (2008). Analysis of Myc-induced histone modifications on target chromatin. PLoS One *3*, e3650.
McCord, R.A., Michishita, E., Hong, T., Berber, E., Boxer, L.D., Kusumoto, R., Guan, S., Shi, X., Gozani, O., Burlingame, A.L.*, et al.* (2009). SIRT6 stabilizes DNA-dependent protein kinase at chromatin for DNA double-strand break repair. Aging (Albany NY) *1*, 109-121.
Mehta, R., Steinkraus, K.A., Sutphin, G.L., Ramos, F.J., Shamieh, L.S., Huh, A., Davis, C., Chandler-Brown, D., and Kaeberlein, M. (2009). Proteasomal regulation of the hypoxic response modulates aging in C. elegans. Science *324*, 1196-1198.
Michishita, E., McCord, R.A., Berber, E., Kioi, M., Padilla-Nash, H., Damian, M., Cheung, P., Kusumoto, R., Kawahara, T.L., Barrett, J.C.*, et al.* (2008). SIRT6 is a histone H3 lysine 9 deacetylase that modulates telomeric chromatin. Nature *452*, 492-496.
Michishita, E., McCord, R.A., Boxer, L.D., Barber, M.F., Hong, T., Gozani, O., and Chua, K.F. (2009). Cell cycle-dependent deacetylation of telomeric histone H3 lysine K56 by human SIRT6. Cell Cycle *8*, 2664-2666.
Michishita, E., Park, J.Y., Burneskis, J.M., Barrett, J.C., and Horikawa, I. (2005). Evolutionarily conserved and nonconserved cellular localizations and functions of human SIRT proteins. Mol Biol Cell *16*, 4623-4635.
Min, L., Ji, Y., Bakiri, L., Qiu, Z., Cen, J., Chen, X., Chen, L., Scheuch, H., Zheng, H., Qin, L.*, et al.* (2012). Liver cancer initiation is controlled by AP-1 through SIRT6-dependent inhibition of survivin. Nat Cell Biol *14*, 1203-1211.
Miyai, T., Maruyama, Y., Osakabe, Y., Nejima, R., Miyata, K., and Amano, S. (2008). Karyotype changes in cultured human corneal endothelial cells. Mol Vis *14*, 942-950.

Morris, B.J. (2013). Seven sirtuins for seven deadly diseases of aging. Free Radic Biol Med *56*, 133-171.
Moschen, A.R., Wieser, V., Gerner, R.R., Bichler, A., Enrich, B., Moser, P., Ebenbichler, C.F., Kaser, S., and Tilg, H. (2013). Adipose tissue and liver expression of SIRT1, 3, and 6 increase after extensive weight loss in morbid obesity. J Hepatol *59*, 1315-1322.
Moser, A.R., Pitot, H.C., and Dove, W.F. (1990). A dominant mutation that predisposes to multiple intestinal neoplasia in the mouse. Science *247*, 322-324.
Moskalev, A., and Shaposhnikov, M. (2011). Pharmacological inhibition of NF-kappaB prolongs lifespan of Drosophila melanogaster. Aging (Albany NY) *3*, 391-394.
Mostoslavsky, R., Chua, K.F., Lombard, D.B., Pang, W.W., Fischer, M.R., Gellon, L., Liu, P., Mostoslavsky, G., Franco, S., Murphy, M.M.*, et al.* (2006). Genomic instability and aging-like phenotype in the absence of mammalian SIRT6. Cell *124*, 315-329.
Munoz-Galvan, S., Jimeno, S., Rothstein, R., and Aguilera, A. (2013). Histone H3K56 Acetylation, Rad52, and Non-DNA Repair Factors Control Double-Strand Break Repair Choice with the Sister Chromatid. PLoS Genet *9*, e1003237.
Murray-Zmijewski, F., Lane, D.P., and Bourdon, J.C. (2006). p53/p63/p73 isoforms: an orchestra of isoforms to harmonise cell differentiation and response to stress. Cell Death Differ *13*, 962-972.
Ng, H.H., Feng, Q., Wang, H., Erdjument-Bromage, H., Tempst, P., Zhang, Y., and Struhl, K. (2002). Lysine methylation within the globular domain of histone H3 by Dot1 is important for telomeric silencing and Sir protein association. Genes Dev *16*, 1518-1527.
Nie, Z., Hu, G., Wei, G., Cui, K., Yamane, A., Resch, W., Wang, R., Green, D.R., Tessarollo, L., Casellas, R.*, et al.* (2012). c-Myc is a universal amplifier of expressed genes in lymphocytes and embryonic stem cells. Cell *151*, 68-79.
Niggeweg, R., Kocher, T., Gentzel, M., Buscaino, A., Taipale, M., Akhtar, A., and Wilm, M. (2006). A general precursor ion-like scanning mode on quadrupole-TOF instruments compatible with chromatographic separation. Proteomics *6*, 41-53.
Nin, V., Escande, C., Chini, C.C., Giri, S., Camacho-Pereira, J., Matalonga, J., Lou, Z., and Chini, E.N. (2012). Role of deleted in breast cancer 1 (DBC1) protein in SIRT1

deacetylase activation induced by protein kinase A and AMP-activated protein kinase. J Biol Chem *287*, 23489-23501.
O'Neill, L.A., and Hardie, D.G. (2013). Metabolism of inflammation limited by AMPK and pseudo-starvation. Nature *493*, 346-355.
Oberdoerffer, P., Michan, S., McVay, M., Mostoslavsky, R., Vann, J., Park, S.K., Hartlerode, A., Stegmuller, J., Hafner, A., Loerch, P.*, et al.* (2008). SIRT1 redistribution on chromatin promotes genomic stability but alters gene expression during aging. Cell *135*, 907-918.
Olivetti, G., Cigola, E., Maestri, R., Lagrasta, C., Corradi, D., and Quaini, F. (2000). Recent advances in cardiac hypertrophy. Cardiovasc Res *45*, 68-75.
Pan, P.W., Feldman, J.L., Devries, M.K., Dong, A., Edwards, A.M., and Denu, J.M. (2011). Structure and biochemical functions of SIRT6. J Biol Chem *286*, 14575-14587.
Parsons, J.L., and Dianov, G.L. (2013). Co-ordination of base excision repair and genome stability. DNA Repair (Amst).
Pavlides, S., Tsirigos, A., Vera, I., Flomenberg, N., Frank, P.G., Casimiro, M.C., Wang, C., Pestell, R.G., Martinez-Outschoorn, U.E., Howell, A.*, et al.* (2010). Transcriptional evidence for the "Reverse Warburg Effect" in human breast cancer tumor stroma and metastasis: similarities with oxidative stress, inflammation, Alzheimer's disease, and "Neuron-Glia Metabolic Coupling". Aging (Albany NY) *2*, 185-199.
Peng, C., Lu, Z., Xie, Z., Cheng, Z., Chen, Y., Tan, M., Luo, H., Zhang, Y., He, W., Yang, K.*, et al.* (2011). The first identification of lysine malonylation substrates and its regulatory enzyme. Mol Cell Proteomics *10*, M111 012658.
Peters, A.H., Mermoud, J.E., O'Carroll, D., Pagani, M., Schweizer, D., Brockdorff, N., and Jenuwein, T. (2002). Histone H3 lysine 9 methylation is an epigenetic imprint of facultative heterochromatin. Nat Genet *30*, 77-80.
Peters, A.H., O'Carroll, D., Scherthan, H., Mechtler, K., Sauer, S., Schofer, C., Weipoltshammer, K., Pagani, M., Lachner, M., Kohlmaier, A.*, et al.* (2001). Loss of the Suv39h histone methyltransferases impairs mammalian heterochromatin and genome stability. Cell *107*, 323-337.

Pihan, G.A., Wallace, J., Zhou, Y., and Doxsey, S.J. (2003). Centrosome abnormalities and chromosome instability occur together in pre-invasive carcinomas. Cancer Res *63*, 1398-1404.

Puigserver, P., Rhee, J., Donovan, J., Walkey, C.J., Yoon, J.C., Oriente, F., Kitamura, Y., Altomonte, J., Dong, H., Accili, D.*, et al.* (2003). Insulin-regulated hepatic gluconeogenesis through FOXO1-PGC-1alpha interaction. Nature *423*, 550-555.

Puigserver, P., and Spiegelman, B.M. (2003). Peroxisome proliferator-activated receptor-gamma coactivator 1 alpha (PGC-1 alpha): transcriptional coactivator and metabolic regulator. Endocr Rev *24*, 78-90.

Puppin, C., Passon, N., Lavarone, E., Di Loreto, C., Frasca, F., Vella, V., Vigneri, R., and Damante, G. (2011). Levels of histone acetylation in thyroid tumors. Biochem Biophys Res Commun *411*, 679-683.

Ram, O., Goren, A., Amit, I., Shoresh, N., Yosef, N., Ernst, J., Kellis, M., Gymrek, M., Issner, R., Coyne, M.*, et al.* (2011). Combinatorial patterning of chromatin regulators uncovered by genome-wide location analysis in human cells. Cell *147*, 1628-1639.

Raval, R.R., Lau, K.W., Tran, M.G., Sowter, H.M., Mandriota, S.J., Li, J.L., Pugh, C.W., Maxwell, P.H., Harris, A.L., and Ratcliffe, P.J. (2005). Contrasting properties of hypoxia-inducible factor 1 (HIF-1) and HIF-2 in von Hippel-Lindau-associated renal cell carcinoma. Mol Cell Biol *25*, 5675-5686.

Revollo, J.R., and Li, X. (2013). The ways and means that fine tune Sirt1 activity. Trends Biochem Sci *38*, 160-167.

Rhee, J., Inoue, Y., Yoon, J.C., Puigserver, P., Fan, M., Gonzalez, F.J., and Spiegelman, B.M. (2003). Regulation of hepatic fasting response by PPARgamma coactivator-1alpha (PGC-1): requirement for hepatocyte nuclear factor 4alpha in gluconeogenesis. Proc Natl Acad Sci U S A *100*, 4012-4017.

Rodgers, J.T., Lerin, C., Haas, W., Gygi, S.P., Spiegelman, B.M., and Puigserver, P. (2005). Nutrient control of glucose homeostasis through a complex of PGC-1alpha and SIRT1. Nature *434*, 113-118.

Rogina, B., and Helfand, S.L. (2004). Sir2 mediates longevity in the fly through a pathway related to calorie restriction. Proc Natl Acad Sci U S A *101*, 15998-16003.

Ronnebaum, S.M., Wu, Y., McDonough, H., and Patterson, C. (2013). The Ubiquitin Ligase CHIP Prevents SirT6 Degradation through Noncanonical Ubiquitination. Mol Cell Biol *33*, 4461-4472.
Sahin, K., Yilmaz, S., and Gozukirmizi, N. (2014). Changes in human sirtuin 6 gene promoter methylation during aging. Biomed Rep *2*, 574-578.
Salvi, J.S., Chan, J.N., Pettigrew, C., Liu, T.T., Wu, J.D., and Mekhail, K. (2013). Enforcement of a lifespan-sustaining distribution of Sir2 between telomeres, mating-type loci, and rDNA repeats by Rif1. Aging Cell *12*, 67-75.
Satoh, A., Brace, C.S., Rensing, N., Cliften, P., Wozniak, D.F., Herzog, E.D., Yamada, K.A., and Imai, S. (2013). Sirt1 extends life span and delays aging in mice through the regulation of Nk2 homeobox 1 in the DMH and LH. Cell Metab *18*, 416-430.
Sayyed, S.G., Gaikwad, A.B., Lichtnekert, J., Kulkarni, O., Eulberg, D., Klussmann, S., Tikoo, K., and Anders, H.J. (2010). Progressive glomerulosclerosis in type 2 diabetes is associated with renal histone H3K9 and H3K23 acetylation, H3K4 dimethylation and phosphorylation at serine 10. Nephrol Dial Transplant *25*, 1811-1817.
Schwer, B., Schumacher, B., Lombard, D.B., Xiao, C., Kurtev, M.V., Gao, J., Schneider, J.I., Chai, H., Bronson, R.T., Tsai, L.H.*, et al.* (2010). Neural sirtuin 6 (Sirt6) ablation attenuates somatic growth and causes obesity. Proc Natl Acad Sci U S A *107*, 21790-21794.
Sebastian, C., Serra, M., Yeramian, A., Serrat, N., Lloberas, J., and Celada, A. (2008). Deacetylase activity is required for STAT5-dependent GM-CSF functional activity in macrophages and differentiation to dendritic cells. J Immunol *180*, 5898-5906.
Sebastian, C., Zwaans, B.M., Silberman, D.M., Gymrek, M., Goren, A., Zhong, L., Ram, O., Truelove, J., Guimaraes, A.R., Toiber, D.*, et al.* (2012). The histone deacetylase SIRT6 is a tumor suppressor that controls cancer metabolism. Cell *151*, 1185-1199.
Seligson, D.B., Horvath, S., McBrian, M.A., Mah, V., Yu, H., Tze, S., Wang, Q., Chia, D., Goodglick, L., and Kurdistani, S.K. (2009). Global levels of histone modifications predict prognosis in different cancers. Am J Pathol *174*, 1619-1628.
Semenza, G.L. (2010). HIF-1: upstream and downstream of cancer metabolism. Curr Opin Genet Dev *20*, 51-56.

Shahbazian, M.D., and Grunstein, M. (2007). Functions of site-specific histone acetylation and deacetylation. Annu Rev Biochem *76*, 75-100.
Shen, J., Ma, W., and Liu, Y. (2013). Deacetylase SIRT6 deaccelerates endothelial senescence. Cardiovasc Res *97*, 391-392.
Skuli, N., Liu, L., Runge, A., Wang, T., Yuan, L., Patel, S., Iruela-Arispe, L., Simon, M.C., and Keith, B. (2009). Endothelial deletion of hypoxia-inducible factor-2alpha (HIF-2alpha) alters vascular function and tumor angiogenesis. Blood *114*, 469-477.
Soga, T. (2013). Cancer metabolism: key players in metabolic reprogramming. Cancer Sci *104*, 275-281.
Su, L.K., Kinzler, K.W., Vogelstein, B., Preisinger, A.C., Moser, A.R., Luongo, C., Gould, K.A., and Dove, W.F. (1992). Multiple intestinal neoplasia caused by a mutation in the murine homolog of the APC gene. Science *256*, 668-670.
Sundaresan, N.R., Vasudevan, P., Zhong, L., Kim, G., Samant, S., Parekh, V., Pillai, V.B., Ravindra, P.V., Gupta, M., Jeevanandam, V*., et al.* (2012). The sirtuin SIRT6 blocks IGF-Akt signaling and development of cardiac hypertrophy by targeting c-Jun. Nat Med *18*, 1643-1650.
Tannahill, G.M., Curtis, A.M., Adamik, J., Palsson-McDermott, E.M., McGettrick, A.F., Goel, G., Frezza, C., Bernard, N.J., Kelly, B., Foley, N.H*., et al.* (2013). Succinate is an inflammatory signal that induces IL-1beta through HIF-1alpha. Nature *496*, 238-242.
Tao, R., Xiong, X., DePinho, R.A., Deng, C.X., and Dong, X.C. (2013a). FoxO3 transcription factor and Sirt6 deacetylase regulate low density lipoprotein (LDL)-cholesterol homeostasis via control of the proprotein convertase subtilisin/kexin type 9 (Pcsk9) gene expression. J Biol Chem *288*, 29252-29259.
Tao, R., Xiong, X., DePinho, R.A., Deng, C.X., and Dong, X.C. (2013b). Hepatic SREBP-2 and cholesterol biosynthesis are regulated by FoxO3 and Sirt6. J Lipid Res *54*, 2745-2753.
Tennen, R.I., Berber, E., and Chua, K.F. (2010). Functional dissection of SIRT6: identification of domains that regulate histone deacetylase activity and chromatin localization. Mech Ageing Dev *131*, 185-192.
Tennen, R.I., Bua, D.J., Wright, W.E., and Chua, K.F. (2011). SIRT6 is required for maintenance of telomere position effect in human cells. Nat Commun *2*, 433.

Thirumurthi, U., Shen, J., Xia, W., LaBaff, A.M., Wei, Y., Li, C.W., Chang, W.C., Chen, C.H., Lin, H.K., Yu, D.*, et al.* (2014). MDM2-mediated degradation of SIRT6 phosphorylated by AKT1 promotes tumorigenesis and trastuzumab resistance in breast cancer. Sci Signal *7*, ra71.

Tian, H., McKnight, S.L., and Russell, D.W. (1997). Endothelial PAS domain protein 1 (EPAS1), a transcription factor selectively expressed in endothelial cells. Genes Dev *11*, 72-82.

Ting, D.T., Lipson, D., Paul, S., Brannigan, B.W., Akhavanfard, S., Coffman, E.J., Contino, G., Deshpande, V., Iafrate, A.J., Letovsky, S.*, et al.* (2011). Aberrant overexpression of satellite repeats in pancreatic and other epithelial cancers. Science *331*, 593-596.

Tissenbaum, H.A., and Guarente, L. (2001). Increased dosage of a sir-2 gene extends lifespan in Caenorhabditis elegans. Nature *410*, 227-230.

Tjeertes, J.V., Miller, K.M., and Jackson, S.P. (2009). Screen for DNA-damage-responsive histone modifications identifies H3K9Ac and H3K56Ac in human cells. EMBO J *28*, 1878-1889.

Toiber, D., Erdel, F., Bouazoune, K., Silberman, D.M., Zhong, L., Mulligan, P., Sebastian, C., Cosentino, C., Martinez-Pastor, B., Giacosa, S.*, et al.* (2013). SIRT6 recruits SNF2H to DNA break sites, preventing genomic instability through chromatin remodeling. Mol Cell *51*, 454-468.

Van Gool, F., Galli, M., Gueydan, C., Kruys, V., Prevot, P.P., Bedalov, A., Mostoslavsky, R., Alt, F.W., De Smedt, T., and Leo, O. (2009). Intracellular NAD levels regulate tumor necrosis factor protein synthesis in a sirtuin-dependent manner. Nat Med *15*, 206-210.

Van Meter, M., Kashyap, M., Rezazadeh, S., Geneva, A.J., Morello, T.D., Seluanov, A., and Gorbunova, V. (2014). SIRT6 represses LINE1 retrotransposons by ribosylating KAP1 but this repression fails with stress and age. Nat Commun *5*, 5011.

Van Meter, M., Mao, Z., Gorbunova, V., and Seluanov, A. (2011). SIRT6 overexpression induces massive apoptosis in cancer cells but not in normal cells. Cell Cycle *10*, 3153-3158.

Vander Heiden, M.G., Cantley, L.C., and Thompson, C.B. (2009). Understanding the Warburg effect: the metabolic requirements of cell proliferation. Science *324*, 1029-1033.
Vinciguerra, M., Santini, M.P., Claycomb, W.C., Ladurner, A.G., and Rosenthal, N. (2010). Local IGF-1 isoform protects cardiomyocytes from hypertrophic and oxidative stresses via SirT1 activity. Aging (Albany NY) *2*, 43-62.
Viswanathan, M., Kim, S.K., Berdichevsky, A., and Guarente, L. (2005). A role for SIR-2.1 regulation of ER stress response genes in determining C. elegans life span. Dev Cell *9*, 605-615.
Wan, F., and Lenardo, M.J. (2010). The nuclear signaling of NF-kappaB: current knowledge, new insights, and future perspectives. Cell Res *20*, 24-33.
Wang, C.Y., Liu, L.N., and Zhao, Z.B. (2013). The role of ROS toxicity in spontaneous aneuploidy in cultured cells. Tissue Cell *45*, 47-53.
Wang, G.L., Jiang, B.H., Rue, E.A., and Semenza, G.L. (1995). Hypoxia-inducible factor 1 is a basic-helix-loop-helix-PAS heterodimer regulated by cellular O2 tension. Proc Natl Acad Sci U S A *92*, 5510-5514.
Warburg, O. (1956). On the origin of cancer cells. Science *123*, 309-314.
Ward, P.S., and Thompson, C.B. (2012). Metabolic reprogramming: a cancer hallmark even warburg did not anticipate. Cancer Cell *21*, 297-308.
Whitaker, R., Faulkner, S., Miyokawa, R., Burhenn, L., Henriksen, M., Wood, J.G., and Helfand, S.L. (2013). Increased expression of Drosophila Sir2 extends life span in a dose-dependent manner. Aging (Albany NY) *5*, 682-691.
White, D., Rafalska-Metcalf, I.U., Ivanov, A.V., Corsinotti, A., Peng, H., Lee, S.C., Trono, D., Janicki, S.M., and Rauscher, F.J., 3rd (2012). The ATM substrate KAP1 controls DNA repair in heterochromatin: regulation by HP1 proteins and serine 473/824 phosphorylation. Mol Cancer Res *10*, 401-414.
Wiesener, M.S., Jurgensen, J.S., Rosenberger, C., Scholze, C.K., Horstrup, J.H., Warnecke, C., Mandriota, S., Bechmann, I., Frei, U.A., Pugh, C.W.*, et al.* (2003). Widespread hypoxia-inducible expression of HIF-2alpha in distinct cell populations of different organs. FASEB J *17*, 271-273.

Williams, S.K., Truong, D., and Tyler, J.K. (2008). Acetylation in the globular core of histone H3 on lysine-56 promotes chromatin disassembly during transcriptional activation. Proc Natl Acad Sci U S A *105*, 9000-9005.
Wise, D.R., DeBerardinis, R.J., Mancuso, A., Sayed, N., Zhang, X.Y., Pfeiffer, H.K., Nissim, I., Daikhin, E., Yudkoff, M., McMahon, S.B.*, et al.* (2008). Myc regulates a transcriptional program that stimulates mitochondrial glutaminolysis and leads to glutamine addiction. Proc Natl Acad Sci U S A *105*, 18782-18787.
Wise, D.R., and Thompson, C.B. (2010). Glutamine addiction: a new therapeutic target in cancer. Trends Biochem Sci *35*, 427-433.
Wu, D., Wu, P., Huang, Q., Liu, Y., Ye, J., and Huang, J. (2013). Interleukin-17: a promoter in colorectal cancer progression. Clin Dev Immunol *2013*, 436307.
Wu, W., and Zhao, S. (2013). Metabolic changes in cancer: beyond the Warburg effect. Acta Biochim Biophys Sin (Shanghai) *45*, 18-26.
Xiang, T., Long, H., He, L., Han, X., Lin, K., Liang, Z., Zhuo, W., Xie, R., and Zhu, B. (2013). Interleukin-17 produced by tumor microenvironment promotes self-renewal of CD133 cancer stem-like cells in ovarian cancer. Oncogene.
Xiao, C., Kim, H.S., Lahusen, T., Wang, R.H., Xu, X., Gavrilova, O., Jou, W., Gius, D., and Deng, C.X. (2010). SIRT6 deficiency results in severe hypoglycemia by enhancing both basal and insulin-stimulated glucose uptake in mice. J Biol Chem *285*, 36776-36784.
Xiao, C., Wang, R.H., Lahusen, T.J., Park, O., Bertola, A., Maruyama, T., Reynolds, D., Chen, Q., Xu, X., Young, H.A.*, et al.* (2012). Progression of chronic liver inflammation and fibrosis driven by activation of c-JUN signaling in Sirt6 mutant mice. J Biol Chem *287*, 41903-41913.
Xie, X., Zhang, H., Gao, P., Wang, L., Zhang, A., Xie, S., and Li, J. (2012). Overexpression of SIRT6 in porcine fetal fibroblasts attenuates cytotoxicity and premature senescence caused by D-galactose and tert-butylhydroperoxide. DNA Cell Biol *31*, 745-752.
Xu, A., Wang, Y., Xu, J.Y., Stejskal, D., Tam, S., Zhang, J., Wat, N.M., Wong, W.K., and Lam, K.S. (2006). Adipocyte fatty acid-binding protein is a plasma biomarker closely associated with obesity and metabolic syndrome. Clin Chem *52*, 405-413.

Yang, B., Zwaans, B.M., Eckersdorff, M., and Lombard, D.B. (2009). The sirtuin SIRT6 deacetylates H3 K56Ac in vivo to promote genomic stability. Cell Cycle *8*, 2662-2663.
Yu, S.S., Cai, Y., Ye, J.T., Pi, R.B., Chen, S.R., Liu, P.Q., Shen, X.Y., and Ji, Y. (2013). Sirtuin 6 protects cardiomyocytes from hypertrophy in vitro via inhibition of NF-kappaB-dependent transcriptional activity. Br J Pharmacol *168*, 117-128.
Yuan, J., Pu, M., Zhang, Z., and Lou, Z. (2009). Histone H3-K56 acetylation is important for genomic stability in mammals. Cell Cycle *8*, 1747-1753.
Yuneva, M., Zamboni, N., Oefner, P., Sachidanandam, R., and Lazebnik, Y. (2007). Deficiency in glutamine but not glucose induces MYC-dependent apoptosis in human cells. J Cell Biol *178*, 93-105.
Zhang, F., Kong, D., Lu, Y., and Zheng, S. (2013a). Peroxisome proliferator-activated receptor-gamma as a therapeutic target for hepatic fibrosis: from bench to bedside. Cell Mol Life Sci *70*, 259-276.
Zhang, G., Li, J., Purkayastha, S., Tang, Y., Zhang, H., Yin, Y., Li, B., Liu, G., and Cai, D. (2013b). Hypothalamic programming of systemic ageing involving IKK-beta, NF-kappaB and GnRH. Nature *497*, 211-216.
Zhang, Y., Shao, Z., Zhai, Z., Shen, C., and Powell-Coffman, J.A. (2009). The HIF-1 hypoxia-inducible factor modulates lifespan in C. elegans. PLoS One *4*, e6348.
Zhong, L., D'Urso, A., Toiber, D., Sebastian, C., Henry, R.E., Vadysirisack, D.D., Guimaraes, A., Marinelli, B., Wikstrom, J.D., Nir, T.*, et al.* (2010). The histone deacetylase Sirt6 regulates glucose homeostasis via Hif1alpha. Cell *140*, 280-293.
Zhu, Q., Pao, G.M., Huynh, A.M., Suh, H., Tonnu, N., Nederlof, P.M., Gage, F.H., and Verma, I.M. (2011). BRCA1 tumour suppression occurs via heterochromatin-mediated silencing. Nature *477*, 179-184.